Indian Journal of Natural Sciences www.tnsroindia.org.in ©IJONS

Vol.9 /Issue 50 /October / 2018 *International Bimonthly* *ISSN: 0976 – 0997*

RESEARCH ARTICLE

Antibiotic Resistance Property of *Streptococcus mutans* and R Plasmid Isolation from Dental Carries Individuals

Jai Shanker Pillai H P[1*], Tewelde G Foto[1] and Mangal Murthi[2]

[1]Faculty of Public Health, St Theresa International College, 1 Moo 6, Rangsit – Nakhon Nayok Road, Klong 14, Bungsan, Ongkharak, Nakhon Nayok, Thailand -26120
[2]Department of PG Studies and Research in Microbiology, Gulbarga University, Kalaburagi, Karnataka, India -585106

Received: 25 May 2018 Revised: 28 Jun 2018 Accepted: 30 July 2018

[*]**Address for Correspondence**
Jai Shanker Pillai H P
Faculty of Public Health,
St Theresa International College,
1Moo 6, Rangsit Nakhon Nayok Road,
Klong 14, Bungsan, Ongkharak,
Nakhon Nayok, Thailand -26120
Email : drjaishankerpillai@gmail.com

ABSTRACT

The present study investigates the antibiotic resistance property of oral *Streptococus mutans* obtained from the dental caries infected individuals. The *Streptococcus mutans* isolates were obtained from the tooth extracts of dental caries and non-dental caries individuals. The effect of four different antibiotics viz., Ampicillin, Amoxicillin, Penicillin G and Tetracycline at six different concentrations (5, 10, 15, 20, 25, 30 µg) was tested. The presence or absence of R plasmid was determined with respect to *Streptococcus mutans* isolates obtained from dental caries and non-dental caries individuals. The resistance of *Streptococcus mutans* to the antibiotics were found to be in the descending order of Ampicillin> Tetracycline> Amoxicillin> Pencillin – G; with a zone of inhibition in the order of 22, 24, 28 and 29 mm diameter respectively. The R plasmid was found to be present in *Streptococcus mutans* isolates obtained from the dental caries individual while it was found to be absent in the non-dental caries individuals.

Key words: Antibiotics resistance, Dental caries, *Streptococcus mutans*, R plasmid.

INTRODUCTION

Tooth decay is the leading cause of tooth loss, leading to odontogenic infections (Rayan *et al.,* 2004). This infectious disease is caused by important oral viridians *Streptococci*. The *S. mutans* is a gram positive, non-spore forming, catalase negative, facultative anaerobic cocci commonly found in the human oral cavity. The bacterium, *S. mutans* is a

significant contributor to tooth decay (Loesche, 1996) and has the ability to cause bacterial endocarditis. It is a member of the viridians *Streptococci* which occurs in chains (Patterson, 1996). Several researchers reported that *S. mutans* possess special character such as resistant to antibiotics. The *S. mutans* isolates have been multi-drug resistant in tradition for several decades and caries pathogens were resistant to specific antibiotic. Normal oral flora of this pathogenic species proved their resistant power against some common antibiotics like cell wall breaking penicillin group for recent decades. Resistant plasmid (R plasmid) is a conjugative feature in the plasmids of the bacterial cells that carry genes encoding resistance to antibiotics, poisons, metal ions, ultraviolet radiation, and bacteriophage (Kennath todar, 2008). In this study, the possible occurrence of *S. mutans* in the tooth extracted samples of dental caries and non caries individuals were studied along with the effectiveness of antibiotics (Ampicillin, Amoxicillin, Penicillin G and Tetracycline). The reason for the antibiotic resistance nature of the pathogenic *S. mutans* was also explained in the context of its plasmid.

MATERIALS AND METHODS

Sample Collection

Extracted tooth samples of dental caries and non caries individuals were collected from Nijalingappa Dental Hospital and Al-Bader Dental Hospital, Kalaburagi, Karnataka state, India. Decayed tooth samples from the patients were collected with a sterile forceps and were emptied into Mitis Salivarius Bacitracin agar, broth-based system (Hi-media, Mumbai). The extracted samples were kept in peptone water (Transport Media) and it was used as per requirement (Syed and Loesche, 1973). The collected samples were plated on 5 mL thiogllycolate broth and incubated at 37 °C for 24h. The stock cultures of the isolates were then prepared in 5 mL Brain-Heart Infusion (BHI) Broth (Hi-Media Laboratories, Mumbai) incubated at 37 °C for 24h and stored at 4 °C. To retrieve the microorganisms, a single pellet of the cultures was resuspended in 5 mL Brain-Heart Infusion (BHI) Broth (Hi-Media Laboratories, Mumbai), followed by incubation at 37 °C for 24h (Yoo *et al.,* 2007).

Bacterial Identification

The isolates were identified on the basis of their morphological, microscopic and biochemical characteristics. The identification criteria done were Colour of the culture, Cell shape, Gram staining, Motility, Catalase, Oxidase, Voges - Proskauer, Carbohydrate fermentation (Mannitol and Sorbitol) and Hemolysis. The colonies were sub-cultured repeatedly for obtaining pure cultures on Mitis Salivarius Bacitracin Agar slants and stored at 4 °C for further investigations (Shklair and Keene, 1974).

Antibiotic Susceptibility test

The disc diffusion test by Kirby-Bauer was employed to check the antibiotic susceptibility of the isolates (Kirby *et al*., 1966). Antibiotics used were Ampicillin, Amoxicillin, Tetracycline, and Penicillin-G. Only selective isolates were used for this assay.

Plasmid isolation

The plasmid from the selected *Streptococcus mutans* isolates of caries and non caries individuals was isolated by rapid boiling method of Holmes and Quigley (1981) modified by Riggs and McLachlan (1986).

Gel Electrophoresis

Plasmid DNA was separated by electrophoresis on a 0.7% agarose gel (w/v) at 50 volts overnight. The gel was stained with Ethidium - bromide, visualized under UV transillumination and photographed as per the standard methods of Aaij and Borst (1972).

RESULTS AND DISCUSSION

All the extracted tooth samples were collected from 20-60 year old, male and female healthy and caries infected individuals as shown in Table 1. It is known from the Table 1, the *Streptococcus mutans* isolates are more in individuals with dental caries infection in comparison to the individuals with non-dental caries (healthy individuals). A total of 134 isolates of *S. mutans* obtained from infected individuals and only 39 isolates are obtained from the healthy individuals.The number of isolates obtained from female infected individuals are 68 where it was only 18 isolates in case of healthy female individuals. The obtained *S. mutans* isolates from infected male were 66 and it was 21 from healthy male individuals. It was very clear from the Table 1, that, the *S. mutans* isolates were significantly more in the infected individuals than in the healthy individuals. The number of isolates obtained for each age group and gender of both healthy and infected individuals were also clearly shown in the Table, which had showed no significant variation with respect to age group and gender of the individuals, but clearing confirming the great variation in the number of isolates obtained from the healthy and infected individuals. From this result it can be clearly confirmed that, *S. mutans* occurs as a normal oral flora of humans and their population is more in the individuals infected with dental caries.

Table 2 clearly depicts the Morphological, Microscopic and Biochemical characteristics of the obtained isolates of *Streptococcus mutans* colonies. The *Streprococcus mutans* colonies appeared as blue coloured round colonies which are small, raised, adherent with irregular margin along the streaked lines on the selective media Mitis – Salivarius Bacitracin Agar medium. All the obtained isolates of *Streptococcus mutans* were confirmed to be positive for the tests such as Gram stain, Voges Prauskauer, Mannitol utilization and Sorbitol Utilization; negative for motility tests, catalase and oxidase. All the *Streptococcus mutans* isolates were also found to be α hemolytic. Table 3 clearly reveals the effect of each of six different concentrations of four different antibiotics namely Ampicillin, Amoxicillin, Penicillin–G and Tetracycline on the *Streptococcus mutans* isolate. It was noted that the zone of inhibition was same i.e. 10 mm diameter, for the Ampicillin and Tetracycline at 5 µg concentration, whereas it was 11 mm and 12 mm for Penicillin G and Amoxycillin at the same concentration of antibiotic. i.e. 5 µg. From this result it is clear that, the antibiotic Amoxycillin produced a higher zone of inhibition, while the least zone of inhibition was by both the antibiotics Ampicillin and Tetracycline at 5 µg concentration. The inhibition zone observed at 10 µg concentration for the antibiotics were in the sequence of; Amoxicillin (16 mm) > Tetracycline (15 mm) > Penicillin -G (14 mm) >Ampicillin (13 mm), referring to the, higher zone of inhibition to the lower zone of inhibition.

The inhibition zone of 20 mm for Amoxicillin, 18 mm for Penicillin–G, 16 mm for Tetracycline and 15 mm for Ampicillin were noted at 15 µg concentration for each of the antibiotics tested. Highest zone of inhibition of 24 mm diameter was observed for Amoxicillin and Penicillin–G at 20 µg concentration, whereas it was only 20 mm and 18 mm for Tetracycline and Amoxycillin. At 25 µg concentration, Penicillin – G produced high zone of inhibition which was 28 mm diameter and Amoxicillin produced 26 mm diameter zone of inhibition which was less than Penicillin – G but higher than Ampicillin and Tetracycline. Both Ampicillin and Tetracycline showed smaller zone of inhibition, i.e. 20 mm compared to other two antibiotics at 25 µg concentration. At 30 µg concentration of each of the antibiotics tested on the *Streptococcus mutans* isolate, the Penicillin – G exhibited greater zone of inhibition i.e.29 mm diameter, next to Penicillin – G was the amoxicillin which showed 28 mm diameter of inhibition zone. The Tetracycline showed 24 mm diameter zone of inhibition and Ampicillin exhibited the lowest inhibition zone i.e.22 mm diameter. Similar results were obtained on *S. mutans* resistance against Penicillin, Amoxycillin and Ampicillin antibiotics (Fani *et al.,*

2007; Dhamodhar *et al.,* (2012). A contradictory result to the Tetracycline resistance of *S. mutans* obtained in the present study was reported by (Devi *et al.,* 2011). Figure 1 shows the picture of plasmid elctrophoresed gel under UV trans illuminator. From the figure 1, it was very clear that the R plasmid band was present in the *Streptococcus mutans* isolates obtained from the dental carries individuals, whereas it was absent in the isolates obtained from the non-dental caries individuals. The *Streptococcus mutans* isolates obtained from the individuals with dental caries showed the presence of R plasmid, due to the antibiotic resistance that these isolates developed as a result of frequent administration of antibiotics to treat the dental caries over the longer period of time. Since the individuals with non-dental caries have not been administered with the antibiotics, the R plasmid was found to be absent in the *S. mutans* isolates obtained from the healthy individuals. From this result it is evident that certain bacteria spontaneously upgrade their genetic setup for their survival by combating the negative effects of antibiotics. Because of the frequent exposure of antibiotics, bacteria may develop antibiotic resistance genes in their plasmid over the period of time.

CONCLUSIONS

From this investigation it can be concluded that, frequent and unscientific method of intake of antibiotics can make the dental caries pathogen, *Streptococcus mutans* to be more antibiotic resistant. So it is advisable to follow the proper and scientific usage of antibiotics to treat the dental caries infections by both health care professionals and the patients. Authors would also like to conclude by pointing that, there is a need to search for newer antibiotics with stronger and wider effectiveness to treat such pathogens which have developed the resistance through their R plasmid over the period of time.

REFERENCES

1. Aaij, C., and P. Borst. 1972. The gel electrophoresis of DNA. Biochim. Biophys. Acta 269:192-200.
2. Devi A, Singh v, Bhatt AB. Antibiotic Sensitivity Pattern of Streptococcus against Commercially Available Drugs and Comparison with Extract of *Punica Granatum*., *International Journal of Pharma and Bio Sciences. 2011: 2(2):504-508.*
3. Dhamodhar P, Sreenivasa Murthy, Channarayappa, Karthik R, Neha G, Shanthakumar SS, George JV. *Antibacterial efficacy of Syzygium aromaticum extracts on multi-drug resistant Streptococcus mutans isolated from dental plaque* samples. J Biochem Tech. 2012;3(5):155-157.
4. Fani MM, Kohanteb J, Dayaghi M. Inhibitory activity of garlic (*Allium Sativum*) extract on *Multidrug-resistant Streptococcus mutans. J Indian Soc. Pedod. Prevdent. 2007: 25:164-168.*
5. Holmes DS, Quigley M.A rapid boiling method for the preparation of bacterial plasmids. *Anal. biochem* 1981: 114:193-197.
6. http://www.textbook of bacteriology .net/author Kenneth todar (accessed on 30.06.08).
7. Kirby WM, Bauer AW, Sherris JC, Turck M. *Antibiotic susceptibility testing by a standardized single disk method. Am J Clin athol. 1966; 45(4):493-496.*
8. Loesche WJ. Microbiology of dental decay and periodontal disease. *In: Baron ST Albrecht, Castro G et al., editors. Baron's Medical Microbiology. Galveston, Texas: University of Texas Medical Branch, 1996, 1169-1170.*
9. Patterson MJ. Viridians Streptococci can cause endocarditis. In: *Baron S, Albrecht T, Castro G, et al., editors. Baron's Medical Microbiology. Galveston, Texas: University of Texas Medical Branch 1996, 199-212.*
10. Rayan KJ, Ray CG, Sherris JC. Sherri's Medical microbiology. An introduction to infectious diseases, 4th edn. New York: Mcgraw-Hill, 2004.
11. Riggs, M.G., McLachlan, A.1986. Biotechnology Techniques 4, 310-313.
12. Shklair IL, Keene HJ. A biochemical scheme for the separation of type five varieties of *Streptococcus mutans. Arch. Oral boil 1974*; 19(11):1079-81.
13. Syed, S. A., and W. J. Loesche. Efficiency of various growth media in recoverying oral bacterial flora from human dental plaque. Appl. Microbiol. . 1973. 26:459- 465.

14. Yoo SY, Park SJ, Jeong DK, Kim KW, Lim SH, Lee SH. Isolation and characterization of the mutans streptococci from the dental plaques in Koreans. J Microbiol 2007; 45:246-55.

Table 1: Number of *Streptococcus mutans* isolates obtained from tooth crevices of the individuals

Age group	Healthy Individuals			Infected Individuals		
	Male	Female	Total	Male	Female	Total
20 – 30	7	5	12	13	15	28
30 – 40	2	6	08	18	14	32
40 – 50	4	1	05	11	15	26
50 – 60	3	3	06	09	11	20
60 - 70	5	3	08	15	13	28
Total	21	18	39	66	68	134

Table 2: Morphological, Microscopic and Biochemical identification of isolates of *Streptococcus mutans*

Sl. No.	Test	Results
1.	Colour	Blue
2.	Cell shape	Chain of round cells
3.	Gram Stain	Positive
4.	Motility	Negative
4.	Catalase	Negative
5.	Oxidase	Negative
6.	VP Test	Positive
7.	Mannitol	Positive
8.	Sorbitol	Positive
9.	Hemolysis	α

Table 3: Antibiotics resistance of *Streptococcus mutans*

Concentration of antibiotics (µg)	Diameter of inhibition zone of antibiotics (mm)			
	Ampicillin	Amoxicillin	Penicillin – G	Tetracycline
5	10	12	11	10
10	13	16	14	15
15	15	20	18	16
20	18	24	24	20
25	20	26	28	20
30	22	28	29	24

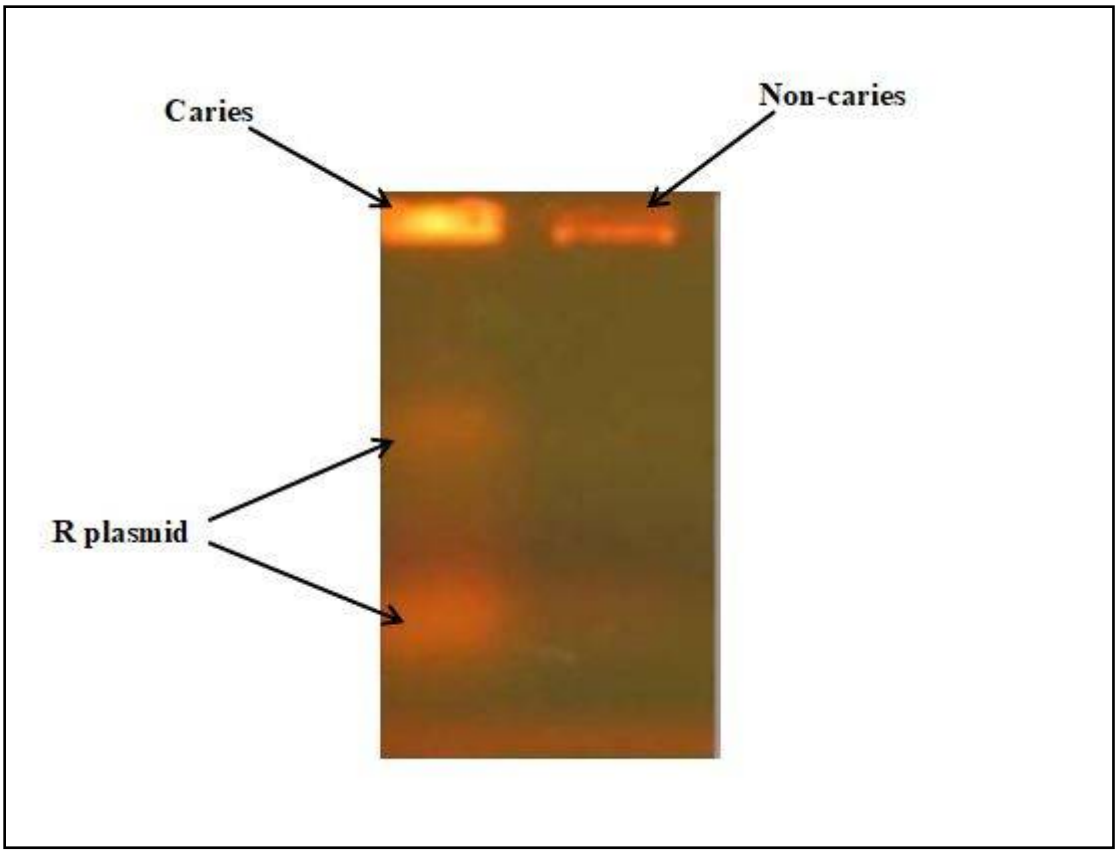

Figure 1: Electrophoresed Gel of Amp® plasmid under UV Tans Illuminator

Indian Journal of Natural Sciences www.tnsroindia.org.in ©IJONS

Vol.9 /Issue 50 /October / 2018 *International Bimonthly* *ISSN: 0976 – 0997*

RESEARCH ARTICLE

Development of Little Millet (*Panicum sumtranse* L.) Based Milk Beverage Using Rheological Properties and Sensory Evaluation

Reni Alagirisami [1,2]* and Gobikrishnan Sriramulu[3]

[1]Research Scholar, Department of Food Processing Technology, Karunya Institute of Technology and Sciences, Coimbatore,Tamilnadu, India-641114.
[2]Department of Food Processing and Preservation Technology, School of Engineering, Avinashilingam Institute for Home Science and Higher Education for Women, India- 641108.
[3]Department of Food Processing Technology, Karunya Institute of Technology and Sciences, Coimbatore, Tamilnadu, India -641114.

Received: 27 June 2018 Revised: 25 July 2018 Accepted: 28 Aug 2018

***Address for Correspondence**
Reni Alagirisami
Research Scholar,
Department of Food Processing Technology,
Karunya Institute of Technology and Sciences,
Tamilnadu, India-641114
Email: renideva@gmail.com

ABSTRACT

Millets play an important role in the food and nutritional security of the world.The present study focused on the use of under exploited little millet (*Panicum sumtranse* L.) flour for the preparation of beverage. In this, the beverage was prepared by mixing the little millet flour with milk at different ratios such as LMS_1 (1:100); LMS_2 (2:100); LMS_3 (3:100); LMS_4 (4:100); LMS_5 (5:100); LMS_6 (6:100); LMS_7 (7:100); LMS_8 (8:100); LMS_9 (9:100); LMS_{10} (10:100) .The rheological properties were analysed.The sensory evaluation also done for the prepared beverages using 9 point hedonic scale.

Keywords: rheology, beverage, little millet flour, sensory Evaluation

INTRODUCTION

Millets are a group of small-seeded grasses grown around the world as cereal crops.Millets ranks as the sixth significant cereal and it feeds one third of the total world population (Saleh *et al.,* 2013).Among the healthy food group, there has been an increased demand for health drinks with high acceptance from consumers. Millets are one of the gifted raw materials for developing health based beverage. These are important food crops in many underdeveloped countries because of their ability to grow even under undesirable weather conditions like reduced rainfall.Among various minor millets, little millet (*Panicum sumatrense L.*) has distinctive nutritional properties, which

are superior in certain constituents when compared to rice and wheat (Menon., 2004). Considering the growing awareness among the consumers regarding the health benefits of millet, there is a need to meet the diversified demands for millet based food products. Value addition and improving health benefits of millets by combining the millet flour at particular ratio with milk then processing it, opens new avenues for the product diversification.In the development of little millet based milk beverage the rheological characteristics and sensory evaluation plays a major role in its overall recognition of the final product. Consideration about rheology of liquid food is a valuable tool in the processing of various liquid beverages (Steffe1996; Rielly, 1997; Sopade and Kiaka 2001). The rheological data obtained were needed for the computation of processes such as pasteurization, evaporation and aseptic processing (Barbosa-Canovas *et al.* 1996; Rao 2007 b). Apart from this the consumer acceptance is more likely dependent on the consistency for the liquid based product (Deswal *et al.,* 2013).The aim of the present study used to develop the little millet based Milk beverage based on the Rheological behaviour and sensory evaluation of the product.

MATERIALS AND METHODS

Raw Materials - Little Millet Flour and Milk

Little millet (*Panicum sumatrense L.*) is rich in fibre, iron and carotene content along with macro and micro-nutrients and has a significant role in providing considerable amounts of antioxidants and Phyto chemicals in the diet (Ushakumari and Malleshi 2007; Pradeep and Guha, 2011).The little millet flour which was used to make millet based beverage was purchased were well dried and cleaned. The outer husk of the millet was removed by using the de-huller then milled using Ball mill. Milling or size reduction of little millet grain, releases the individual starch granules (Bao and Bergman, 2004).The milled flour was sieved to remove the unwanted foreign material present in it.

The particle size of the Little millet flour used to develop the milk based millet beverage was in the range of 270.3 nm size that was measured by using Particle analyzer and the milk with 3.0% Fat and 8.5% SNF was used. Other ingredients used to make this beverage were sucrose and Elachi essence. Elachi essence was added mainly to improve the flavor of the beverage.

Total Soluble Solid Content

The sucrose or table sugar is added to maintain total solid content of 20-22^{o} Brix level in the prepared beverage. The TSS was determined by an Erma hand refracto meter (reading at 20 °C) and was expressed as °Brix.

Preparation of Little Millet Based Milk Beverage

For the preparation of the millet beverage, little millet flour, Milk, sucrose and Elachi essence were used as ingredients. Before mixing the flour to the milk of 3.0 % fat and 8.5 % SNF the proper total solid content of 20-22^{o} Brix for the milk was maintained. To determine, the best and suitable consistency required for the preparation of beverage was done by mixing the Little Millet flour to milk at different ratio such as LMS_1 (1:100); LMS_2 (2:100); LMS_3 (3:100); LMS_4 (4:100); LMS_5 (5:100); LMS_6 (6:100); LMS_7 (7:100); LMS_8 (8:100); LMS_9 (9:100); LMS_{10} (10:100). Then this prepared mix was heated until the flour in the milk get gelatinization and finally the prepared mix was added with few drops of elachi essence. The protocol followed for the preparation of milk based little millet flour beverage was shown in Fig. 1.

Rheological Measurements

Adserson Patron Rheometer was used to perform the rheological measurements. Each experiment had a test temperature control using peltier system with a tolerance of ± 0.1°C. Viscosity of different samples was measured using plate and cone configuration (Cone diameter=20 mm; Cone angle=2°) in the shear rate range of 0.1 to 100 s^{-1}. The samples were effectively mixed using a magnetic stirrer to attain uniform consistency before loading into the Rheometer. The sample was brought into the lower plate using a spatula and filled up the gap by lowering the upper cone down to the designated gap. Rheological measurement was subsequently started after 2–4 min to allow for temperature equilibrium. All the measurements were carried out in triplicate and average is reported. A fresh sample was used in each measurement.

Sensory Evaluation

Prepared beverage samples such as LMS_1 (1:100); LMS_2 (2:100); LMS_3 (3:100); LMS_4 (4:100); LMS_5 (5:100); LMS_6 (6:100); LMS_7 (7:100); LMS_8 (8:100); LMS_9 (9:100); LMS_{10} (10:100) were evaluated for its sensory characteristics by a panel of 10 judges using 9 point Hedonic scale (stone et.al.,1974).

RESULTS AND DISCUSSION

Flow Behaviour of Little Millet based Milk Beverage

Figure 2 depicts the apparent viscosity-shear rate relationship of experimental data obtained for Little millet beverage with TSS content of 20°Brix at different preparation ratio such as LMS_1 (1:100); LMS_2 (2:100); LMS_3 (3:100); LMS_4 (4:100); LMS_5 (5:100); LMS_6 (6:100); LMS_7 (7:100); LMS_8 (8:100); LMS_9 (9:100); LMS_{10} (10:100) and exhibited non-Newtonian pseudo plastic behaviour.

The role of apparent viscosity in the sensory perception of the beverage is also significant from consumer standpoint (Szczesniak, 1979).Apparent viscosity may be the response to different physical stimuli as a function of the flow characteristics of a particular food under study (Yanes et al. 2002; Shama and Sherman 1973; Christensen, 1987). The sensory thickness, or oral viscosity, of shear-thinning fluids depends on the shear stress applied to the fluid in mouth. It has been found that a shear stress developed in mouth at a constant shear rate is generally perceived as the stimulus associated with the oral evaluation of viscosity (Wood, 1968). The Consistency K, Flow index n and flow behaviour of the beverage samples was given in the Table 1.For the prepared samples such as LMS_1 (1:100); LMS_2 (2:100); LMS_3 (3:100) LMS_4 (4:100); LMS5 (5:100); LMS_6 (6:100); LMS_7 (7:100); LMS_8 (8:100); LMS_9 (9:100); LMS_{10} (10:100) the flow behaviour indices, n varied in the range of 0.1430 - 5. 9978and the consistency coefficients, k were in the range of 0.893 –17.7 $Pa.s^n$. In this shear thinning behaviour obtained for all samples. The best result was obtained based upon the quantity of flour added during beverage preparation, flow index n, consistency k and apparent viscosity. From the obtained result flow index n value was less than 1 for all samples. In this, for the samples LMR1, LMR2, LMR3, LMR4, LMR5, LMR6 the n value was in the range between 0.1430 to 0.7885 and showing shear thinning behaviour. From LMR7, LMR8, LMR9, and LMR10 the n value was in the range between 1.9107 to 5. 9978. The shear thinning behaviour was always accepted for the beverages. The consistency value also increases based upon the increased amount of the flour for the beverage preparation.

It is evident from Fig. 3 that the apparent viscosity at any given shear rate decreases for all samples. In the starting point, the apparent viscosity towards the shear rate showed the highest value for all the samples. The high apparent viscosity was observed for the LMS_{10} (10:100) sample and lowest value for the LMS_1 (1:100) sample. It showed that apparent viscosity in the initial or starting point of the flow behaviour influenced by the addition of flour during preparation. These results indicate that concentration of the flour has a significant effect on the apparent viscosity of

little millet based milk beverage as indicated by shift in flow curves as the concentration increases and showed the shear thickening behaviour. ANOVA result shows that there is a significant difference in value of apparent viscosity at different concentration for entire range of shear rate under study (1 % level of significance).

Sensory Evaluation

Beverage prepared at different ratios of little millet flour along with milk LMS_1 (1:100); LMS_2 (2:100); LMS_3 (3:100); LMS_4 (4:100); LMS_5 (5:100); LMS_6 (6:100); LMS_7 (7:100); LMS_8 (8:100); LMS_9 (9:100); LMS_{10} (10:100) evaluated was given in the for its sensory characteristics by a panel of 10 judges using 9 point Hedonic scale. (Stone et.al.,1974).The best result obtained for the LMS_4 (4:100) sample.

CONCLUSION

The effects of flour concentration were examined in this study. From the result, it can be stated that the apparent viscosity of the little millet based beverage decreased considerably with the increase in the shear rate, indicating its pseudoplastic behaviour. The values of consistency index, k and flow index n was found to be strongly dependent on the quantity or ration of the flour added for the beverage .Based upon the consistency, flow index, and sensory evaluation LMR4(4:100) was best for the development of little millet based beverage.

ACKNOWLEDGEMENTS

We would like to thank Karunya University and Avinashilingam University, Coimbatore, Tamilnadu, India for their support to carry out this research.

REFERENCES

1. Bao, J. and Bergman, C.J., 2004. The functionality of rice starch. In *Starch in food* (pp. 258-294).
2. Barbosa-Cánovas, G.V., Kokini, J.L., Ma, L. and Ibarz, A., 1996. The rheology of semiliquid foods. In *Advances in Food and Nutrition Research* (Vol. 39, pp. 1-69). Academic Press.
3. Christensen, C.M. and Casper, L.M., 1987. Oral and nonoral perception of solution viscosity. *Journal of Food Science*, *52*(2), pp.445-447.
4. Deswal, A., Deora, N.S. and Mishra, H.N., 2014. Optimization of enzymatic production process of oat milk using response surface methodology. *Food and Bioprocess Technology*, *7*(2), pp.610-618.
5. Menon, M.V., 2004. Small millets call for attention. *World*, *4*, pp.63-64
6. Pradeep, S.R. and Guha, M., 2011. Effect of processing methods on the nutraceutical and antioxidant properties of little millet (Panicum sumatrense) extracts. *Food chemistry*, *126*(4), pp.1643-1647.
7. Rao, M.A., 2007. Application of rheology to fluid food handling and processing. In *Rheology of Fluid and Semisolid Foods*(pp. 427-469). Springer, Boston, MA.
8. Rielly, C.D., 1997. Food rheology. In *Chemical engineering for the food industry* (pp. 195-233). Springer, Boston, MA.
9. Saleh, A.S., Zhang, Q., Chen, J. and Shen, Q., 2013. Millet grains: nutritional quality, processing, and potential health benefits. *Comprehensive Reviews in Food Science and Food Safety*, *12*(3), pp.281-295.
10. Shama, F. and Sherman, P., 1973. Identification of stimuli controlling the sensory evaluation of viscosity II. Oral methods. *Journal of texture studies*, *4*(1), pp.111-118.
11. Sopade, P.A. and Kiaka, K., 2001. Rheology and microstructure of sago starch from Papua New Guinea. *Journal of Food Engineering*, *50*(1), pp.47-57.
12. Steffe, J.F., 1996. *Rheological methods in food process engineering*. Freeman press.

13. Stone, H., Sidel, J., Oliver, S., Woolsey, A. and Singleton, R.C., 2004. Sensory evaluation by quantitative descriptive analysis. *Descriptive Sensory Analysis in Practice*, pp.23-34.
14. Szczesniak, A.S., 1979. Classification of mouthfeel characteristics of beverages. *Food texture and rheology*, pp.1-20.
15. Ushakumari, S.R. and Malleshi, N.G., 2007. Small millets: Nutritional and technological advantages. *Food uses of small millets and avenues for further processing and value addition, Ed. Krishnegowda, K. and Seetharam, All India Coordinated Small Millets Improvement Project, ICAR, UAS, Bangalore, In*.
16. Wood, F.W., 1968. Psychophysical Studies on the Consistency of Liquid Foods. *Rheology and Texture of Food Stuffs, SCI Monograph*, (27), pp.40-49.
17. Yanes, M., Durán, L. and Costell, E., 2002. Effect of hydrocolloid type and concentration on flow behaviour and sensory properties of milk beverages model systems. *Food hydrocolloids*, *16*(6), pp.605-611.

Table 1. Consistency K, Flow index n and Flow behaviour of the beverage samples

Samples	Consistency K	Flow Index n	Flow behaviour
LMR 1	0.893 Pa.s ^1.82	0.1430	shear thinning
LMR 2	1.524 Pa.s ^1.92	0.2520	shear thinning
LMR 3	2.007 Pa.s ^1.89	0.2889	shear thinning
LMR 4	3.893 Pa.s ^1.89	0.3526	shear thinning
LMR 5	6.893 Pa.s ^1.89	0.5947	shear thinning
LMR 6	8.308 Pa.s^0.64	0.7885	shear thinning
LMR 7	10.815 Pa.s^0.0907	1.9107	shear thickening
LMR 8	12.51 Pa.s^0.01	2.9526	shear thickening
LMR 9	15.25 Pa.s^0.01	4.9978	shear thickening
LMR 10	17.7 Pa.s^0.01	5. 9978	shear thickening

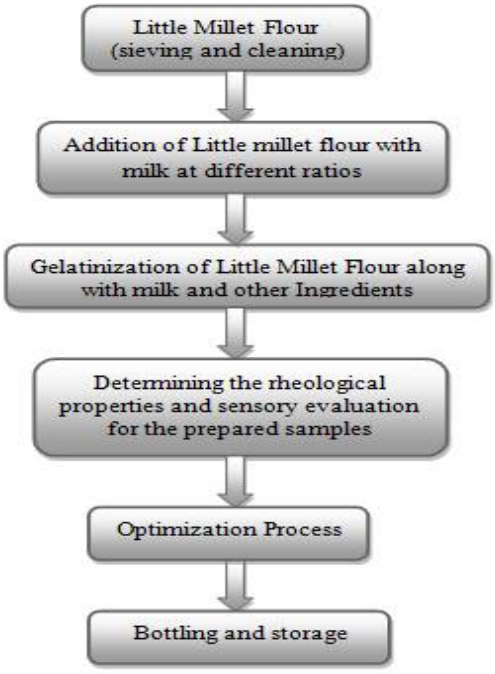

Fig. 1 Flow chart for the Processing of Little millet (*Panicum sumatrense L*) based beverage

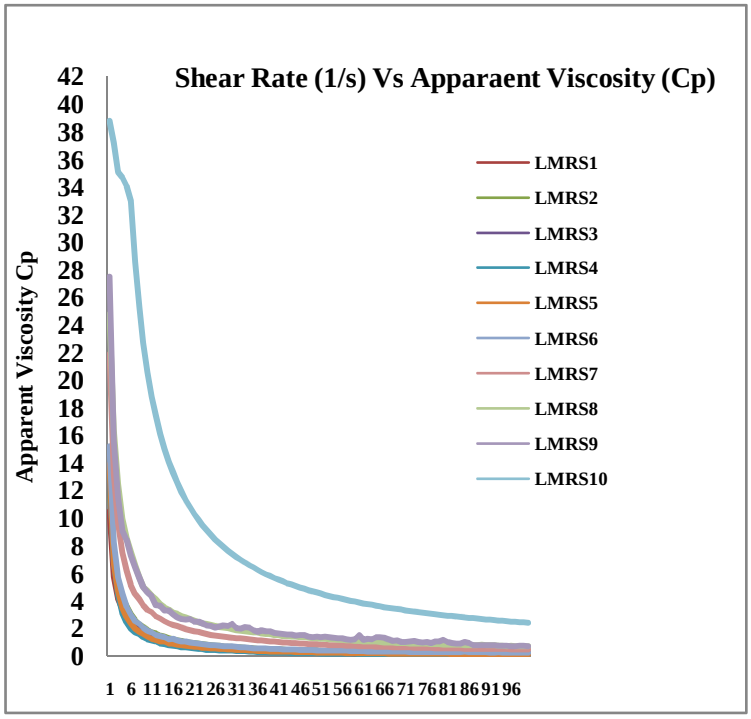

Fig. 2. Shear rate Vs Apparent Viscosity (Cp)

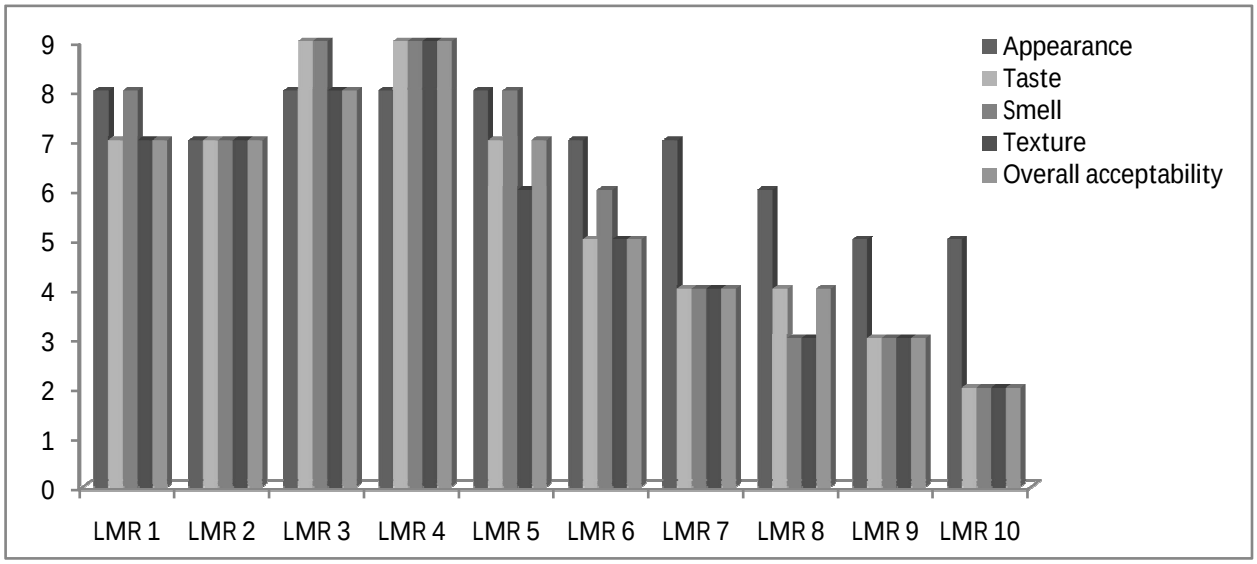

Fig. 3. Sensory Evaluation of the prepared samples

Indian Journal of Natural Sciences www.tnsroindia.org.in ©IJONS

Vol.9 /Issue 50 /October / 2018 *International Bimonthly* *ISSN: 0976 – 0997*

RESEARCH ARTICLE

The Effectiveness of Extracellular Matrix Derived from Bovine Urinary Bladder Matrix on Spinal Cord Injury in Dog

Salah H.A.AL-Ameri[1*] and Hameed A.K.AL-Timemi[2]

[1]Department of Surgery and Obstetrics, College of Veterinary Medicine, Universityof Al- Qasim Green, Iraq.

[2]Department of Surgery and Obstetrics, College of Veterinary Medicine, University of Baghdad, Baghdad, Iraq.

Received: 26 June 2018 Revised: 27 July 2018 Accepted: 25 Aug 2018

[*]**Address for Correspondence**
Salah H.A.AL-Ameri
Department of Surgery and Obstetrics,
College of Veterinary Medicine,
Universityof Al- Qasim Green, Iraq.

ABSTRACT

Spinal cord injury has a limited capacity to repair; therefore, medical interventions are necessary for treatment of injuries. Using urinary bladder sub mucosa powder as a scaffold is a new approach. The aim of this study is to evaluate the effect of urinary bladder sub mucosa powder on regeneration of thecanine spinal cord injury model. For this purpose, twelve adult local breed dogs were divided into two equal group (n=6).Group I (positive control group) subjected to dorsal laminectomy with left lateral hemisection defects was treated with phosphate buffer saline, andgroup II (scaffold group) subjected to with left lateral hemisection defects then urinary bladder sub mucosa powder 0.01mg filled the site of hemisection defects. Comprehensive studies were including the clinical signs andhistopathological examination. Motor and sensory improvements were assessed by open field locomotor scale, including, gait, proprioceptive positioning and nociception, were evaluated weekly from the first week to the end of the study 16 weeks PO. The clinical evaluation of motor and sensory functions revealed significant ($p \leq 0.05$) differences between the scaffold and the control groups. However, the sensory function indicated the prognosis of sensation during on 112 days PO in treated group compared with control group. Histological findings in treated group revealed a reduction in tissue loss from secondary processes as well as in diminished glial scarring tissue, prominent remyelination regenerative nerve fibers, and remarkable angiogenesis at the 112th PO. The conclusion of study, it is proved the clinical efficacy of scaffold grafting as a tool for induction of neuroregeneration after traumatic spinal cord injury.

Keywords: Spinal cord injury, Scaffold, Functional Recovery, Regeneration.

INTRODUCTION

Worldwide, approximately 90 million people suffer from spinal cord injury (SCI), the incidence in developed countries vary from one to five persons per 100.000, the main causes are motor vehicle accidents, fall, violence and sports injuries [1].The pathology varies with the force of spinal cord compression, the duration of compression, the displacement of the spinal cord, the acceleration of the impacting forces, and the kinetic energy absorbed at the time of spinal cord impact [2]. There are three phases of SCI response that occur after injury [3]. Upon primary injury, there is immediate mechanical damage to neural and other soft tissues, including endothelial cells of vasculature, this phase is associated with hemorrhage, localized edema ,loss of microcirculation by thrombosis and mechanical damage, and loss of vasculature autoregulation, all of which further exacerbate the neural injury [4]. In the secondary phase (which occurs over a time course of minutes to weeks) the devastating effect of ischemic cellular death, ionic shifts, and edema continue from the acute phase, inflammatory cells invade the spinal cord parenchyma. Apoptosis occurs and involves reactive gliosis that includes the increased expression of glial fibrillary acidic protein (GFAP) and astrocytic proliferation. Finally, in the chronic phase, which occurs over a time course of days to years, apoptosis continues, together with scarring, demyelination and cyst formation [5]. There are many cues that influence the growth and regeneration of nerve fiber. One of these is biomaterials help rebuild damaged tissues [6].Biomaterials, with their own intrinsic biological activity that would encourage endogenous tissue repair without the need for additional bioactive molecules such as exogenous growth factors or peptides, may provide high treatment effectively together with relative ease of application and scalable manufacturing potential [7].The aim of this work is to evaluate the clinical efficacy of urinary bladder sub mucosa powder as a scaffold for regeneration of the canine spinal cord injury model

MATERIALS AND METHODS

The whole fresh urinary bladders were harvested from a slaughtered cow at the local abattoir and UBM-ECM prepared as a decellularized scaffolddescribed and applied previously by [8,9] The decellularized UBM sheets(Fig.1A) allowed to set slightly before being transferred to −20 °C for 24 hours then transferred to the deep freezer at -80°C for 5days and the scaffolds was later freeze dried in a freeze drier (FTS Systems Bulk Freeze Dryer Model 8–54) for lyophilization till it is completely dried for 4 days at −50 °C (Fig.1B).The powder has been sterilized by 60°C in oven at 16 hours, later kept in a sterile container before use (Fig.1c).This study was conducted on twelve adult local breed dogs aged 8 to 12months old, with a body weight between 10 and 15 kg. The animals were kept in separate cages and given broad-spectrum antibiotics and antihelmintic. All procedures used in this study were approved by the College of Veterinary Medicine, University of Baghdad. Dogs were randomly divided into two groups. Both groups compromised of animals were left lateral hemisections at the second lumbar vertebrae (L2).Group I (positive control group) was treated with phosphate buffer saline.Group II (scaffold group) was treated by urinary bladder sub mucosa powder 0.01mg filled the gap between the proximal and the distal ends of the spinal cord. Thendura was repaired to prevent cerebral spinal fluidleakage. The animals from both groups were sacrificed on day 112 post operations (PO) forhistopathological examination.

Anesthetic Protocol

The dogs were fasted for two hours prior to the anesthesia. Induction of anesthesia was achieved by intramuscular injection of a mixture of 15mg/kg Ketamine hydrochloride (Kepro®, Holland), 5mg/kg of Xylazine hydrochloride (Xyla®, Holland) [10].

Surgical Protocol

The dogs were positioned in sternal recumbence. Make a surgical incision over the dorsal midline to include L1-L3. Use a periosteal elevator to subperiosteally elevate epaxial muscles from dorsal spinous processes, laminae, articular facets, and pedicles of L2 vertebrae. Use Gelpi retractors to facilitate gentle retraction of epaxial musculature during dissection.Remove the interarcuate ligament using sharp dissection with a No. 11 scalpel blade and remove the exposed dorsal spinous processes to the level of the dorsal lamina with large, single-action duckbill rongeurs. Once the inner cortical layers of both laminae have been reached, the soft periosteal can be palpated with a dental spatula, gently penetrate periosteum and remove fat tissue surrounded of spinal cord. (Fig.2A), Longitudinal incision of the meninges, Left lateral hemisections were achieved with surgical blade No 10 under a magnify lens (Fig.2B).Haemostasis was achieved by using gel foam and irrigates the wound with room-temperature physiologic saline solution to dislodge any remaining bone fragments from soft tissue. In scaffold group the hemisection of the spinal cord was implantation with a 0.01mg UBM- powder filled between distal stumps and the proximal stumps of spinal cord (Fig.2C). Then dura matter was closed by 4/0 Vicryl and harvest a piece of subcutaneous fat place it over the laminectomy site to help prevent dural adhesions. Close the fascia and epaxial muscles with 3-0 Polydioxanone simple continuous sutures. Close subcutaneous tissue and skin routinely (Fig.2D).All animals were given postoperative analgesia Tramadol hydrochloride (Trabar® Switzerland, 100 mg) 0.2 ml/kg intramuscular administered at 12-hour intervals for three consecutive days.

Clinical Signs Evaluation

Motor Functions Evaluation

All dogs were subjected to neurological assessment, the gaitof each animal in the different groups wasassessed before and after surgery, daily from the first day to the end of the study on day 112 PO assessment was done using modified Tarlov Scale [11]. Knuckling was graded based on normal, mild, moderate to severe.

Sensory Functions Evaluation

The sensory functions of the spinal cord injury were recorded weekly starting from the end of the 3rd week to the end of the study on day 112 PO. Sensory functions and clinical signs scoring were evaluated by using the Texas Spinal Cord Injury Scale (TSCIS) [12]. The superficial nociception was tested induced by pricking the lateral aspect of leg and planter surface of foot by needle, deep nociception was evaluated by pinching the most distal portion of each digit on both limbs with forceps squeezing, which were recorded as positive response, indicative of recovery.

Neurohistopathological Procedure

On the 112th postoperative day, animals (n = 12) were anesthetized with Ketamine and xylazine and euthanized by intracardial injected of formaline 10%. The spinal cord was left in bone overnight embedded in 10% neutrant buffer formalin, then removed, and post fixed in the same fixative for at least 1 week. A 3 cm-long segment of the spinal cord containing the lesion site anda series of 5μm thick longitudinal sections at middle and transverse at proximal anddistal segment was collected. Hematoxylin–eosin staining were performed usingstandard protocols, and the slides were specifically evaluated the cystic cavity formation, orientation of regenerative nerve fibers in white matter, number of regenerative neuron cells in gray matter, scar tissue formation at the site of hemisection the spinal cord.

Statistical analysis

All data were expressed in means and standard deviation of themean (M ± SD). Statistical comparisons between groups wereperformed using Statistical Package for the Social Sciences (SPSS) 16.0 software (non-parametric tests), Kruskal Wallis and Mann-Witney tests. A p value of ≤ 0.05 was considered significant.

RESULTS

Clinical Assessment of Motor and Sensory Function

There was a statistically significant difference in modified Tarlov scoring between scaffoldgroupand positive controlgroups.In group I, the animals were able to stand or walk few steps. Knuckling was mild, and remained until the end of the study.Sensation of the lateral leg sensation, toe pinch and the toe prick remained absentuntil end of the study. In group II, the interesting finding was that the animals regained normal gait ability on day 91 PO (Tab. 1). The knuckling in group II were significant difference ($p \leq 0.05$) compared with group I (Tab. 2). Sensation of the hind limb was regained and the lateral aspect leg, toe prick were appeared on days 99,105 postoperative respectively where toe pinch response appeared on 85 day PO (Tab. 3). However, the sensory clinical signs improved in group II were significant difference ($p \leq 0.05$) compared with group I.

Histopathological Observations

The histopathological sections at the site of the spinal cord injury in group I, showedlarge cystic cavity surrounded by glial scar formation due to proliferation of reactive astrocytes and still there is a gap between pre and post transection area (Fig.4. A), inthe white matter showedmarked vacculation and demyelination axons (Fig.5. A), In addition, hyperatrophy and proliferation of astrocytes, apoptosis of oligodentrocytes and proliferation of active microglia cells (Fig.6 A).Group II showednarrow cavity containing blood vessels, surrounded by dense regenerative nerve fiber, wide glial cell (Fig.4. B), in white matter market reduction in the number of swollen vacuolated nerve fiber with prominent remyelination regenerative nerve fibers (Fig.5B), multiple regenerative neurons were seen in the grey matter and good orientation regenerative nerve fibers were detected in the cross sections of the white matter (Fig.6. B).

DISCUSSION

Results of this study showed the gait progressed early developed in the group II compared to the group I. This result suggested that the potential therapeutic effects of scaffold used in this study urinary bladder matrix can reduce inflammation, while increasing functional tissue remodeling, However, urinary bladder matrix (UBM) can regulate M1/M2 phenotypes in infiltrating macrophage and resident microglia, which differ considerably from monocyte derived macrophages.Cherry *et al*[13]reported in a rodent traumatic brain injury (TBI) model, urinary bladder matrix (UBM) injected into the brain did not detectably activate microglia or astrocytes, while decreasing the lesion volume and increasing functional recovery.Zhang *et al*[14] showed in a rodent spinal cord injury model, M2-like macrophage-derived factors were shown to reduce astrocyte activation, which in turn reduced M1-like macrophage infiltration via a putative feedback mechanism. However, the knuckling disappeared in all animals in the group II and this might be due to the role of UBM effeteness functional recovery on the site of hemisection defects on day 112 PO, which enhanced early innervation of the extensor and flexor muscle that controls normal locomotion of the limb andthat promote myelin sheath formation and neovascularization, reduced inflammatory reaction and reduction edema as a result relief pain which result from injure of spinal cord.[15]Reported thatafter UBM is applied *in vivo*, ECM bioscaffolds are rapidly invaded and degraded by macrophages and other immune cells. During degradation, release growth factors and cytokines, like VEGF, TGF, PDGF, and bFGF that contributes to healing.The degree of sensory

reflexes included superficial nociception and deep nociception, gradually regaining function; the dogs in group II showed lateral aspect leg, toe prick were present on day's 99 and 105 PO respectively where toe pinch response appeared on day 85 PO. Therefore, animals in the control group did not regain sensation even by end of the study.Improvement of motor and sensory functions could indicate that regenerated axons organizing their growth, preventing gliosis in the damaged area and enhancing neural recovery of spinal cord injury. The absorption action of the UBM decreases the level of fibrinogen and fibrin production derived from fibrinogen, which leads to decreased fibrosis (scar tissue) at the site of the hemisectionsspinal cord. Decreased fibrosis will facilitate the extension and direction of axons to align and orientate correctly. This result is similar to the findings of Xue*etal* [16]. That showed that ECM transposition had more newly developed nerve fibers and less scar tissue.

The histological sections findings at the site of the hemisections spinal cord in the group II showed considerable improvement and acceleration of myelin sheath formation, neovascularization so that spinal cord regeneration compared to the group I. Meanwhile, the group I histology at the site of thehemisections spinal cord showed sever vacculation of the nerve fibers in the white matter this attributed by key pro-inflammatory cytokines which lead to the secondary cascades of events that occur after several hours to days of spinal cord injury which include the mitochondrial dysfunction which lead to failure of aerobic energy metabolism and finally lead to production of free oxygen radicals which cause lipid peroxidation and lead to increase vascular permeability, local ischemia, and intraneuronal edema, and degenerate axons. These findings coincide with Tsai *etal*. [17].

The vacuolation in the gray matter result from degenerated and necrotized neurons, the neuronal cell necrosis result from ischemia which occurs after spinal cord secondary injury, Ischemia results from inadequate blood supply to the tissue lead to hypoxia and reduction in perivscular PH from accumulation of acid metabolites such as lactate this tissue perfusion may increase cellular damage by promoting the influx of free radicals and other toxic byproducts, which are in agreement with the study conducted by [18].In the group II showeddecrease cystic cavity surrounded by dense regenerative nerve fiber and associated with proliferation of oligodendrocytes and microglial cells and small capillaries, in white matter market reduction in the number of swollen vacuolated nerve fiber with prominent remyelination regenerative nerve fibers, in gray matter marked reduction in the number of atrophied neurons.The UBM treatment preserved white matter integrity and improve long-term neurological function after SCI. Two potential mechanisms might underlie these improvements. First, ECM may directly promote axonal growth and myelination.

Multiple components of the ECM, *e.g.* tenascin-C, laminin, and integrins, have been shown to facilitate oligodendrocyte progenitor cell (OPC) proliferation and migration, as well as their differentiation into mature myelination oligodendrocytes [19].The second explanation for the white matter protection afforded by ECM might be an indirect effect from microglia. Microglias are among the most potent regulators of SCI repair and regeneration. Microglia undergoes phenotypic polarization in response to SCI injury [20] However, the UBMto release a wide range of neurotrophic factors, such as NGF, BDNF, CTNF, and GDNF and VEGF such as VEGF and HGF that promote myelin sheath formation and neovascularization. This result agreement with study conducted by Zhang *et al.* [21] these findings clearly demonstrated that chemically extracted a cellular muscle grafts provided useful biometrics to enhance axon sprouting in the injured spinal cord.

In conclusion; depending on the clinical and histopathological findings, the present study confirmed that novel natural urinary bladder matrix powder showed reduced cystic cavity formation, good orientation of regenerative nerve fibers in white matter, increased number of regenerative neuron cells in gray matter, increased angiogenesis and minimal scar tissue formation at the site of hemisection the spinal cord. These histopathological findings of spinal cord regeneration supported the clinical signs in motor and sensory test in a period of 16thpostoperative week because the UBM showed both mechanical and chemical support to the injured spinal cord regeneration.

REFERENCES

1. Holtz, A. and Levi, R. (2006). Effect of methylprednisolone incompression trauma to the feline spinal cord. J. Neurosurg. 55: 200 –208.
2. Bunge, R. P.; Puckett, W. R.; Becerra, J. L. (1993). Observations onthe pathology of human spinal cord injury. A review andclassification of 22 new cases with details from a case of chroniccord compression with extensive focal demyelination. Adv. Neurol.,59: 75–89.
3. Hulsebosch, C. E. (2000). Recent advances in pathophysiology andtreatment of spinal cord injury. Adv. physiol. Edu. 26: 238 – 255.
4. Hagg, T., and Oudega, M. (2006). Degenerative and spontaneous regenerative processes after spinal cord injury. Journal of neurotrauma. 23(3-4): 263-280.
5. Allan, S. M., and Rothwell, N. J. (2003). Inflammation in central nervous system injury. Philosophical Transactions of the Royal Society B: Bio. Sci. 358(1438):1669-1677.
6. Kabu, S., Gao, Y., Kwon, B. K., and Labhasetwar, V. (2015). Drug delivery, cell-based therapies, and tissue engineering approaches for spinal cord injury. Journal of Controlled Release. 219: 141-154.
7. Tukmachev, D., Forostyak, S., Koci, Z., Zaviskova, K., and Sykova, E. (2016). Injectable extracellular matrix hydrogels as scaffolds for spinal cord injury repair. Tissue Engineering Part A. 22(3-4): 306-317.
8. Rosario, D. J., Reilly, G. C., Glover, M., and MacNeil, S. (2008). Decellularization and sterilization of porcine urinary bladder matrix for tissue engineering in the lower urinary tract. Regen.Med.3:145-153.
9. Eberli, D., Atala, A., and Yoo, J. J. (2011). One and four layer acellular bladder matrix for fascial tissue reconstruction. Journal of Materials Science: Materials in Medicine. 22(3): 741-751.
10. Flecknell, P. (2003). Anesthesia of rodent and rabbits. In Veterinary anesthesia and analgesia. D. McKelvey and K. Hollingshead (Eds.), 3rd (ed). pp. 350-386. St. Louis, Missouri U.S.A.
11. Tarlov, I. M., Klinger, H., and Vitale, S. (1953). Spinal cord compression studies: I. experimental techniques to produce acute and gradual compression. AMA Archives of Neurology and Psychiatry. 70(6): 813-819.
12. Levine,G.J., Levine, J. M., Budke, C. M., Kerwin, S. C., Au, J., and Slater, M. R. (2009). Description and repeatability of a newly developed spinal cord injury scale for dogs. Preventive veterinary medicine.89(1-2): 121-127.
13. Cherry, J. D., Olschowka, J. A., and O'Banion, M. K. (2014). Neuroinflammation and M2 microglia: the good, the bad, and the inflamed. Journal of neuroinflammation. 11(1): 98.-105.
14. Zhang, L., Zhang, F., Weng, Z., Brown, B. N., and Chen, J. (2013). Effect of an inductive hydrogel composed of urinary bladder matrix upon functional recovery following traumatic brain injury. Tissue engineering Part A. 19(17-18): 1909-1918.
15. Badylak, S. F. (2004). Xenogeneic extracellular matrix as a scaffold for tissue reconstruction. Transplant immunology. 12(3-4): 367-377.
16. Xue, H., Zhang, X. Y., Liu, J. M., Song, Y., and Chen, D. (2013). Development of a chemically extracted acellular muscle scaffold seeded with amniotic epithelial cells to promote spinal cord repair. Journal of biomedical materials research Part A, 101(1): 145-156.
17. Tsai, M. C., Shen, L. F., Kuo, H. S., and Chak, K. F. (2008). Involvement of acidic fibroblast growth factor in spinal cord injury repair processes revealed by a proteomics approach. Molecular & Cellular Proteomics.7(9): 1668-1687.
18. Amar, A. P. (2008). Pathogenesis of acute spinal cord injury and theoretical bases of neurological recovery. Surgical management of spinal cord injury: controversies and consensus. 1-17.
19. Wu, Y., Wang, J., Shi, Y., Pu, H., Leak, R. K., and Chen, L. (2017). Implantation of brain-derived extracellular matrix enhances neurological recovery after traumatic brain injury. Cell transplantation. 26(7): 1224-1234.
20. Wang, G., Zhang, J., Hu, X., Zhang, L., Mao, L., and Chen, J. (2013). Microglia/macrophage polarization dynamics in white matter after traumatic brain injury. Journal of Cerebral Blood Flow and Metabolism. 33(12):1864-1874.

21. Zhang, X. Y., Xue, H., Liu, J. M., and Chen, D. (2012). Chemically extracted acellular muscle: a new potential scaffold for spinal cord injury repair. Journal of Biomedical Materials Research Part A, 100(3):578-587.

Table 1: Statistical Analysis of Motor Clinical Observation on days 56 and 112 in all groups

Groups days	Mean ± SE		LSD value
	Group I	Group II	
56	B 0.50±0.28 b	B 4.25±0.25 a	0.884 *
112	A 1.25 ± 0.25b	A 6.00±0.00 a	0.533 *

[a,b,] Values (Mean ± SE) having with the different small letters in same row and big letters in same column differed significantly (p ≤0.05).

Table 2: Statistical analysis of knuckling function tests on days 56 and 112 in all groups

Groups days	Mean ± SE		LSD value
	Group I	Group II	
56	B 1.75 ± 0.04 b	B 2.38 ± 0.05 a	0.502 *
112	A 2.38 ± 0.08 b	A 3.75 ± 0.11 a	0.833 *

[a,b,c]Values (Mean ± SE) having with the different small letters in same row and big letters in same column differed significantly (p ≤0.05).

Table 3: Mean Time of Sensory Function Test Observation in the in all groups on day112 PO

Mean time Groups	Lat. Aspect Leg Sense	Toe prick	Toe pinch
Group I	N	N	N
Group II	+99days	+105days	+85days

Table 4: Statistical analysis of Sensory Clinical Observations in in the all group on day112 PO

Sensory Signs	Group I	Group II
Lat. Aspect Leg Sense	0 ± 0^{b}	1 ± 0^{a}
Toe pinch	0 ± 0^{b}	1 ± 0^{a}
Toe prick	0 ± 0^{b}	1 ± 0^{a}

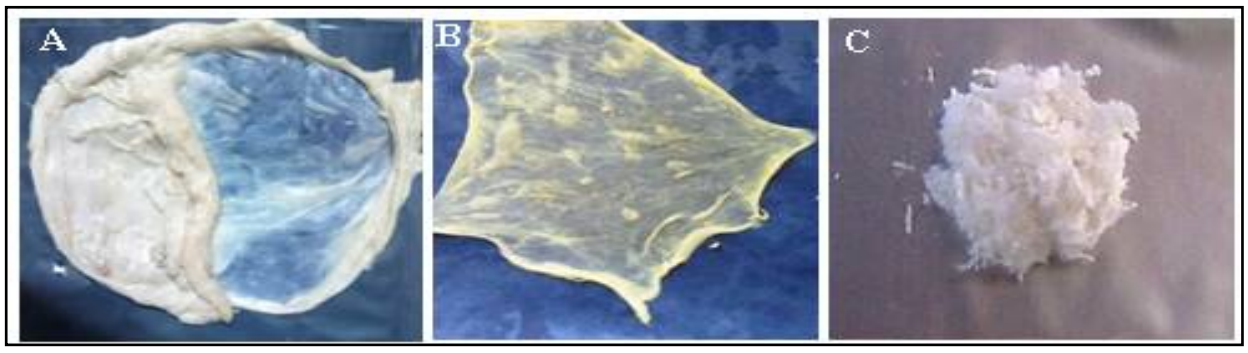

Figure 1: Photograph shows steps of bovine UBM-powder preparationA. Mechanical separation of mucosal and seromuscular layers from the submucosa of bovine urinary bladder B. Prepared urinary bladder sheet C. Lyophilizing the urinary bladder sheet and then comminuted into powder.

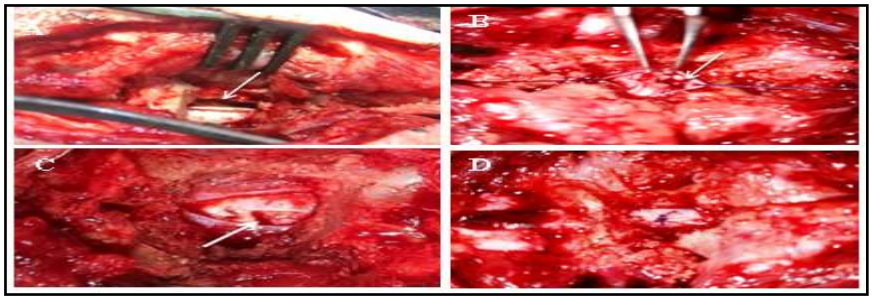

Figure 2: Photograph showing the initial steps for hemicordectomy A. spinal cord covered by meninges (arrow) B. left lateral hemisection of the spinal cord (arrow) C. implantation scaffold between distal and the proximalstumps of spinal cord (arrow) D. closed dura matter.

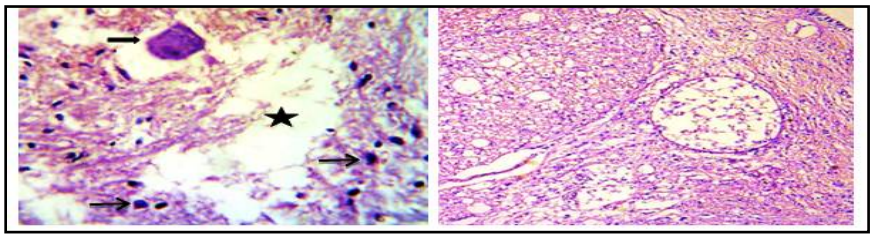

Figure 3: Light micrographs at the site of the spinal cord injury in Group (I)A. shows large cystic cavity (star) surrounded by glial scar formation due to proliferation of reactive astrocytes (thin arrows) and neuronal degenerative (thick arrow).In Group (II)Appear of narrow cavity containing blood vessels surrounded by dense regenerative nerve fiber with wide glial cell (thick arrows) H&EX40.

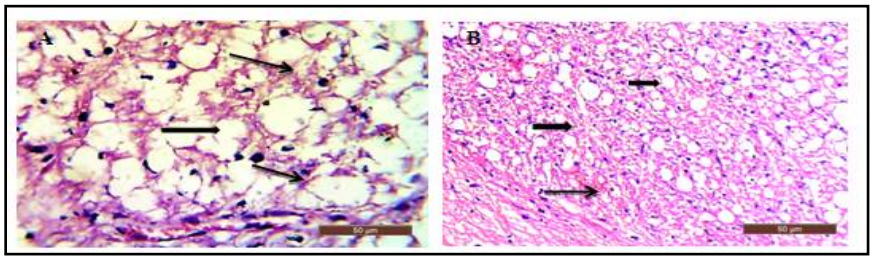

Figure 4: Light micrographs at the site of the spinal cord injury in Group (I)A. shows markedvacuolation (thick arrow) and demyelination axons in white matter (thin arrow).In Group (II)B. shows appear of marked reduction in the number of swollen vacuolated nerve fiber with prominent remyelination regenerative nerve fibers (thick arrows) with proliferation glial cells (thin arrows) H&EX40.

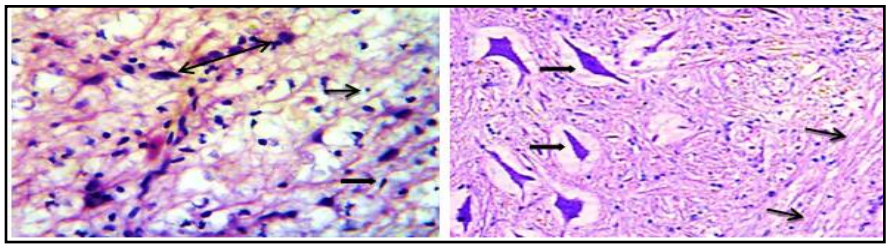

Figure 5: Light micrographs at the site of the spinal cord injury in Group (I) A. shows hyper atrophy and proliferation of astrocytes (double head arrow), apoptosis of oligodentrocytes(thin arrow) and proliferation of active microglia cells (thick arrow). Group (II) B. Appear of multiple regenerative neurons were seen in the grey matter (thick arrows) and good orientation nerve fibers with axons were detected in the cross sections of the white matter (thin arrows) H&EX40.

RESEARCH ARTICLE

Preparation and Characterization of ZnO Nanorods and Analysis of the Effect of Photo Irradiation on the Physical Properties of Polymer Nano Composites

Ahmed Mishaal Mohammed[1*], Hameed K. AL-Duliami [2] and Marwa A. Mekhlif [1]

[1]Department of Chemistry, College of Science, University of Anbar, Ramadi, Iraq.
[2]Department of Chemistry, College of Education for Pure Sciences, University of Anbar, Ramadi, Iraq.

Received: 23 June 2018 Revised: 25 July 2018 Accepted: 27 Aug 2018

[*]**Address for Correspondence**
Ahmed Mishaal Mohammed
Department of Chemistry,
College of Science,
University of Anbar,
Ramadi, Iraq.

ABSTRACT

This study investigatedthe photodegradation of polyvinyl alcohol (PVA) based nanocomposites with different weight ratios of Zinc oxide (ZnO) nanorods prepared hydrothermally.Scanning electron microscopy, atomic force microscopy,and X-ray diffraction analysis are utilized to study the morphological characteristics and size of ZnO nanorods were studied via, where, films were made by mixing with a polymer solution at different weight percentages of1%, 2%, 3%, 4%, and 5% and a thickness of 70±5 μm. The as-prepared samples were exposed to photoradiation at a wavelength of 356 nm at different time points. The photodegradation of the prepared films with and without additives were assessed with Fourier transforminfrared spectroscopy and ultraviolet-visible spectroscopy to monitor the changes in hydroxyl coefficient, carbonyl coefficient and dissociation constant (K_d), which was used to illustrate the effect of ZnO nanorod addition. The prepared ZnO nanorods showeda wide range of applications inPVAphotodegradation.In addition to the mean chain scission and degradation degree, the molecular weight and chain scission decreased in the presence of the ZnO nanorods, and this observation was consistent with that described in other studies.

Keywords: Zinc oxide, Polymer, Photodegradation, Polyvinyl alcohol.

INTRODUCTION

Nanotechnology involves the preparation of nanoscale materials [1].ZnO is one of the versatile and technologically important semiconducting materials that exhibit a direct and wide band gap (3.3eV). It has been extensively explored because of its electrical, and piezoelectric [2-6], chemical [7], optical [8], and magnetic [9] properties. ZnO has also

been recognized as an important material because of its wide applications, such as catalysts [10],semiconductors [11], gas sensors [12], ultraviolet (UV)-shielding materials [13], piezoelectric devices [14], photochemicals [15],polymer coatings [16],and antibacterial agents [17].ZnO is a multifunctional material,as such,studies on ZnOnanoparticleshave focused on their preparation through various methods, including solid-state reaction [9], microwave-assisted method [18],flame spray pyrolysis [19],sol-gel method [20],hydrothermal method [21],sonochemical route [22],and mechanochemical methods [23].ZnO films have been prepared via several techniques, such as electrochemical deposition [24], chemical vapor deposition (CVD) [25], hydrothermal or solvothermal methods [26],spay pyrolysis technique [27],electrodeposition [28], chemical bath deposition [29], sputtering [30], metal-organic CVD [31], evaporation[32], molecular beam epitaxy, atomic layer epitaxy [33, 34], and pulsedlaser deposition [35].According to the importance of polyvinyl alcohol (PVA) as water-soluble transparent polymer extensively, it has been used in industries ,as well as , it is considered as an excellent physical and chemical properties, good chemical resistance, non-toxicity, biodegradability, good film formation capacity, and high crystal modulus. The fact is that, PVA is utilized in as ahydrolyze form with 85% hydrolysis degree [36]. Indeed, it is a polymer which has various pharmaceutical, biomedical, and technological applications [37]. For example, it can be applied to coat ZnO [38], Ag [39], and titanium dioxide [40]. In this study, a new type of ZnO nanorods was prepared by using hydrothermal method and used as a UV photoinducer for PVA degradation.

MATERIALS AND METHODS

Chemicals

It is important to note that the deionized distilled water was involved to make all the solutions. In addition, the standard metal ion solution, Zinc nitrate hexahydrate [$Zn(NO_3)_2{\cdot}6H_2O$], was commercially obtained from Aldrich. Anyhow, the analytical grade of this study was based on all of the chemicals and reagents.

Growth Layer Preparation

In this process, 0.5 g of zinc nitrate, 5 g of hexamethylenetetramine, and 100 ml of deionized water were placed in a beaker and mixed using a magnetic stirrer for 1 hrs. At room temperature. The prepared growth layer solution was placed in another beaker where seed-coated substrates were immersed. The resulting mixture was kept in an oven at 90°C for 3 hrs. Slides were taken out from the beaker and rinsed with water to separate residuals. The substrates were subjected to annealing at 500°C for 1 hrs. The ZnO nanorods were prepared at pH values of 7.5.

Sample

The first step of preparing the specimens which represented by films was based on dissolving PVA with a constant concentration of 10% w/v of the polymer solution, where, this polymer dissolved in deionized waterat 40 ^{o}C.This stock solution was mixed with 1ml of the used ZnO nanorods as the stabilizer of weight ratios (1% , 2% , 3% , 4% , and 5%)and casted using glass flakes to form PVA films with a thickness of70 ±5µm.The films were then cut into parts of 1.5 cmx3cm for measurements.

The Samples Irradiation

An accelerated irradiator, assembled to the one in a laboratory, supplied with a power of 125 Watts and a light filter with a length of 356 nm for 16 hrs. was used to irradiate the specimens. Under many circumstances, the samples were located in vertical and parallel orientations subjected to the lamp to make sure that the light fell on vertically over the films tube. Therefore, the films positions periodically were changed to ensure the light coincidence. Polymeric films with and without PVA were irradiatedwith UV at different periods, ranging from4 hrs. to 16 hrs.(Table 2).

The Studies of Spectral

Variations of the polymeric films were examined through fouriertransformer infrared (FT-IR) spectroscopy, measurementof the growth level of the hydroxyl group (I_{OH}) and carbonyl group (I_{CO}) as means of PVA degradation behavior under light of fact, and UV measurements to determine the absorbed band intensities calculated before and after irradiation was administered [41].

Morphological analysis

Morphological analysis is mainly performed to describe the state of degradation. In this process, molecules become reflected on a polymer surface because of the effect of high-energy light (UV), thereby changing the color of the surface or the color of the whole polymer this phenomenon reflects the loss of the physical, andelectrical,mechanical properties, thereby causing softness and pitting on external surfaces [42].

Material Characterization

X-ray diffraction (XRD) with CuKα radiation (λ = 1.5418 Å) was conducted to investigate the phase composition and crystalline properties of the sample.The quality of surface morphology and the quantity of elemental composition were analyzed through scanning electron microscopy (SEM) and atomic force microscopy (AFM).The chemical functional groups of the sample that did not undergo annealing were characterized through FT-IR.

RESULTS AND DISCUSSION

Structural Characterization

Fig. 1 shows the XRD pattern of the sample powder compared with that of ICDD no 01-076-0704 as the standard reference of the ZnO phase. The diffraction peaks indexed to (100), (002), (101), (102), (110), (103), and (112) planes were observed, confirming the ZnO hexagonal wurtzite structure. The scanned 2θ axis of the XRD graph, showed that three strong peaks at 31.73º, 34.38º, and 36.20º were attributed to (100), (002), and (101) ZnO planes, respectively (Table 1).

SEM Measurements

We identified the morphological characteristic and structures of the particles and measured the grain size of the samples prepared hydrothermally.Fig.2shows the SEM micrograph of the ZnO nanorodssynthesized hydrothermally at different magnifications.

AFM Measurements

AFM is essential for studying the morphological characteristics of ZnO nanorods. Quantitative information from individual ZnO can be generated through the software-based image processing of AFM data. Individual particles determination was based on the size information (length, width, and height) and other physical properties (morphological characteristics and surface texture).AFM can be functioned in liquid or gas media, therefore, this capability is considered as highly advantageous for the characterization of ZnO. In our study, AFM was applied to analyze the morphological characteristics and size of the particles and the topography of the ZnO surface structure. As noticed in Fig. 3, the AFM images presenting the two - and three-dimensional views of the surface structure of the ZnO nanorods, which were grown hydrothermally. The images indicated that the ZnO nanorods had small particles size distribution with a diameter of 52.16 nm

FT-IR Spectroscopy

The FT-IR spectra of all of the samples, palletized with KBr were recorded from 400 $cm^{-1}$to 4000 cm^{-1}(Fig. 5). The spectra consisted of seven vibrational bands. The transmittance spectrum of the as-deposited ZnO film showed the main absorption bands centered at 1222.79 and 3431.13cm^{-1}, and several small features were located at 528.46, 867.91, 1504.37, 1635.52, 2329.85, 2887.24 and 3014.53 cm^{-1}. The absorption bands that centered at 484.10and 528.46 cm^{-1} could be associated with ZnO bond vibration, compared with that of the standard FT-IR of the ZnO powder. A strong peak at 3431.13 $cm^{-1}$was observed in the as-deposited ZnO film, which is sensitive to the stretching vibrations of –OH [28]. The other absorption bands at 2887.24, 1635.52, and 867.91 cm^{-1} can be related to N–H and, N–O bonds [30].

UV–vis Spectroscopy

The process of characterizing the optical absorption properties of the ZnO nanorods involved conducting UV–vis spectroscopy, where, the UV–vis absorption spectra of the samples was achieved at a room temperature [43] and were recorded in the wavelength range of 200 –800nm through a Shimadzu UV 3600 UV–vis–NIR spectrometer (Shimadzu Corporation, Kyoto, Japan).The photodegradation of the PVA films at different concentrations was studied through UV–vis spectroscopy, by exposing the PVA films to UV radiation for a given period to change the color of the filmsto yellowish. This change indicated the photolysis of the polymer (Table 2) . Through observing the absorption spectrum in terms of time irradiation, these films varied and reflected when calculating the rate of decomposition (K_d) via recording the absorption spectrum of UV and during the process at different times of irradiation. We observed that the absorption spectrum of these films varied in terms of the time of irradiation as shown in Fig.6.

The rate of change in the absorption spectrum with respect to the time of irradiation was .dependent on the ZnO nanorod additive concentration, which increasedas the ZnO nanorod concentration increased due to the increase in the active substance content (Figs.7–11). To calculate the rate constant ofthe photolysis of polymeric films in the presence of the ZnO nanorod additive, where,the relationship between the time of irradiation and the logarithm of absorption (A_∞-A_t) was drown as shown in (Figs. 12–16).The slope apparently shown as a straight line, indicating that the interaction light of this ZnO nanorod was of the first class, which was the constant determinant rate of photolysis (K_d) atvarious concentrations under the same conditions was previously determined as noticed in (Table 3).This result suggested that $K_d$was sensitive to additive concentrations,whose increase was consistent with those described in previous studies [44].This finding confirmed that the additive accelerated the interaction between the light and polymer

FT-IR Spectrum of PVA

The exposure of pure PVA to high-energy rays with a wavelength of 356 nm alteredthe FT-IR spectrum [45] and yielded two broad bands.The first band of the carbonyl group (C=O) appeared at 1600–1700 cm^{-1}, which increased with irradiation time [46]. This band was present with few values before the films were irradiated because of the stress induced by thermal oxidationduring manufacturing (Fig.17). The second band of the hydroxyl and hydro peroxide polymer appeared at 3200-3600 cm^{-1}, where the absorbance increasedas the ZnO concentration increased (Fig.19).Therefore, the coefficients of the increase in the absorption of I_{OH} and I_{CO} were high at high additive concentrations (Tables 4, and 5and Figs. 20 and 21) as calculated using the base-line method [47].These results showed correspondence of the values calculated from the decomposition constant values (highest K_d). The calculations via the viscometer method showed the average molecular weight of the polymeric film before and after addition, suggesting that the average molecular weight decreasedas the irradiation time was extended. The additive concentration of the ZnO nanorodwas comparable with that of the reference becauseof the fragmentation of the polymeric chains (Tables 6, and 7), and the viscous molecular weight rapidly decreased at the beginning of

irradiation [48].Consequently, the most apparent results revealed that the bonds between the polymer chains were formed randomly along the polymeric chain, where, this observation was firmly established by the linear relationship of the average chain scission (S) and the degree of degradation(α) through time [44], revealing that Sand α of the chips of pure PVA were less than those supported by the ZnO nanorod additive. This study provided a basis for using ZnO nanorods as a good catalyst to photodegrade plastic materials, reduce environmental pollution, and accelerate their decomposition.

CONCLUSION

Rod-like ZnO nanorods were successfully synthesized hydrothermally in a nanosize range with a diameter of approximately 52.16 nm. The synthesized ZnO nanopowder obtained exhibited good crystallinity.The addition of ZnO nanorods increased the photodegradation rate because of the absorption of UV light. The degradation rate increased when the nanorodswere exposed to irradiation for16hrs.By studying the impact of different concentrations of ZnO nanorodson polymer degradation, we found that the rate of polymer degradation increased asthe concentration of each ZnO nanorod increased. These results and the calculated average viscous molecular weight, average numerical S, andαconfirmedthe increasein the photodegradation rate.

REFERENCES

1. Zhou, B. and Balee, R., "Groenendaal, nanoparticle and nanostructure catalysts: technologies and markets", Nanotech. Law Business, Vol. 2, 222-231(2005).
2. Tang, Z. K., Wang, G. K., Yu,P., Kawasaki, M., Ohtomo, A., Koinuma, H. and Segawa, Y., "Room-temperature ultraviolet laser emission from self-assembled ZnO microcrystallite thin films",Appl. Phys. Lett. Vol. 72(25), 3270 - 3278(1998).
3. Kind, H., Yan, H., Law, M., Messer, B. and Yang, P., " Nanowire ultraviolet photodetectors and optical switches", Adv. Mater. Vol. 14, 158 - 164(2002).
4. Suchada, W., Tomoaki, M.,Yoshinori, H.,Yoichiro, N.,Hidenori, M.,and Wisanu, P., "Synthesis and characterization of ZnO nanorods by hydrothermal method ", Materialstody: Proceedings, Vol. 5 (5) , 10964 - 10969 (2018).
5. Pushpitha, R.,Bruno, L., Sahuban, M., Chandramohan, R., and Srikumar, S.,"Preparation and characterization of Mn doped ZnO nanorods" , Physics of the Solid State, Vol. 60 (5), 1011 - 1015 (2018).
6. Youngjo, T., Dongseok, P., and Kijung, Y.,"Characterization of ZnO nanorod arrays fabricated on Si wafers using a low-temperature synthesis method", Journal of Vacuum Science & Technology B,Vol. 24, 2047 - 2052 (2006).
7. Suwanboon, S., Amornpitoksuk, P., Bangrak, P. and Randorn, C., "Physical and chemical properties of multifunctional ZnO nanostructures prepared by precipitation and hydrothermal methods",Ceramics International, Vol. 40, 975- 983(2014).
8. Labuayai, S., Promarak, V. and Maensiri, S., "Synthesis and optical properties of nanocrystalline ZnO powders prepared by a direct thermal decomposition route",Applied Physics A,Vol. 94, 755 – 761(2009).
9. Yılmaz, S., Nisar, J., Atasoy, Y., McGlynn, E., Ahuja, R., Parlak, M. and Bacaksız, E., "Defect-Induced room temperature ferromagnetism in B-Doped ZnO", Ceramics International, Vol. 39, 4609-4617(2013).
10. Suwanboon, S., Amornpitoksuk, P., Sukolrat, A. and Muensit, N., "Optical and photocatalytic properties of La-Doped ZnO nanoparticles prepared via precipitation and mechanical milling method", Ceramics International, Vol.39, 2811-2819(2013).
11. Zhang, C.,"The influence of post-growth annealing on optical and electrical properties of P-Type ZnO films", Materials Science in Semiconductor Processing,Vol. 10, 215-221(2007).
12. Yu, A., Qian, J., Pan, H., Cui, Y., Xu, M., Tu, L., Chai, Q. and Zhou, X., "Micro-Lotus constructed by Fe-Doped ZnO hierarchically porous nanosheets: preparation, characterization and gas sensing property",Sensors and Actuators B: Chemical,Vol. 158, 9-16(2011).

13. Li, R., Yabe, S., Yamashita, M., Momose, S., Yoshida, S., Yin, S. and Sato, T. , "Synthesis and UV-shielding properties of ZnO- and CaO-Doped CeO_2 via soft solution chemical process", Solid State Ionics,Vol. 151, 235-241. (2011).
14. Seo, M., Jung, Y., Lim, D., Cho, D. and Jeong, Y.,"Piezoelectric and field emitted properties of controlled ZnO nanorods on CNT yarns",Materials Letters,Vol. 92, 177-180(2013).
15. Mousa, M., Bayoumy, W. and Khairy, M., "Characterization and photo-chemical applications of Nano-ZnO prepared by wet chemical and thermal decomposition methods",Materials Research Bulletin, Vol. 48, 4576-4582(2013).
16. Qin, L., Shing, C., Sawyer, S. and Dutta, P.S., "Enhanced ultraviolet sensitivity of zinc oxide nanoparticle photoconductors by surface passivation",*Optical Materials*, Vol. 33, 359-362(2011).
17. Talebian, N., Amininezhad, S.M. and Doudi, M. "Controllable synthesis of ZnO nanoparticles and their morphology-dependent antibacterial and optical properties",Journal of Photochemistry and Photobiology B: Biology,Vol. 120, 66-73 , (2013).
18. Sharma, D., Sharma, S., Kaith, B., Rajput, J. and Kaur, M., "Synthesis of ZnO nanoparticles using surfactant free in-air and microwave method",Applied Surface Science, Vol. 257, 9661-9672(2011).
19. Lee, S.D., Nam, S.H., Kim, M.H. and Boo, J.H.,"Synthesis and photocatalytic property of ZnO nanoparticles prepared by spray-pyrolysis method",Physics Procedia,Vol. 32, 320-326(2012).
20. Ba-Abbad, M.M., Kadhum, A.A.H., Bakar, M., A., Takriff, M.S. and Sopian, K. 'The effect of process parameters on the size of ZnO nanoparticles synthesized via the sol-gel technique", Journal of Alloys and Compounds, Vol. 550, 63-70(2013).
21. Aneesh, P.M., Vanaja, K.A. and Jayaraj, M.K.,"Synthesis of ZnO nanoparticles by hydrothermal method", Proceedings of SPIE, Vol. 6639, 66390J-1-66390J-9(2007).
22. Kazeminezhad, I., Sadollahkhani, A. and Farbod, M.,"Synthesis of ZnO nanoparticles and flower-like nanostructures using nonsono- and sono-electrooxidation methods",Materials Letters,Vol. 92, 29-32(2013).
23. Stanković, A., Veselinović, L., Škapin, S., Marković, S. and Uskoković, D.,"Controlled mechanochemically assisted synthesis of ZnO nanopowders in the presence of oxalic acid",Journal of Materials Science, Vol. 46, 3716-3724(2011).
24. Elias, J., Tena-Zaera, R, and Levy-Clement, C., "Effect of the chemical nature of the anions on the electrodeposition of ZnO nanowire arrays", , J. Phys. Chem. C, Vol. 112 (15) 5736-5741(2008).
25. Sato, H., Minami, T., Miyata, T., Takata, S., Ishii, M., "Transparent conducting ZnO thin films prepared on low temperature substrates by chemical vapour deposition using $Zn(C_5H_7O_2)_2$", Thin Solid Films,Vol. 246 (1-2), 65-70 (1994).
26. Yang, H., Song, Y., Li, L., Ma. J., Chen. D., Mai, S., Zhao, H., "Large-scale growth of highly oriented ZnO nanorod arrays in the Zn-NH_3·H_2O hydrothermal system", Cryst. Growth Des., Vol. 8 (3), 1039-1043 (2008).
27. Ambia , M. G., Islam , M. N., and Hakim , M. O., " The effects of deposition variables on the spray pyrolysis of ZnO thin film",J. Mater. Sci. Vol. 29 (24) 6575-6580 (1994).
28. Izaki, M., " Transparent zinc oxide films prepared by electrochemicalreaction", Appl. Phys. Lett. Vol. 68, 2439-2445 (1996).
29. Ennaoui, A., Weber, M., Scheer, R., Lewerenz, H. J., "Chemical-bath ZnO buffer layer for $CuInS_2$ thin-film solar cells", Sol. Energy Mater. Sol. Cells Vol. 54(1-4), 277-286 (1998).
30. Stolt, L., Hedstrom, J., Ruckh, M., Kessier, J., Velthaus, K. O. and Schock, H. W., "ZnO/CdS/$CuInSe_2$ thin-film solar cells with improved performance", Appl. Phys. Lett. Vol. 62 , 597-604 (1993).
31. Wenas, W., Yamada, A., Konagai, M. and Takahashi, K., "Metalorganic chemical vapor deposition of ZnO using D_2O as oxidant",J. J. Appl. Phys. Vol. 33 (3A), 283-290 (1994).
32. Huang, M. H., Wu, Y., Feick, H., Weber, E., Yang, P., " Catalytic growth of zinc oxide nanowires by vapor transport",Advances Mater. Vol. 13 , 113-119 (2001).
33. Sang, B., Konagai, M., "Growth of transparent conductive oxide ZnO films by atomic layer deposition", J. J. Appl. Phys, Vol. 35 (5B), 602-608 (1996).

34. Steven, C., and John, L., "Atomic layer epitaxy of aluminum nitride: Unraveling the connection between hydrogen plasma and carbon contamination",*ACS Appl.Mater. Interfaces,* Vol. 10 (23), 20142-20149 (2018)
35. Zhang, Y., Russo, R. E., Mao, S. S., "Femtosecond laser assisted growth of ZnO nanowires",Appl.Phys.Lett. Vol. 87, 133115 – 133118 (2005).
36. Wang, H.H., Shyr, T.W. and Hu, M.S., "The elastic property of polyvinyl alcohol gel with boric acid as a cross-linking agent", Journal of Applied Polymer Science, Vol.74, 3046-3052(1999).
37. Scotchford, C., Cascone, M., Downes, S. and Giusti, P.,"Osteoblast responses to collagen-PVA bioartificial polymers *in Vitro*: The effects of cross-linking method and collagen content", Biomaterials,Vol. 19, 1-11(1998).
38. Chandrakala, H., Ramaraj, B. and Lee, J.H., "Polyvinyl alcohol/carbon coated zinc oxide nano-composites: Electrical, optical, structural and morphological characteristics",Journal of Alloys and Compounds, Vol. 580, 392-400(2013).
39. Shin, J., Kim, Y., Lee, K., Lim, Y.M. and Nho, Y.C., "Significant effects of sodium acetate, an impurity present in poly(vinyl alcohol) solution on the radiolytic formation of silver nanoparticle" , Radiation Physics and Chemistry, Vol. 77, 871-876(2008).
40. Hebeish, A., Abdelhady, M. and Youssef, A., "TiO_2nanowire and TiO_2nanowire doped Ag-PVP nano-composite for antimicrobial and self-cleaning cotton textile" ,Carbohydrate Polymers, Vol. 91, 549-559(2013).
41. Skuzina, S.I. and Mikhailov,A.I., "Institute of problems of chemical physics russian academy of science, high energychemistry, Vol. 44 (1), 667-673 (2010).
42. Taraq, A., J., "Copolymerization study of (N-Acryloy Amide) monomer with buty acrylate and determination of the reactivity ratio",Journal of Pure Science, Vol. 1 (2), 80-88 (2007).
43. Cimitan, S., Albonetti, S., Forni, L, Peri, F., Lazzari, D., " Solvothermal synthesis and properties control of doped ZnO nanoparticles", J. Colloid. Interface Sci., Vol. 329, 73-80 (2009).
44. Hameed K., and Abdul Hameed H., "A study of effect of copper (Π)-complex (Cu-BHBH) on the photo degradation of poly styrene films", International Journal of Applied and Natural Sciences, Vol. 3 (3), 123-134 (2014).
45. Yang, J., Wang, Y., Kong, J., Jia, H., and Wang, H., "Synthesis of ZnO nanosheets via electrodeposition method and their optical properties, growth mechanism" , Opt. Mater., Vol. 46 , 179-185 (2015).
46. Li, X., Cheng, S. , Deng, S., Wei, X., Zhu, J., and Chen, Q., "Direct observation of the layer-by-layer growth of ZnO nanopillar by in situ high resolution transmission electron microscopy", Sci. Rep., Vol. 7, 40911-40919 (2017).
47. Belkhalfa, H., Ayed, H., Hafdallah, E., Aida, A., and Ighil, R., "Characterization and studying of ZnO thin films deposited by spray pyrolysis: effect of annealing temperature" , Optik, Vol. 127(4) , 2336-2340(2016).
48. Gawali, S., Mahadik, S., Pedraza, F., Bhosale, C., Pathan, H., Jadkar, S., "Synthesis of zinc oxide nanorods from chemical bath deposition at different pH solutions and impact on their surface properties", J. Alloy. Compd., Vol. 704, 788-794(2017).

Table 1. The structural parameters of ZnO nanorods as obtained from XRD analysis.

2θ(degree)		
hk1	**Observed**	**JCPDS**
100	31.73°	31.76°
002	34.38°	34.42°
101	36.20°	36.25°
102	47.54°	47.53°
110	56.56°	56.60°
103	62.80°	62.86°
112	67.80°	67.96°

Table 2.Absorbance values of the PVA with thickness 70±5 μm containing different concentrations of the ZnOnanorods and calculated at 283.5 nm spectrum measurements of UV–Vis with time

Irradiation Time (hrs.)	Absorbance				
Concentration %	0.0	4	8	12	16
PVA	0.108	0.137	0.160	0.200	0.273
PVA + 1 % ZnO	0.111	0.243	0.310	0.412	0.486
PVA + 2% ZnO	0.112	0.364	0.607	0.685	0.850
PVA + 3 % ZnO	0.113	0.466	0.723	0.802	0.916
PVA + 4 % ZnO	0.114	0.543	0.825	0.932	1.100
PVA + 5% ZnO	0.117	0.573	0.884	0.994	1.215

Table 3. Values constants of rate decomposition K_d of the ZnO nanorods in PVA films

Concentrations %	K_d(Sec) $^{-1}X10^{-4}$
1	5.361
2	6.245
3	6.541
4	6.7417
5	6.789

Table 4. Coefficient growth values carbonyl (I_{CO}) with irradiation time for PVA containing concentrations different of the ZnO nanorods

Irradiation time (hrs.) / Wt. % of Addition	Carbonyl Index (I_{CO})				
	0.0	4	8	12	16
PVA	0.378	0.551	0.649	0.800	0.902
PVA + 1 ZnO	0.396	0.632	0.683	0.839	1.173
PVA + 2 ZnO	0.401	0.666	0.831	1.008	1.400
PVA + 3 ZnO	0.439	0.965	1.045	1.183	1.608
PVA + 4 ZnO	0.469	0.993	1.293	1.373	1.930
PVA + 5 ZnO	0.496	1.066	1.379	1.632	2.121

Table 5. Coefficient growth values hydroxyl (I_{OH}) with irradiation time for PVA containingconcentrationsdifferent of the ZnO nanorods

Irradiation time (hrs.) / Wt. % of Addition	Carbonyl Index (I_{OH})				
	0.0	4	8	12	16
PVA	0.272	0.505	0.563	0.733	0.810
PVA + 1 ZnO	0.282	0.586	0.625	0.793	1.113
PVA + 2 ZnO	0.303	0.655	0.706	0.982	1.252
PVA + 3 ZnO	0.340	0.839	0.954	1.086	1.582
PVA + 4 ZnO	0.393	0.860	1.195	1.287	1.747
PVA + 5 ZnO	0.408	0.933	1.270	1.551	2.069

Table 6. Values calculated from measuring of the viscous molecular weight for pure PVAchips

Time Irradiation (hrs.)	$\overline{(M_v)}x10^3$	$(M_v)^2x10^9$	$\frac{dM_v}{dt} = \frac{M_{v0} - M_{vt}}{t}$	Degree of Polymerization P	$\frac{1}{P}x10^{-4}$	Deg. Degree *a x10*$^{-3}$	Ava. Chain Scission (S)
0	51.404	2.642	∞	1168.272	8.559	0.0	0.0
4	41.591	1.729	0.681	945.250	10.579	0.202	0.235
8	35.809	1.282	0.541	813.840	12.278	0.371	0.433
12	31.405	0.986	0.462	713.750	14.010	0.545	0.636
16	28.379	0.805	0.399	644.977	15.504	0.694	0.810

Table 7.Values calculated from measuring of the viscous molecular weight for PVA with concentration 4 %ZnO nanorods

Time Irradiation (hrs.)	$\overline{(M_v)}x10^3$	$(M_v)^2x10^9$	$\frac{dM_v}{dt} = \frac{M_{v0} - M_{vt}}{t}$	Degree of Polymerization P	$\frac{1}{P}x10^{-4}$	Deg. Degree *a x 10*$^{-3}$	Ava. Chain Scission (S)
0	51.404	2.642	∞	1168.272	8.559	0.0	0.0
4	38.282	1.465	0.911	870.045	11.493	0.293	0.342
8	31.988	1.023	0.674	727.000	13.755	0.519	0.606
12	27.925	0.779	0.543	634.659	15.756	0.719	0.839
16	24.603	0.605	0.465	559.159	17.884	0.932	1.088

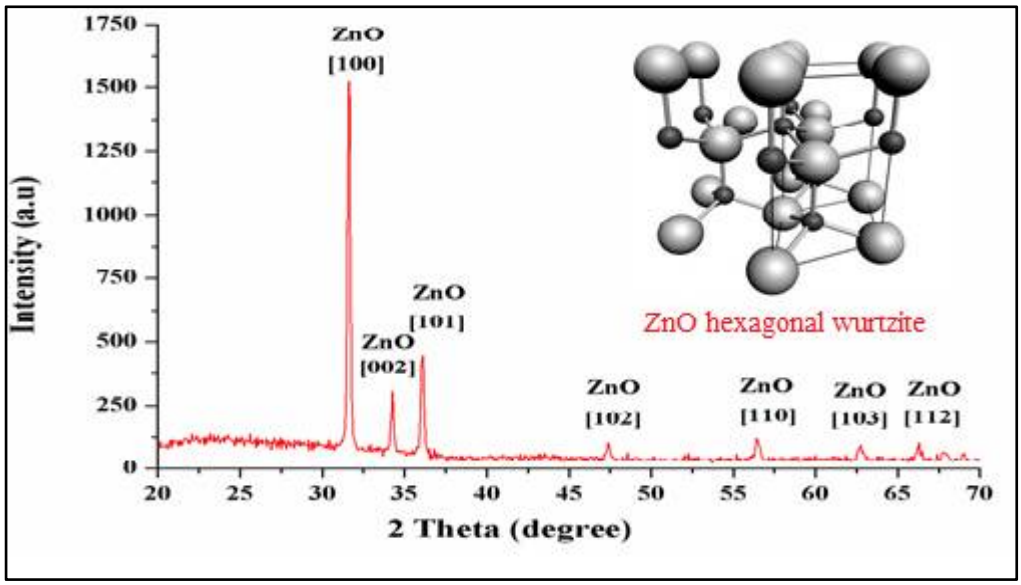

Fig.1. X-ray diffraction pattern of ZnO nanorods compared to standard ZnO phase (ICDD no 01-076-0704).

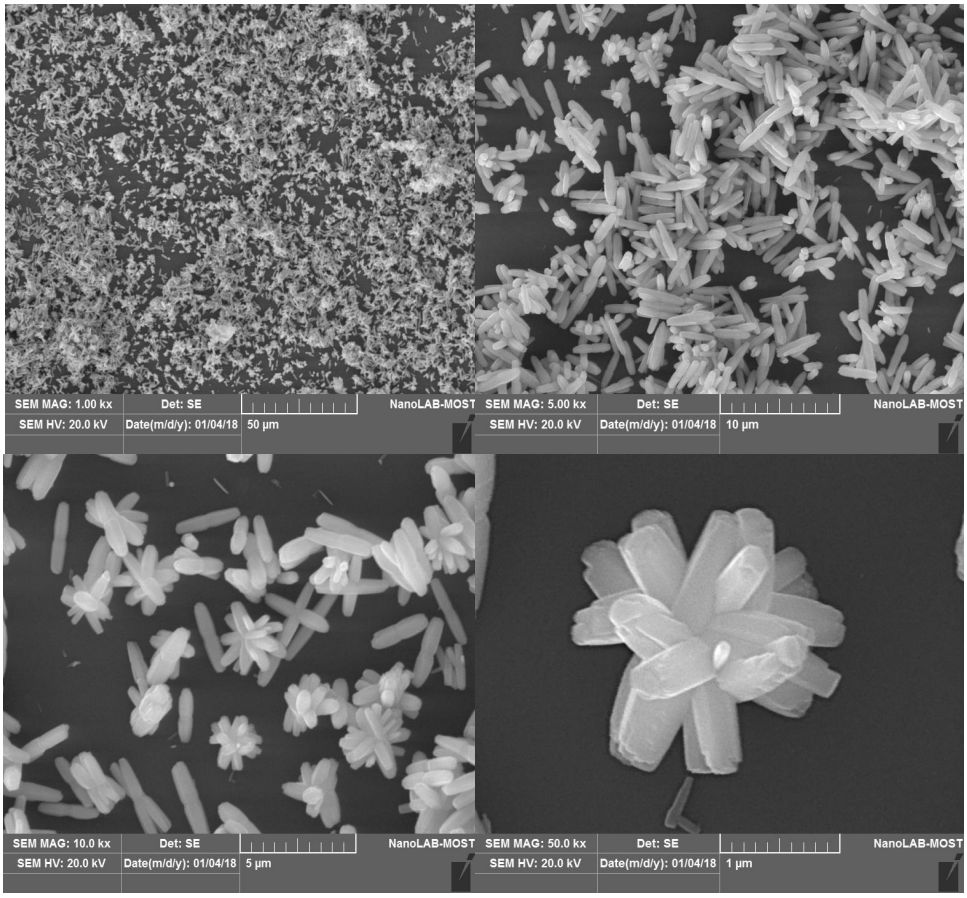

Fig. 2. SEM micrograph of ZnO nanorods synthesized in different magnification

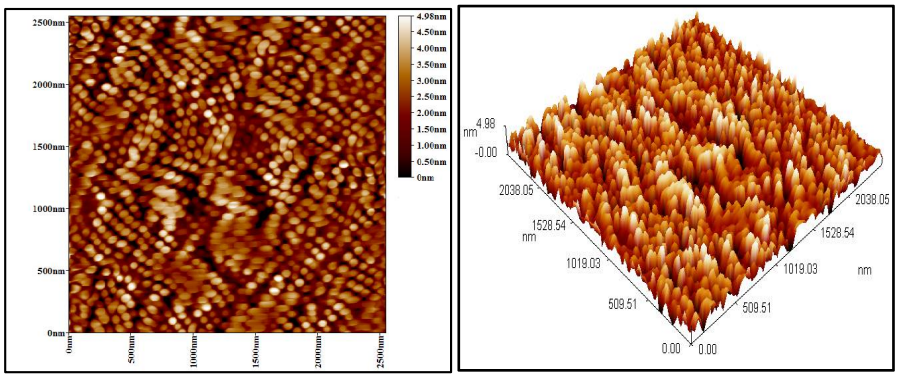

Fig. 3. AFM image of 2-dimensional and 3-dimensional of ZnO nanorods

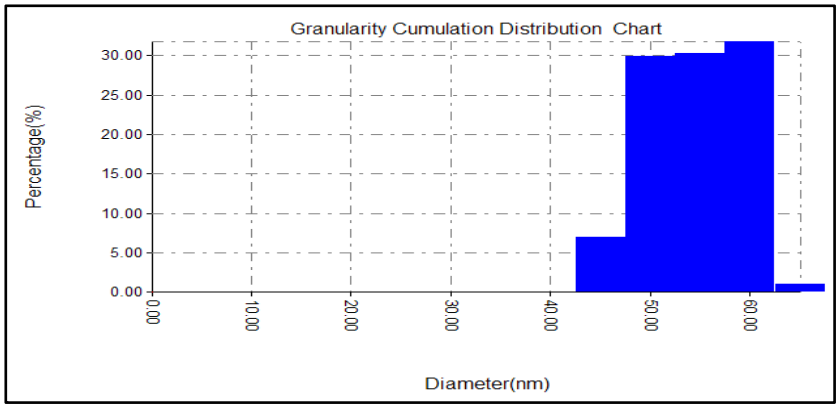

Fig.4. The average distribution for ZnO nanorods of diameter 52.16 nm

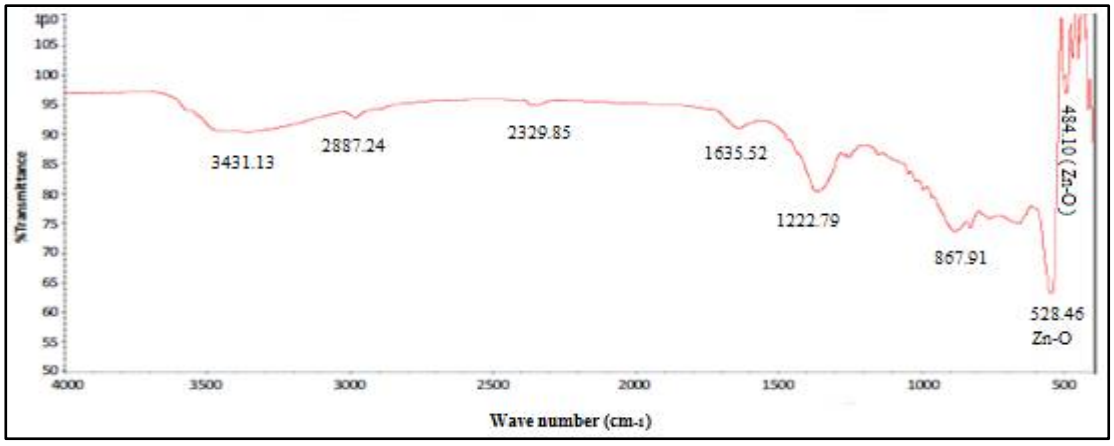

Fig. 5. FT-IR spectrum of ZnO nanorods

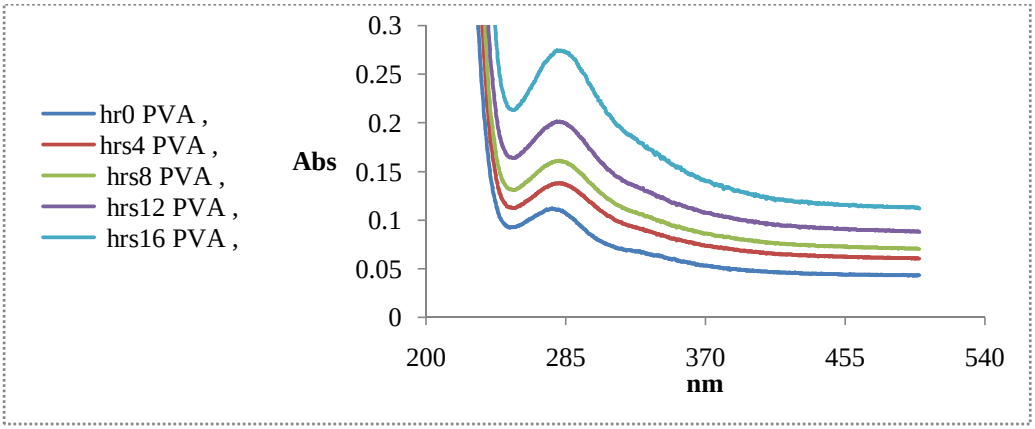

Fig.6. Change in the spectrum of UV–Vis for pure PVA with thickness70±5 μm at different times of irradiation

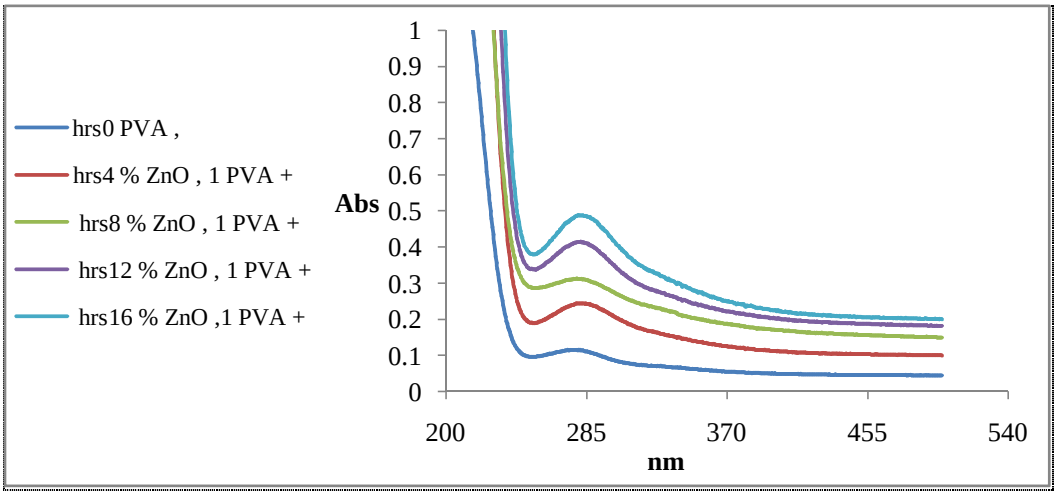

Fig.7.Change in the spectrum of UV–Vis for PVAcontaining concentration (1%) of the ZnO nanorods with thickness 70±5 μm at different times of irradiation

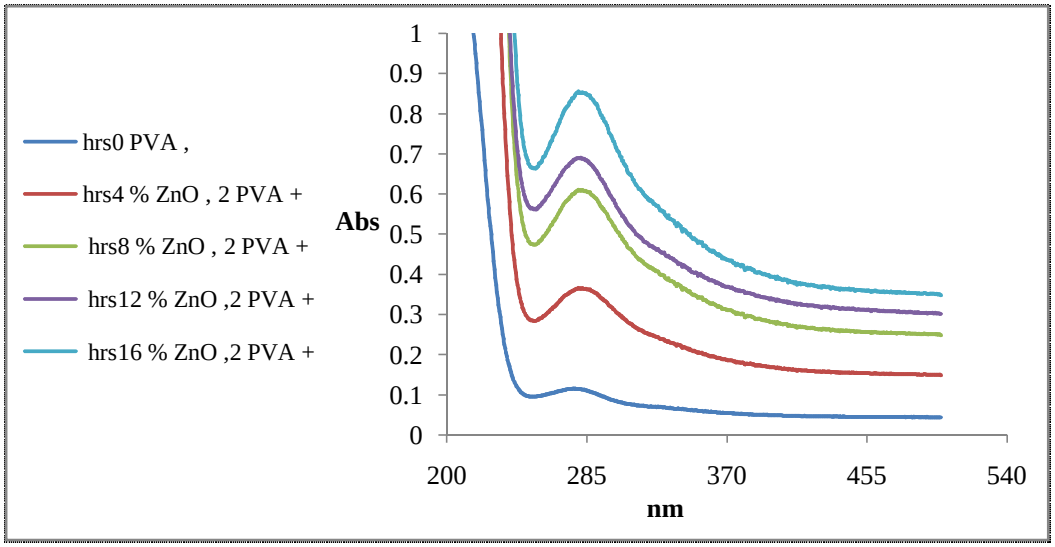

Fig. 8.Change in the spectrum of UV–Vis for PVAcontaining concentration (2%) of the ZnO nanorods with thickness 70±5 μm at different times of irradiation

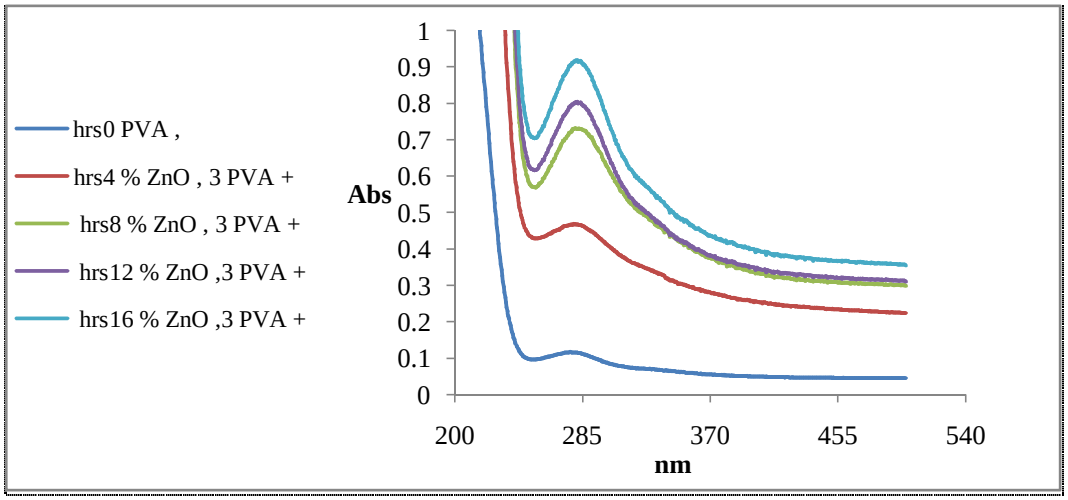

.

Fig. 9.Change in the spectrum of UV–Vis for PVAcontaining concentration (3%) of the ZnO nanorods with thickness 70±5 μm at different times of irradiation

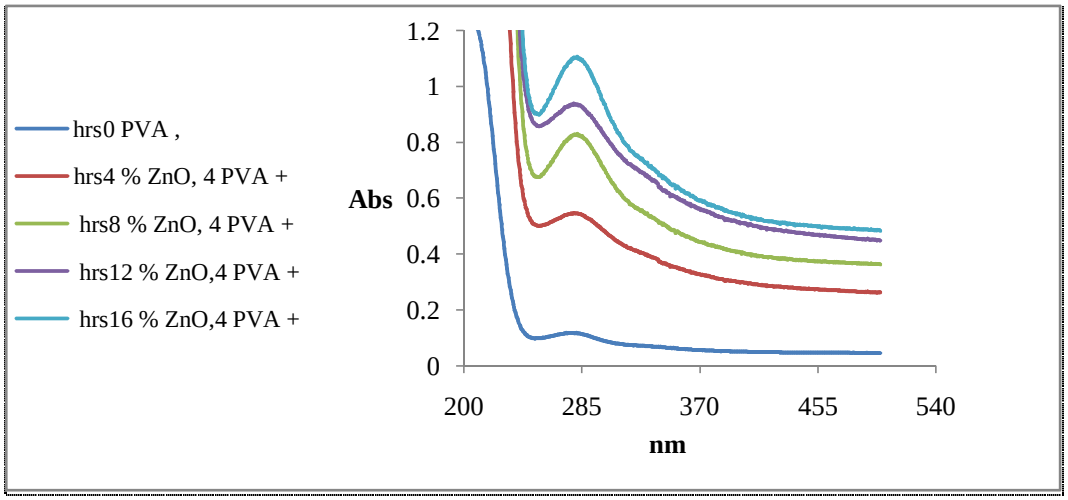

Fig. 10.Change in the spectrum of UV–Vis for PVAcontaining concentration (4%) of theZnO nanorods with thickness 70±5 μm at different times of irradiation

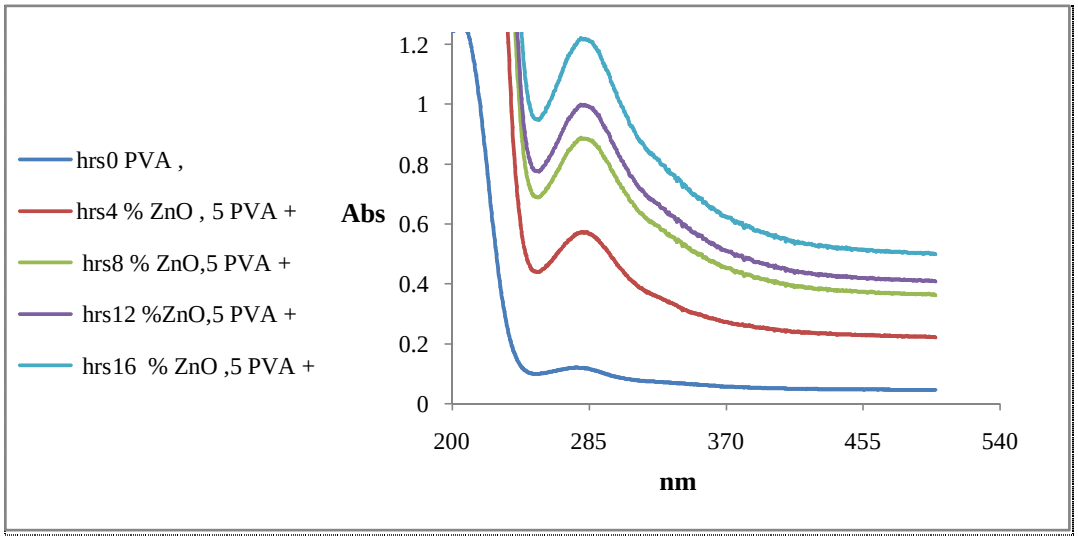

Fig. 11.Change in the spectrum of UV–Vis for PVAcontaining concentration (5%) of the ZnO nanorods with thickness 70±5 μm at different times of irradiation

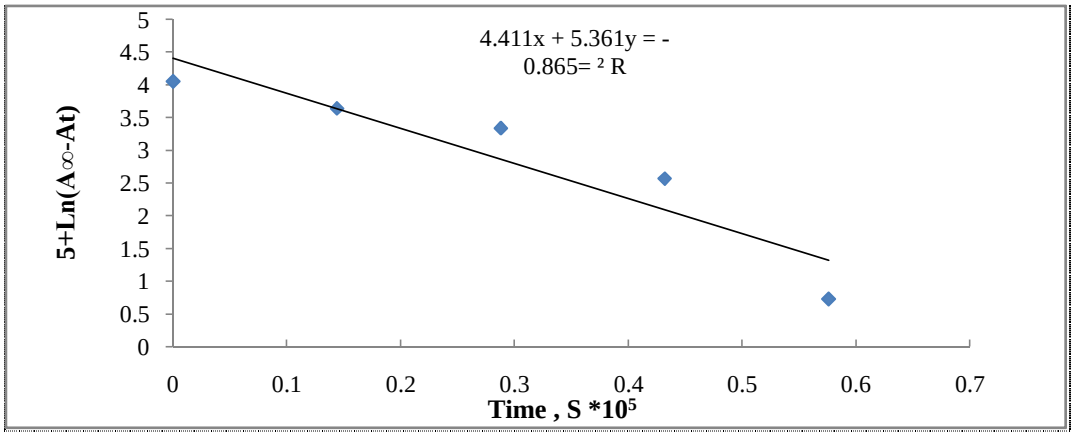

Fig. 12. The relationship between the logarithm of PVA films containing of ZnO nanorods with thickness70±5 μm and concentration (1%) with irradiation time

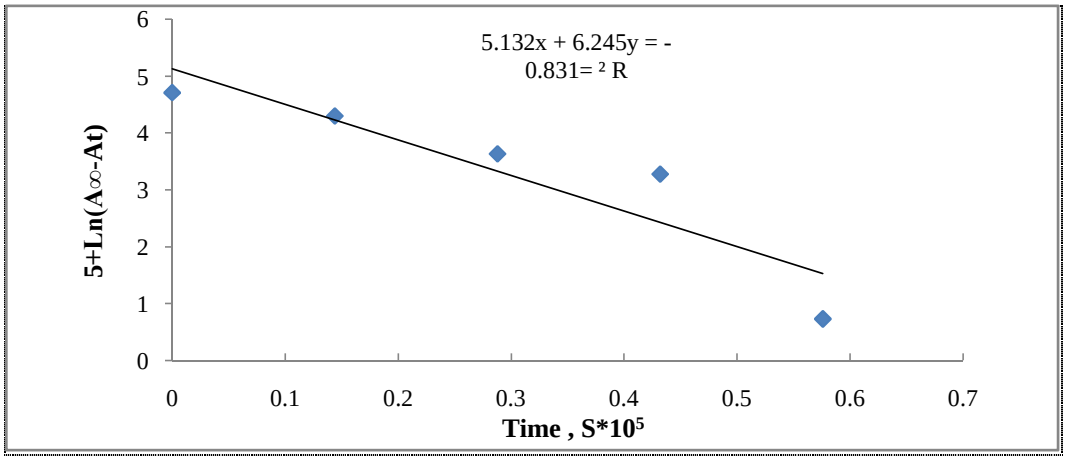

Fig. 13. The relationship between the logarithm of PVA films containing of ZnO nanorods with thickness70±5 μm and concentration (2%) with irradiation time

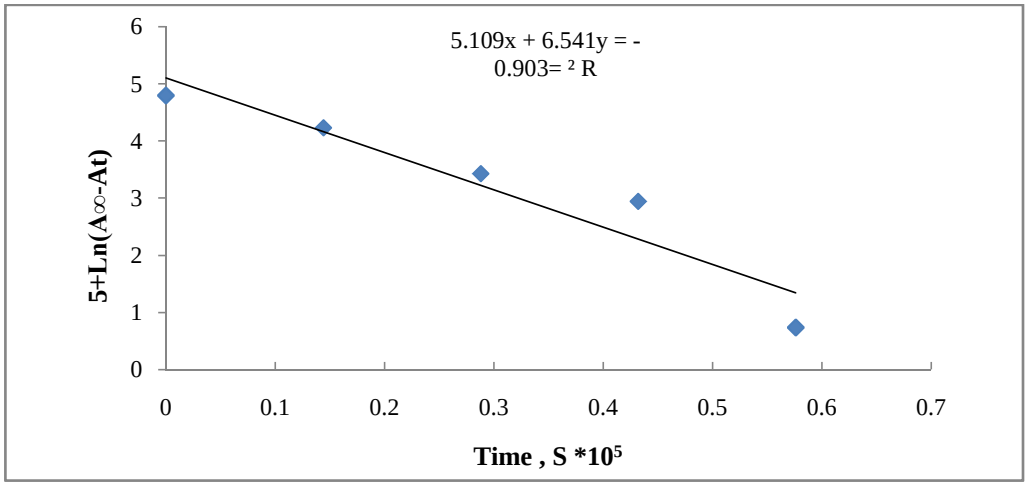

Fig. 14. The relationship between the logarithm of PVA films containing of ZnO nanorods with thickness70±5 μm and concentration (3%) with irradiation time

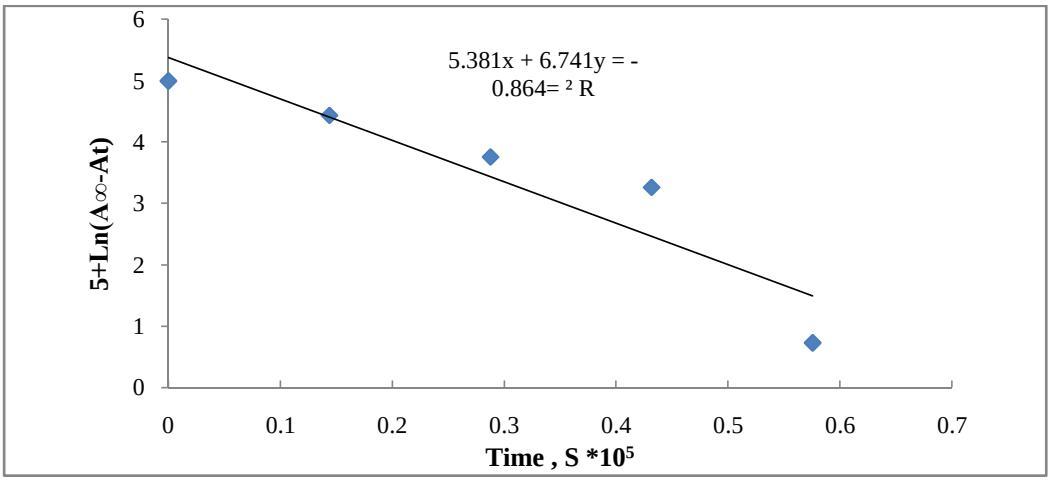

Fig. 15. The relationship between the logarithm of PVA films containing of ZnO nanorods with thickness70±5 μmand concentration (4%) with irradiation time

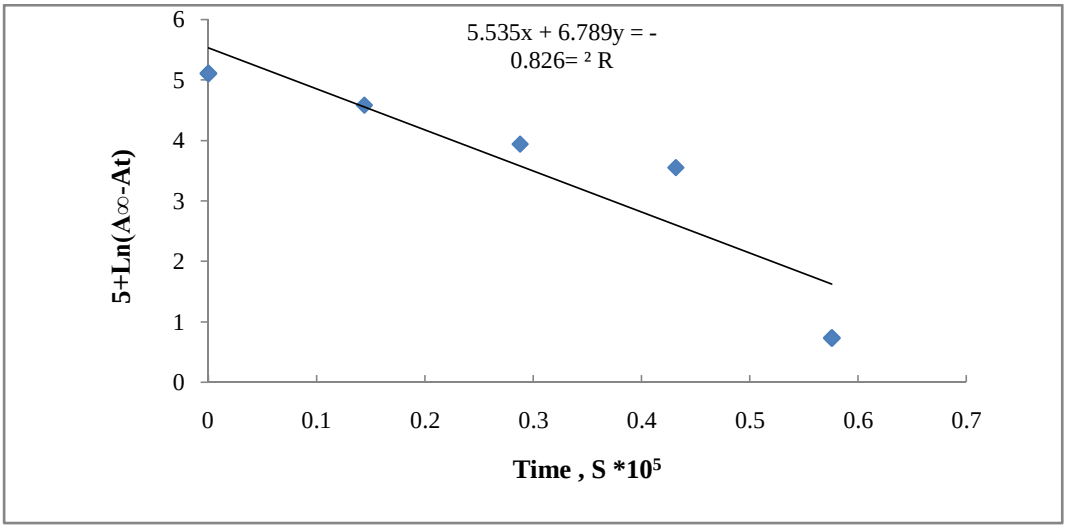

Fig. 16. The relationship between the logarithm of PVA films containing of ZnO nanorods with thickness70±5 μm and concentration (5%) with irradiation time

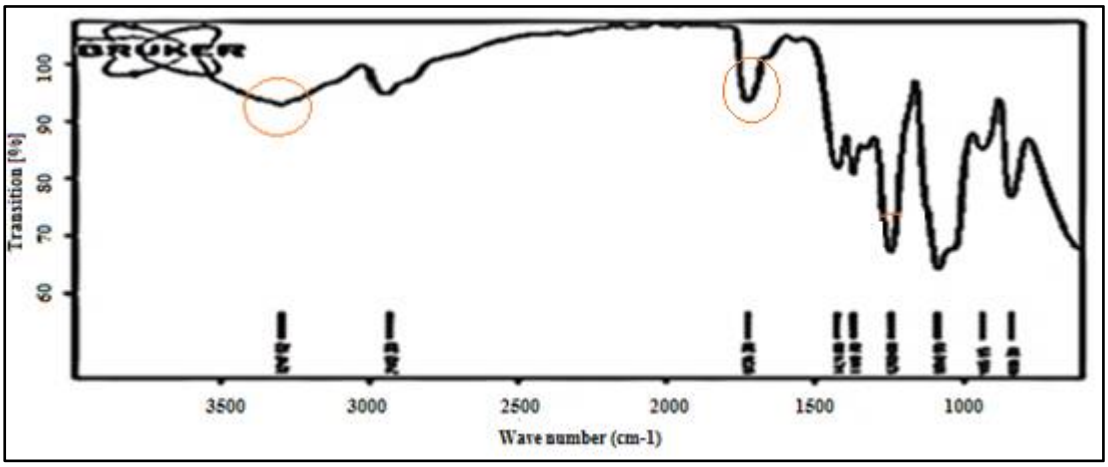

Fig. 17. FT-IR spectrum of pure PVA film with thickness 70±5 μm before irradiation

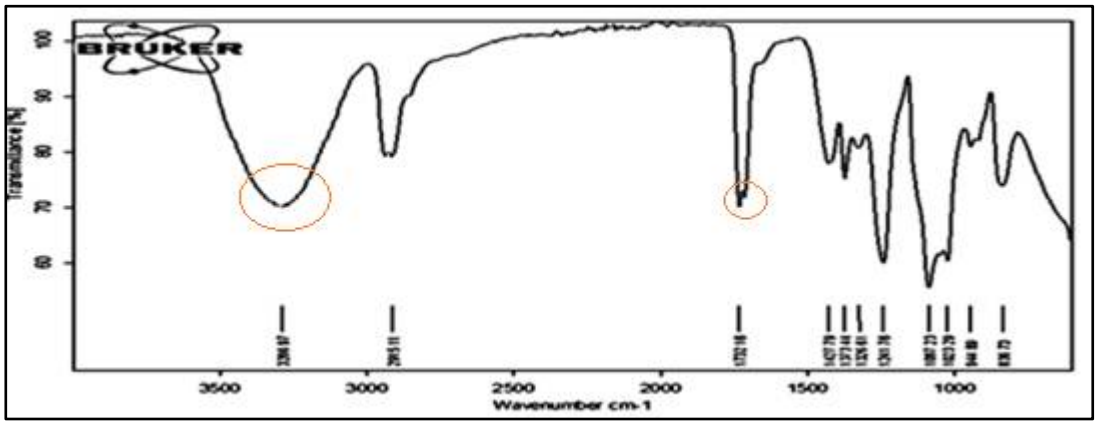

Fig. 18. FT-IR spectrum of pure PVA film with thickness 70±5 μmand the time of irradiation16 hrs.

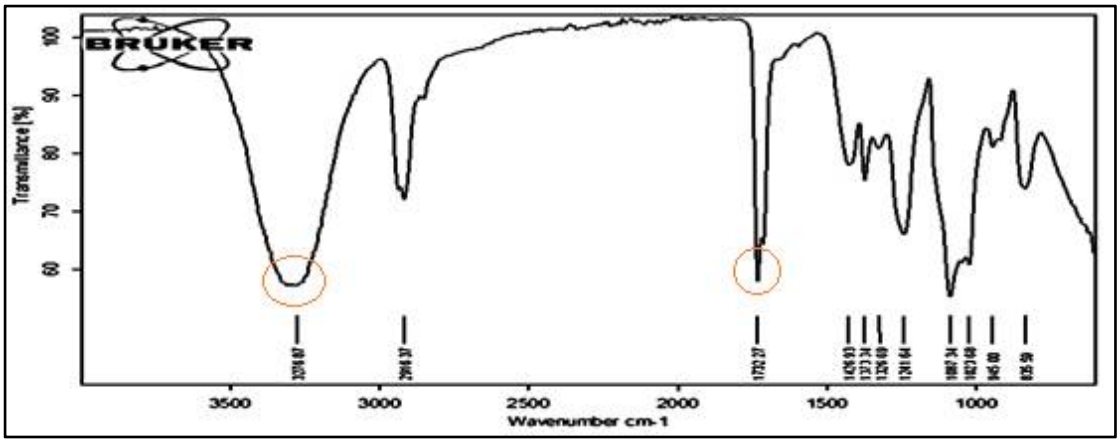

Fig. 19. FT-IR spectrum of PVA film with thickness 70±5 μm containingconcentration (5 %) of the ZnO nanorods and the time of irradiation 16 hrs.

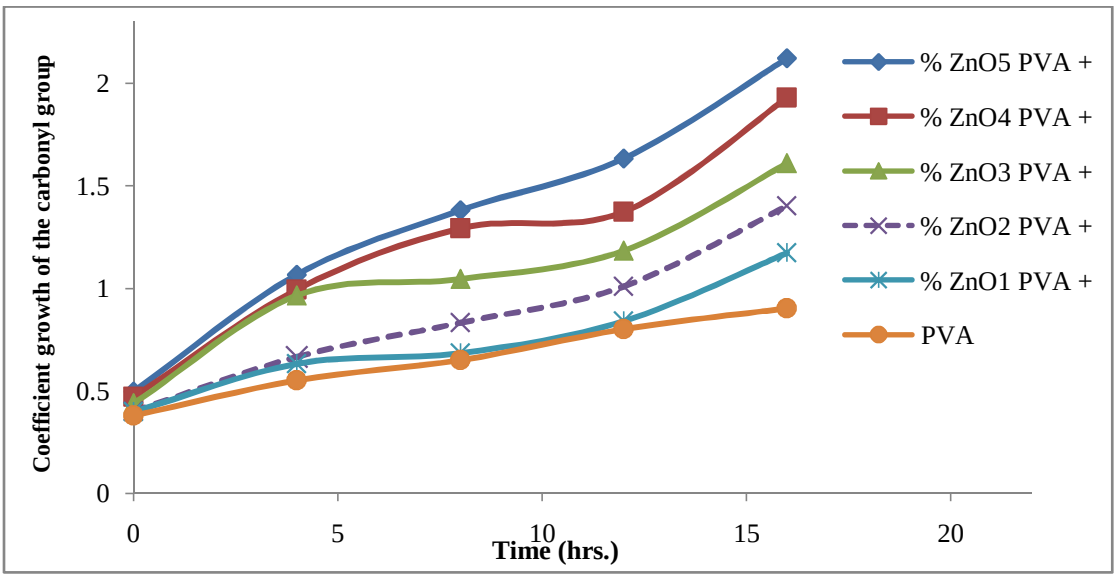

Fig. 20. The relationship between the absorption coefficient of the carbonyl and irradiation time of the results listed in the (Table 4)

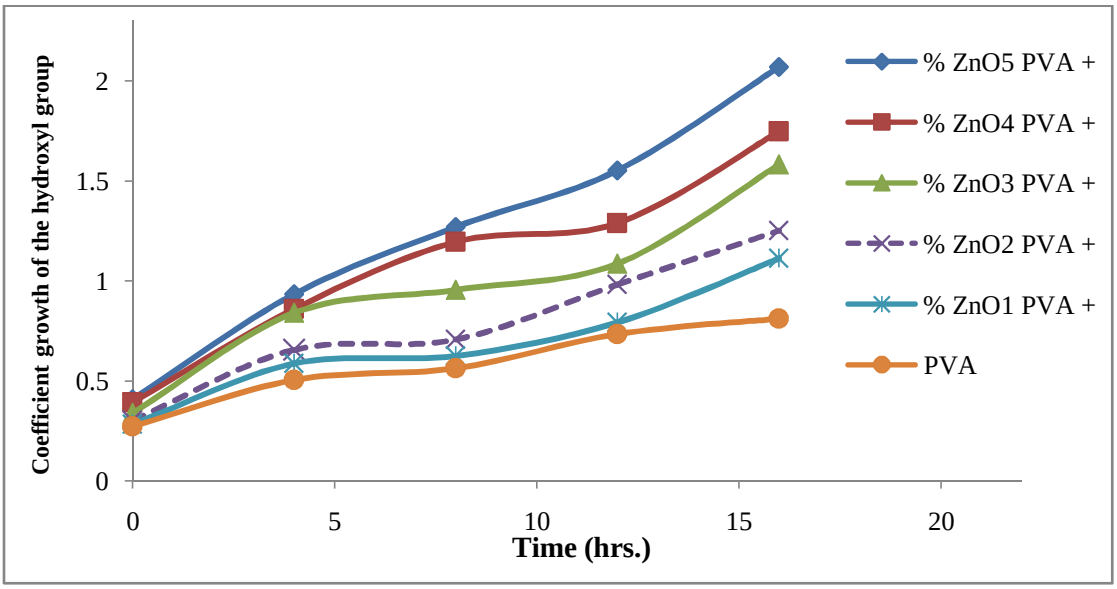

Fig. 21. The relationship between the absorption coefficient of the hydroxyl and irradiation time of the results listed in the (Table 5)

Indian Journal of Natural Sciences www.tnsroindia.org.in ©IJONS

Vol.9 /Issue 50 /October / 2018 *International Bimonthly* *ISSN: 0976 – 0997*

RESEARCH ARTICLE

Molecular Detection of *Babesia bigemina* in Water Buffaloes in Iraq

Moayad Jilab Abid[1*] and Saleem Amin Hasso[2].

[1] College of Veterinary Medicine, University of Baghdad, Baghdad, Iraq.
[2]Professor, Department of Internal and Preventive Veterinary Medicine, College of Veterinary Medicine, University of Baghdad, Baghdad, Iraq.

Received: 26 June 2018 Revised: 24 July 2018 Accepted: 27 Aug 2018

[*]**Address for Correspondence**
Moayad Jilab Abid
College of Veterinary Medicine,
University of Baghdad,
Baghdad, Iraq.
Email: moayadjilab@gmail.com

ABSTRACT

The present study was conducted to investigate the prevalence of Babesiabi *gemina* in water buffaloes in AL-Qadisiya, Najaf and Babylon governorate, Iraq. A total of 320 blood samples were randomly collected from buffaloes from three governorates of Iraq. All the samples were examined for diagnosis of *Babesia bigemina* infection using blood smear examination and PCR for detection of specific DNA.Out of these, Light microscopic examination of blood smears revealed *Babesia bigemina* infection in 2.19%(7/320), while 22.81% (73/320) samples were found positive for *B. bigemina* DNAon polymerase chain reaction (PCR) using the organism-specific primers derived from 18S ribosomal RNA (rRNA) gene of *B. bigemina*. The higher infection rates were 25.22% (29/115) in AL-QadisiyaWhereas, the lower infection rate was 20% (21/105) in Babylon and 23% (23/100) in Najafsamples without significant difference (P>0.05). The highest rate 51.28% of infection with *B.bigemina* was recorded in August, while the lower rate was 0% in December and Januarywith significant difference (P<0.05). Rate of infection in females of buffaloes was 26.16% (45/172) more than in males18.92% (28/148) with significant (P< 0.05) difference.An expected size of 1124-bp PCR product was visualized on agarose gel electrophoresis with all the 73 samples, and three of the products was further cloned and sequenced *B. bigemina* local isolates Blood-Buffalo IQ1(MG461642), IQ2(MH356480.1) and IQ3(MH356481.1)Basic Local Alignment Search Tool (BLAST) analysis of *B. bigemina* sequences generated in the present study share identity at 18S rRNA gene nucleotide sequence level. Furthermore, These local Iraqi *B. bigemina* sequences were found to be closely related with the cognate gene nucleotide sequences of *B. bigemina* from Ugenda where 100% nucleotide identities was observed. This study shows valuable information regarding the survey of *B. bigemina* in water buffaloes in the middle region of Iraq which will likely be very beneficial for the management and control programs of this disease.

Key words: *Babesia bigemina*, Blood, Water Buffaloes, PCR, Iraq

INTRODUCTION

Babesia parasites are responsible for important diseases of large economic, social, and epidemiological impact (1).*Babesiabigemina* is a tick-borne intraerythrocytic protozoan parasite that causes bovine babesiosis in tropical and sub-tropical areas and constitutes one of the most important diseases affecting cattle industry worldwide (2)and (3).Microscopic techniques like Giemsa stained blood smear is the most appropriate for the diagnosis of acute babesiosis but the low sensitivity of this method do not permit to identify the carrier animals (4). The acute infection can readily be diagnosed by direct microscopic examination of Giemsa-stained blood smears, in subclinical cases; this may be impractical due to low levels of parasitemia (5). Bovine babesiosis is an important tick-borne disease, transmitted by Rhipicephalus species (6). Microscopic techniques like Giemsa stained blood smear is the most appropriate for the diagnosis of acute babesiosis but the low sensitivity of this method do not permit to identify the carrier animals(4).The disease In buffaloes are characterised by fever, weakness, ataxia, hemoglobinuria, anemia, anorexia, suspended rumination, reduced milk yield, depression and presence of intraerythrocytic parasites (7)and (8). Several serological methods have been standardized for the diagnoses of babesiosis have been extensively employed in epidemiological field studies. Among the drawbacks of these techniques is the occurrence of cross-reactions between *B. bovis* and *B. bigemina* (9). Molecular tests, such as PCR assays, are highly specific and sensitive method over the existing diagnostic techniques for the diagnosis of subclinical infections (10).Therefore, DNA amplification methods, which are more sensitive and specific than other conventional methods may facilitate and be used as a powerful tool for the diagnosis of babesiosis (11). The aims of the present study will include detection of *Babesia bigemina* in buffalo in middle governorates of Iraq by more than one test along with the clinical findings of the positive animals for *B.bigemina.* As well as, Genotyping of the diagnosed *Babesia bigemina* in blood through gene sequences

MATERIALS AND METHODS

Blood Samples Collection

Blood samples were collected in EDTA from the jugular veins of 320 buffaloes at three governorates in the middle areas of Iraq. The samples were stored on ice until they were returned to the laboratory and placed at (–20°C). Blood samples from buffaloes with known *B. bigemina*infections (supplied by Laboratories of Veterinary Medicine Collage, Baghdad University).

Microscopy

Thin blood smears were prepared on a clean glass slide, Fixed with Methanol for 1 minute and Stained with Giemsa stain (1:10 dilution) for 30minutes. After staining, slides were washed with tape water and dried in air. Finally the stained slides under 100x magnification of Olympus microscope were observed for *Babesia bigemina*, by studying their morphological individuality described by (12).

DNA Extraction

Genomic DNA was isolated from the whole blood samples by using gSYAN DNA mini kit extraction kit (Frozen Blood protocol) Geneaid. USA, and done according to company instructions: Nine hundred microliters of RBC lysis solution was added to 300µl of whole blood sample to disrupt the RBCs and release of parasite in the medium. Samples were incubated for (1-3) minutes at room temperature, centrifuged at 14,000 rpm for one minute and supernatant was discarded leaving behind 10-20µl of residual liquid containing the parasite.Extracted DNA was eluted in 50 µl of DNA elution buffer and stored at −20°C until further analysis. DNA concentration was determined using a NanoDrop® ND-1000 (NanoDrop Technologies Inc., Wilmington, USA).

PCR amplification

For specific detection ofPCR *B. bigemina* primer that used in this study were design in this study by (13) provided by (Bioneer company, Korea) shown in (table 1) were used for ribotyping. PCR reaction was performed to obtain the 1124 bp amplified products over 35 cycles by 94ºC for 5 min., 94ºC for 30 sec., 50ºC for 30 sec., 72ºC for 45 sec. and completed with a final extension step of 7 min. at 72ºC. Finally the amplified DNA fragments were analyzed after electrophoresis on 1% agarose gel.

Data management and analysis

The data of the present study were carried out statistically by Social Science Statistics and the Statistical Package For Social Sciences version 23 for Windows Software and Microsoft Excel 2010. Chi-square test was used for the assessment of association between the variables studied. An estimate was considered statistically significant if its P value was less than an α level of significance of 0.05. (14).

RESULTS

The analysis on 320 blood samples from buffaloes that were subjected to PCR showed that 22.81 % (73/320) were positive for *Babesia bigemina* and revealed an expected PCR product of 1124 bp in length (Fig.1). From the blood smear slides, 2.19 %(7/320) were positive for *Babesia bigemina*. The comparison between the results that obtained by microscopic examination using Giemsa stain and by PCR technique,the PCR method recorded the high percentage (22.81%) of infection in compared to the blood smears, which recorded low percentage (2.19%) , with significant (P< 0.05) difference between the two methods,table (2).The study revealed that all three governorates showed the presence of infection with *B. bigemina* in buffaloesat variable rates. The higher infection rates were 25.22% (29/115) in AL-Qadisiyaand 23%(23/100) in Najaf, Whereas the lower infection rate was 20% (21/105) in Babylon samples without significant difference (P>0.05), table(3).The study demonstrated that the infection rate of infection in females was 26.16% (45/172) more than in males 18.92% (28/148) with significant difference (P<0.05)table (3).The infection with *Babesia bigemina* in buffalo in three governorates was demonstrated along the months of the study with significant difference (P<0.05). The highest rate 51.28% of infection with *B. bigemina* was recorded in August, while the lower rate was 0% in December and January table (3). As shown in figure (2) Phylogenetic tree analysis based on the partial sequence of 18S ribosomal rRNA gene in local *Babesia bigemina* Blood isolates that used for genetic relationship analysis. The evolutionary distances were computed using the Maximum Composite Likelihood method by phylogenetic tree UPGMA method (MEGA 6.0 version). The local *Babesia bigemina*(Blood-Buffalo-IQ1, Blood-Buffalo-IQ2 and blood Buffalo-IQ3 isolate) were show closed related to NCBI-Blast *Babesia bigemina* Uganda isolates (KU206291.1) whereas, other the NCBI-Blast *Babesia bigemina* isolates were show different and out of tree.

DISCUSSION

In the present study a total of 320 blood smears were collected, staining with Giemsa stain and examined microscopically for *Babesia bigemina*. The total infection rate by examined blood Giemsa stain was 7/320 (2.19 %). Using PCR primers previously shown to be specific and sensitive in the detection of *B. bigemina* In blood collected from buffaloes in Iraq detected 1124bp DNA fragments of *B. bigemina* in 22.81% of the samples. Most commonly used method for the diagnosis of Babesiosisis blood smearing in acute cases but in carrier stages where the infection is too low, where more sensitive tools are needed; because microscopy does not detect the infection in early stage or carrier stage and PCR is most reliable and sensitive method. In our study some animals were symptom less but their infectivity was shown by PCR indicating *Babesia bigemina* carrier stage which showed the same result as described by (15).Buffaloes are generally a resistance animal when compared to other domestic livestock. This is particularly impressive because most of them, especially the water buffaloes, live in humid and hot regions that are willing to

have several infectious agents (16). Although the reason is not clear, the effect on buffaloes is often less deleterious than that on other animals.(17) and (18) considered blood smear as the gold standard in diagnosis of different species of Babesia especially *B.bovis* and *B.bigemina*.(19) recorded 1% in the Amazon region of Brazil by microscopic examination, while in the northwestern states of India, microscopic examination revealed *Babesia bigemina* 4.7% of buffaloes tested (20).These differences in infection rate by traditional blood smear stained with Giemsa stain might due to difference in sample size, breed of examined animals, climatic condition of study areas, endemic of parasites in study areas or due to difference in the resistance of the examined local breed and availability of vector ticks (21). Through this study it was confirmed that PCR technique ismore sensitive and specific in detecting low level of infections if carrier animals as compared to light microscopy technique.The results of our study are in observations were reported by (22) who studied the carrier cattle infected with babesia by using PCR amplification. The results in this study are also in relevance with the studies conducted by (10) regarding carrier animals.

These results were in agreement with the most studies concerned this object (23) in Egypt and (24) in India who mentioned that besides the high sensitivity of PCR technique it still the most specific and sensitive test in detecting *Babesia bigemina* in carrier animals as declaring by (25).Regarding the infection rates according to the different study areas indicated that AL-Qadisiya governorate showed the highest rate of infection by PCR technique 25.22% followed by Najaf 23% and Babylon20% without significant difference (P>0.05),these findings are supported by many authors about the availability of the vector ticks of Babesiosis and other blood parasites in these regions.These localities have similar weather conditions around the year as they are located closely in hot and humid incentral of Iraq. Tick infestation in these areas is high due to the favorable temperature conditions, commonly during hotter months of the year.These result differ with (35) who showed molecular assays was dependent to localities of sampled animals. The prevalence of babesiosis correlates with the geographic distribution and changing environmental conditions, especially global warming (36). The relative prevalence of *B. bigemina* by PCR amplifying for 18S rRNA gene which showed prevalence of the disease in North-eastern region higher than in western region of Punjab (37).(38) showed that the prevalence of subclinically infected carriers increased from February till December even if the animals were indoors and no ticks were present.

The prevalence then dropped dramatically six months later. Regarding gender of the infected animals showed infection rate (26.16 %) in female compared to male (18.92%) with significant difference (P<0.05). Sex have been demonstrated to play a role in determining host susceptibility to Babesia infection (29). In this study, females were found more susceptible to babesia infection as compared to the male animals. These findings disagree with (30), and other scientists (15) reporting a higher prevalence in male than in female animals. While (31) and (32) considered that infection rate with babesiosis in female and male infected animals were similar. Concerning sex susceptibility to infection, current study showed higher rate of infection in female buffaloes. The physiology of the females during pregnancy and lactation period which is associated with hormonal and immunological changes could explain this finding (33). The reason for the higher infection rate in females than males could be the exposure to some stress that cause severe clinical cases, such as parturition and lactation. Such breakdowns in immunity are most likely to occur if there is a superimposed infection with a different parasite (34). (35) Concluded that these differences of positivity for molecular assays were verified to reproductive status of sampled animals. Distributing the cases according to months of the study , August 2017, showed the highest rate of infection 51.28 % compared with zero in December and January 2018 with significant difference(P<0.05).

The distribution of infection was highest in summer followed by autumn and lowest in cold months. (26) and (27) observed high infection rate in April and early summer months which they considered as the most suitable environmental condition for breeding and activation of tick vector, also (28) found the infection with Babesiosis may begin in the first period (May and July) and reach the peak at second period (September and October) of year. These differences may be due to the delayed rain season to late summer during 2017 in Iraq and neighboring countries. Phylogenetic tree analysis was based on the partial sequence of 18S ribosomal rRNA gene in local *Babesia bigemina* Blood isolates used for the confirmative genetic detection. According to the created phylogenetic tree, *B. bigemina*

grouped with *B.bigemina* (KU206291.1). This indicate the presence of strain diversity of *B. bigemina* isolates from Iraq with strains of other countries recorded in gene bank, these finding were supported by (39),figure (2). In this study, the local *Babesia bigemina* Blood-Buffalo-IQ1, blood Buffalo-IQ2 and blood Buffalo-IQ3 isolates found to have 100% nucleotide identities with NCBI-Blast *Babesia bigemina* Uganda isolates (KU206291.1), that mean it have a very close phylogenetic relation with isolate from Uganda. Whereas, the other NCBI-Blast *Babesia bigemina* isolates showed different and out of tree. Thus, close genetic relatedness was observed between *B. bigemina* isolates from Iraq with Uganda rather than its neighboring countries. This study on phylogenetic relation of local *B. bigemina* of buffalo isolates with other isolates throughout the world may be considered as the earliest report of its kind from Iraq. This study provides important data for understanding the epidemiology of tick-borne diseases and it is expected to improve the approach for diagnosis and control of tick-borne diseases in Iraq.

These results were agreement with (40) who showed that *B. bigemina* isolates from north-eastern India found to have have a very close phylogenetic relation with isolates from Argentina and Kenya. Thus, close genetic relatedness was observed between *B.bigemina* isolates from this region of India with Argentina and Kenya rather than its neighbouring country China. In the constructed tree, *B.bigemina* isolate (KU206291.1) was related to *B. bigemina* (IQ1, IQ2 and IQ3) local isolates with Nucleotide sequence identity 100%, 100% and 100% respectively. whereas, other the NCBI-Blast Babesia species were show different and out of tree, indicating presence of strains diversity with other strains of neighboring countries recorded in gene bank, these finding were supported by(41)and (42).This study provides essential data for understanding the epidemiology of tick-borne disease as *B. bigemia* and it is expected to improve the methods for detection and control of tick-borne diseases in Iraq.

ACKNOWLEDGEMNTS

The authors are highly indebted to departmental colleagues for their support. I would like to thanks Higher Education Commission, Iraq for their research grants.

REFERENCES

1. Bock R, Jackson L, De Vos A, Jorgensen W. Babesiosis of cattle. Parasitology (2004). 129(Suppl S1): S247-S269.
2. McCosker, P.J., (1981). The global importance of babesiosis. In: Ristic, M., Kreier, J.P. (Eds.), Babesiosis. Academic Press, New York, pp. 1–24.
3. Kuttler, K.L. (1988). World-wide impact of babesiosis. In :Ristic M (Ed), Babesiosis of Domestic Animals and man .CRC.Press.Boca Raton, FL: 1-22.
4. Singh J, Tuli A, Singla LD. (2003) Mixed Anaplasma and Babesia infection outbreak in crossbred cattle. Punjab Vet J. 3(2): 73– 74
5. Bose R, Jorgensen WK, Dalgliesh RJ, Friedhoff KT, De Vos AJ(1995). Current state and future trends in the diagnosis of babesiosis. Vet Parasitol. 57(1-3): 61-74.
6. Oliveira-Sequeira TCG, Oliveira MCS, Araujo JP, Amarante AFT. (2005) PCRbased detection of *Babesiabovis* and *Babesiabigemina* in their natural host *Boophilusmicroplus* and cattle. Int J Parasitol; 35(1): 105-111.
7. Wright IG, Goodger BV, Buffington GD, Clark IA, Parrodi F, Waltisbuhl DJ (1989). Immunopathophysiology of babesial infections. Trans R Soc. Trop. Med. Hyg. 83 Suppl:11-13.
8. Patel, P.A, Modi, M.C., Chaudhary, P.M., Patel, S.P. and Joshi, A.H. (2011). A rare case of babesiosis in Mehsana buffalo. Int. J. Agro Vet. Med. Sci., 5: 383-384.
9. Passos, L.M.F., Bell-Sakyi, L., Brown, C.G.D., (1998). Immunochemical characterization of in vitro culture-derived antigens of Babesiabovis and Babesiabigemina. Vet. Parasitol. 76, 239–249.

10. Figueroa JV, Chieves LP, Johnson GS, Buening GM. (1992). Detection of *Babesiabigemina* infected carriers by polymerase chain reaction amplification. J ClinMicrobiol. 30: 2576– 2582
11. Aktas M, Altay K, Dumanli N. (2005). Development of a polymerase chain reaction method for diagnosis of *Babesiaovis* infection in sheep and goats. Vet Parasitol. 133:277–281.
12. Soulsby, (1982),Helminths, Arthropods and Protozoa of Domesticated Animals7th Edition, BaillereTindall, London.P. 456-475.
13. Guido, F.C.L., Angela, P.S., Lloyd, H. L. and Claudio, R. M., (2002). Cien. Anim. Barasil., 3: 27-32.
14. Field, A. (2005) . Discovering Statistics using SPSS for Windows – Second Edition, Sage Publications Ltd.
15. Durrani AZ, Kamal N, (2008).Identification of ticks and detection of blood protozoa in friesian cattle by polmerase chain reacton test and estimation of blood parameters in district Kasur, Pakistan, Trop Anim Health Prod. 40(6), 441-447.
16. Cockrill W.R., "The water buffalo: a review, "British Veterinary Journal,vol.137,pp.8–16,1981.
17. Mesplet, M.; Palmer, G.H.; Pedronic, M.J.; Echaided, I.; Christensen , M.F. and Schnittgger, L.(2011). Genome-wide analysis of peptidase content and expression in a virulent and attenuated Babesiabovis strain pair. Mol.Biochem.Parasitol;179(2):111-113.
18. Palmer, G.H. (2002). Babesiosis. In Encyclopedia of life sciences. Macmillian Publishers Ltd., Nature Publishing Group, London ,United Kingdom. pp:1-8.
19. Silveira JAG , de Oliveira CHS , Silvestre BT , Albernaz TT , Leite RC , Barbosa JD , Oliveira CMC , Ribeiro MFB. (2016) Molecular assays reveal the presence of Theileria spp. and Babesia spp. in Asian water buffaloes (Bubalusbubalis, Linnaeus, 1758) in the Amazon region of Brazil.Ticks and Tick-borne Diseases, 7(5):1017-1023
20. Miranpuri G.S. (1988) Ticks parasitising the Indian buffalo (*Bubalusbubalis*) and their possible role in disease transmission Veterinary Parasitology Volume 27, Issues 3–4, P. 357-362.
21. Salih DA, Julla II, Hassan SM, El Hussein AM, Jongejan F. (2008) Preliminary survey of ticks (Acari: Ixodidae) on cattle in Central Equatoria State, Southern Sudan.Onderstepoort J Vet Res. 75(1):47-53.
22. Fahrimal, Y., Goff, W.L. and Jasmer, D.P., (1992). J. clin. Microbiol., 30: 1374-1379.
23. Ibrahim HM, AdjouMoumouni PF, Mohammed-Geba K, Sheir SK, Hashem IS, Cao S, Terkawi MA, Kamyingkird K, Nishikawa Y, Suzuki H, Xuan X. (2013)Molecular and serological prevalence of Babesiabigemina and Babesiabovis in cattle and water buffalos under small-scale dairy farming in Beheira and Faiyum Provinces, Egypt. Vet Parasitol. 15;198(1-2):187-92. doi: 10.1016/j.vetpar.2013.08.028. Epub 2013 Sep 6.
24. Maharana, BR.; Tewari, AK.; Saravanan ,BC . and Sudhakar, NR.(2016). Important hemoprotozoan diseases of livestock ; Chalange in current diagnostics and therapeutic: An update. Vet. World; 9(5):487-495.
25. Saad F; Khaisroom M ;Khan K; and Akber N. (2015). Prevalence and Molecular Detection of Babesiosis in the Slaughter Animals of Peshawar .KhyperPakhunkhawa Pakistan . Int.J.Curr.Microbiol. App.Sci; 4(8):1030-1036.
26. Simuunza, M.C. (2009). Differential diagnosis of tick –borne diseases and population genetic analysis of Babesiabovis and Babesiabigemina .Ph.D. thesis . Faculty of Veterinary Medicine –University of Glasgow.
27. Mustafa, B.H.S.(2011). Study on some epidemiological factors of hard tick (Ixodidae) in sheep in Sulaimania Province with trial to immunize rabbits against larval extracts of Hyalommaanatolicumanatolicum .Ph.D. Thesis, Sulaimania University.
28. Afkar M. Hadi , A.M.A. Al- Amer (2012) Isolation of Theileria and Babesia from gut and ovary of hard ticks: Hyalomma a. anatolicum in Baghdad. Diyala Agricultural Sciences Journal, 4(2) 1 – 8

29. Aguilar-Delfin,I., Homer,M.J.,Wettstein,P.J. and Persing,D.H.(2001). Innate resistance to Babesia infection is influenced by genetic background and gender. Infect.Immun; 69: 7955-7958.
30. Iqbal F, Fatima M, Shahnawaz S, Naeem M, Shaikh R, Ali M, Shaikh A, Aktas M, Ali M. (2011) A study on the determination of risk factors associated with babesiosis and prevalence of Babesia sp., by PCR amplification, in small ruminants from Southern Punjab (Pakistan).Parasite. Aug;18(3):229-34.
31. Al-Thabhawi, Khowla Hussein Sabbar.(2015).Molecular Ddetection of Babesiabovis and Babesiabigemina in cattle in Al-QadisiyahProvince.M.Scthesis.College of Veterinary Medicine./University of Al-Qadisiyah.
32. Lemma, F., Adugna, G. and Dirsha, D.(2016). Prevalence of Bovine Babesiosis in and Around Jimma Town South Western Ethiopia . Adv. Bio. Res; 10(1).:37-42.
33. Sappenfield E, Jamieson DJ, Kourtis AP. (2013) Pregnancy and susceptibility to infectious diseases. Infect. Dis. Obstetrics Gynecology. 213:1–9.
34. Radostits, O. M., Gay, C.C., Hinchcliff, K.W. and Constable , P. D.(2007). Veterinary Medicine . A text book of the diseases of cattle, sheep, pigs, goats and horses .10th ed.London .Saunders Elseveir. :1483-1493.
35. da Silva JB1, André MR, da Fonseca AH, de Albuquerque Lopes CT, da Silva Lima DH, de Andrade SJ, Oliveira CM, Barbosa JD (2013)Molecular and serological prevalence of Babesiabovis and Babesiabigemina in water buffaloes in the north region of Brazil. Vet Parasitol. Nov 8;197(3-4):678-81.
36. Slenning BD. (2010) Global climate change and implications for disease emergence. Vet Pathol. 47:28–33.
37. Sharma A. , Das SinglaL., Ashuma, Kaur BatthB., and KaurP. (2016)Clinicopatho-Biochemical Alterations Associated with Subclinical Babesiosis in Dairy Animals J Arthropod Borne Dis. 10(2): 258–266.
38. Terkawi MA1, Huyen NX, Shinuo C, Inpankaew T, Maklon K, Aboulaila M, Ueno A, Goo YK, Yokoyama N, Jittapalapong S, Xuan X, Igarashi I.(2011) Molecular and serological prevalence of Babesiabovis and Babesiabigemina in water buffaloes in the northeast region of Thailand. Vet Parasitol. 10;178(3-4):201-7.
39. Ica A, Vatansever Z, Yildirim A, Duzlu O, Inci A. (2007)Detection of Theileria and Babesia species in ticks collected from cattle.Vet Parasitol. 1;148(2):156-60. Epub 2007 Jul 5.
40. Laha R, Mondal B, Biswas SK, Chand K, Das M, Sarma D, Goswami A, Sen A. (2015). Detection of Babesiabigemina infection in cattle from north-eastern India by polymerase chain reaction and its genetic relatedness with other isolates.Trop Anim Health Prod. 47(3):633-6.
41. Saravanan BC, Das S, Siju SJ, Tewari AK, Sankar M, Kataktalware MA, et al. *Babesiabigemina* infection in yak (*Poephagusgrunniens* L.): (2013)Molecular detection and characterization. Vet Parasitol.194:58–64.
42. Ravindran R, Sreekumar C, Saravanan BC, Udaykumar M, Tewari AK, Kumar S, *et al.*(2010)Genetic variation among Indian isolates of *Babesiabigemina*. J Vet Parasitol. ;24:159–63.

Table1. Primers used for amplify the DNA of *Babesia bigemina*

Amplicon		Nucleotide Sequence	Product length	Reference
18SrRNA gene	F	TGGCGGCGTTTATTAGTTCG	1124bp	(13)
Babesia bigemina	R	CCACGCTTGAAGCACAGGA		

Table 2. infection rate with *Babesia bigemina* by blood smear staining and PCR technique

Diagnostic test	No. of tested animals	No. of positive	Percentage
Blood smear	320	7	2.19 %
PCR		73	22.81 %

Table 3. Infection Rate with *Babesia bigemina* by PCR assay on basis of location, sex and months of Study

Item		No. of examined buffaloes	No. of infected buffaloes	Frequency
Location	AL-Qadisiya	115	29	25.22%
	Najaf	100	23	23%
	Babylon	105	21	20%
Total		320	73	22.81%
Sex	male	148	28	18.92%
	female	172	45	26.16 %
Total		320	73	22.81 %
Months	June	45	13	28.89 %
	July	34	13	38.24 %
	August	39	20	51.28 %
	September	35	17	48.57 %
	October	28	7	25 %
	November	38	2	5.26 %
	December	35	0	0
	January	32	0	0
	February	34	1	2.94 %
Total		320	73	22.81 %

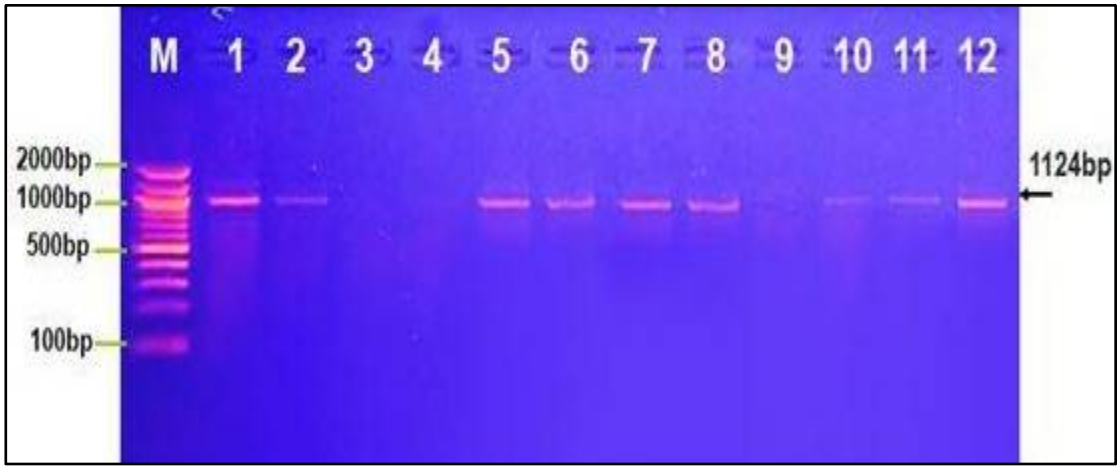

Fig.1. Agarose Gel Electrophoresis Image Shows the PCR Product Analysis of 18S ribosomal RNA Gene of *B. bigemina*positive DNA in buffalo blood Samples. Lanes (1, 2, 5, 6, 7, 8, and 10, 11, 12) were positive samples at 1124bp product size.

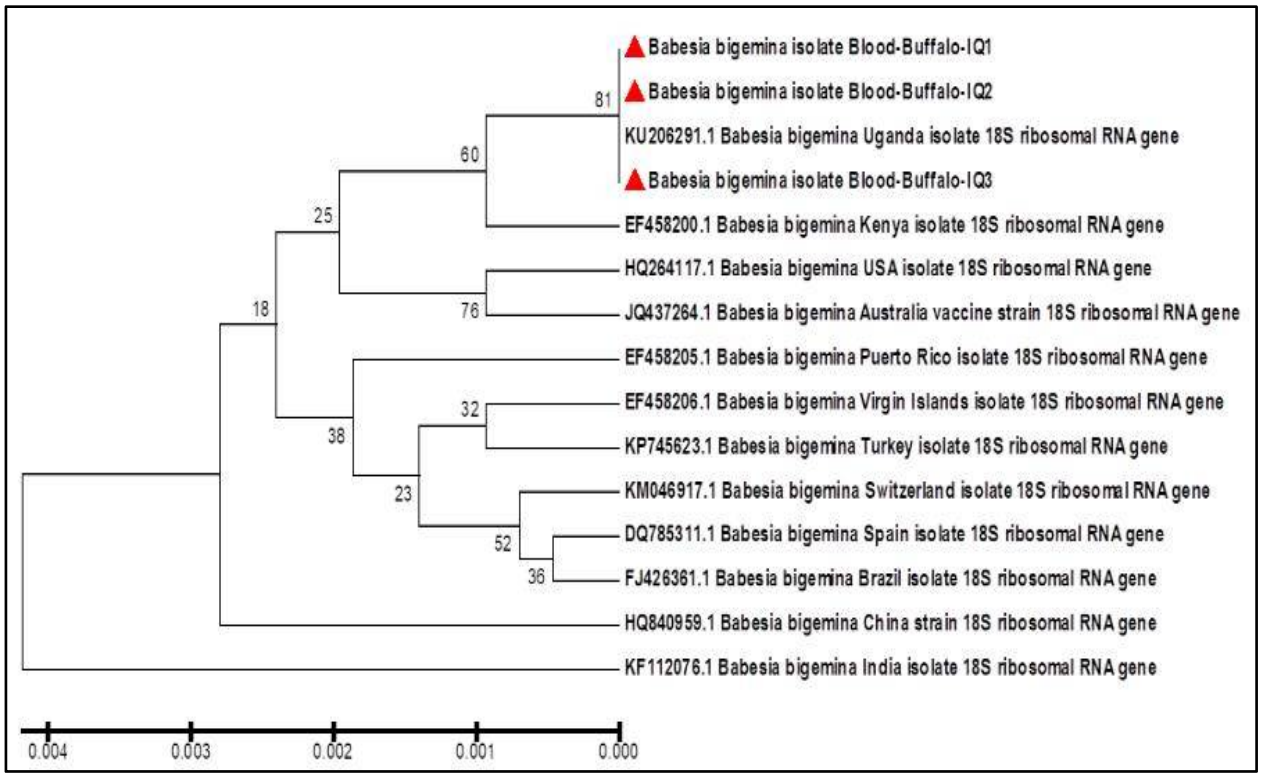

Figure 2. Phylogenetic tree analysis of local *Babesiabigemina* in blood of buffaloes for genetic relationship analysis.

Indian Journal of Natural Sciences www.tnsroindia.org.in ©IJONS

Vol.9 /Issue 50 /October / 2018 *International Bimonthly* *ISSN: 0976 – 0997*

RESEARCH ARTICLE

Effect of Plant Density and Fertilizer Application on the Incidence of Maize Stem Borer

S.Suganya kanna*

Assistant Professor (Agrl. Ento.), Agricultural College and Research Institute, Tamil Nadu Agricultural University, Kudumiyanmalai - 622 104, Pudukkottai, Tamilnadu, India.

Received: 26 June 2018 Revised: 23 July 2018 Accepted: 27 Aug 2018

*Address for Correspondence
S.Suganya kanna
Assistant Professor (Agrl. Ento.),
Agricultural College and Research Institute,
Tamil Nadu Agricultural University,
Kudumiyanmalai - 622 104,
Pudukkottai, Tamilnadu, India.
Email: sugaento@yahoo.co.in

ABSTRACT

Optimum spacing and fertilizers application are one of the cultural practices that are generally prophylactic in natures and are frequently the first line of defence against crop pests. These tactics are environmentally safe as they do not have significant disruption effects on non target organisms and environmental quality. The field trial on impact of spacing and fertilizers against maize stem borer infestation on pre release hybrids revealed that there was no significant difference among hybrids and spacing, where higher dose of fertilizer dose (125% RDF) showed higher infestation and dead hearts.

Keywords: Maize, Spacing, Fertilizer, Stem borer, Incidence.

INTRODUCTION

Maize is a promising option for diversifying agriculture in upland areas of India. The area is slowly expanding to meet out food and feed demands in livestock and poultry industry besides blooming as commercial crop for farmers' livelihood. On the other hand, continuous cropping of maize will lead to the occurrence of pests. About 139 insect-pests cause varying degree of damage to maize crop. Among all the insect pests of stem borer *C. partellus* is the most notorious pest found throughout India. The survey conducted all over Tamil Nadu on the incidence of pests on maize revealed that maize stem borer is emerging as serious pest which causes greater yield loss. The economic injury level is 2.09 to 2.42 larvae per plant (Manjunath and Mallapur. 2017).

The integrated pest management strategies are adopted to manage the increasing pest menace in maize. As integral part in IPM, cultural practices like selection of variety, time and manner of planting, tillage, sanitation, fertilizer and

irrigation, spacing, harvesting and off season operations are adopted under field condition. Among this spacing and fertilizer application are key practices in maize which make the environment less/more favorable for the pest.

MATERIALS AND METHODS

A field experiment was carried out during *Rabi* season of the year 2012-13 under irrigated condition to study the growth and performance of three pre-release maize hybrids VMH 08013, VMH 08014 and CMH 08282 (COH (M)6) in comparison with the released maize hybrid (COH (M) 5) under various plant density (60 x 20 cm and 60 x 25 cm) and varied fertilizer levels (75% , 100% and 125% RDF). The experiment was laid out under split-split plot design, replicated thrice with the treatments given in Table 1. The field observation on maize stem borer was done on total number of plants, stem borer infected plants were recorded and statistically analysed.

RESULTS

The results revealed that there was no significant difference among hybrids and spacing, where higher dose of fertilizer dose (125% RDF) showed higher infestation (38.15%) and dead hearts (10.25%) followed by 100 percent RDF (33.50 and 9.77%) and 75 per cent RDF (21.33 and 9.15%), respectively (Table 1). Singh and Singh (1969), N leads to tilting of balance of the carbon to nitrogen ratio in the plant. Greater N supply causes the formation of thin, succulent cell walls that enhance survival of young borer larvae. Among yield CMH (M) 6 recorded higher yield (8634 kg/ha) followed by VMH 08014 (7198 kg/ha), VMH 08013 (7284 kg/ha) and CO H (M) 5 (6152 kg/ha). Although higher dose of fertilizer 125 per cent RDF recorded higher infestation, yield was higher (7698 kg/ha) followed by 100 per cent RDF (7363 kg/ha) and 75 per cent RDF (6947 kg/ha). Setamou *et al.* (1995) found that average cob weight losses due to borer activity decreased linearly with N application. This indicated that under the prevailing damage levels, the positive effect of N fertilization enhanced plant vigor, and surpassed the negative effect of increased borer's feeding.

The present results suggested that optimum doses of nitrogen fertilizer which are sufficient for proper crop production should be applied for minimum pest damage because increasing the nitrogen application leads to an increase in *C. partellus* population. The nitrogen fertilizer application plays a major role in integrated pest management tactic in the control of *C. partellus* population, development and infestation on maize crop

REFERENCES

1. Manjunath Chouraddi and C.P. Mallapur . 2017. Assessment of crop loss and economic injury level of maize stem borer, *Chilo partellus* (Swinhoe). *Journal of Entomology and Zoology Studies,* 5(4): 1530-1535.
2. Sétamou M., Schulthess F., Bosque-Perez N.A., Th omas-Odjo A. 1995. The effect of stem borers on maize subjected to different nitrogen and silica treatments, with special reference to *Sesamia calamistis* Hampson (Lepidoptera: Noctuidae). *Entomologia Experimentalis et Applicata* , 77: 205-210.
3. Singh T.P., Singh R, 1969. Incidence of stemborer (*Chilo zonellus* Swinhoe) and lodging in Jaunpur variety of maize under different fertility levels of nitrogen. *Indian J. Entomol*., 31: 158–160.

Table 1. Effect of hybids, plant density and nutrient management on incidence of maize stem borer

Treatments	Plant Infestation (%)	Dead Hearts (%)	Yield (Kg/ha)
Main plot treatments (Plant density)			
S_1: 60 x 20 cm (83333 plants ha^{-1})	31.75	8.75	7116
S_2: 60 x 25 cm (66666 plants ha^{-1})	30.80	9.35	7516
SEd	1.53	0.38	169.8
CD(0.05%)	NS	NS	NS
Subplot treatments (Pre-release maize hybrids)			
H_1: VMH 08013	32.65	8.82	7198
H_2: VMH 08014	29.60	9.15	7284
H_3: CO H (M) 6	30.50	9.00	8631
H_4: CO H (M) 5	32.55	9.25	6152
SEd	1.78	0.48	243.1
CD(0.05%)	NS	NS	529.6
Sub-Sub plots (Fertilizer levels)			
F_1: 75 % RDF (187.5: 56: 56 kg NPK ha^{-1})	31.33	9.15	6947
F_2: 100 % RDF (250: 75: 75 kg NPK ha^{-1})	33.50	9.77	7363
F_3: 125 % RDF (312.5: 94: 94 kg NPK ha^{-1})	38.15	10.25	7698
SEd	1.53	0.42	166.5
CD(0.05%)	2.15	NS	336.9

RDF- Recommended dose of Fertilizer

Indian Journal of Natural Sciences www.tnsroindia.org.in ©IJONS

Vol.9 /Issue 50 /October / 2018 *International Bimonthly* *ISSN: 0976 – 0997*

RESEARCH ARTICLE

Detection of Intestinal Parasites by Using Microscopic Examination and Molecular Diagnosis of *Ancylostoma spp* in Domestic Dogs in Baghdad City -Iraq

Ahmed Shalan Jasim* and Azhar Ali Faraj

Department of Parasitology, College of Veterinary Medicine, University of Baghdad, Iraq.

Received: 25 June 2018 Revised: 27 July 2018 Accepted: 29 Aug 2018

*Address for Correspondence
Ahmed Shalan Jasim
Department of Parasitology,
College of Veterinary Medicine,
University of Baghdad, Iraq.

ABSTRACT

The current study was designed for detection of intestinal parasites by traditional and molecular diagnosis of hook worms in domestic dogs. The fecal specimens were collected from 180 domestic dogs in Baghdad city during the period from beginning of October 2017 to March 2018. Results of microscopic examinations revealed that six genera/species gastrointestinal parasitesin domestic dogs (*Ancylostoma spp*, *Trichuris vulpis*, *Toxocara canis*, *Isospora spp*, *Taenia spp., Giardia spp*). There was a statistical difference in prevalence between dogs aged < 6 months (44.44%) and those aged ≥ 6 months (20%). Results revealed that the intestinal parasite infection among females (33.33%), are more than males (31.11%) . Among 180 fecal samples which we taken from them 100 samples randomly selected and subjectedto molecular diagnosis of *Ancylostoma* spp.The use of PCR analysis of the DNA isolated from 100 fecal samples showed that 30% have *Ancylostoma spp*. positive and revealed an expected PCR product of 18 S gene *(*900bp), for *Ancylostoma spp* of 18 S genes.Phylogenic tree inferred the degree of relatedness between 18SrRNA sequence deposited in the international nucleotide bank sequence database (NCBI). Furthermore this identification was verified via 18SrRNA sequence of the parasite 3 using Blastn algorithm. Sequence recorded in the Genbank under accession numbers MH508247.1, MH508246.1, MH508245.1 to *Ancylostoma caninum, Ancylostoma duodenale Ancylostoma ceylanicum,* respectively.

Keywords: Intestinal parasites, *Ancylostoma* spp.,PCR, Phylogenic tree, Iraq.

INTRODUCTION

Dogs may harbour numerous intestinal parasites, including protozoa, cestodes, trematodes and nematodes (Kaewthamasorn et al., 2006). Among parasites, the gastrointestinal ones may affect dog' well-being, causing clinical signs like listlessness ,vomiting, diarrhoea, poor growth rate, anaemia and sometimes even death, especially in

puppies (Savioliet al., 2006;Jittapalapong et al., 2007). Furthermore, some canine parasites, such as *Toxocara canis* and hookworms may cause diseases, such as visceral and ocular larva migrans and others, including Cryptosporidium spp., Giardia spp., *Echinococcus multilocularis* and *Dipylidium caninum* have the potential to infect humans, either via direct contact or via exposure to contaminated environment (Oliveira-Sequiera et al., 2002; Traub et al., 2004b).Diagnosis of intestinal parasites depend on microscopic examination and molecular assay are a range of DNA based methods for the detection of intestinal parasites (Oliveira-Arbex et al., 2016). However, due to the little studies that related to the prevalence of intestinal parasites infections in domestic dogs in Baghdad city in Iraq. The present study was designed to detection of intestinal parasites, using molecular diagnosis of *Ancylostoma spp* and phylogenic analysis in domestic dogs in Baghdad city, Iraq.

MATERIALS AND METHODS

Samples Collection

One hundred and eighty faces samples of domestic dogs were collected from different areas in Baghdad city during the period from the beginning of October2017-March2018. Direct fresh fecal samples (about 20 g) were compiled by using disposable plastic gloves and putted into in clean containers. The samples were conveyed to the Parasitological laboratory - Veterinary Medicine College - University of Baghdad.

Microscopic examination of fecal samples

Each fecal sample was divided into two parts the first one for the microscopic examination (Direct wet smear, flotation method and sedimentation method) aspreviously described by Coles (1974), while the second part was kept at -20 ^{o}C for molecular diagnosis (PCR).

DNA Extraction

Extraction of DNA from previously 100 fecal samples collected were subjected to DNA extraction using kit of promega company USA according to manufacturer's instructions. Primers used for the PCR amplification were Forward strand primers 5'-GAC TGC GGA CTG CTG TAT-'3 and Reverse strand primers 5'-AAG TTC AGC GGG TAG TCA-'3 (Liu et al.,2013).

Data Management and Analysis

All data were subjected to statistical analysis by using SAS software (2010). The differences among the prevalence were assessed by chi square test. $P<0.05$ is considered significant.

RESULTS

The results of the microscopic examination of fecal samples collected from domestic dogs revealed six species of genera/species of intestinal parasites and the differences among their proportions were significant (P=0.005) (Table 1)(figure 1-6). The total infection rate of intestinal parasites in dogs was 32.22% (58/180). According to age group, there was a significant (P=0.0004) difference in the prevalence between dogs aged < 6months and those aged ≥ 6 months) (Table 1). The result showed that the difference in the infection rates with intestinal parasite in females 33.33% (30/90), and males 31.11% (28/90) were not significant (Table 3).

Prevalence of *Ancylostoma* in dogs using PCR Technique

The use of PCR technique was aimed to detect *Ancylostoma species* which spread in the areas. PCR analysis of the DNA isolated from 100 fecal samples showed that 30% have *Ancylostoma spp*. positive and revealed an expected PCR product of 900 bp in length (Table 4)(Figure7).

Sequence Alignment of 18S RNA Gene

Figure (8) Show theamplification and sequenced analysis of 18S *(900* bp) of the rRNA gene of each isolate was successfully achieved. PCR product = 900bp 18S ribosomal RNA. The result showed a strain of *Ancylostoma caninum*which has the highest similarities with JQ812694.1 USA accession number 100% while the lowest similarities with KC755028.1 China accession number 99.1% and MF371322.1 Brazil accession numbers 99.1%. The other accession number of *Ancylostoma caninum*has a lower grade in similarities with MH508247.1 Iraq the accession number is 99.8%, AJ920347.2 Poland accession number is 99.8%, and KP844735.1 Australia accession number 99.4%. The strain of *Ancylostoma Ceylanicum* the higest was with JF960369197.9 Malaysia accession number 98.2% and LC036567.1 Guinea accession number is 98.2% while the lowest was similarities with MH508345.1 Iraq the accession number 97.1%. The other accession number of Ancylostoma *Ceylanicum*has lower grade in similarities with, DQ464371.1 Poland the accession number is 97.9 %.While the strain of *Ancylostoma duodenale*showed a highestsimilaritiy with AB504715.1Thailand the accession number 97.7% while the lowest similarities with EU344797.1 China accession number 96.7% and the other accession number of *Ancylostoma duodenal*has a lower grade in similarities with KU996371.1 India accession number is 97.5% and MH508246.1 Iraq accession number 97.5 %(Figure 9).

DISCUSSION

Microscopic examination

Dogs frequently contain several intestinal parasites which are zoonotic and considered important to human health. Our study identified six parasite genera/species which was in agreement with previous studies (Hadi and Faraj, 2016; Hasson, 2014; Klimpel et al., 2010). This study showed that an overall prevalence of dogs intestinal parasitic infection of 32.22%. which was lower than the 52.4% obtained by Fontanarrosa et al. (2006) in Buenos Aires, Argentina, but much higher than the overall prevalence (12.5%) reported by Little (2009) in the United States. The vast differences in overall prevalence was expected and is most likely due to the differences in the geographic regions of sampling, as well as the type of sampling and method of detection.The results of present study showed that the highest rate of infection in young dogs was 44.44%(40/180). The effect of age on the incidence of parasitic infestation is severe. This effect is in agreement with Abere et al(2013) who mentioned that the parasites prevalence was strongly associated with age. In addition, the same researcher referred that the parasite prevalence was higher in young dogs than adults. Furthermore, Ahmed et al., (2014) and Jenan et al.,(2015) mentioned that the infection in puppies was higher than adults.

These results might be due to low immunity in young ages or probably as a consequence of single or repeated exposures (Ramírez-Barrios et al., 2004).The results of our study show that, there was a closely infection rate between males and females, this results was agreement with previous studies (Mirzaei, 2010; Zelalem and Mekonnen, 2012). This could be due to both sexes exposed to same environmental condition.Canine hookworm species eggs are difficult to differentiate microscopically (Traub et al., 2004a). Differences in size and shape have been documented although they require a high experiance in microscopic detection (Lucio-Forster et al., 2012). Molecular methods have been used to diagnose intestinal parasites in dogs, as well as to differentiate hookworm species (Liotta et al., 2012b; Ngui et al., 2012). This is the first study to detection hookworm infection in Iraq using molecular assay. Molecular techniques are more advantageous for hookworm identification as they are rapid and more sensitive. Molecular

methods for diagnosis of *Ancylostoma* spp as more sensitive and specific tools have been increasing used to detect *Ancylostoma* spp in carrier dogs. It is recognized even relative amount of DAN of the parasite (Rehman et al*.,* 2017).

PCR Examination

In present study using PCR technique showed that the high rate of infection with *Ancylostoma spp* (30%). This finding was in accordance with previous studies in other countries where Liu *et al*.(2013) who reported with *Ancylostoma caninum* was 54.90% and *A. ceylanicum* was 40.20% in cats . Assam, India, the prevalence of hookworms in dogs was found to be 98%using acombination of PCR and conventional microscopy (Traub et al., 2004b). Difference in above results may be attributed to differences of environmental and climatic conditions, number of samples was examined, methods used in their diagnosis and poor animals health.

Sequence of 18S RNA Gene and Phylogenetic Analysis

The present study was the first study on *Ancylostoma spp* genotypes that isolated from domestic dogs in Iraq. Based on available information obtained from NCBI GenBank. Three samples selected randomly and send to NICEM co. (Seoul, South Korea). The sequences have been registered in NCBI under accession numbers (GenBank accession no. MH508247.1), (GenBank accession no. MH508246.1),(GenBank accession no. MH508245.1) to *Ancylostoma caninum , Ancylostoma duodenale and Ancylostoma ceylanicum.* For phylogenic analysis. Comparative analysis 18S Gen sequenences Iraq of *Ancylostoma spp* with global breedsof *Ancylostoma spp* was similarities of 100%-97.7%. (GenBank accession no. MH508247.1), Iraq of *Ancylostoma caninum* was similarities of with (GenBank accession no. JQ812694.1), USA , (GenBank accession no. AJ920347.2), Poland, (GenBank accession no. KP844735.1), Australia, (GenBank accession no. KC755028.1), China, and(GenBank accession no. MF371322.1), Brazil respectively.The (GenBank accession no. MH508245.1) Iraq of *Ancylostoma Ceylanicum* was similarities 0f with (GenBank accession no. DQ464371.1) Poland ,(GenBank accession no. LC036567.1) Guinea and(GenBank accession no.JF960369.1) Malaysia. And. (GenBank accession no. MH508246.1) Iraq *Ancylostoma duodenale* were grade in similarities with(GenBank accession no. KU996371.1) India, (GenBank accession no. AB504715.1) Thailand and (GenBank accession no. EU344797.1) China.

The result of phylo00genic tree show similarities between Iraq strain of *Ancylostoma spp* that isolated from domestic dogs and globale strain may demonstrate rapprochement related to ancestral propinquity This are in line with which who found(Ngui *et al* ., 2012) .The existence of resemblance between the breeds that have been isolated in Iraq and the world breeds that have been isolated in groups far from Iraq may be due to related to same group or breed because of import of domestic dogs and guard dogs from these countries this was agreed with(Abubucker *et al* .,2008; Yang *et al* ., 2012).

REFERENCES

1. Abere T, Bogale B, Melaku A: Gastrointestinal helminth parasites of pet and stray dogs as a potential risk for human health in Bahir Dar town, north-western Ethiopia, Vet World. 2013; 6: 388-392.
2. Abubucker S, Martin J, Yin Y, Fulton L, Yang S P, Hallsworth-Pepin K, Mitreva M :The canine hookworm genome: analysis and classification of *Ancylostoma caninum* survey sequences. Mol Biochem Parasit 2008;157: 187-192.
3. Ahmed WM, Mousa WM, Aboelhadid SM, Tawfik, MM :Prevalence of zoonotic and other gastrointestinal parasites in police and house dogs in Alexandria, Egypt. Vet World. 2014;7: 275-280.
4. Coles EH: Veterinary clinicaly ., pathology ,2edth.W,B.Sanunders comp., Philadelphia:1974: pp474.

5. Fontanarrosa M F, Darío V, Julia B, Diego F E:An epidemiological study of gastrointestinal parasites of dogs from Southern Greater Buenos Aires (Argentina): Age, gender, breed, mixed infections, and seasonal and spatial patterns. Vet. Parasitol. 2006; 136:283-295.
6. Hadi A M, FarajAA: Prevalence of gastrointestinal Helminthes and protozoa among stray dogs in Baghdad. The Iraqi J Vet Med. 2016; 40:1-4.
7. Hasson RH : Stray dogs internal parasites from Baquba City, Diyala Province, Iraq. J Nat Sci Res.2014; 4: 30-38.
8. Jenan M K, Shaimaa A M, Nuha K K: Epidemiological Study of Zoonotic Gastrointestinal Parasites in Police and House Dogs in Baghdad governorate/ Iraq. MRVSA. 2015 ; 4: 18-26.
9. Jittapalapong S, Inparnkaew T, Pinyopanuwat N, Kengradomkij C, Sangvaranond, A, Wongnakphet S : Gastrointestinal parasites of stray cats in Bangkok metropolitan areas, Thailand. Katsetsart J. Natl Scie. 2007: 41, 69-73.
10. Kaewthamasorn K, Niwetpathomwat A , Assrasakaron S,Wongsamee S, Tiawsirisup SAP: Surveillance of canine gastrointestinal parasites fecal samples from public areas of Bangkok, Thailand. J. Anim. Vet. Advan. 2006; 5: 1209–1213.
11. Klimpel S, Heukelbach J, Pothmann D, Ruckert S : Gastrointestinal and ectoparasites from urban stray dogs in Fortaleza (Brazil): High infection risk for humans, Parasitol. Res. 2010; 107: 713-719.
12. Liotta, JL, Youn H, Aksel S, Bienhoff SE, Bowman DD: Prevalence of Ancylostoma braziliense in Dogs From Alachua and Marion Counties, Florida, United States. J Parasitol. 2012b; 98: 1039-1040.
13. Little, Susan E, Eileen M J, David L, Renee PJ, Mark E P, Byron L B, Dwight D B, Scott M, Todd T, Lon R, David A : Prevalence of intestinal parasites in pet dogs in the United States. Vet Parasitol.2009; 166:144-152.
14. Liu Y, Zheng G, Alsarakibi M, Zhang X, Hu W, Lu P, Lin L, Tan L Luo Q, Li G : Molecular Identification of *Ancylostoma caninum* Isolated from Cats in Southern China Based on Complete ITS Sequence. BioMed Res Int. Article ID 868050, (2013).6 pages http://dx.doi.org/10.1155/2013/868050.
15. Lucio-Forster A, Liotta JL, Yaros JP, Briggs KR, Mohammed, HO, Bowman DD: Morphological differentiation of eggs of Ancylostoma caninum,Ancylostoma tubaeforme, and Ancylostoma braziliense from dogs and cats in the United States. J Parasitol.2012;98, 1041-1044.
16. Mirzaei M : Prevalence of Stray Dogs with Intestinal Protozoan Parasites in Iran. American J Anim Vet Scie. 2010; 5 : 86-90.
17. Ngui R, Lim YA, Traub R, Mahmud R, Mistam MS : Epidemiological and genetic data supporting the transmission of Ancylostoma ceylanicum among human and domestic animals.PLoS Negl Trop Dis..2012;6:15-22.
18. Oliveira-ArbexAP, David EB, Oliveira-Sequeira TCG,Katagiri S, Coradi ST, Guimara S: Molecular identification of *Ancylostoma* species from dogs and an assessment of zoonotic risk in low-income households, Sa˜o Paulo State, Brazil. J. Helminthol. 2016;88:1-6.
19. Oliveira-Sequeira T C G, Amarante A F T, Ferrari T B, Nunes, L C : Prevalence of intestinal parasites in dogs from São Paulo State, Brazil. Vet Parasitol. 2002; 103, 19-27.
20. Ramírez-Barrios Roger A, Barboza-Mena G, Muñoz J, Angulo- Cubillán F, Hernández E, González F, Escalona F: Prevalence of intesetinal parasites in dogs under veterinary care in Maracaibo, Venezuela. Vet Parasitol. 2004; 121:11-20.
21. Rehman A , Akhtar R, Akbar H , Riaz F , Rashid I , Shehzad W, Islam S , Bajwa AA , Waqas M :First report of the molecular detection of *Ancylostoma caninum* in Lahore, Pakistan: the threat from pets.Vet Med. 2017; 62: 559–564.

22. SAS.2010.SAS/STAT Users Guide for Personal Computer. Release 9.1. SAS Institute, Inc., Cary, N.C., USA.Shore Garcia, L. Practical guide to diagnostic parasitology. ASM press, 349.
23. Savioli L, Smith H, Thompson A:Giardia and Cryptosporidium join the 'neglected diseases initiative'. Trends parasitol. 2006; 22, 203-208.
24. Traub RJ, Robertson ID, Irwin P, Mencke N, Thompson RCA: The prevalence, intensities and risk factors associated with geohelminth infection in tea-growing communities of Assam, India. Trop Med Intl Health.2004b; 9: 688–701.
25. Traub RJ, Robertson ID, IrwinP, Mencke N , Thompson RCA :Application of a species specific PCR-RFLP to identify Ancylostoma eggs directly from canine faeces. Vet. Parasitol. 2004b; 123:245–255.
26. Yang Y, Zheng J, Chen J : Cloning, sequencing and phylogenetic analysis of the small GTPase gene cdc-42 from Ancylostoma caninum. Exper parasitol.2012; 132: 550-555.
27. Zelalem G and Mekonnen A. (2012). Prevalence of Gastrointestinal Helminthes among Dogs in Bahir Dar Town, Ethiopia. World Appl. Sci. J. 19 (5): 595-601. Mirzaei M : Prevalence of Stray Dogs with Intestinal Protozoan Parasites in Iran. American J Anim Vet Scie. 2010; 5 (2): 86-90.

Table 1: Infection rate of intestinal parasitesin domestic dogs

Parasites	Positive	(%)	Chi-square value	P
Ancylostoma spp	20	(11.11%)	16.49	0.005
Toxocara spp	12	(6.66%)		
Trichuris vulpis	8	(4.44%)		
Taenia spp	4	(2.22%)		
Giardia spp	10	(5.55%)		
Isospora spp	6	(3.33%)		
Total	58	(32.22%)		

Table 2: Infection rate of intestinal parasitein domestic dogs according to age

Age	No .exam	No.infected	(%)	Chi-square value	P
<6 months `	90	40	44.44	12.31	0.0004
≥ 6 months	90	18	20.00		
Total	180	58	32.22		

P<0.05

Table 3: Prevalence of intestinal parasite in domestic dogsaccording to sex

Sex	No.exam	No. infected	(%)	Chi-square value	P
Male	90	28	31.11	0.10	0.74
Female	90	30	33.3		
Total	180	58	32.22		

P > 0.05

Table 4: Infection rate of intestinal parasites in dogs by PCR

Test	No. Examined	Positive	Percentage (%)
PCR	100	30	30

Figure 1: Show egg of *Ancylostoma*(X10*)*

Figure 2: Show eggs of *Toxocara spp* (X10)

Figure3: Show eggs of *trichuris vulpis* (X10)

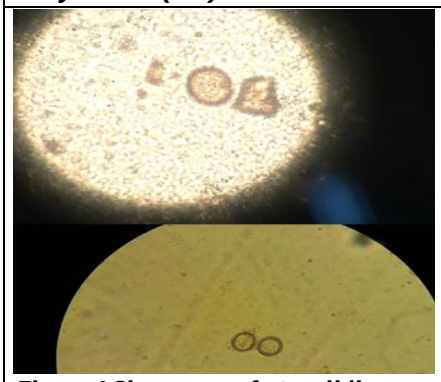

Figure 4:Show eggs of *taeniidi spp* (*X*10)

Figure 5: Show cystof *Isospora spp* (X40)

Figure6: Show cyst of *Gardia* spp (X 40)

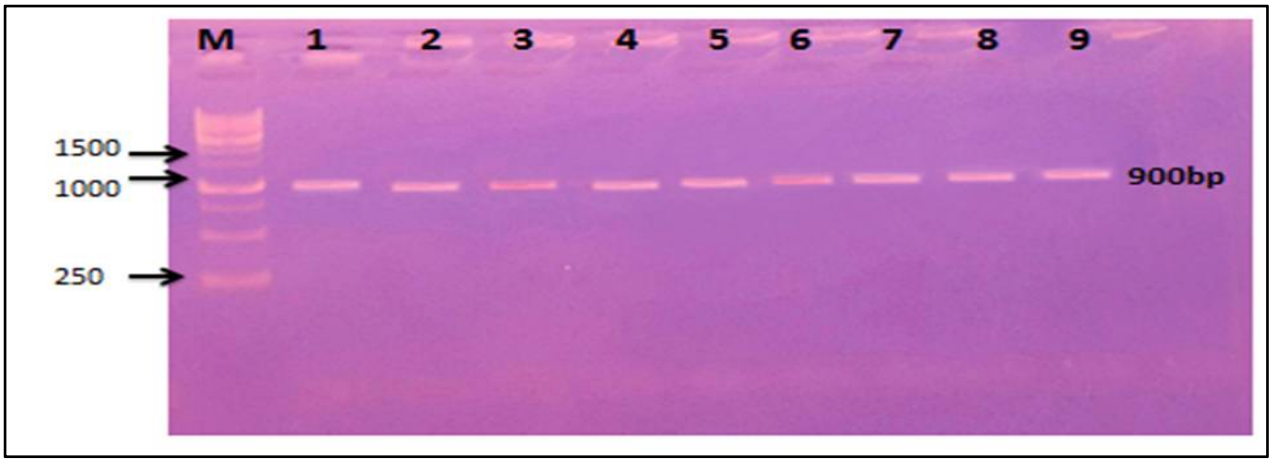

Figure 7: Gel electrophoresis of PCR product of *18 S gene (*900bp), for *Ancylostoma spp* using 1% agarose gel at 60volt /cm for 1 hour. Lane 1- 9: PCR product positive for *18 S* gen

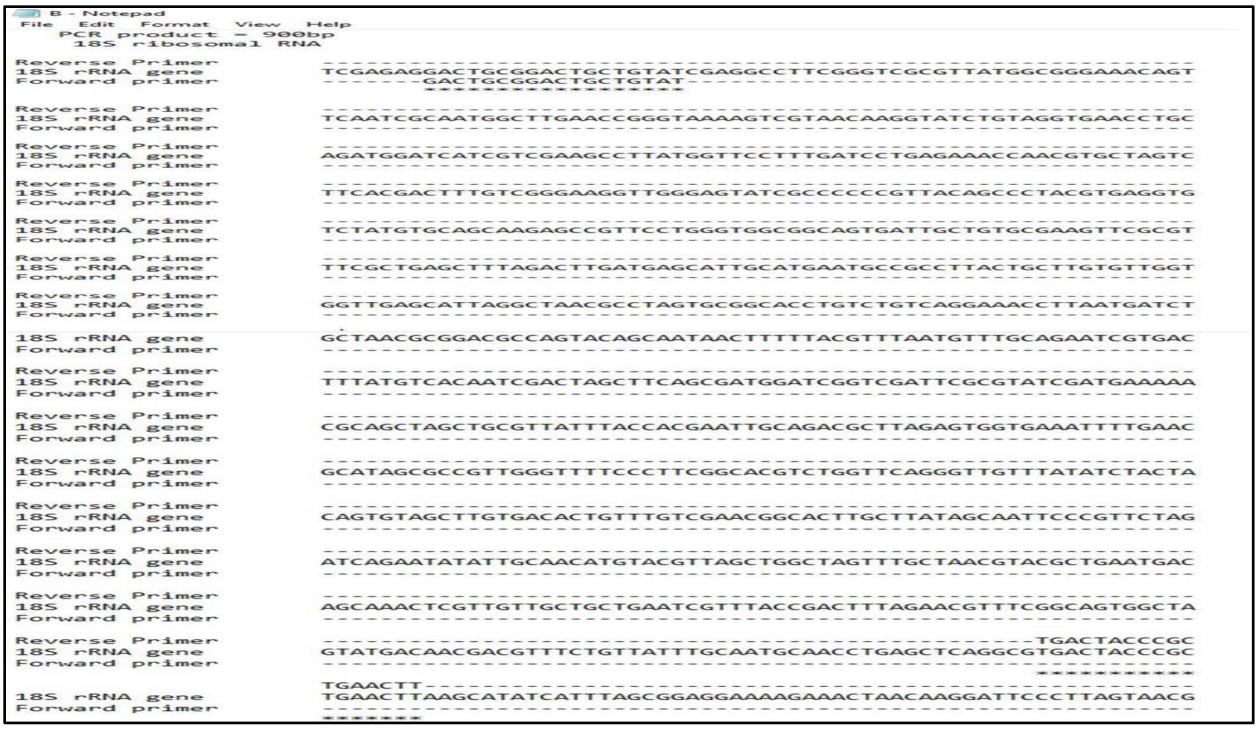

Figure 8: The confirmation of PCR Product size (900 bp) by alignment of 18SrRNA gene with Forward and Reverse primers.

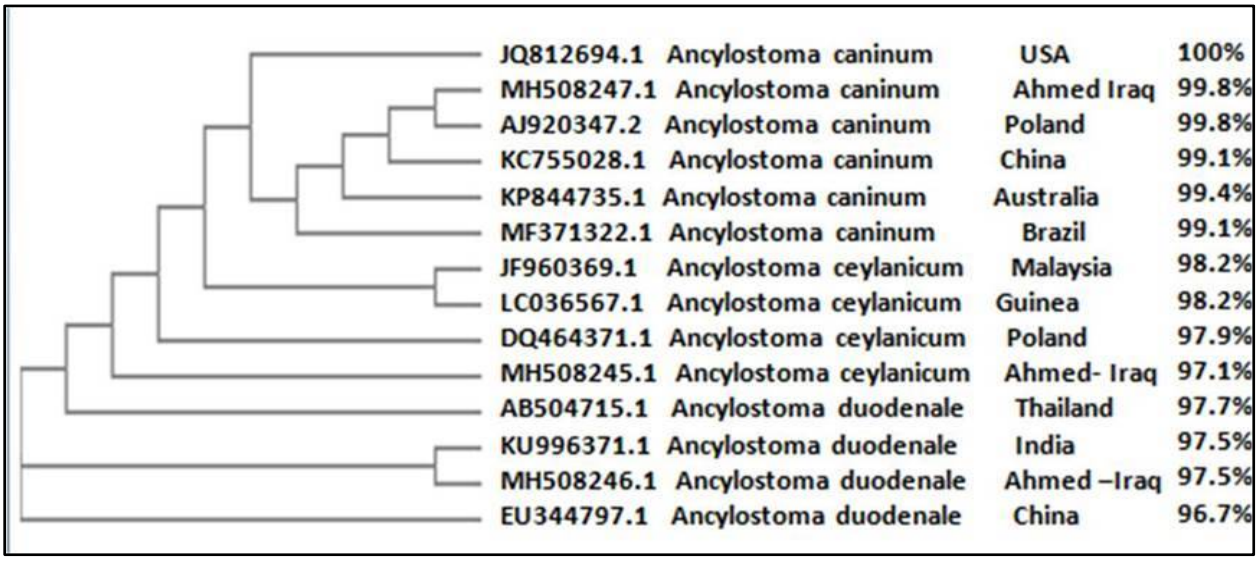

Figure(9):Phylogenic tree inferred the degree of relatedness between 18SrRNA sequence deposited in the international nucleotide bank sequence database(NCBI) furthermore this identification was verified via 18SrRNA sequence of the three different sequenced parasites using Blastn algorithm. Sequence recorded in the GenBank under accession numbers MH508247, MH508246, MH508245 to *Ancylostoma caninum, Ancylostoma duodenale and Ancylostoma ceylanicum,* respectively in dogs

Indian Journal of Natural Sciences www.tnsroindia.org.in ©IJONS

Vol.9 /Issue 50 /October / 2018 *International Bimonthly* *ISSN: 0976 – 0997*

RESEARCH ARTICLE

Role of Nox and O_3 in Micro Climate Change: Policy Dimension and Human Facet Impact for Quetta (Pakistan)

Safdar ShahKhan[1]*, Faiza Akhtar[2], Saleem Iqbal[3], Malik M. Akhtar[4], Badar Moghira[5] and Moiz Uddin[6]

[1]Department of Environmental Management, General Muhammad Musa Government Degree College, Quetta.
[2]Department of Environment Management and Policy, Balochistan University of Information Technology, Engineering & Management Sciences (BUITEMS**)**, Quetta, Balochistan,
[3]Department of Mathematics, University of Balochistan.
[4]Department of Environment Management and Policy, Balochistan University of Information Technology, Engineering & Management Sciences (BUITEMS**)**, Quetta, Balochistan,
[5]Department of Environment Management and Policy, Sarghoda University Lahore Campus, Lahore
[6]Department of Physics, University of Balochistan.

Received: 22 June 2018 Revised: 26 July 2018 Accepted: 29 Aug 2018

*__Address for Correspondence__
Safdar ShahKhan
Department of Environmental Management,
General Muhammad Musa Government Degree College,
Quetta, Pakistan.
Email: safdarshahkhan@ymail.com

ABSTRACT

Climate change poses risk to millions of peoples due to extreme weather events, crop failures and other related emergencies. Nowadays, these events are occurring with greater frequency. In climate change researchmore emphasis is given to temperature and CO_2 but other pollutants are also of prime importance. Therefore to improve the understanding of the complex interactions of the climate, ecosystems, and human activities, the research study explores the effects of NOx and O_3 along with other climatic parameters at micro climate change level in Quetta valley.Data was collected at twelve monitoring sites in Quetta city. The result of the study indicate rise in annual maximum temperature is 1.10°C and precipitation data indicates net change is 8.45 mm (based on recorded data on temperature and precipitation 1901-2015).The correlation between O_3 and NOx was 1:1.57 respectively and CalculatedMoment Correlation Co-efficient between NOx and O_3 is r = 0.980. The data was analysed using geo-statistical analyst tool in ArcGIS. The paper discuss the role of micro climate changes and its effects on human. At the end a strategic management plan is suggested to control the effects of micro climate change in Quetta city.

Key words: Micro Climate Change, Nitrogen dioxide, Ozone, Quetta, Management Policy Direction.

INTRODUCTION

Ephemeral Primer

Micro climate changes at global and regional levels are of prime concern for the environmentalists. Micro climate indicates expected weather conditions at a given location over time.The modifications in the micro climate system are caused by changes in forcings which is either positive (lead to warming) or negative (lead to cooling) (Doherty et al., 2013). Micro climate forcing accrued due to natural or anthropogenic process. Changes in natural forcings have always occurred but now anthropogenic forcings have accelerate the impact of micro climate change at local level(Guenther et al., 2012). The key factors responsible for anthropogenic forcing are population explosion, rapid industrial development, resource depletion and alteration in the atmospheric chemical composition. The major pollutants responsible for the deterioration atmicro level are Carbon Dioxide, Oxide of Nitrogen (NO_x), Ozone (O_3), Oxides of Sulphur (SO_x), Carbon Monoxide, Hydrocarbon (HC) and Particulate Matters (PM) (Prather and Ehhalt, 2001). Continued emissions of these pollutants make change in the atmospheric patterns—in the size, natural climate variations, and local weather for example—La Niña events changes weather patterns in some regions and make these regions wetter and cooler. In a similar way, Polar strong winds contribute to irregular colder winter in North Atlantic Oscillation which has contributed several recent cold winters in Europe, Eastern North America and northern Asia (Royal Society Publication, 2009).

Impact of Climate Change at Global Level

Climate change impact due to rise in sea-level has been determined by expansion in water volume, as water warms-melting of glaciers occurred in most parts of the world. The rise in sea level at any location depends on a variety of factors; such as regional geological processes, rebound of the land weighted down by ice sheets, rise or sink of the land and changes in winds pattern that are moving ocean water toward coasts. Occurred fluctuations also influence the amounts of water stored on land. The effects of rising water level are felt most acutely in the increased frequency and intensity of occasional storm surges. If greenhouse gases continue to increase on their current trajectories, it is feared that sea level further rises from 0.5 to 1 m (1.5 to 3 feet) by 2100. But rising sea levels will not stop in 2100; as the sea continues to take up heat and glaciers continue to melt faster it has drastic effects in subsequent centuries. In response to continue warming; the Greenland and Antarctic Ice Sheets will continue to lose mass, whereas the colder parts of Antarctica could start to gain mass as they receive more snowfall from warmer air that contains more moisture (Cornwall, 2016).

The climate change due to rise of 2°C is irresistible and intolerably dangerous that causes multiple dreadful impacts on huge human population living on planetary ecosystems (IPCC, 2007). As glaciers are the source of fresh water that provide crops for 50 million people if the glaciers begin to melt quickly; farming could collapse in many parts of Africa and Asia due to flooding. More than 10 million extra people are affected by Coastal flooding. Further; 300,000 people are affected every year by climate-related diseases such as malaria and diarrhoea (Moore and Semple, 2005). One third of the world's species will become extinct as the 2°C rise occur and it is going to be difficult for other habitats to adapt these changes quickly. Water becomes scarcer in many part of the world, with the increases in temperature coinciding with a peak in world population and the extra demand on food and water resources. As consequences of 2°C which stands for strong chance of drought and storm and pose a threat to the civilized society, leading potentially to the conflict and suffering that go with failed states and mass migrations.

The climate changes also have threatening effects on agriculture yield, Fisheries and forest; reducing productivity and income growth (ADB, 2009). Changes in climate affect irrigation requirements for all the cropping seasons. The production of rice, maize wheat, potato and other temperate crops in the past few decades have gone down about 50% (MoE, 2009) due to ever increasing water stress arising mainly from temperature rise (UNFCCC, 2007). The

fisheries sectors also depend on water. Since the solubility of oxygen in water decreases with higher temperature, it effects the fish production. Moreover, if the flow of river is reduced in dry season the freshwater migratory fish hatchlings will face a survival problem in the rivers because of increased salinity due to sea level rise (ADB, 2009). In forest; trees are captive carbon dioxide. As the world becomes warmer, the trees start releasing more CO_2 than they absorb, making the planet progressively even warmer; this will cause melting of the permafrost which would in turn give out more greenhouse gases and dieback of the forest (Kull et al., 2003). Impacts of climate change are more devastating in northern Pakistan, India and western China especially in the isolated, marginal areas such as mountains, dry lands and deserts which are deficient in natural resources.

There is strong evidence between health of the people and climate change. The implications of the planetary changes involved with climate change touch nearly every sector of health care and promotion. It is estimated that if the rise in temperature is 1°C; it would lead to loss of $ 4.18 million to the net revenue per annum. The phenomenon is already contributing to the deaths of nearly 400,000 people a year and costing the world more than $1.2 trillion, wiping 1.6% annually from global GDP. By 2030, the researchers' estimate the cost of climate change and air pollution combined will rise to 3.2% of global GDP, with the world's least developed countries forecast to bear the brunt, suffering losses of up to 11% of their GDP. The costs of protecting low-lying and coastal areas from the sea could reach 270 billion dollars a year by 2100, the third world's countries such as Bangladesh and Vietnam will have to depend on debt from rich countries to protect their land (Shamim et al., 2013). If the temperature rise to 4°C, the limits for human adaptation are likely to be exceeded in many parts of the world, while the limits for adaptation for natural systems would largely be exceeded throughout the world. The climatic distribution of those impacts will depend on regional climate shifts as well as the adaptive capacity of specific populations, with increased vulnerability among those suffering from poor health and poverty. If climatic changes continues unchecked in the region at local level, these impacts are almost certain to get worse and their impacts are felt first at national level than at global scale.

Climatic Parameters and NO_x - O_3 Relation

Temperature is chosen as the prime factor in defining the relationship between the weather and short or longer-term climate changes that create VOC and Ozone formation (Fusco, 2003). Increasing temperatures generally lead to increased VOC emissions, which is important in NOx formation, resulting in higher ozone levels (Sillman et al., 1990). Temperature serves as a proxy for meteorological conditions and defines the rates of chemical reactions important for ozone formation. In formation of ozone by absorption of sunlight involve reacting chemicals (Jacob and Winner, 2009); therefore sunny and cloudless days are more favourable to ozone formation (Murazaki and Hess, 2006). Besides temperature there are other factors responsible for climatic changes that play vital role in formation of ground-level ozone i.e. increased drought, shifts in weather patterns that lead to stagnant air events and heat waves (Sánchez et al., 2005; Isaksen, 2009). In climate change process the more emphasis is given to the temperature and CO_2 but other pollutants are also of prime important in the climate change process. Therefore to improve the understanding of the complex interactions of the climate system, ecosystems, and dependent human activities, this research see the effect of climate change due to NO_x and O_3 in Quetta Valley (Pakistan).

MATERIALS AND METHODS

The pollutants (NOx and Ozone) were measured using Mobile Pollution Monitoring Lab. For NOx an automatic analyzer 42C, made by Thermo Environmental Instrumental, USA was used for the present study. The model 42C chemiluminescence's NO-NO_2- NOx analyzer combines proven detection technology and advance diagnostics to offer unsurpassed flexibility and reliability. For Ozone an automatic analyzer Model 8810, Control Ltd, U.S.A. based on UV photometry was employed for surface ozone measurements. The data was collected at twelve different sites in Quetta valley. The duration of measurement was 15 minutes and monitoring was carried out continuously for forty

eight hours at a site and was repeated over the nine months for all the twelve seasons. In addition to these measurements the wind speed, humidity, and temperature at all sites were also recorded.

Kriging Method in GIS

The study area's topographic map (1:50,000), used to create a thematic map, contains comprehensive information about the study area boundaries, road network and towns within Quetta District. There were twelve air samples were used in ArcGIS 10.1 applying x and y coordinates. To develop NO_x and O_3 distribution zones, a Kriging method was employed in current analyses in ArcGIS environment using geo-statistical analyst tool.Kriging is useful for the development of potential contamination maps between factors and in this study NO_x and O_3 concentrations are mapped. To design the distribution map, the NO_x and O_3 concentrations in air were categorized into twelve levels using the manual method. NO_x and O_3 concentrations in air are the factor affecting air quality and leads to climate changes in local/regional system.

Research Area

Quetta is a funnel shape valley and the capital city of Balochistan, Pakistan and lies between $66^0 15' 00''$ to $67^0 15' 00''$ Easting and $30^0 00' 00''$ to $30^0 25' 00''$ Northing in the survey of Pakistan Topo-sheets 34 N/3 & 4 and 34 J/15 & 16. The main valley of Quetta or Shal proper (comprising an area of 1720 sq. km), which unites the two sides at the toe of the horse-shoe, is a parallelogram about sixteen miles by eight (khan et al., 1986). The general character of the district is mountainous. The mountains are intersected by long narrow valleys consisting of flat alluvial plains with pebbly slopes rising on either side.In Quetta city, the twelve prime locations are selected according to the guidelines provided by the UNEP for the collection of data i.e. residential, commercial and industrial areas, near high ways etc.

RESULTS

Results with Automatic Analyzer (NO_x)

Oxides of nitrogen include both nitric oxide (NO) and NO_2. Both substances are normally calculated in emissions inventories as NO_2 because NO is ultimately converted to NO_2. Therefore levels NO_x are routinely reported as nitrogen dioxide (NO_2) equivalents. The result of NOx in Quetta city is shown in table-1.

Diurnal and Seasonal Variation of NOx

The results show that Quetta has a marked maximum NO_2 concentration between 6.00 P.M. to 7.00 P.M. (18.00 hours to 19.00 hours). The level of the NO_2 rises from 8 A.M. to 7.00 P.M. and then starts declining from 8 P.M. to 7 A.M. in the morning. The level at day time lies between 21.17 ppb and 69.90 ppb. The concentration level at night time lies between 17.14 ppb to 46.65 ppb. The average concentration of NOx in Quetta Valley is 33.69 ppb. Concentrations at all sites remain relatively consistent suggesting that NO_2 concentrations are evenly distributed throughout the city i.e. average concentration at all sites is 33.69 ppb. A higher concentration was observed in the months of June/ July at site-6 i.e. 69.90 ppb. Minimum Value recorded at day is 21.17 By-pass Eastern and maximum value recorded at 46.65 on Gawaldi choak site-4. It is due the fact that this site lies at the center of the city, where the population density is high and roads are congested with high traffic density. The lowest concentration also recorded at site-11 is 17.14 ppb in the month of February. NO_2 has more concentration in summer (June/July) and gradually decreases with the arrival of winter and level arises as the blossoms spring starts. Concentration of NOx with 24 Hours Day & Night Variation in Quetta Valley is shown in figure-1.

Results with Automatic Analyzer Ozone (O_3)

Ozone (O_3) is a pollutant that is not emitted directly, but is formed as a product of very complex reaction of NO_x and Hydrocarbon in the presence of sun light. The results are shown in the table-2

Diurnal Variation andSeasonal Variation of Ozone

The results show that Quetta has a marked maximum O_3 concentration between 2.00 P.M. to 3.00 P.M. (14.00 hours to 15.00 hours). The level of the O_3 rises from 8 A.M. to 2 P.M. and then starts declining from 4 P.M. to 6 A.M. in the morning. The annual mean average level at day time lies between 17.76 ppb and 47.94 ppb. The concentration level at night time lies between 11.55 ppb to 37.82 ppb. At site-6 at Meazan Choak (Commercial) the level of average concentration of Ozone is observed to be higher as compared with other sites having maximum in the months of June/ July. It is due the fact that this site lies at the center of the city, population density is high and roads are congested with high traffic density. The lowest concentration recorded at site-2 Satellite Town (Residential Area) is 11.55 ppb in the month of October/ November. The Ozone concentration is higher due to the fact that it is also a congested area and near the main bus stand. At site-3 the average Ozone concentration is lowest however its minimum level at night is highest as compared to other two sites. Most probable cause is being an industrial site and that all the vehicular and operational activities increases and is at their peak during night. Ozone has more concentration in summer (June/July) and gradually decreases with the arrival of winter and level arises slightly as the blossoms spring starts. Seasonal average O_3 concentration ranges from 11.55 ppb to 47.94 ppb. The study shows that, even when suitable meteorological conditions occurs, levels (annual mean average is 28.89ppb) are much below the standard of WHO i.e.50 ppb to 60 ppb. The twenty four variation of O_3 is shown in figure-4 and Concentration of O_3 at day and night time at twelve sites in Quetta Valley is presented in figure-5-6 respectively. Variations of Ozone and NO_x in Quetta Valley Figure 7:

Correlation between O_3 and NO_x

For calculation of correlation coefficient between Ozone and NO_x, their seasonal average values are taken as X and Y. For n pairs of observations the following formula was employed

$$r = \frac{n\sum XY - (\sum X)(\sum Y)}{\sqrt{[n\sum X^2 - (\sum X)^2][n\sum Y^2 - (\sum Y)^2}}$$

r = 0.996

The results of the study show that there is well defined correlation between NO_x and O_3. The calculated Moment Correlation Co-efficient is r = 0.996; which is direct and positive. The twenty four hours variation of NO_x and O_3 shows the same pattern all over the year and the rising and falling ratio of Ozone and NO_x is found by a ratio of 1: 1.57. The correlation of tropospheric ozone and NOx in the environment and its transformation to O_3 are dependent on weather and climate conditions and dependent on the metrological changes; such as humidity, temperature variation, wind speed, radiations, rain, drought period, etc. Year wise average concentration of NOx and Ozone from 2005-2016 in Quetta Valley is indicated in table-4.

Micro Climate Changes in Quetta Valley-Pakistan

Climate change in the Quetta valley is occurring due to natural and anthropogenic sources. The data from 1960-2014- indicates that total rise in the annual minimum temperatures of the Quetta is 0.99 °C and the total increase in the annual maximum temperature is 1.12°C Valley (Pakistan Meteorological Department, 2015; Qamr-uz-Zaman et al., 2009). Long-term mean maximum temperature series of Quetta shows the rise of 2°C per decade and total increase is

1.25°C. Future trends indicate that there is a much larger percentage of land area showing significant change in minimum temperature (5°C) than maximum temperature. Percentile based spatial change indicates that the daily minimum temperature will become higher and weather becomes warmer as compared to the increase of daily maximum temperature in summer whereas in winter the change in maximum threshold temperature become higher.

In Quetta, Pakistan long term precipitation data (1901- 2014) is also analyzed and the net change for all the analyzed period was found 8.45 mm. However, the major change in precipitation trend was observed in the period 1955-2014 (last 60 years), which exhibited a net change of 56.4 mm which is quite significant compared to the data between 1901-1953 (first 53 years) with only 2.2 mm of change. The analysis further shows the average annual rainfall for Quetta is 212.9 millimeters (8.58 inches). Due to the shift in the weather pattern; Quetta was affected by La-Nina phenomenon from 1998 to 2001. In that period severe drought was observed in North Balochistan that received 30% less rain while South Balochistan received 60% less rain (Drought in Quetta, 2015).At the peak of the drought in year 2000, the city received just 60 millimetres (2.4 in) of rainfall, while almost no rainfall or snowfall was observed in winter season (Severe Cold Wave in Quetta, 2010.). The drought enveloped the whole country and resulted in 30% below normal rains in Pakistan. At least 1.2 million people in Balochistan mostly in Quetta Valley were affected by drought, and over 100 died, mostly because of dehydration.The average values (based on data for 100 years) of temperature, precipitation, rain, humidity over the year (on monthly basis) is given in table-5

Micro climate changes also affect the meteorological transport processes. In Quetta concentration at ground level ozone mainly relies on the meteorological condition of the environment. The spatial distribution and rate of emissions has a vital effect on the pollution levels responsible for climate change. The mountain valley has a strong influence on the prevailing winds through a direct funneling effect and creates more complex thermal circulations. The mountains also serve as barriers, which keep the pollutants with minimum dispersion and allow their levels to build up over time. Quetta valley with bowl shaped topography is a favorable site for trapping the pollutants at night time also. In morning; solar heating destabilizes the surface air as a result photochemical reaction produced ozone in the atmosphere. During summer the level are high due to high temperature and duration of sun light is longer. In winter months, comparatively low value of ozone is attributed to low ambient temperature and low UV radiation intensities (Shahkhan et al., 2004). Quetta lies outside the range of the monsoon currents. Therefore it does not have any washout effect throughout the seasons. The pollutants remain in circulation for longer period in air and settled particles are likely to be re-suspended due to dryness of weather. The wind speed also enhances this phenomenon (Shahkhan et al., 2007).

The micro climate changes also have threatening effects on agriculture yield, fisheries and forest; reducing productivity and income growth (ADB, 2009). Changes in climate affect irrigation requirements for all the cropping seasons. The production of rice, maize wheat, potato and other temperate crops in the past few decades have gone down about 50% in Quetta valley (MoE, 2009) due to ever increasing water stress arising mainly from temperature rise (UNFCCC, 2007).Fruits trees in the region are dying off on a large scale. A reduction of 50% were noted especially in Apple trees in Quetta, Mastung, northern areas of Balochistan, and date palms in Makran have succumbed to diseases. The water table due to climate change in Quetta Valley has declined to 300 feet in the last 40 years. Presently the water table is falling at the rate of 10-15 feet per year. With continued decline in the level of groundwater without adequate recharge, the soil sediments became increasingly compressed, causing the land to subside. The quality of drinking water in Quetta city is deteriorating in taste, odor, appearance, and have pathogens. In Quetta 75% of households are effected by water borne diseases and children more susceptible to these diseases. Statistics shows that 44% of the residents are affected by Diarrhea, GI 25%, Cholera 21%, Typhoid 5%, and 5% other diseases. The estimated cost of illness beared by the Quetta's residents is about Rs. 2098,808 annually. On average, annually each household is paying Rs. 10,494 for water borne diseases cost (Butt and Khair, 2014). Besides that increases of 20 % in Eye diseases have been reported in Balochistan (Ophthalmological Society of Pakistan, 2017). Asimpacts of climate change are more devastating in isolated, marginal areas such as mountains, dry lands and deserts which are deficient in natural resources and Quetta lies in such region which have deficient of resources,

have dry mountains, arid land and deficient of water resources therefore worst effects of climate change are observe in Quetta valley.

Beside natural phenomena major anthropogenic factor responsible of Micro Climate Change is the contribution of transport sector, which is the main source of NOx generation in Quetta Valley. The city is designed only for 50,000 vehicles but there are more than 200,000 vehicles plying on the roads in Quetta city. These vehicles emits more NOx in the atmosphere due to the poor maintenances of engines, high loading factors, improper fuel, lube mixture, substandard silencers and the use of smuggled oil/petrol/diesel in both light and heavy vehicles-The smuggled fuels are of low standard and have high Sulphur /Lead contents (Shahkhan, 2007). Beside that the secondhand vehicles engines (diesel and petrol) are imported and smuggled from Japan and other European countries after their economically useful life is over and these engines are rebuilt/overhaul or reconditioned for use in the Quetta city. These types of vehicles produce more NOx due to imperfect overhauling and low technological availability. Further city's roads are narrow and congested which created frequent traffic jam. The traffic jams also occurred due to the mixing of motorized and non-motorized mode of transport. In Quetta there are thousands of hand carts, donkey carts, horse carts plying on the roads and they do not observe strict traffic laws and when they mix within the traffic, they create frequent traffic jams. In frequent traffic jams, the drivers give unnecessary acceleration to the engine and produce NOx and other pollutants. The insufficient and non-effective pollution control and poor law and order condition has also aggravated this situation. In addition to fugitive emission from vehicles from factories (bricks kilns, stone crushing plants, marble cutting and polishing plants, ceramic, etc.), and construction activities are the other major sources of Climate Change in Quetta city.

The cause and consequences of micro climate change are often localized and its affects are felt first at the local level and it affects local people. These localized impacts then cascade to have national and international ramifications and felt by the people around the globe. These weather systems usually travel over the earth's surface and allow the atmospheric effects to move downwind for several hundred kilometers (Air Quality 2003).For example in Asia, major weather patterns are conducive to trans-boundary transport of air pollutants from land to sea and reverse in summer. In Quetta Valley the dust fall occurs in summer; this dust is transported hundreds of kilometers from the desert of Iran and Turkey to the arid zones of Balochistan (Pakistan). Thus pollutants are not restricted to one region and are carried out from country to country in the region.In the last decade Pakistan has faced extreme weather patterns, and consistently remained in the top 10 Global Climate Risk Index. Furthermore, research by German-watch reveals that between 1994-2013 Pakistan lost $ 3,988.92 million (annual-average), or approximately 0.77 percent of its annual GDP, as a direct or indirect consequence of extreme climatic conditions (Farooqi and Aftab, 2015).At global scale, the phenomenon is responsible for causing400,000 deathsper year and costing the world more than $1.2 trillion, wiping 1.6% annually from global GDP. By 2030, it is estimated that climatic related cost will be double i.e. 3.2% of world GDP, with the world's least developed countries forecast to bear the brunt, suffering losses of up to 11% of their GDP. If climate change continues unchecked, these impacts are almost certain to get worse. Therefore it is the responsibility to manage such risks through the linkage of local, national, and global scales.

Policy Recommendation to Manage Micro Climate Change

In developing cities such as Quetta Pakistan; the sources are natural and anthropogenic. The natural sources can be minimized but anthropogenic sources can be controlled through proper planning. In Quetta city the growth had been unplanned and haphazard which results in many environmental and health issue creating dissatisfaction among the residence of the city. The anthropogenic sources identify for the cause of climate degradation are urbanization and vehicular density. Therefore the study recommends strategic guidelines for the management of micro climate change for cities that are effected by the urbanization and vehicles pollution.

- Renewal Plan for management of micro climate change reduction in Quetta City is formed by the concept of "Garden City". In semi-arid zones like Quetta which have scarcity of rain fall and lies in non-monsoon range.

Therefore concept of urban forestry should be introduced in Quetta city. Special emphasis will be given on plantation of trees that require less water with broader leaves and public should also generate green areas that will also helpful in controlling the micro climate change. It will also give beautiful look to the city and enhanced ascetic sense within people and that will also reduce tension among the general public.

- In Quetta the weather is dry and have low rain. Therefore to reduce the effect of climate change agriculture sector should focus on breeding for high yielding; heat- and cold tolerant; drought resistant; and short duration agriculture and food varieties. The water conserving technologies like drip irrigation, sprinkler, and precision levelling etc. can be applied in Quetta valley.
- Development and promotion of a floriculture strategy is required for Quetta Valley to abate the effects of micro climatic changes. The concept can be enhanced by applying the technique of growing flowers in plastic tunnels and placed it at different places in Quetta city. This will reduce the effect of pollution effects especially dust blown across the Quetta Valley and control the climate change. Floriculture will also improve the socio-economic conditions of farmers.
- Proper urban planning is the key for micro climate change reduction. Poor urban planning resulting in the close proximity of industry to residences has led to increased climate change' effects in residential areas. Improvement should be made in the building codes. The buildings constructed without rules and total absence of squares, green areas, parks and gardens should be demolished. The unauthorized interventions on buildings and on public spaces caused a tightening of services roads and the increase in the traffic jams in the city. Therefore the building codes must be applied or if they have any they short come should be modified according to the new situations.
- In micro climate changes the main anthropogenic source of NOx and O_3 is due to vehicular emission. The Vehicular pollution can be checked by regular tune up of engine, in time oiling and proper maintenance will also reduce the effect of NOx and O_3, installing catalytic converter, avoiding by using smuggle diesel or petrol; which is more polluting and contain high Sulphur and Lead ratio, by engine modification to have fuel efficient lean mixtures to reduce the NOx and O_3 effect and other pollution produced. Government should ban the import of second hand engine from Japan or other European countries. As most of the engine are old and completed their economically useful life. They generated more NOx, O_3 and other types of pollution. Government should give incentives for the replacement of old vehicles with new ones by tax reduction plan. Provincial EPA authorities work together Traffic police for emission testing programs to reduce NOx and O_3 pollution in Quetta city and remove faulty and unsafe vehicles from roads.
- To minimize the effects of micro climate change technology based solution should be adopted such as to develop comprehensive road network GIS maps for monitoring the traffic flow. The GIS monitoring program should be installed in the vehicles that shows the traffic situation in the area. Government should gave subsidy and reduce the internet/ GIS charges especially on GIS vehicular instruments. This will help to avoid the frequent traffic jam and unnecessary accelerating the vehicles producing more NOx and O_3.
- Plan and implement transport solution is another strategy to control the micro climate changein developing cities. To establish traffic databases or inventory profiles of roads and identify congested road sections and intersections that showing high population density and high usage of public and non-motorised transport. The government should promote walking; cycling, buses, mass transit, and other less polluting public transport alternativesbecause in developing countries due to urbanization the vehicular density on the roads are growing very fast. A decline in traffic flow, particularly through the promotion of public transportationsuch as use of railways, subways, metro bus services and use of non-fuel means of transportation- bicycles. This will also resolve the problem of climate changeand significant level of NOx and O_3reduction in the area.
- In future planning the government should make laws for roads planning keeping in mind the population increase. The designed future planned roads must have minimum width of 320 feet or more, the roads are design two ways. Separate road lane for slow moving vehicle may also be constructed. The existing roads can

be improved by imposing the traffic management plans, effective road maintenance areuseful in reducing NOx and $O_3$from existing roads networks. Ban on motorized and non-motorized traffic should be imposed on roads especially donkey-horse carts, to avoid frequent traffic jams.

- For the management for climate change, the most important is the strict implementation of law in order to control the climate change menace. Ambiguities in the law should be avoided.
- As the micro climate changes due to NOx and O_3 effects the human health. Therefore improve surveillance by developing health information systems to rapidly collect, share and disseminate information relevant to micro climate change using electronic means and mobile phone technology. Use this intelligence to identify critical areas for research.
- Designing and executing policies to mitigate and combat the micro climate change impacts, relying hugely on institutional set up, is responsibility of federal and provincial level ministries and departments. Effective and enhance role of EPA and other government organizations are very important in controlling the climate changeespecially in growing urban city. These organizations can give the permission of the projects such as industrial zones, residential projects, silence zones etc. after proper environment impact assessment studies. They can lounge knowledge and awareness program, which is a key for change and in public awareness programs they highlight the ill effects of climate changeon the society and on the environment. Participation of the commonman is needed in process of controlling the climate changeproblem. There is also need for education and capacity building for stakeholders involved in policy and planning development.
- Technical assistance should be provided by the developed nations to upgrade capacity of developing countries to handle the micro level climate change management. Effective research is essential to find the potential solutions forclimate change**.**If we rectify the micro climate change at local or small level than the global climate becomes healthy and many of our problems do not exist.

CONCLUSIONS

Environmentalists warned climate change as “threat multiplier”, which intensify already acknowledged security threats such as resource scarcity, disease, drought and displacement of the population and biodiversity. In Quetta; due to high urbanization and density influx of population, there already exist a heavy burdenof environmental stress on land and other natural resources, leading to severe degradation of the resources. Erratic and intensive rains, changes in precipitation patterns, late monsoons, dry winters, prolonged dry spells and increases in temperature enhance the phenomena of climate change and causes severe destruction in the environment of Quetta Valley. Additional pressure due to climate change will be difficult to sustain. Unfortunately, the impact of climate change is more felt in the developing countries which have inadequate capacity, resource shortage, and poor physical and institutional infrastructure to handle with and timely respond to the impacts of climate change. Currently there is no quick fix through technology to control the effects of climate change. The quick fix only occurs through the modification in our behaviour, if large number of people take appropriate steps, including supporting governmental regulations aimed at reducing greenhouse gas emissions it will slow the pace of climate related disaster in near future. At small-scale the impact of microclimate management measures is similar in diverse locations around the globe.But there is a necessity to observe microclimatic characteristics at multiple scales and consider cumulative actions, rather than to simply assess the importance of microclimate independently at each scale.

REFERENCES

1. ADB, 2009. Building climate resilience in the agriculture sector in Asia and in the Pacific. Asian Development Bank, Annual Development Report, p. -9.

2. Air Quality in Asia and the Pacific, 2003. *An analysis in relation to national and international standards, Economic and social commission for Asia and Pacific*, pp-65-67,
3. Butt M. and Khair S. M., 2014. Cost of Illness of Water-borne Diseases: A Case Study of Quetta. *J. App. Em. Sc. Vol 5, Issue 2, pp-133-146.*
4. Calderon G.L., Mora T.A, Fordham, Valencia S.G., Chung, C.J, Rodriguez, A.A.,2003. Respiratory damage in children exposed to urban pollution *Pediatr pulmonol*, pp-148-61,
5. Cornwall W**.,** 2016. Efforts to link climate change to severe weather gain ground *Science* Vol. 351, Issue 6279, pp. 1249-1250 DOI: 10.1126/science.351.6279.1249
6. Deepak P., Sapkota B., Manohar L., Kaga S.A., Kondo A. and Inoue Y., 2006. Ground level ozone concentrations and its association with NOx and meteorological parameters in Kathmandu valley, Nepal, *Atmospheric Environment* 40:8081-8087
7. Delfino R.J., Murphy M., Becklake, M.R., 1998. Emergency room visits for respiratory illness among the elderly in Mouteral: Association with low level ozone exposure, *Environ. Res Sect* A:66-77,
8. Derwent, R.G., Jenkin, M.E. Saunders, S.M. Pilling, M.J. Simmonds, P.G. Passant, N.R. Dollard G.J., Dumitrean P. and Kent, A., 2003. Photochemical ozone formation in North West Europe and its control, *Atmospheric Environment* 37 (14):1983–1991,
9. Doherty R. M., Wild O., Shindell D. T., Zeng G., MacKenzie I. A, Collins W. J., Fiore A. M., Stevenson D. S., Dentener F. J., Schultz M. G., Hess P., Derwent R. G., and Keating T. J., 2013. Impacts of climate change on surface ozone and intercontinental ozone pollution: A multi-model study, *Journal of Geophysical Research: Atmospheres* 118:1–20, doi:10.1002/jgrd.50266
10. Drought in Quetta". UN.org.pk. Retrieved 31 July 2015.
11. Farooqi H. K. and Aftab, I., 2015. The Climate Club. THE NEWS Paper, December, 13, 2015, retrieved on 16 February 2016.
12. Fusco, A.C. and Logan, J.A., 2003. Analysis of 1970-1995 trends in tropospheric ozone at Northern Hemisphere mid-latitudes with the GEOS-CHEM model, *J. Geophys. Res*.,45-60
13. Godlee, F., Walker, A., 1992. "Health and the environment", *British Medical Journal*, London, 47:321-54,
14. Guenther, A. B., Jiang, X. Heald, C. L. Sakulyanontvittaya, Duhl T. Emmons, L. K. and Wang X. 2012. The Model of Emissions of Gases and Aerosols from Nature version 2.1 (MEGAN2.1): An extended and updated framework for modeling biogenic emissions, *Geosci. Model Dev*.5:1471–1492, doi:10.5194/gmd-5-1471-2012.
15. IPCC, 2007. Climate change 2007: *The physical science basis. IPCC working group I fourth assessment report: summary for policymakers*, IPCC, Geneva
16. Isaksen, I. S. A., 2009. Atmospheric composition change: Climate chemistry interactions, *Atmos. Environ*.43:5138–5192, doi: 10.1016/j. *atmosenv*.2009.08.003.
17. Jacob, D.J., and Winner, D.A. 2009. Effect of climate change on air quality. *Atmospheric Environment* 43(1):51–63.
18. Kennet W. and Cecil F.W., 1998. *Air pollution Its origin and control*, Harper Collins Publishers, pp-371-74,
19. Khan S.N., Younas M., Mohsin A. Kazim & Hussain S.A., 1986. *Environmental geology, mineral, raw material and aggregate resources of Quetta valley, Balochistan, Pakistan* P- 1-2 GSP Rec. Vol. LXXVI- Environmental Geology.
20. King, J.S., Pregitzer, K.S., Zak, D.R., Sober, J., Isebrands, J.G., Dickson, R.E., Hendrey, G.R. and Karnosky, D.F., 2001. Fine-root biomass and fluxes of soil carbon in young stands of paper birch and trembling aspen as affected by elevated atmospheric CO_2 and tropospheric O_3. *Oecologia* 128:237-250.
21. Kull, O., Tulva, I. and Vapaavuori, E., 2003. Influence of elevated CO_2 and O_3 on Betula pendula Roth crown structure. *Annals of Botany*91: 559-569.
22. Liu, H. Jacob, D.J. Bey, I. Yantosca, R.M. Duncan, and Sachse, G.W., 2003. Transport pathways for Asian pollution outflow over the Pacific: Inter B.N. annual and seasonal variations*, J. Geophys. Res.*, 674-686
23. MoE. 2009. *Climate Change Vulnerabilities in Agriculture in Pakistan*. Ministry of Environment, Government of Pakistan, Annual Report. pp.1-6.
24. Moore G.W.K. and Semple, J.I.,2005. A Tibetan Taylor cap and a halo of stratospheric ozone over the Himalaya, *Geophysical Research Letters*, vol. 32 pp-1–4

25. Murazaki, K., and Hess, P., 2006. How does climate change contribute to surface ozone change over the United States?, *Journal of Geophysical Research*, vol. 111:D05301. doi:10.1029/2005JD005873.
26. O-Nei MS, Loomis D and Borja Aburto, 2004. Ozone area social conditions and mortality in Maxico City, *Eviron. Res* pp- 234-42,
27. Ophthalmological Society of Pakistan, Quetta, The national conference on eye diseases, organized by the 17 September, 2017
28. Pak-EPA (Pakistan Environmental Protection Agency), 2007. "Ambient Air and Water Quality Investigation in Quetta." Pakistan Environment Programme. http://www .environment.gov.pk/PUB-PDF/Ambient%20AW%20Quetta.pdf.
29. Pak-EPA (Pakistan Environmental Protection Agency), 2015. "Daily PM2.5, SO2, NO2, O3, and CO data collected by the Pak-EPA." Unpublished report. Islamabad.
30. Pak-EPA/JICA April, 2006. Measurement of NO2 concentration in different cities of Pakistan using Diffusion samplers (Karachi, Islamabad, Peshawar, Lahore and Quetta), April 2006, Pak-EPA/JICA
31. Pakistan Meteorological Department, 2015. Pakistan Meteorological Department. Retrieved 25 July 2015.
32. PMD-GCISE, 2007. *Pakistan Meteorological Department & Global Change Impact Studies Center joint project report on climate change and its impacts*, June 2007
33. Prather, M. and Ehhalt, D., 2001. *Atmospheric chemistry and greenhouse gases, in Climate Change*: The Scientific Basis: The IPCC Working Group I Third Assessment Report, Cambridge Univ. Press, New York,.
34. Qamar-uz-Zaman, Arif, M., Rashool, G., Afzaal, M., 2009. *Climate change indictors of Pakistan*, Pakistan Meteorological Department, technical report, PMD No. 22/2009, August 2009.
35. Royal Society Publication, 2009. Climate Change Evidence & Causes: *An overview from the Royal Society and the US National Academy of Sciences*
36. Sánchez, M.L. Torre B. de, García M.A. and Pérez, I., 2005. Ozone concentrations at a high altitude station in the central massif (Spain), *Chemosphere*60: 576–584,
37. Sapkota and Dhaubhadal, 2002. Atmospheric turbidity over Kathmandu valley, *Atmospheric Environment* 36:1249–1257.
38. Severe Cold Wave in Quetta 20 December, 2010. Urduwire.com. Retrieved 25 July 2015.
39. ShahKhan S., Usmani, S.H., Naseem, S. and Khan F., 2004. "Concentration of Ground Level Ozone (O_3) in Quetta City",*Research Journal, Balochistan Study Centre*,University of Balochistan, xii-xiii: 37-46,
40. ShahKhan Safdar, 2007. M.phil thesis, *Empirical Modeling of Toxic and Other Airborne Matter in Quetta Valley*, Department of Physics "University of Balochistan, 2007.
41. Shakoor U., Saboor A., Ali I., and Mohsin, A.Q., 2011. Impact of Climate Change on Agriculture: Empirical Evidence from Arid Region. *Pak. J. Agri. Sci., 48(4):327-333*
42. Shamim U., Hasan A.B.M. and Zillurr, R. M., 2013. Change in Temperature over Bangladesh Associated with Degrees of Global Warming. *Asian Journal of Applied Science and Engineering,* 2(2) ISSN 2305-915X
43. Sillman, S., Logan, J. and Wofsy, S., 1990. The Sensitivity of Ozone to Nitrogen Oxides and Hydrocarbons in Regional Ozone Episodes. *Journal of Geophysical Research* 95(D2):1837–1851.
44. Task Force on Hemispheric Transport of Air Pollution (TF-HTAP), 2007. *Hemispheric Transport of Air Pollution 2010*, Part A: Ozone and Particulate Matter, Air Pollut. Stud., 16, edited by: T. J. Keating, and A. Zuber, U. N. Econ. Comm. Eur., Geneva, Switzerland, available at: http://www.htap.org.
45. Task Force on Hemispheric Transport of Air Pollution (TF-HTAP), 2011. *Hemispheric Transport of Air Pollution 2010*, Part A: Ozone and Particulate Matter, Air Pollut. Stud., 17, edited by: F. Dentener, T. Keating, and H. Akimoto, U. N. Econ. Comm. Eur., Geneva, Switzerland, available at: http://www.htap.org.
46. UNFCCC, 2007. *Climate change: Impacts, vulnerabilities and adaptation in developing countries*. United Nations Framework Convention on Climate Change, UN.
47. World Bank Report, 2010. *Institutional Analysis of Air Quality Management in Urban Pakistan*. Study commissioned by the World Bank. Washington, DC: World Bank. cleanairinitiative.org /portal/system/files/.../AQM_Draft_Final_Report.pdf

Table 1. NO_x (ppb) level in Quetta city (Source Compiled)

Sites		Level in June-July		Level in Oct-Nov		Level in Jan-Feb.		Ave
		Min	Max	Min	Max	Min	Max	
Site-1 Jinnah Road (Commercial Area)	Day	28.90	60.20	24.75	55.35	25.35	52.80	41.23
	Night	27.95	44.65	23.55	40.50	21.80	41.45	33.32
Site-2 Satellite Town (Residential Area)	Day	30.55	56.55	26.35	52.35	25.40	50.85	40.34
	Night	26.75	42.55	27.00	38.35	25.80	40.45	33.48
Site-3 Sirki Road (Industrial Area)	Day	28.30	59.90	23.30	55.85	26.80	45.35	44.92
	Night	28.05	43.50	24.20	37.90	20.70	40.00	32.39
Site-4 Gawalmundi Choak (Com-Residential)	Day	29.70	62.22	25.65	57.38	27.63	62.18	44.13
	Night	27.84	46.65	24.50	42.53	21.80	41.45	34.12
Site-5 Khudaiadad road junction (Com-Res)	Day	31.27	60.55	26.38	52.35	25.40	50.85	41.12
	Night	25.92	40.55	27.98	39.13	25.80	40.45	33.30
Site-6 Meazan Choak (Commercial)	Day	29.78	69.90	24.34	60.40	27.88	47.85	43.35
	Night	27.81	45.50	21.12	39.67	23.60	44.00	33.62
Site-7 Police Lane near Girls College	Day	25.18	52.45	22.45	54.13	24.93	52.72	38.62
	Night	22.01	39.65	19.89	45.78	21.27	44.91	32.24
Site-8 Sumungli Road near EPA office	Day	28.51	56.55	28.23	52.35	27.89	50.72	40.69
	Night	26.81	42.55	25.12	38.13	24.10	40.23	32.82
Site-9 Joint Road Chamman Phattak	Day	29.60	59.90	25.37	55.85	27.60	56.9	42.54
	Night	27.82	43.50	22.25	39.99	24.14	41.91	33.26
Site-10 Sariab Road (Balochistan University)	Day	34.18	60.20	26.17	65.35	32.18	66.99	47.51
	Night	30.23	44.65	22.64	43.54	23.14	45.17	34.89
Site-11 By-pass Eastern	Day	25.76	48.95	21.30	45.39	21.17	42.72	34.22
	Night	21.88	40.56	19.90	36.05	17.14	38.28	28.99
Site-12 Airport Road	Day	27.72	49.70	25.70	52.18	26.23	55.13	39.44
	Night	23.81	39.15	24.26	37.94	22.20	36.21	30.59

Table 2. O_3 (ppb) level in Quetta city Source Compiled

Sites		Level in June-July		Level in Oct-Nov		Level in Jan-Feb.		Ave
		Min	Max	Min	Max	Min	Max	
Site-1 Jinnah Road (Commercial Area)	Day	24.60	44.50	20.35	40.20	22.70	40.50	32.14
	Night	17.90	32.65	13.65	28.45	17.00	30.05	23.28
Site-2 Satellite Town (Residential Area)	Day	23.50	41.55	19.30	37.75	20.15	40.20	30.41
	Night	18.55	31.85	11.55	27.20	18.45	33.05	23.44
Site-3 Sirki Road (Industrial Area)	Day	24.05	41.15	23.25	37.95	21.00	36.75	30.69
	Night	19.92	32.01	15.85	27.05	16.15	30.05	23.50
Site-4 Gawalmundi Choak (Com-Residential)	Day	22.43	42.11	24.40	44.23	23.56	46.94	33.95
	Night	20.32	34.76	17.32	29.09	18.43	32.78	25.45
Site-5 Khudaiadad road junction (Com-Res)	Day	23.76	44.23	22.60	46.90	25.89	45.35	34.79
	Night	17.61	34.98	25.62	37.82	23.54	34.97	29.09

Site-6 Meazan Choak (Commercial)	Day	25.70	47.94	25.87	46.78	25.90	47.23	36.57
	Night	19.97	36.12	18.67	35.45	16.40	32.78	26.57
Site-7 Police Lane near Girls College	Day	22.78	42.13	20.18	41.68	18.60	41.76	31.17
	Night	16.90	35.87	18.32	31.80	15.87	39.76	26.42
Site-8 Sumungli Road near EPA office	Day	23.62	45.54	21.35	44.21	23.79	43.15	33.61
	Night	18.99	30.66	15.83	24.41	19.53	32.17	23.59
Site-9 Joint Road Chamman Phattak	Day	25.17	44.33	21.18	43.45	17.76	43.47	32.56
	Night	18.29	34.98	16.56	35.90	16.88	37.07	26.13
Site-10 Sariab Road (Balochistan University)	Day	25.53	44.59	19.73	39.97	24.71	43.42	32.99
	Night	19.15	33.38	12.95	25.22	20.46	34.45	24.27
Site-11 By-pass Eastern	Day	20.27	41.51	19.67	40.96	17.78	41.76	30.33
	Night	16.91	36.00	17.99	30.18	14.87	37.96	25.65
Site-12 Airport Road	Day	22.68	44.55	22.35	44.72	23.17	42.69	33.36
	Night	17.39	31.26	14.88	23.98	19.75	33.71	23.49

Table 3.Results of Correlation between O_3 and NO_x Source Compiled

Seasons	O_3 Concentration X	NO_x Concentration Y	X^2	Y^2	XY
Level in June-July	29.22	39.09	853.81	1528.03	1142.21
Level in Oct-Nov	27.23	35.85	741.47	1285.22	976.19
Level in Jan-Feb	29.26	35.82	856.15	1283.07	1048.09
∑	85.71	110.76	2451.43	4096.32	3166.49

Table 4. Average Concentration of NOx and O_3 from 2005-2017 in Quetta Valley

Year	NOx	Ozone	Source
2005		27.61	(Shahkhan, 2007) ***(Pak-EPA/JICA , 2006;*** 2007)
2006		29.98	
2007	37.58	34.68	(World Bank Report, 2010).
2008	40.76	44.48	
2009	54.78	31.35	
2010	52.67	35.76	
2011	49.76	40.12	(Pak-EPA, 2015)
2012	45.95	34.43	
2013	41.78	31.07	
2014	38.78	30.10	
2015	37.21	26.67	
2017	33.69	28.89	Compiled

Table 5. Mean Value of (based on 100 years) Temperature, Precipitation, Humidity and Rain of Quetta Valley. Source Meteorological Department 2016

Months	Mean Temperature (°C)		Precipitation (millimeters)	Relative Humidity (%)	Rain (Inches)
	Minimum	Maximum			
January	10.79	-3.36	56.74	65.76	1.796
February	12.92	-0.87	48.98	64.85	1.416
March	18.68	3.44	55.01	57.30	2.05
April	24.84	8.30	28.26	48.45	0.516
May	30.42	11.51	5.96	36.82	0.438
June	35.25	15.93	1.08	31.43	0.05
July	35.90	19.86	12.71	40.53	0.576
August	34.84	17.87	12.07	39.97	0.239
September	31.36	10.90	0.29	36.28	0.253
October	25.46	3.84	3.90	36.27	0.42
November	19.18	-0.88	5.27	45.83	0.228
December	13.33	-3.18	30.45	59.46	1.5
Annual Mean	24.42	6.95	21.73	46.91	0.78

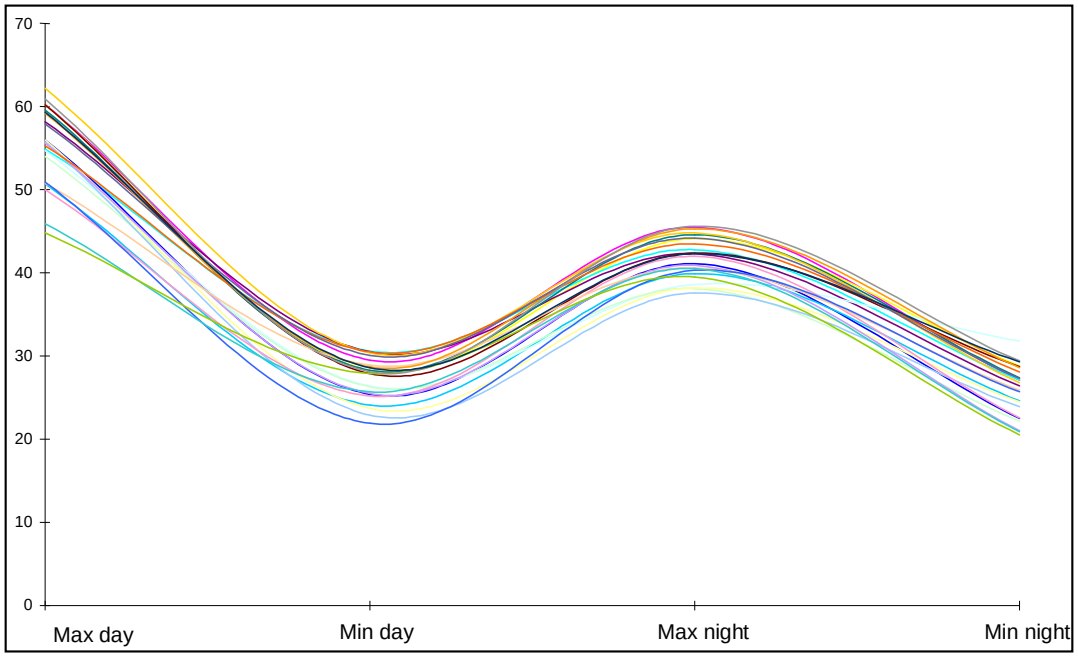

Figure 1. Concentration of NOx with 24 Hours Day & Night Variation in Quetta Valley. Source compiled

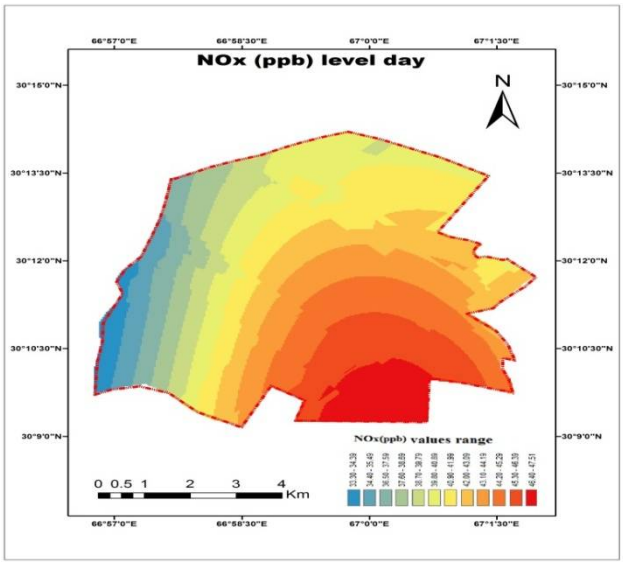

Figure 2. Concentration of NOx at day time at twelve sites in Quetta Valley. Source compiled

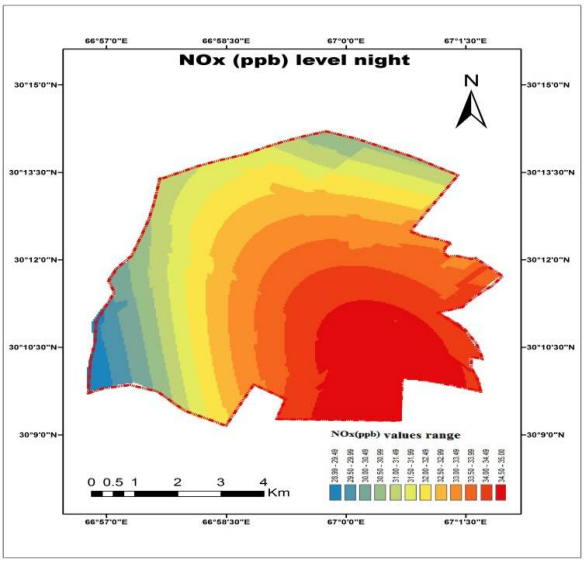

Figure 3. Concentration of NOx at night time at twelve sites in Quetta Valley. Source compiled

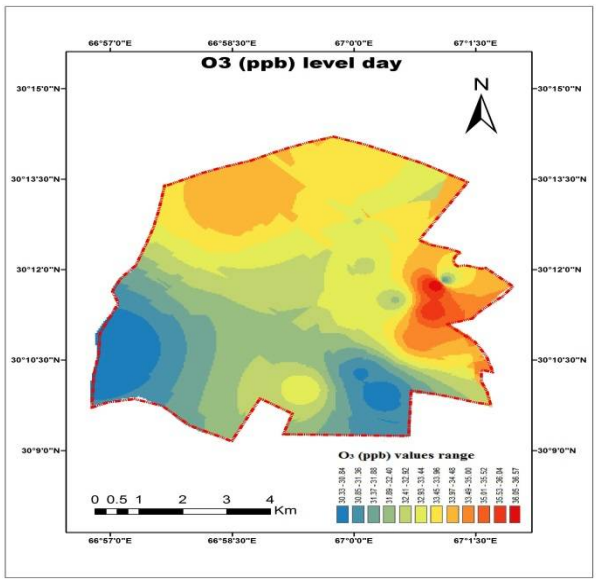

Figure 4. Concentration of O_3 with 24 Hours Day & Night Variation in Quetta Valley. Source Compiled

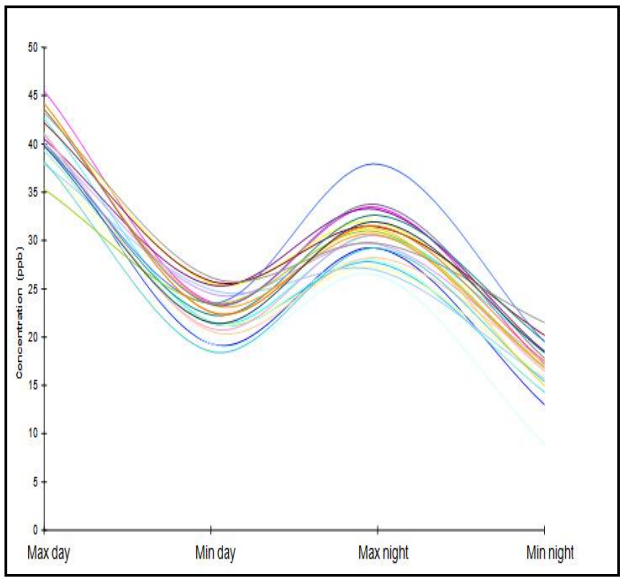

Figure-5: Concentration of O_3 at day time at twelve sites in Quetta Valley. Source compiled

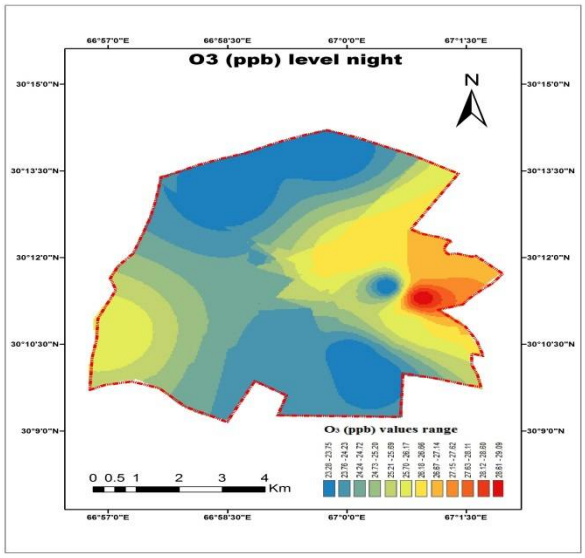

Figure-6: Concentration of O_3 at night time at twelve sites in Quetta Valley. Source compiled

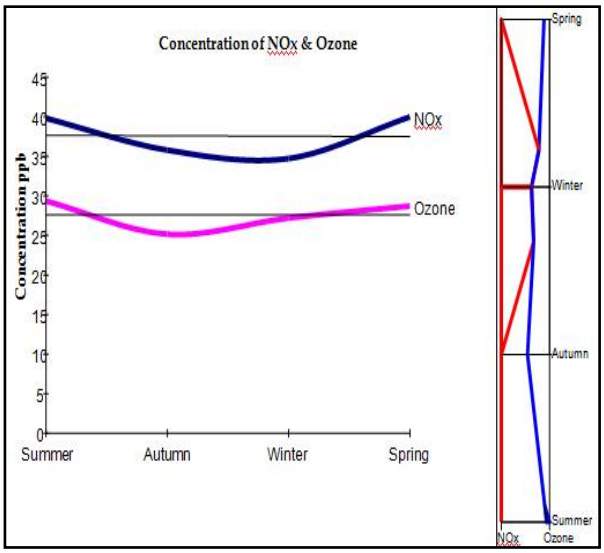

Figure 7: Variations of Ozone and NO_x in Quetta Valley. Source Compiled

Indian Journal of Natural Sciences www.tnsroindia.org.in ©IJONS

Vol.9 /Issue 50 /October / 2018 *International Bimonthly* *ISSN: 0976 – 0997*

RESEARCH ARTICLE

Histological and Histochemical Features of the Fore Stomach in Indigenous Gazelle (*Gazella subgutturosa*)

Ahmed Saad Al-A araji* and Dhyaa Ab. Abood

Department of Anatomy and Histology, College of Veterinary Medicine, University of Baghdad, Baghdad, Iraq.

Received: 23 Jun 2018 Revised: 25 July 2018 Accepted: 29 Aug 2018

***Address for Correspondence**
Ahmed Saad Al-A araji
Department of Anatomy and Histology,
College of Veterinary Medicine,
University of Baghdad,
Baghdad, Iraq.
Email : sabahali503@yahoo.com

ABSTRACT

Present work wasinvestigatedthe histochemical features of the parts of fore stomach in Gazella.A total six Gazella were used. The tissue sections were stained with H&E, Masson's trichrom and Combine Alcian blue & PAS stains.Thethree parts of fore stomach (rumen, reticulum & omasum) were displaying papillated mucosa which showed the highest laminae were seen in omasum (20.8±1.1 mm).In rumen the papilla were simple type and not displaying branching.In all parts the papilla were lined with keratinized stratified squamous epithelium which showed highest epithelium in the rumen (483.2±7 µm). In rumen the lamina propria was not muscular type in contrary those of reticulum and omasum. The tunica muscularis was smooth type showed three layers in rumen, while in reticulum and omasum was two layers and the thickest muscularis was seen in rumen (1.98±0.4 mm). The histochemical results showed no glycogen in the epithelial cells of rumen while in reticulum and omasum the epithelium showed little glycogen.

Keywords: Gazella, fore stomach,rumen , reticulum, omasum , histochemical

INTRODUCTION

In ruminant stomachs the first three parts; rumen, reticulum and omasum are non-glandular parts while the fourth part (Abomasum) is a glandular [1]. The digestive tract of the ruminants has attentionbecause of involve differences in biodiversity across species [2].Ruminants fore stomach stores and converts the coarse foods into highly nutritious products[3]. Rumen is an important parthas ability to store large quantities of forages, has papillated mucosa which, it dose fermentation the cellulose and source of vitamin A of microbial population in the rumen digests, rumen also

absorbs most of the volatile fatty acids [4],[5].The reticulum is a pouch-like structure has rows of folds (laminae) and on the surface of the laminae is short conical projections that are called papillae which are passiveabsorption of fatty acids[4][6].The omasum has a layered mucosa which thrown is into long sheets"laminae", in addition that there are short papillae on the laminae, theomasum has functionsserves in dehydration and it squeezed and compressed by contractions tocrush the food particles so they are small enough[4],[6]&[7]. The Anatomy of the ruminants forestomach varies amongvarious ruminant species[6],[8], [9], [10],such variations could be presents in histological aspect,scanty histological literatures on the fore stomach of indigenous gazella.The Gazella subgutturosa is settles and distributed in Azerbaijan, Iran, Afghanistan, Pakistan, Uzbekistan and Iraq, in Iraq the Gazella was recorded in the north to southern provinces of Iraq [11] [12] [13].Gazella subgutturosa has saved in several nature reserves located in many provinces including, the district of AL Madaen in the outskirts of the capital Baghdad, an area of (157) acres, where ksiab-reservoir to save the species and varieties from the risk of extinction, includes Gazella subgutturosa which involved in this study. [13].The aim of the present workis to investigatethe histological and histochemical features of the fore stomach in indigenous Gazelle.

MATERIALS AND METHODS

Six male indigenous Gazelle (2-5 years old) with a mean body weight of 18.5±0.21 kg have used in this study. The Gazelle were obtained from (AL-Madaen Animal Reservoir) in Baghdad. The study was conducted in department of Anatomy and Histology at College of Veterinary Medicine-University of Baghdad. The animals were euthanized by slaughterer, immediately after being slaughtered the parts of the stomachs have beenwashing up and fixed by 10 % neutral buffered formalin sol. (PH 7.4). The rumen, reticulum and omasum had been separated and small specimens of each partwere collected for histological and histochemical studies. After well fixation the specimens havedehydrated withup graded series of ethanol (70-100%) (2 hours each), cleared with two changes of xylen solution (one hours each), embedded two changes of paraffin bath (two hours each) and sectioned at 5-7 µm. Sections have stained with hematoxylin & eosin, Masson's trichrom stain, combine Alcian blue (AB) (pH 2.5) & Periodic Acid-Schiff (PAS)stains [14].The slides were captured by using future Winjoe microscopy camera, china.

Statisticalanalysis

The data of papillae thickness and height, thickness of tunica muscularis and epithelial height were represented by (Mean±SE). A post-hoc (Tukey &Dunkun) analysis was applied toachievesignificant differences ($P<0.05$).

RESULTS

Rumen

The mucosa of the rumen wasthrown into papillae which revealed variable size and shape. Papillae were long and short types, the long type had to be tongue-like shape, while the short papillae were conical shape(fig.1&2). Each papilla was lined by keratinized stratified squamous epitheliumof four layers cells types (basale, spinosum, granulosum andcorneum), the epithelium was rested on a lamina propria which composed of densely packed collagen bundles which was well vascularized contained capillaries and there were no muscle fibers have been seen in the papillae(fig.3).The tunica submucosa was merged with lamina propria due to absent of muscularis mucosa which showed blood vessels companying connective tissue (fig.4). The tunica muscularis of rumen showed three layers; inner circular, middle oblique and outer longitudinal layers of smooth muscle bundles. The inner and middle layers were the thickest layers (fig.5). The histometrical measurements showed that the rumen had the thickest tunica muscularis and epithelial height (Tab.1).

Reticulum

The mucosa of the reticulum was thrown into short conical like laminae that covered with short papillae (displaying subdivision into secondary papillae) (Fig.6). Each lamina was lined by keratinized stratified squamous epithelium, (fig.7).The reticulum had a muscularis mucosa and the lamina propria wasa thin layer composed ofcollagen bundles

that pass along the length of papilla core and intermingled by bundle of smooth muscle of muscularis mucosa, it was well vascularized (fig.7). The tunica muscularis of reticulum showed two layers; inner most circular and outer most longitudinal layers of smooth muscle bundles, both layers were had the same thickness (fig.8).

Omasum

The mucosa of the omasum was displaying very longest laminae (Fig.9). Each lamina was lined by thin layer of keratinized stratified squamous epithelium showed thick layer of keratin and the lamina propria was composed of two thin layers of collagen bundles that pass along the length of lamina core and intermingled by bundle of smooth muscle of muscularis mucosa (fig.10). The tunica muscularis of rumen showed two layers; inner most circular and outer most longitudinal layers of smooth muscle bundles, bothhad the same thickness (fig.9). The histometrical measurements showed that the rumen had a significant thickest tunica muscularis and epithelial height, while the omasum had the longest lamellae (Tab.1).The histochemical sections with combine Alcian blue and PAS satin of rumen showed no glycogen or mucopolysaccharidewere found in the epithelial cells (fig.11) while the epithelial cells of the reticulum and omasum showed light reaction for PAS satin and the lamina propria was positive for Alcian blue stain (fig.12).

DISCUSSION

This is the first data about the histological features fore stomach of the indigenous Gazella subgutturosa which participatingin a comparison with other descriptions in small and large ruminants.The current results showed that the three compartments of fore stomach was consisted of four ideal histological tunica (mucosa, submucosa,muscularis and serosa) it was similar that in buffalo, bovine, camel, sheep and goat[15][16][17][18][19].The current results showed the ruminalmucosa had simple not branched papilla which varies in size and shape also the core of papilla was a muscular such records were accords with results of [15][16]&[20], the reticulum and omasum of gazella the laminae were branched into secondary once which similar those in other small and large ruminants [16], [21] ,[7],[22],[19],on the other hand in sheep there was tertiary laminae in omasum [21], further more divisions of mucosal papillae or lamina suggests the more role in the omasal functions in crushing the forage particles so they are small enough to pass on to the abomasum and be useful [4]. In Gazella the epithelial lining of the three compartments were keratinized stratified squamous epithelium, such result agree with results of [16][23], [17],[21],[20],[22], [19].The current result revealed many of capillaries in the sub epithelium of rumen and reticulum which referred for the important role of these parts of fore stomach in absorption of volatile fatty acids[4],the reticulum is the site of the sorting mechanism [25].

The current results revealed that the fore stomach of Gazella was similar other ruminants had muscularis mucosa which well developed and extended into the core of the reticular papilla and omasal laminae [16], [21], this results suggests that the smooth muscle fibers are responsible for contraction of reticular papillae and omasal laminae during rumination and digestion.In Gazella the ruminal tunica muscularis revealed three layers of smooth muscle bundles which were contrary those in goat [16] and sheep [25].In Gazella the rumen had the thickest tunica muscularis which accords with the ability of this part to store large quantity of food alsohad the epithelial height such observation revealed that this part had an active epithelial reabsorption consequently the result compatible with result of[26], [27][10],[4]. The current result revealed the ruminal papillae were smallest while the omasum had the largest [26].In Gazella the histochemical results revealed no glycogen or mucopolysaccarides were found in the epithelial liningof the rumen while the that of the reticulum and omasum showed light amount glycogen or mucopolysaccarides and the lamina propria has acidic mucopolysaccarides such results disagree with result of ([15] in Buffalo and[23] in red deer and [28] in sheep who mentioned that mucopolysaccaridesare distributed in all tunica of fore stomach with high densities in the mucosal layer.Presence of positive PAS mucosubstances in the lining epitheliumreveals that the neutral mucosubstances playa role in the absorption[29][30][31],the neutral mucosubstancesservea protection the underlying tunica from chemical and physical damage during trituration processes [32], also other literature revealed presence of neutral mucopolysaccarides in epithelial cells of the sheep and red deer during prenatal development [20],[22], [7],[28],the mucopolysaccarides in early embryonic life could playan

important roles in the development of the epithelial cells in addition serve as a protective barrier against some harmful acidic materials in the amniotic fluid, [33],on the other hand the presence of neutral mucopolysaccharide plays a role in adaptation of omasal mucosa against acid compounds which produced bymicrobial fermentation in reticulum[21].

REFERENCES

1. Eurell JA, FrapplerBL.Dellmann's textbook of veterinary histology. 6th Edn., Baltimore, MD: Williams and Wilkins. 2006;86-194.
2. Langer P.Vergleichend-anatomischeUntersuchungen am Magen der Artiodactyla. II. UntersuchungenamMagen der Tylopoda und Ruminantia. GegenbaursMorphologischesJahrbuch. 1973;119: 633–695.
3. Stumpff F, Martens H, Bilk S, Aschenbach JR, Gabel G.Cultured ruminal epithelial cells express a large-conductance channel permeable to chloride, bicarbonate and acetate. Pflugers Arch Eur J Physiol.2009; 457:1003-22.
4. Rush IG. Rumen Physiology for the Rancher. Proceedings, The Range Beef Cow Symposium XXI, December 1, 2 and 3, Casper, WY2009 .
5. Clauss M, Hummel J, VöllmJ,.Lorenz A, Hofmann R. The allocation of a ruminant feeding type to the okapi (Okapiajohnstoni) on the basis of morphological parameters. 2006 ;253-270.
6. Hofmann RR. Evolutionary steps of eco physiological adaptation and diversification of ruminants: a comparative view of their digestive system. Oecologia. 1989;78 :443-457.
7. Redondo E, Franco A, Masot1 J. Morphometric and immunohistochemical study of the omasum of red deer during prenatal development. J Anat. 2005 ; 206: 543–555.
8. Clauss M, Kaiser T, Hummel J. The morphophysiological adaptations of browsing and grazing mammals. In: Gordon, I. J. &Prins, H. H. T. (eds.).The ecology of browsing and grazing. Springer, Heidelberg.2008; 47–88.
9. Clauss M, Hofmann RR, Fickel J, Streich W J, Hummel J. The intraruminalpapillation gradient in wild ruminants of different feeding types: implications for rumen physiology. J Morphol. 2009 ;270: 929–942.
10. Clauss M, Hume ID, Hummel J. Evolutionary adaptations of ruminants and their potential relevance for modern production systems. Animal. 2010 ;4:7: 979–992.
11. Habibi K, Thouless CR, Lindsay N. Comparative behavior of sand and mountain gazelles. Journal of Zoolo. 1993; 229:41-53.
12. Abood DA, Hussein ZM. Histological features of Vomer nasal organ in Indigenous Gazelle (*Gazella subgutturosa*). J EntomolZoolo Studies. 2017; 5.4: 598-604.
13. Abood DA, Hussein ZM. Histological and Histochemical Features for Jacobson's Glands in Male Gazella subgutturosa. Indian J Natural Sci. 2018; 8. 46: 13107- 13114.
14. Bancroft JD. Marilyn G. Theory and practice of histological techniques. 6th Ed. London: Elsevier Limited; 2008; 168-173.
15. Ahmed SG, Al-Asadi FS. Histochemical Study of Mucopolysaccarides In Stomach Of Buffalo (Bubalus-Bubalis). Bas.J.Vet.Res.2016 ; 15.1:292-299.
16. Garcia A, Masot J, Franco A, Gazquez A, Redondo E.Immnunohistochemical evaluation of the goat fore stomach during prenatal development. J Vet Sci. 2014;15.1: 35-43
17. Naghani ES, AkradiL.Histogenesis of rumen in one-humped camel (Camelusdromedarius). Pak Vet J. 2012 ; 32.2: 269-272.
18. Poonia A, Kurmurpawan, Kurmarparveen. Histomorphological studies on the rumen of the sheep (ovisaries).HaryanaVeterinary. 2011 ;50:49-52.
19. Stallcup OT, Kreider DL, Rakes JM. Histological Development and Histochemical Localization of Enzymes In 'Rumen And Reticulum In Bovine Fetuses. J him Sci.1990 ; 68:1773-1789.
20. Masot AJ, Franco AJ, Redondo E. Morphometric and immnunohistochemical study of the abomasum of red deer during prenatal development. J Anat. 2007 ;211:376–386.

21. Redondo E, Masot J,García A, Franco A. Ontogenesis of the omasum: a comparative analysis of the Merino sheep and Iberian red deer. HistolHistopathol. 2011 ; 26: 1135-1144.
22. Franco AJ, Redondo E, Masot AJ. Morphometric and immnunohistochemical study of the reticulum of red deer during prenatal development. J Anat. 2004; 205: 277–289.
23. Zitare I, Pilmane M, Jemeljanovs A. Histomorphology of the digestive system of red deer (Cervuselaphus L.) in Latvia.J Vet Med Anim Health.2013 ;5.4: 99-106.
24. Clauss M, Hofmann RR. The digestive system of ruminants, and peculiarities of (wild) cattle. In: Melletti, M. & Burton, J. (eds.), Ecology, evolution and behaviour of wild cattle: implications for conservation. Cambridge University Press, Cambridge 2014.
25. Pfannkuche H, Schellhorn C,Schemann M, Gabel G.Intrinsic innervation patterns of the smooth muscle in the rumen and reticulum of lambs. J Anat. 2004; 204: 293–299
26. Sauer C, Hammer C, Bertelsen MF, Tütken T, Clauss M, Hammer S. Quantitative macroscopic digestive tract anatomy of the beira(Dorcatragusmegalotis). J Zoo and Aquarium Res. 2016 ; 4.4:147-179.
27. Pérez W, Vazquez NJ.Gross anatomy of the gastrointestinal tract in the Brown Brocket deer (Mazamagouazoubira). Morphol Sci. 2012 ; 29.3:148-150.
28. Franco AJ, Robina A, Regodon S, Vivo JM, Masot AJ, Redondo E. Histomorphometric analysis of the reticulum of the sheep during development. HistolHistopath. 1993 ; 8: 547-556.
29. Grau A, Crespo S, Sarasquete MC, González de Canales ML. The digestive tract of the amberjack SeMadumerili, Risco: A light and scanning electron microscope study. J Fish Biol. 1992; 41: 287-303.
30. Ferrans RP, Tan JD, De la Cruz M.C. Development of the digestive tract of milk fish, Chanoschanos (Forskal): histology and histochemistry. Aquaculture, 1987; 61:241 -257.
31. Ezeasor DN, Stokoe WM. Scanning electron microscopic study of the gut mucosa of the rainbow trout Salmogairdneri Richardson. J Fish Biol. 1980; 17:529-539.
32. Gisbert E, Sarasquete C, Williot P, Castelló F. Histochemistry of the development of the digestive system of Siberian sturgeon during early ontogeny. J. Fish Biol. 1999;55: 596-616.
33. Moore KLEmbriologiaclinica. Interamericana. Mexico. 1985; 262-273.

Table 1: show the height, thickness of papilla or (laminae), thickness of tunica muscularis and epithelial height of rumen, reticulum & omasum.

Parts	Height of Papilla/mm	Thickness of papilla/mm	Thickness of tunica muscularis/mm	Epithelial height/µm
Rumen	6.34±0.2	0.710±0.4	1.98±0.4 *	483.2±7 *
Reticulum	9.84±0.8	0.521±0.9	1.21±0.3	391.9±9
Omasum	20.8±1.1 *	0.671±0.9	1.46±0.6	407.4±8

(*) represents significant differences at level of (P<0.05)

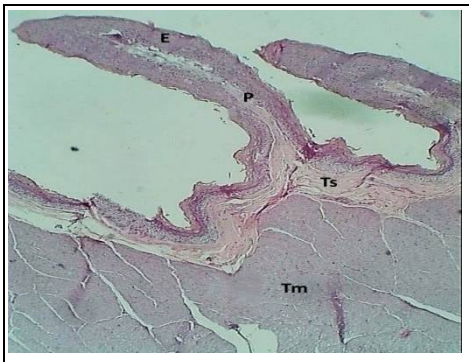

Figure 1: Section rumen shows: Ruminal papillae (arrows), epithelium (E), proprial core (P), tunica submucosa (Ts) andtunica muscularis (Tm). H&E stain.40x

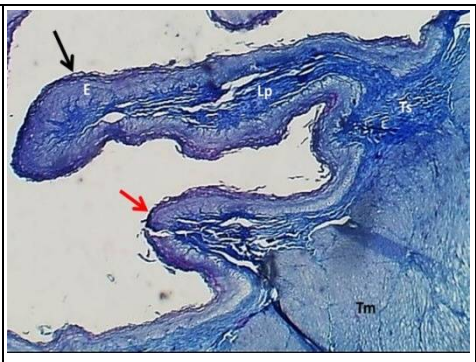

Figure 2: Section rumen shows: long ruminal papillae (Black arrow), short papilla (Red arrows), epithelium (E), lamina propria (Lp), tunica submucosa (Ts) & tunica muscularis (Tm). Masson's trichrom stain.100x

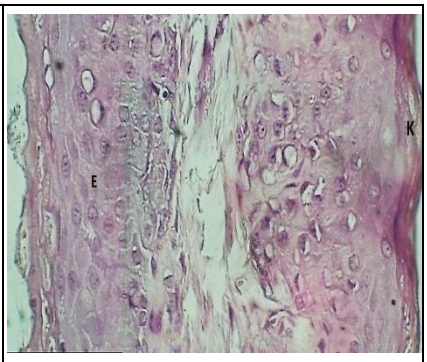

Figure 3: magnified section of ruminal papilla shows: stratified squamous epithelium (E) & keratin layer (K). H&E stain.400x

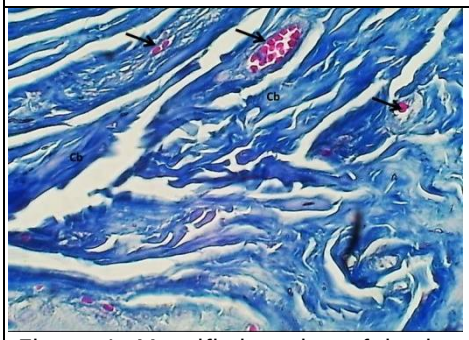

Figure 4: Magnified section of lamina propria submucosa shows: collagen bundles (Cb) and blood vessels (arrows) Masson's trichrom stain.400x

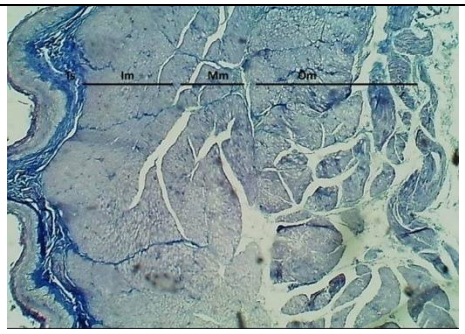

Figure 5: Section at the wall of the rumen shows: inner layer (Im), middle layer (Ml) outer layer(Ol), submucosa (Ts). Masson's trichrom stain.40x

Figure 6: Section of reticulum shows: Primary papilla (Pp), secondary papilla (Sp) lamina propria (p), smooth muscle (Sm), muscularis mucosa (mm), inner muscularis (Im) & outer muscularis (Om). H&E stain.40x

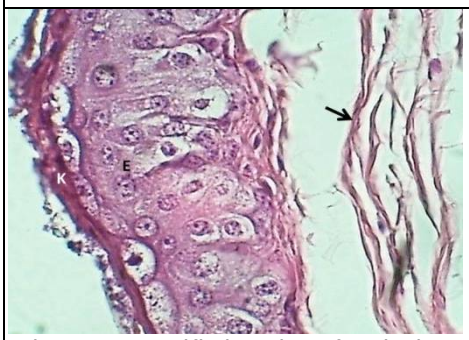

Figure 7: Magnified section of: reticulum show: epithelium (E), keratin layer (K)& collagen fibers (arrow). H&E stain.400x

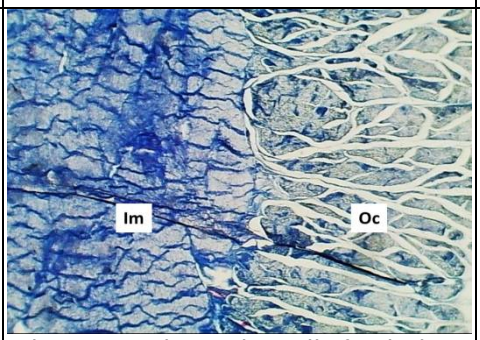

Figure 8: Section at the wall of reticulum shows: inner circular layer (Im) & outer longitudinal layer of smooth muscle fibers (Om) of tunica muscularis. Masson's trichrom stain.40x

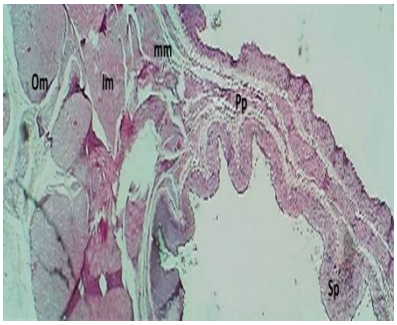

Figure 9: section of Omasum shows: primary papilla (Pp), secondary papilla (Sp), muscularis mucosa (mm), inner muscularis (Im) & outer muscularis (Om). H&E stain.40x

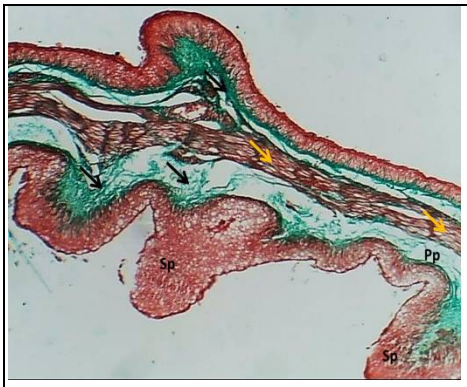

Figure 10: section of omasal papilla shows: primary papilla (Pp), secondary papilla (Sp), smooth muscle of muscularis mucosa (yellow arrows),& collagen bundles (Black arrows). H&E stain.100x

Figure 11: Section rumen shows: negative reaction of ruminal epithelium for PAS (E), keratin layer (K) & lamina propria (Lp). Combined Alcian blue PAS stain.100x

Figure 12: Section omasum papilla shows: light positive reaction of ruminal epithelium for PAS (E), keratin layer (K) & lamina propria (Lp). Combined Alcian blue PAS stain.100x

Indian Journal of Natural Sciences www.tnsroindia.org.in ©IJONS

Vol.9 /Issue 50 /October / 2018 *International Bimonthly* *ISSN: 0976 – 0997*

RESEARCH ARTICLE

Fats of Animal Origin: Health Perspectives

S.K. George[1]*, M.T. Dipu[2], K.Lalu[2] and Muhammad Aslam M K[2]

[1]Assistant Professor, Base Farm, Kolahalamedu, Kerala, India.
[2]Kerala Veterinary and Animal Sciences University, Pookode, Wayanad, Kerala, India.

Received: 25 Jun 2018 Revised: 27 July 2018 Accepted: 30 Aug 2018

***Address for Correspondence**
S.K. George
Assistant Professor,
Base Farm,
Kolahalamedu,
Kerala, India.
Email : skgeorge31@gmail.com

ABSTRACT

Foods of animal origin such as meat, fish, eggs and milk are important sources of vital nutrients including proteins. However, a large population of the world avoids one or other type of these precious foods. Reason being the, reports of food hazards and risk factors related to chronic diseases of the digestive and circulatory system caused by the intake of fat and cholesterol. Therefore, during the present time, more important is the classification of dietary fat based on their effect on human health as unhealthy fats and healthy fats. Unhealthy fats include *trans* fatty acids, saturated fats and cholesterol. Healthy fats are generally unsaturated fats and they come from vegetable and marine sources. Foods of animal origin are rich in saturated fat and cholesterol compared to marine/vegetable origin foods. Among the various red meats' chevon, is a high quality protein source along with a healthy fat with minimal cholesterol content. In chicken and pork, above 50% of the total fat is unsaturated. Recent studies suggest that conjugated linoleic acid, a Tran's fatty acid in ruminant milk and meat have major health benefits. Researchers are working to develop designer milk, meat and egg that contain higher levels of a "healthy fat" that they say could fight cancer and heart diseases. It can be concluded that animal origin fats have both beneficial and harmful effects. Therefore, judicious selection and consumption of animal origin foods will help to lead a healthy life with a healthy body.

Keywords: effect, animal, nutrients, system, healthy, benefits, origin

INTRODUCTION

Animal origin foods such as meat, fish, eggs and milk are important source of easily digested proteins of high biological value and of some other valuable nutrients. However, a large population in various parts of the world

avoids one or other type of these precious foods. Various theories exist in the world which explains the reasons behind the evading of foods of animal origin. One such is related with the transmission of certain zoonotic diseases by foods of animal origin. Recent reports of food hazards and risk factors related to chronic diseases of the digestive and circulatory system have been cited in support of this theory. The present paper attempts an examination of the available scientific evidence of the beneficial and harmful effect on human health associated with the consumption of fats of animal origin. To better understand the topic, brief information of the types of fats in our diet and the importance of normal lipid profile is also discussed.

Dietary Fat

Apart from carbohydrate, fat is also a major source of energy for the body, precursor for synthesis of various biological compounds and aids in the transportation and absorption of fat soluble vitamins. Both animal and plant origin food products contain fat and it is important for proper growth, development, reproduction and maintenance of good health. There are two main types of dietary fats based on the chemical composition: unsaturated and saturated. During the present period, more important is the classification of dietary fat based on their effect on human health as unhealthy fats and healthy fats.

Unhealthy Fats

Unhealthy fats includes trans fatty acids (trans fat), saturated fats and cholesterol. Trans fat is the common name for unsaturated fat with *trans*-isomer fatty acids. *Cis* and *trans* are terms that refer to the arrangement of the two hydrogen atoms bonded to the carbon atoms involved in the double bond. In the *cis* arrangement, the hydrogen's are on the same side of the double bond while in the *trans* arrangement, the hydrogen's are on opposite sides.Trans fats can be monounsaturated or polyunsaturated, but never saturated. Trans fats are rare in nature but is produced during food production process. Trans fat is formed when liquid oils are turned into solid fats, such as 'vanaspathi' or margarine. During the process of hydrogenation, in presence of metal catalyst hydrogen is added to vegetable oils to increase the shelf life, taste and flavor. The consumption of trans fats increases the risk of coronary heart disease by raising levels of "bad" LDL cholesterol and by lowering the levels of "good" HDL cholesterol. Apart from this trans fats also occur as vaccenic acid and conjugated linoleic acid (CLA) in meat and dairy products from ruminants. Human intake of trans fatty acids therefore originates from foods containing industrially produced partially hydrogenated fat, and from beef, chevon, mutton and dairy fat.

Saturated fats are found in "hard fats," in many animal products such as milk, curd, butter, cheese, yoghurt, meat, and vegetable products such as palm kernel oil and coconut oil. The longer the chain, the harder the fat will be and thus, the higher its melting point. When a person's diet is high in saturated fats, these fats tend to clump together in the body and form deposits, along with protein and cholesterol, and then lodge in the cells, organs and blood vessels. This can lead to many health problems, including heart disease, obesity, and even. High dietary cholesterol content is found in dairy fats, organ meats such as liver, and egg yolk. High intake of cholesterol raises low-density lipoprotein (LDL or "bad") cholesterol in the blood, which increases the risk of developing coronary heart disease. To reduce the risk of developing heart disease, the goal is to decrease the overall level of LDL cholesterol in the diet. Reducing the amount of saturated fat, trans fat, and cholesterol in the diet will help in decreasing the LDL cholesterol level and thus prevents heart diseases.

Healthy fats

Healthy fats are generally unsaturated fats and they come from vegetable and marine sources. They include olive oil, canola oil, peanut oil, corn oil and fish oil. The unsaturated fats are classified into monounsaturated and polyunsaturated. Poly unsaturated fatty acids are further classified, based on the position of the omega carbon atom.

Omega-3 Fatty acids

The most common omega-3 fatty acids are eicosapentaenioic acid (EPA), docosahexaenoic acid (DHA) and alpha-linolenic acid. EPA and DHA are abundant in fishes and remains liquid at room temperature. It is said that they protect fish by providing a body fat that stays fluid even in very cold temperatures. It is said that eating fish twice a week an mee the requirement of omega-3 fatty acids needed per day to reduce the risk of heart disease.

Omega-6 Fatty acids

The most common omega-6 fatty acid is gammalinolenic acid (GLA) which is abundant in vegetable oils

Essential fatty acids

Fatty acids are either essential or nonessential. A fatty acid is considered essential if the body is unable to synthesize it and the only way it can be obtained is through the diet. In addition, it is considered essential if a deficiency will cause a disease. There are basically three essential fatty acids. They are linoleicacid, linolenic acid and arachidonic acid.

Lipid Profile

The lipid profile includes cholesterol, triglycerides, high-density lipoprotein (HDL), very low-density lipoprotein (VLDL), low-density lipoprotein (LDL), cholesterol to HDL ratio, and LDL to HDL ratio in the blood.

Cholesterol

Total cholesterol is used to measure lipid status and metabolic disorders. Cholesterol is essential for life, but is also connected with the occurrence of atherosclerosis. The normal value of cholesterol in blood after 8-10 hrs of fasting should be less than 200 mg/dL. Unsaturated dietary fats lowers the bad (LDL) cholesterol levels, while increasing good cholesterol (HDL). Saturated fats raise the total blood cholesterol while the trans fats are even worse than saturated fats, since they not only raise the bad LDL cholesterol, but also lower the good HDL cholesterol.

Triglycerides

Like cholesterol, triglycerides are used to measure lipid status and metabolic abnormalities. Triglycerides are the major component of the lipoproteins chylomicrons and VLDL. They may be elevated in hypothyroidism, diabetes, chronic liver, kidney and pancreas diseases, some genetic types of hyperlipidemia, alcohol abuse, estrogen and certain medications.

HDL (High-Density Lipoprotein)

HDL is called the "good cholesterol". It tends to carry cholesterol away from tissues. That is, even if their total cholesterol and LDL cholesterol levels are normal, people with reduced levels of HDL have an increased risk of early cardiac disease. HDL levels, to be considered "normal," should be minimum 35 - 40 mg/dL. Anyone whose HDL level is below 40 mg/DL should consider taking steps to increase their HDL. This is the case even if total cholesterol and LDL cholesterol levels are within the normal range. In addition to changes in dietary practices, HDL level can be elevated by performing aerobic exercises and by loosing weight.

LDL (Low-Density Lipoprotein)

"Bad" cholesterol is associated with low density lipoproteins (LDLs). LDLs carry cholesterol in the blood to body cells. High levels of LDLs are usually associated with elevated blood cholesterol and an increased risk of heart disease due to cholesterol and fat being deposited in the blood vessels. These fatty deposits decrease the interior size of the arteries so the blood supply is reduced, thus increasing the risk of heart disease and stroke. It is part of the lipid profile and is one of the more important "risk factors" for atherosclerotic disease. LDL is the cholesterol component that control the synthesis of cholesterol in the liver.

Very Low Density Lipoprotein (VLDL)

VLDL is a type of lipoprotein and helps carry triglycerides to the liver and other parts of the body.

Cholesterol to HDL Ratio

The Cholesterol to HDL ratio is a calculation of the risk for heart disease. It is optimal to have a low ratio. A low ratio indicates that total cholesterol is comprised mostly of HDL particles. This ratio is considered the most important indicator for coronary atherosclerosis.

Foods of Animal Origin

Milk

Milk is a complex physiological liquid that simultaneously provides nutrients and bioactive components that facilitate the successful postnatal adaptation of the newborn infant by digestive maturation, development of gut-associated lymphoid tissues and by the establishment of beneficial microflora in the gut. Milk fat contains a number of components having precise functional properties (Spreer, 1998). Sphingolipids and their active metabolites in milk may exert antimicrobial effects either directly or upon digestion.The milk fat of cattle and buffalo is rich in long chain saturated fatty acids while that from sheep and goats is rich in medium-chain triacylglycerols. Fatty acids C6:0, C8:0 and C10:0 can be found in the milk of goats up to 15–18 %, and in sheep milk up to 12–14 %, while only 5–9 % in the milk of cows. The nature of fat content in sheep and goat milk, in comparison with cow milk, presents advantages for consumer health. The low molar mass of medium-chain fatty acids and their solubility in water facilitate the action of digestive enzymes, making hydrolysis faster and more complete than that of long-chain fatty acids (Alferez *et al*., 2001).

Eggs

Eggs are nutrient rich as they have high-quality protein, essential vitamins and minerals and are only 75 calories a serving. Eggs contain folate, a B vitamin that reduces birth defects and cardiovascular disease. Next to milk, eggs are one of the best dietary sources of vitamin D, which aids in the absorption of calcium. The total fat content in the yolk of an egg is 4.5g while that in egg white only 0.06 g. Of the total fat in an egg yolk, 1.6 g is saturated fat, 0.02 g is trans fat and 184 mg is cholesterol

Meat

Fat deposition pattern

1. Internal fat – surrounds the organs
2. Intermuscular/seam fat – between the muscles
3. Subcutaneous fat –under the skin
4. Intramuscular fat/marbling – within the muscle

Chevon

Goat meat or chevon cuts have fat content 50%-65% lower than beef and have between 42%-59% less fat than lamb. In addition, the percentage of saturated fat in goat meat is 40% less than chicken meat and is far below beef, pork and mutton. Unsaturated fatty acids predominate in goat meat (68.5% to 72.3%). Cholesterol content of chevon is similar to that of beef, lamb, pork, and chicken. Evidences indicates that chevon, regardless of age, breed, or region, will supply a high quality protein source along with a healthy fat with a minimal cholesterol intake risk. In addition, chevon contains comparatively higher values of minerals such as iron and potassium with a low sodium level. Chevon is a rich source of B Vitamin, thiamine

Pork

Lean pork contains only 1.2% fat. Over 50% of the fat present in pork is unsaturated the type that is comparatively better for health. Pork is a good source of protein (22.8%) and essential amino acids. Pork is rich in Vitamin B_1 (Thiamine), with 100g meat containing almost 90% of our daily requirement of this nutrient. Thiamine is important for general vitality, cellular metabolism and energy production. Pork is a source of Vitamin B_{12}, an important nutrient for keeping the nervous system healthy. In addition pork is rich in the mineral zinc which can help to boost the immune response.

Chicken

Skin less chicken contains only 0.9% fat. Over 60% of the fat present in chicken is unsaturated, the type that is better for health. Chicken is an excellent source of protein (22.5%) and essential amino acids.

Beef

Around 50% of the beef fat is saturated and may adversely affect the lipid profile. Beef also contains ruminant unsaturated trans fatty acids. Unlike the trans fatty acids produced industrially in partially hydrogenated vegetable oils, the trans fatty acids in beef has some favorable effect on health. Emerging findings from experimental animal studies, suggest that the *trans* fatty acid, conjugated linoleic acid (CLA), particularly rumenic acid (c9, t11, isomer) which is produced in beef (Dhiman *et al*., 2005), may have a favorable influence on blood lipid levels and cardio vascular disease risk.

Rabbit meat

Recently, the nutritional value of rabbit meat has been reviewed by several authors (Hernández and Gondret, 2006), showing that rabbit meat has a high nutritional value compared with other meats. Rabbit meat is a lean meat rich in proteins of high biological value and it is characterized by high levels of essential amino acids. Furthermore, it is also an important source of highly available micronutrients, such as vitamins and minerals. Also, rabbit meat does not contain uric acid and has a low content of purines. Rabbit meat is characterized by its lower energetic value compared with red meats due to its low fat content. Fat content varies widely depending of the carcass portion from 0.6 to 14.4% with an average value of 6.8% for the whole carcass (Hernández and Gondret, 2006) with the loin being the leanest part of the carcass (1.2% of lipids). Fatty acid composition of rabbit meat is characterized by high content of polyunsaturated fatty acids. The amount of cholesterol in rabbit meat is about 59 mg/100 g of muscle which is lower than those present in meat from other species (61 mg in pork, 70 mg in beef, 81 mg in chicken).

Designer foods

Designer foods are the results of the attempts conducted by scientists to alter the nutrient composition of foods of animal origin to provide a healthy diet to the consumers. Companies has developed designer eggs which are designed for health conscious people who prefer a low cholesterol egg combined with the health benefits of omega 3 fatty acids and Vitamin E. By feeding flax seed to the hen, the omega-3 fatty acids (alpha-linolenic fatty acid) combined with the hens' own conversion of alpha-linolenic acid to eicosapentaenoic acid (EPA) and docosahexaenoic acid (DHA), allow the egg to be enriched with higher than normal omega- 3 levels.Researchers are working to develop milk that contains higher levels of a "healthy fat" that they say could fight cancer and heart disease. Recent studies suggest that conjugated linoleic acid have major health benefits. Studies reveal that the principal dietary sources of conjugated linoleic acid come from animal products, particularly ruminants or animals that eat plants and grasses.

CONCLUSION

Animal origin fats have both beneficial and harmful effects. Judicious selection and consumption of animal origin foods will help to lead a healthy life with a healthy body.

REFERENCES

1. Alférez M.J.M., Barrionuevo M., López Aliagua I., Sanz Sampelayo M.R., Lisbona F., Campos M.S. 2001. The digestive utilization of goat and cow milk fat in malabsorption syndrome. .*Dairy Sci.* 68, 451–461.
2. Dhiman T.R., Nam S.-H.N., Ure A.L, 2005. Factors affecting conjugated linoleic acid content in milk and meat. *Crit.Rev.Food Sci.Nutr.* 45, 463–482 (2005).
3. Hernández P., Gondret F. 2006. Rabbit Meat Quality. *In: Maertens L., Coudert P. (Eds.). Recent Advances in Rabbit Sciences. ILVO, Merelbeke, Belgium, 269-290.*
4. Spreer, E. 1998. Milk and Dairy Product Technology. Ed. Marcel Dekker, Inc. New York, NY. pp. 39–41.h

Indian Journal of Natural Sciences www.tnsroindia.org.in ©IJONS

Vol.9 /Issue 50 /October / 2018 *International Bimonthly* *ISSN: 0976 – 0997*

RESEARCH ARTICLE

Application of Chitosan as a Natural Antimicrobial and Antioxidant Agent for Extension Shelf Life of Meat

Huda N. Jasim* and Marwa R. Hassan

Department of Veterinary Public Health, College of Veterinary Medicine, University of Baghdad, Baghdad, Iraq.

Received: 24 Jun 2018 Revised: 26 July 2018 Accepted: 30 Aug 2018

***Address for Correspondence**
Huda N. Jasim
Department of Veterinary Public Health,
College of Veterinary Medicine,
University of Baghdad,
Baghdad, Iraq.
Email : hudhudh60@yahoo.com, doctormrh2@gmail.com

ABSTRACT

Chitosan is the deacetylation derivative of chitin, which is the second most abundant polysaccharide found in nature after cellulose and commonly found in the shells and exoskeletons of crustacean, which are available in large quantities as waste products and by products of the shellfish industry. The present study described the effectiveness of different concentrations of chitosan solutions (0.25%, 0.5% , 1%) as a preservative on some quality characteristics of meat, as microbiological quality, lipid stability and organoleptic characteristic during 10 days of refrigerated storage. The microbiological quality and shelf life of meat treated with different concentrations of chitosan (0.25%, 0.5% and 1%).was investigated. The meat were evaluated for microbiological counts (total bacterial count, total psychotropic bacteria and total coliform bacteria) on 1, 7 and 10 days of storage. Microbial counts increased gradually *(*$p \leq 0.05$*)* in all samples during storage but the rate of increase was lower in 0.5% and 1% chitosan dipped samples with the mean value 7.12±0.16 , 6.79±0.29 respectively compared with control samples . There is a significantly decrease ($p \leq 0.05$) in the total psychotropic count with a long lag phase from the beginning of the storage period, the meat samples dipping in 0.5%,1% chitosan decreased significantly ($p \leq 0.05$) up to 10 days of storage and reached 6.63±0.07 CFU/g and 5.60±0.06 CFU/g respectively. In addition, the rate of *coliform* proliferation was generally slower than that of the control samples, reached 4.75±0.09 and 4.61±0.13 CFU / g respectively there was a decrease bacterial contamination of meat samples dipping in 0.25% chitosan but this decrease was not significantly difference ($p \leq 0.05$) after 10 day of storage. There were significant differences ($p \leq 0.05$) among the samples preserved in chitosan 0.5%, 1% in TBARS value 0.44±0.02, 0.36±0.01 compared with those of the control sample 1.49±0.05 after 10 days of storage. The pH values of the control samples were found to increase ($P \leq 0.05$) at the end of the storage period while samples which treatments with chitosan 0.5% ,1% inhibited the increase in pH during the storage period which caused the pH to reach a level of only 6.38±0.10, 5.98±0.03 compared with that measured for the control 6.92±0.04. The last part of present study was an attempt to know the effect of chitosan on organoleptic characteristic, all chitosan treated samples (0.5%, 1%) received good sensory attributes than the control samples, which after 7 days became unacceptable. Higher microbial counts and lipid oxidation in samples without chitosan treatment might be the

reason for their early spoilage. While meat samples treated with chitosan had a better sensory appearance and showed highly improvement of organoleptic characteristics.

Keywords: polysaccharide, microbial, meat, control, samples, chitosan

INTRODUCTION

Meat and meat products make important nutritional contribution to the diet of the people. It is recognized as a highly nutritious food being an excellent source of high quality protein, containing a good balance of the essential amino acids and having high biological value. Meat is also highly desired food, which frequently is the center of meal all around the world. The increase in meat consumption and production gives rise to various problems in handling, processing, preservation and storage, marketing and distribution till it reaches to the consumer [1] [2] [3].Chitosan is mostly applied as a food preservative and as a component of packaging material, not only to retard microbial growth in meat, but also to improve the quality and shelf life of meat [4]. It is a polysaccharide found in the shells of crabs and shrimps and the cell walls of fungi, It was investigated as an antimicrobial material against a wide range of target organisms like algae, bacteria, yeasts and fungi in experiments involving in vivo and in vitro interactions with chitosan in different forms. It has attracted attention as a potential natural food preservative [5].

Besides its antimicrobial effect, it possesses ant oxidative effects in foods. Chitosan also slows putrefaction by reducing lipid oxidation, which is currently one of the greatest economic problems facing the meat industry. It is one of the main causes of deterioration in the quality of meat and meat products during their storage and processing [6]. It is also maintaining the sensory quality of meat during storage. and has been shown to enhance the microbiological, chemical, odor and color qualities of the product [7].Chitosan has a number of uses in food industry such as lipid binding food additives, emulsification property ,dye absorption capacity , and the other properties of chitosan such as water binding capacity, bioactivity and toughness makes it an attractive material for food industry. It is Generally Recognized as Safe (GRAS) [8]

MATERIALS AND METHODS

Preparation meat samples for microbiological and chemical analysis

The meat from sheep animals were purchased from a local butcher in Baghdad governorate. In the lab, samples were divided into 5 groups for dipping (1 min.) in different solutions. The first group was served as control. The second group dipped in acetic acid 0.1% ,the third group was dipped in chitosan 0.25%, the fourth group was dipped in chitosan 0.5% and the five group was dipped in chitosan 1% .Samples were left to dry for 20 min. then each meat samples was packaged individually in polyethylene bag and put in the refrigerator until analysis. Three packages for each treatment were analyzed after 1, 7 and 10 days of refrigerated storage.

Preparation of chitosan solutions

An appropriate volume of chitosan stock solution at a concentration of 1.0 % (w/v) was aseptically diluted in distilled water to get final concentrations of 0.1, 0.15, 0.2, 0.25, 0.5, 1 % (w/v), followed by stirring to homogenize [9].

Susceptibility Test

Preparation of chitosan-impregnated discs with chitosan solution was carried out. Clean thick what man Cellulose filter papers were cut it as standard circular antibiotic like disc by appropriate applicator and distributed in sterile

plates for autoclaving before treatment with different chitosan concentrations. Sterile cooled filter papers were impregnated properly by each concentrated solution in each plate separately, and then left to absorb and adsorb the active ingredients in each concentration for twenty minutes. Preparation of freshly 0.5 McFarland culture broth of (10^5 cfu/ml) and distributed thoroughly on Muller-Hinton agars, then transferring each impregnated chitosan discs by sterile applicator and distributed evenly in inoculated plates (4-5 discs/plate) and incubated at 37 C^0 for 24 hours [10].Depending on diffusion rate for each impregnated disc, measuring size of inhibition zones to nearest millimeter, then determine minimum inhibitory for each concentration [11].

Determination the cut-off values (gradient concentration)

Each chitosan solution was added directly into sterile liquid agar to get final concentrations of 0.1%, 0.15%, 0.2%, 0.25%, 0.5%, 1% (w/v) .Each chitosan concentrations was poured into each Petri dish and afterwards allowed to stand until all the plates became solid. Viable cells were enumerated by spread plating of 0.1 mL aliquot of cell suspension dilution series (10^5) onto the surface of agar. The plates were triplicated and incubated at 37 °C for 72 h in the incubator. The grown colonies were then counted and compared with the control. Cut–off value of each chitosan was determined as the lowest concentration of each chitosan solution required to inhibit half log bacterial growth after incubation at 37 °C for 72 h completely [12].

Microbiological Analysis

The hygienic microbial quality tests which includes the total aerobic bacterial counts, total psychotropic counts (p.c) and coliforms plate counts (CPC), were made for each collected meat sample to reflect completely the sanitary condition of the meat throughout refrigerated storage. Twenty five grams of each sample had been homogenized in 225 ml sterile buffer Peptone water BPW solution, Decimal serial dilutions (10^{-1} to 10^{-7}) for every meat sample had been organized in sterile 0.1 % (wt/v) peptone water as a diluent and then pour plated in duplicate for each dilution on to nutrient agar at 45°C for both the total aerobic bacterial counts and psychrotrophic counts, i.e. one milliliter from each dilution was transferred to petri dish and mixed with 15 ml of nutrient agar and violet red bile agar at 45°C. The total aerobic bacterial colonies were enumerated after aerobic incubation at 37°C for 48 hours while the psychotropic colonies were enumerated after aerobic incubation at 7°C for 10 days. The coliform colonies were enumerated after aerobic incubation for 24 hours at 32°C.

Antioxidant activity assays (Thiobarbituric Acid reactive substance- TBARS values) Test

A common method used for quantitating malonaldehyde (MDA), a primary lipid peroxidation product, was performed in triplicates over a 1 , 7 and 10 day period on refrigerated samples according to Vyncke, the use of Thiobarbituric acid (0.375gm), hydrochloric acid (0.25M) and triochloroacetic acid (15%). Take 200µL from sample, 1000 µL thiobarbituric acid (0.375gm) and triochloroacetic acid(15%) 4000 µL Set sample tube at water bath 100 C0 for 15 minutes cool sample and centrifuge for 5 minutes. read supernatant at a wave length 532nm. read the blank (0.2ml 26 water instead of sample) on the same wave length(Beuge and Aust ,1978 modified with the aid of [13].

PH value

The PH value of meat samples were measure with PH meter. For this, meat samples was grinded by a blender then 5 gm of every meat samples (control and meat samples dipping in different concentrations of chitosan) after storage at refrigerator have been homogenized in 45 ml distilled water for 5 min. The pH of meat homogenate was measured for period storage after 1 day up to 7 day, 10 days. Then PH value was determined from the reading of PH meter. Calibration method was applied to probe of pH meter with standard buffer at 4.00 and 7.00

Organoleptic characteristics of the samples

Meat samples (about 100 g) were cooked by boiled in water. Sensory assessment was accomplished on meat prepared with chitosan and stored at 4 C^0 after 1, 7, 10 days storage.

Statistical analysis

Statistical analysis was performed using SAS software (Statistical Analysis System - version 9.1). Two-way ANOVA was applied and least significant differences (LSD) post hoc test was performed to assess significant differences among means. $P < 0.05$ was considered statistically significant.SAS.2010.SAS/STAT Users Guide for Personal Computer. Release 9.1.SAS Institute, Inc., Cary, N.C., USA

RESULTS

Disc susceptibility profile with Cut-Off Values determination (log count) for different chitosan concentrations

Table 1. provides the inhibition region diameters determined by disc diffusion for every chitosan concentration with cut off value have been preceded so as to determination of the threshold interface or cut-off breakpoints values that inhibit bacterial population. Cut-Off values dedication are defined as the lowest concentration of antimicrobial that will inhibit the visible growth of total bacterial count after overnight incubation.

Potency of chitosan as antimicrobial substance

The total bacterial count

The result showed the total bacterial counts after 10 days of refrigerated storage were affected significantly ($p \leq 0.05$) by dipping the meat samples in chitosan 0.5% and 1% reach 7.12±0.16 and 6.79±0.29 respectively compared with negative and positive control. Although There was a decrease in total bacterial count of meat samples dipping in 0.25% chitosan solution reach 9.10±0.48 but this decrease was not significantly difference ($p \geq 0.05$) after 10 day of storage at 4 C^0.

The total psychotropic bacterial count

The result in table 2. showed the psychotropic count of untreated meat samples (control) and acetic acid treated samples increased and reached at a value of 7.42±0.02 CFU/g and 7.34±0.01 CFU/g after day 10 of refrigerated storage, while the chitosan treated meat samples (0.5% , 1%) show a significantly decrease in the total psychotropic count ($p \geq 0.05$), up to 10 days of storage and reached 6.63±0.07 CFU/g and 5.60±0.06 CFU/g respectively which indicate the good effect of chitosan in maintain the quality of meat during storage period.

The Total coliform count

The effects of different chitosan concentrations on the growth of coliform bacteria are presented in Table 3.The rate of coliform proliferation of the chitosan treated samples was generally slower than that of the control samples after 10 days of refrigerated storage. There was a significant difference ($p \geq 0.05$) between the control and the samples treated with chitosan 0.5% and 1%. The coliform count in meat samples dipped in chitosan 0.5%, 1% reached 4.75±0.09 and 4.61±0.13 CFU / g respectively. In general, the rate of microbial proliferation of the chitosan treated samples was

slower than that of the control samples. The growth of total aerobic bacteria, psychotropic bacteria, and coliform bacteria on meat samples was effectively inhibited by chitosan 0.5%, 1% within the 10 days of refrigerated storage.

Chemical analysis

Antioxidant activity assays (Thiobarbituric Acid reactive substance-TBARS values)

Table 5. showed the antioxidant effects of chitosan on TBARS values of meat during 1 ,7,10 days of refrigeration storage. The TBARS values of all samples increased significantly with the extension of the storage period. There had been tremendous variations ($p \leq 0.05$) among the samples preserved in chitosan 0.5% ,1% in TBARS value in comparison with those of the negative (control) and positive controls (acetic acid sample) for every sampling during storage showing that those concentrations had highly protective effects against lipid oxidation in meat samples . The antioxidant impact changed into more potent in the 0.5% ,1% chitosan treated samples than within the 0.25% chitosan treated samples at all storage times.

PH value

Table 6. shows the effect of chitosan on the pH of meat samples during refrigerated storage at 4 C^0 for 1, 7, 10 days, at the end of the storage period chitosan treatments inhibited the increase in pH to some extent during the storage period. Treatment with 0.5%, 1% had the best effect, which caused the pH to reach a level of only 6.38±0.10, 5.98±0.03 compared with that measured for the negative and positive control 6.92±0.04, 6.88±0.04 respectively. No significant difference was measured with the samples treated with 0.25% ($P \geq 0.05$), which reached final pH levels of 6.87±0.13.

Sensory evaluation

The results presented in table 7. show the changes for color ,mouth feel, odour, flavor and appearance and overall acceptability of cooked meat samples submitted to different treatments of chitosan concentrations during refrigerated storage after 1,7 and 10 days of storage. The sensory attributes for odor, taste, color ,mouth feel and appearance after 7 days for the negative and positive control samples became unacceptable. While meat samples treated with chitosan (0.25% ,0.5%) had a better sensory appearance than the control and acetic acid samples and showed highly improvement of organoleptic characteristics. This observation suggests that chitosan has a good effect on the sensory attributes of meat.

DISCUSSION

Minimum inhibitory concentration for chitosan solution were proceeded in order to determination of the threshold interface or cut-off breakpoints values that inhibit bacterial growth. chitosan at concentrations 0.1% ,0.15% , 0.2% showed no inhibition zone was observed and there is no effect on total bacterial count whereas chitosan at concentration 0.25% showed some inhibitory effects with inhibition zone size (7 mm) and mean bacterial count 6.53 log compared with the other chitosan concentration (0.1% 0.15% 0.2%). Chitosan at concentration 0.5%, 1% showed the powerful inhibitory effect with inhibition zone size (18, 22 mm respectively), and the bacterial count 6.53, 6.16 log respectively. In order to obtain the optimum antimicrobial effectiveness of chitosan in this present study, several factors influencing the antimicrobial activity of chitosan, such as concentration, pH ,molecular weight and degree of deacetylation (DDA) of chitosan had to be optimized With regard to the application of chitosan for meat preservation, so, chitosan was used for meat preservation under improved conditions, [14]. The antimicrobial effect of chitosan regarded mainly to interaction of chitosan with membranes or cell wall components , resulting in increased permeability of the membranes and leakage of cell material from tissue or due to water binding capacity and inhibition of various enzymes by chitosan [15]. Chitosan cause destruction of the membrane of bacteria. Electrostatic forces in the structure of chitosan between the NH+3 groups and the negative residues which compete with the Ca2+

for electronegative sites on the membrane surface caused changes in the permeability of membrane wall [14] .This changes cause provokes internal osmotic imbalances and consequently prevent from the growth of bacteria. It is also because the hydrolysis of the peptidoglycans in the microorganism wall, leading to the leakage of intracellular electrolytes such as potassium ions and other low molecular weight components such as proteins, nucleic acids, glucose, and lactate dehydrogenaseor it may be due to Binding of chitosan with microbial DNA, which leads to the inhibition of the mRNA and protein synthesis is another mechanism for the antimicrobial effects of chitosan.[14]

.It is also act by chelation of metals, suppression of bacterial elements , chitosan possesses high chelating capacity for various metal ions (including Ni2+, Zn2+, Co2+, Fe2+, Mg2+, and Cu2+) in acid conditions, and it has been widely applied for the removal or recovery of metals in different industries. Metal ions that combine with the cell wall molecules of microorganisms are crucial for stability of the cell wall [16]. Also chitosan has ability for binding to essential nutrients to microbial growth.17 it is also has bio absorbent activity[17] and can absorb nutrients of bacteria and may inhibit their growth. The fact that pH of the treated meat samples with Chitosan increased slowly during storage at refrigerator temperature in compered with the control samples was probably due to an effective inhibitory activity of chitosan on proteolytic bacteria which causing decomposition of nitrogenous compounds. The present results show that chitosan at concentration (0.5 %, 1%) retarded the pH increase of meat to a value of 6.38 and 5.98 at the end of a 10-day of refrigerated storage, respectively

The effectiveness of chitosan on the oxidative stability of meat has already been demonstrated. The mechanism by which this inhibition takes place is thought to be related to the chelation of free iron, which is released from hem proteins during heat processing or storage [17]. The Higher microbial counts in samples without chitosan might be the reason for their early spoilage [18]. Moreover, lipid oxidation products and the production of ammonia from protein breakdown by microbes may have resulted in the production of off-odor, which may have been the cause for the poor sensory attributes of samples not receiving chitosan treatment on the 10th day of storage. While the lower total bacterial counts and lower MDA values indicates depression of rancid and spoilage flavor of meat prepared with chitosan thereby causing in more acceptance throughout the entire period of refrigerated storage [19].

CONCLUSIONS

Chitosan is a versatile material with proved antimicrobial activity. It is increase the shelf life and improve the microbial safety parameters of meat and meat products. Chitosan was a good antioxidant properties for shelf life extension of meat during refrigeration. On the basis of the results obtained antioxidant and antimicrobial properties could be a potential alternative natural product for synthetic food additive replacement and also could meet consumer safety requirement. It was also improved the sensory properties of meat during refrigeration.

REFERENCES

1. Apple, J. K., and Yancey, J. W. S. (2016). 138 the quandaries of measuring meat quality.Journal of Animal Science, 94(supplement2), 64e65.
2. Grunert, K. G., Bredahl, L., and Brunsø, K. (2004). Consumer perception of meat quality and implications for product development in the meat sectorda review. Meat Science, 66(2), 259e272.
3. Valous, N. A., Zheng, L., Sun, D. W., and Tan, J. (2016). Quality evaluation of meat cuts. In *Computer Vision Technology for Food Quality Evaluation (Second Edition)* (pp. 175-193).
4. Vasilatos, G. C., and Savvaidis, I. N., (2013). Chitosan or rosemary oil treatments, singly or combined to increase turkey meat shelf-life. International journal of food microbiology, 166(1), 54-58.
5. Rao, M. S.; Chander, R., and Sharma, A., (2005). Development of Shelf-stable Intermediate-moisture Meat Products Using Active Edible ChitosanCoating and Irradiation. Journal of food science, 70(7), m325-m331.

6. Darmadji, P., and Izumimoto, M., (1994). Effect of chitosan in meat preservation. Meat Science, v. 38, n. 2, p. 243-254.
7. Abd El-Rehim, H. A.; Zahran, D. A.; El-Sawy, N. M.; Hegazy, E. S. A., and Elbarbary, A. M., (2015). Gamma irradiated chitosan and its derivatives as antioxidants for minced chicken. Bioscience, biotechnology, and biochemistry, 79(6), 997-1004.
8. Food, U. S. (2001). Drug Administration Center for Food Safety and Applied Nutrition Office of Food Labeling June 11, 1998. Center for Food Safety and Applied Nutrition Office of Nutritional Products, Labeling and Dietary Supplements August, 30.
9. Ko, J. A.; Park, H. J.; Park, Y. S.; Hwang, S. J., and Park, J. B. (2003). Chitosan microparticle preparation for controlled drug release by response surface methodology. *Journal of microencapsulation*, *20*(6), 791-797
10. Liu, N.; Chen, X. G.; Park, H. J.; Liu, C. G.; Liu, C. S.; Meng, X. H., and Yu, L. J. (2006). Effect of MW and concentration of chitosan on antibacterial activity of Escherichia coli. *Carbohydrate polymers*, *64*(1), 60-65
11. No, H. K., Park, N. Y., Lee, S. H., and Meyers, S. P. (2002). Antibacterial activity of chitosans and chitosan oligomers with different molecular weights. *International journal of food microbiology*, *74*(1-2), 65-72
12. Andrews, J. M. (2001). Determination of minimum inhibitory concentrations. *Journal of antimicrobial Chemotherapy*, *48*(suppl_1), 5-16
13. Wysocka, M., Kubin, M., Vieira, L. Q., Ozmen, L., Garotta, G., Scott, P., and Trinchieri, G. (1995). Interleukin-12 is required for interferon-γ production and lethality in lipopolysaccharide-induced shock in mice. *European journal of immunology*, *25*(3), 672-676
14. Bilinski, B., and Chibowski, E. (1983). The determination of the dispersion and polar free surface energy of quartz by the elution gas chromatography method. *Powder Technology*, *35*(1), 39-45
15. Young, D. H.; Köhle, H., and Kauss, H. (1982). Effect of chitosan on membrane permeability of suspension-cultured Glycine max and Phaseolus vulgaris cells. *Plant Physiology*, *70*(5), 1449-1454
16. Kurita, K., Chemistry and application of chitin and chitosan. Polymer Degrad. Stabil., 1998, 59, 117–120.
17. Knorr, D. (1991). Recovery and utilization of chitin and chitosan in food processing waste management. *Food technology (USA)*.
18. No, H. K.; Meyers, S. P., Prinyawiwatkul, W., and Xu, Z. (2007). Applications of chitosan for improvement of quality and shelf life of foods: a review. *Journal of food science*, *72*(5), R87-R100
19. Cerveny, J.; Meyer, J.D. and P.A. Hall, (2009). Microbiological Spoilage of Meat And Poultry Products In: Compendium Of The Microbiological Spoilage, Of Foods And Beverages. Food Microbiology and Food Safety, W.H. Sperber and M.P. Doyle (Eds.). Springer Science and Business Media, NY, pp. 69-868. DOI: 10.1007/978-1-4419- 0826-1-3.

Table 1. Size of Inhibition Zone (mm) and Cut-Off Values determination for different chitosan concentrations

Chitosan concentration	Size of inhibition zone(mm)	Cut-off values determination (titer or log
Control	None	7.02
Acetic acid	None	7.11
Chitosan 0.1%	None	7.09
Chitosan 0.15%	None	7.05
Chitosan 0.2%	None	7.01
Chitosan 0.25%	7	6.53*
Chitosan 0.5%	18	6.16
Chitosan 1%	22	5.98

*Minimum cut of value of chitosan that inhibit spoilage bacteria.

Table 2. Mean ± Standard Error of the total bacteria count (log10) of meat samples dipped in different chitosan concentrations during 10 days of refrigerated storage

No	Group	1 day	7 days	10 days
1	Control	C7.29±0.14a	B 8.89±0.37a	A9.38±0.15a
2	Acetic acid	C7.16±0.12a	B 8.32±0.15a	A9.27±0.15a
3	Chitosan 0.25%	C7.02±0.13a	B 8.08±0.14a	A9.10±0.48a
4	Chitosan 0. 5%	C5.92±0.10b	B 6.20±0.14b	A7.12±0.16b
5	Chitosan 1%	C4.72±0.11c	B 5.00±0.14c	A6.79±0.29c
LSD		0.6057		

Table 3.The total psychotropic bacterial count (log10) of meat samples dipped in different chitosan concentrations during 10 days of refrigerated storage

No	Group	1 day	7 days	10 days
1	Control	C5.86±0.03a	B6.44±0.05a	A7.42±0.02a
2	Acetic acid	C5.79±0.03a	A6.37±0.05a	A7.34±0.01a
3	Chitosan0.25%	B5.78±0.03a	B6.34±0.05a	A7.32±0.01a
4	Chitosan 0. 5%	C4.65±0.03b	B5.81±0.02b	A6.63±0.07b
5	Chitosan 1%	C3.48±0.03c	B4.67±0.03c	A5.60±0.06c
LSD		0.1194		

Table 4. The Total coliform count (log10) of meat samples dipped in different chitosan concentrations during 10 days of refrigerated storage

No	Group	1 day	7 days	10 days
1	Control	C4.78±0.07a	B5.45±0.10a	A6.53±0.07a
2	Acetic acid	C4.56±0.16a	B5.41±0.11a	A6.42±0.08a
3	Chitosan0.25%	C4.52±0.15b	B5.32±0.11a	A6.39±0.09a
4	Chitosan 0.5%	C3.47±0.10b	B3.80±0.03b	A4.75±0.09b
5	Chitosan 1%	C2.94±0.12c	B3.30±0.12c	A4.61±0.13c
LSD		0.3086		

Table 5. TBARS values of meat samples dipped in different chitosan concentrations during 10 days of refrigerated storage.

No	Group	1 day	7 days	10 days
1	Control	C0.29±0.01a	B1.29±0.03a	A1.49±0.05a
2	Acetic acid	C0.26±0.01a	B1.27±0.05a	A1.44±0.05a
3	Chitosan 0.25%	C0.24±0.01a	B1.26±0.03a	A1.43±0.04a
4	Chitosan 0. 5%	C0.14±0.01b	B0.31±0.03b	A0.44±0.02b
5	Chitosan 1%	C0.12±0.01b	B0.28±0.01b	A0.36±0.01b
LSD		0.0984		

Table 6. PH values of meat samples dipped in different chitosan concentrations during 10 days of refrigerated storage

No	Group	1 day	7 days	10 days
1	Control	C6.11±0.03a	B6.63±0.04a	A6.92±0.04a
2	Acetic acid	B5.97±0.05a	B6.55±0.04a	A6.88±0.04a
3	Chitosan 0.25%	C5.94±0.04a	A6.56±0.04a	A6.87±0.13a
4	Chitosan 0. 5%	B5.67±0.05b	A6.12±0.05b	A6.38±0.10b
5	Chitosan 1%	B5.48±0.03c	A5.96±0.05c	A5.98±0.03c
LSD		0.1707		

Table 7. Effect of different concentrations of chitosan on sensory characteristics of cooked meat during 10 days of storage

Meat samples	1 day	7 day	10 day
Control	-ve	+ve	+ve
Acetic acid	-ve	+ve	+ve
Chitosan 0.25%	-ve	+ve	+ve
Chitosan 0.5%	-ve	-ve	-ve
Chitosan 1%	-ve	-ve	-ve

(+ve) There is adversely effect on organoleptic characteristic. (-**ve**) There is no adversely effect on organoleptic characteristic

Indian Journal of Natural Sciences www.tnsroindia.org.in ©IJONS

Vol.9 /Issue 50 /October / 2018 *International Bimonthly* *ISSN: 0976 – 0997*

RESEARCH ARTICLE

Assessment of *In vitro* X-Ray Radiation Overexposure by Cytokinesis - Block Micronucleus Assay in Human Peripheral Blood Lymphocytes (HPBLs) in Saudi Population

Mashael A. Alotaibi,1* Entisar S. Alsuhaibani[2] and Ghazi A. Alsbeih[3]

[1]Department of Biology, Faculty of Sciences, Aljouf University, Kingdom of Saudi Arabia
[2]Department of Zoology, Faculty of Sciences, King Saud University, Kingdom of Saudi Arabia
[3]Radiation Biology Section, Biomedical Physics Department, King Faisal Specialist Hospital & Research Centre.

Received: 26 Jun 2018 Revised: 28 July 2018 Accepted: 31 Aug 2018

*Address for Correspondence
Mashael A. Alotaibi
Department of Biology,
Faculty of Sciences,
Aljouf University,
Kingdom of Saudi Arabia
Email : maotaibi2017@gmail.com, ealsuhaibani@ksu.edu.sa, galsbeih@kfshrc.edu.sa

ABSTRACT

The cytokinesis-block micronucleus assay as Rapid biodosimetry tool is required to assist with triage in the case of ionizing radiations exposure, whether medical, occupational or accidental that leads to deleterious biological consequences like mortality or carcinogenesis. Here, we aimed to evaluate the relationship of DNA damage parameters; micronuclei (MNi) frequencies, binucleated cells (BNCs) and nuclear division index (NDI) of peripheral blood lymphocytes cells (PBLcs) taken from healthy donors with x-ray radiation dose rate.We performed prospective analysis on 20 peripheral blood lymphocytes samples taken from healthy volunteers. The blood samples were irradiated with single X-rays doses of 320 KeV with dose rate of 0.913 Gy/min and blood samples were exposed at the dose levels of 0, 0.5, 1, 2, 3, 4, and 5 Gy. The blood samples were then cultured for 72 h at 37°C and processed following the International Atomic Energy Agency standard procedure with slight modifications. We observed significantly increase in the average number of micronuclei with increasing radiation dose as compared with control subjects, the highest average number of MNi (400.700±14.343) was found in irradiated female lymphocytes at 5Gy dose, while minimum average numbers of MNi (0.700±14.343) was in non-irradiated female lymphocytes samples. The number of micronuclei in BNCs cells for healthy tended to be greater in females relative to males at lower doses of radiation (0.5- 2Gy), but this effect was not statistically significant at high doses (3–5 Gy). Average numbers of binucleated cells and nuclear division index were significantly decreased by increasing radiation dose as compared with control groups. The increased

number of nuclei following high radiation doses could represent a negative impact on public health especially that of workers exposed to radiation.

Keywords: cytokinesis-block micronucleus assay, micronuclei, biodosimetry, cytogenetic, X-rays, and lymphocytes

INTRODUCTION

Radiation exposure due to radiotherapy or following a large-scale radiological accident, or detonation of either a small radiological dispersal device or an improvised nuclear device in a populated area can damage the human tissues considerably (Iyer R, Lehnert BE 2000, Singh VK, et al. 2012; Garty G 2010). The ability to achieve an accurate estimate of the absorbed radiation dose is critical for people exposed to significant levels of ionizing radiation, as this information can predict the short-and/or long-term health implications and provide evidence needed for effective counseling. Cases of overexposure to radiation are typically rare and have a limited number of potential casualties. However, in these isolated cases, the primary focus is on providing the most accurate dose estimate, considering details of the exposure, such as the type and quality of the radiation and the uniformity, duration, and timing of the exposure (Ainsbury EA 2010; Rothkamm K 2013). DNA (genetic material) that exists in the nucleus and mitochondria of most cells has been recognized as most critical target for transferring ionizing radiation in living tissue is (Steenken S 1989).

Cytogenetic methods are potential tools to assess radiation damage and to support triage, medical treatment decisions, and prognosis of radiation casualties. Chromosomal aberration is widely known as cytogenetic indicators used in the field of radiobiology to evaluate the effects of exposure to ionizing radiation (Thierens H, et al.2002), especially dicentric chromosome assay (DCA) and the in vitro cytokinesis-block micronucleus (CBMN) assay have been established as the main biodosimetry tests for ionizing radiation exposure (WHO 2014). The CBMN assay, developed by Fenech and Morley in 1985, is a reliable method to quantify chromosome breakage and loss in nucleated cells (Fenech M & Morley AA 1985; Tucker JD 2013). The CBMN assay is a very reliable standardized technique in the field of radiation biology established to assess in vivo radiation exposure of occupational, medical, and accidentally exposed individuals and to assess individual in vitro cancer susceptibility or radiosensitivity (Thierens H et al. 1999, Sari-Minodier I et al. 2007 and Fucic A et al. 2008). In vitro MN test with CBMN of human peripheral blood lymphocytes has been used extensively to study chromosomal damage induced by ionizing radiation or chemicals (Mill AJ et al. 1996) Because radiation-induced MN has is strongly correlated with a radiation dose and quality dependence, micronuclei can be used as a biological dosimeter for radiation protection purposes (Hall EJ et al. 2012) and MN assay has been recommended by the International Atomic Energy Agency (IAEA. 2011]

The CBMN assay works by assessing micronuclei (MNi), which can occur when small acentric chromosome fragments are not incorporated into the daughter nuclei during cell division. Instead, they are enveloped by a nuclear membrane and appear as small nuclei, known as micronuclei, in the cytoplasm outside the main daughter nuclei. Micronuclei can arise during exposure to various clastogenic agents and are the result of non- or mis-repaired DNA double strand breaks. Micronuclei can also contain whole chromosomes that lag at anaphase during nuclear division and by consequence are not incorporated in the main nuclei. In the CBMN assay, the scoring of micronuclei is restricted to once-divided cells, which are recognized by their binucleate (BN) appearance, after inhibition of cytokinesis by cytochalasin B. This restriction prevents confounding effects caused by variable cell division kinetics (Fenech M & Morley AA 1985). Due to its good reliability and reproducibility, the CBMN assay has become one of the standard cytogenetic techniques for genetic toxicology testing in human and mammalian cells in general (Deng B, et al. 2015; Shahane SA, et al. 2016). In addition, scoring of micronuclei in the CBMN assay is easy and quick, making it much less labor-intensive than the DCA method and an attractive option for population triage in the case of large-scale radiation accidents, as well as for large-scale assessments of genetic damage in radiation workers receiving a

high dose of radiation (Deng B, et al. 2015). The main aim of this study was to assess the effect of overexposure to radiation on the peripheral blood lymphocytes cells isolated from the blood of Saudi volunteers as a reliable biomarker for measuring the emerging DNA damage, this assessment was carried out by visual scoring the micronuclei frequency, micronucleated cells and The nuclear division index in 1000 peripheral blood lymphocytes cultures of non-irradiated (control) and irradiated (0.5-5Gy) lymphocytes samples

MATERIAL AND METHODS

Blood Sampling

This study is a prospective study performed in six-month period between May and October 2016. a total of 20 Peripheral blood samples were collected from nonsmoking and apparently healthy human volunteers had no history of exposure to radiation and did not suffering from any serious acute or chronic illness in Sulaiman Al Habib Hospital. The age range was between 25 and 35 years that consist of 10 males and 10 females. Aliquots of 2 mL of whole blood were drawn in heparinized vials using a vacutainer system (Becton Dickinson, Germany). Blood was taken from study Subjects with informed consent and the approval of a local ethics committee.

Exposure of HPBLs to X-ray radiation

In vitro, Heparinized blood samples were irradiated immediately after venipuncture at 37°C using single X-ray doses with a mean photon energy of 320 keV (filtered with 1 mm) using X RAD 320 System (Precision X-Ray, United States). The dose rate was approximately 0.913 Gy/min and to obtain a calibration curve, blood samples were exposed at the dose levels of 0, 0.5, 1, 2, 3, 4, and 5 Gy. The irradiation was performed according to IAEA procedure (IAEA 2011), after irradiation, blood samples were kept at 37°C in to allow for any chromosomal repair to take place.

Isolation and culture of Lymphocyte

Blood culture and harvest procedures were conducted according to the instructions in the IAEA manual (IAEA 2011) with minor modifications. Briefly, 0.5 ml of peripheral blood samples (non-irradiated and irradiated) was added to 4.5 ml of RPMI 1640 culture medium (Sigma, USA) enriched with L-glutamine containing 10-15% fetal calf serum, 2% penicillin, 3% streptomycin and stimulated with 3% phytohaemagglutinin (Sigma, USA) at 37 ˚C . After 48 hours of culture, 45 µl Cytochalasin B (Sigma Aldrich) was added to the samples. After 72 hours of incubation, cells were collected by centrifuging the blood **s**ample at 800 rpm for 5 minutes. The collected cells were suspended in 6 ml of cold hypotonic solution (0.075 M cold KCl), centrifuged at 800 rpm for 5 min. the cells were fixed in methanol: Glacial acetic acid (6:1) for 3 times.

Slide preparation and Micronuclei scoring

To prepare the microscopic slides, the fixed cells were dropped on the glass slides, air-dried and stained with 5% aqueous solution of Giemsa dye Sigma Aldrich) for 15 min. Assessment of slides was carried out using Nikon microscope with ×100 magnification to determine the numbers of micronuclei in cytokinesis-blocked according to the criteria proposed by (Fenech M, Morley AA 1985 and IAEA 2011). A total of 1000 lymphocytes were examined for the Number of binucleated cells and the Number of micronuclei

Statistical Analysis

The data of this study were compiled into the computerized data file and frequency and statistical description (Mean, SE) were divided using SPSS statistical software V. 19. We used statistical analysis of variance (ANOVA) test and least significantly difference (LDS) at level of significance was set to $P<0.05$.

RESULTS

In the preliminary study, lymphocytes cultures of non-irradiated (control) and irradiated peripheral blood samples were subjected to the cytokinesis-block micronucleus assay according to standard protocol as described by (Varga et al. 2004) as a valuable dose assessment method in cases of radiation overexposure with or without physical dosimetry data. Visual scoring the frequencies of binucleated cells (BNCs), micronuclei (BNi) and Nuclear division index (NDI) on 1000 peripheral blood lymphocytes samples exposed to X-rays from 0.5 to 5 Gy as compared with control samples Table 1. The (NDI) was significantly higher in non-irradiated male control lymphocytes cultures (0.918±0.03, 0.89±0.03) and gradually increased by increasing x-ray dose, while minim average numbers of NDI (120±0.03) was in irradiated male lymphocytes with 5Gy dose. Study results showed that the highest average numbers of BNCs scored in 1000 non-irradiated and irradiated lymphocytes cultures were found in non-irradiated male samples (920.40±30.038) and relatively decreased in accordance with increase radiation dose in both sex, while minim average numbers of BNCs (120.40±30.038) was in irradiated male lymphocytes at 5Gy dose Figure 1 (a). We observed that the number of MNi scored in BNCs increased proportionally with radiation dose rate ($R^2 = 0.89$; Figure 1(b). The highest average number of MNi (400.700±14.343) was found in irradiated female lymphocytes at 5Gy dose, while minimum average numbers of MNi (0.700±14.343) was in non-irradiated female lymphocytes samples Figure 2.

The effects of gender on DNA damage measured using micronuclei frequencies in peripheral blood lymphocytes was firstly reported by Fenech and Neville (1994). Our observations in this study indicated the influence of gender on the average of micronuclei scores in Binucleated lymphocyte cells for healthy tended to be greater in females relative to males (Mean; 191.671±5.421 and 233.443±5.421) respectively as represented in Figure 3. However, this was only true at lower doses of radiation (0.5–2 Gy), but at high doses (3–5 Gy), there was no statistically significant difference in the average number of MNi between groups 4 Gy4: female (399.7) and male (291.8) and Gy5: female (400.7) and male (224.7) Figure 1(b).

DISCUSSION

The present study investigated the effects of X-ray irradiation on human peripheral blood lymphocytes (HPBLs) by evaluating DNA damage using CBMN assay, which is a simple, rapid, and reliable tool for assessing radiation-induced cytogenetic damage (Sram RJ, et al 2016; Bolognesi C, et al. 2017). In general, Parameters of BNCs, MNi and NDI were significantly and dose dependently changed after irradiation by 1 – 5 Gy as compared with control subjects. On the other hand cellular proliferation decreased with increasing radiation dose, in agreement with previous work on HPBL irradiated with X-rays (Heimers A, et al 2005). We also investigated differences in DNA damage following irradiation with X-rays by measuring MN in binucleated cells. The mean baseline frequency of MN in non-irradiated lymphocytes was similar to that of previous reports and was within the expected range (WHO 2014). At higher doses, damage is likely to occur, leading to a decrease in cellular proliferation and increased cytogenetic damage, thereby increasing cell death (Müller WU & Rode A 2002). The biological responses of irradiated cells also depend on the dose rate (Konopacka M & Rogoliński J 2011). Specifically, a decreased dose rate can result in decreased micronuclei formation in HPBL, possibly due to efficient repair (Konopacka M & Rogoliński J 2011; Vral A, et al. 1992). NDI is a measure of cytostasis and cell death (cytotoxicity) as a marker of cell proliferation. The rationale behind NDI is cells with greater chromosomal damage are less likely to enter cell division or cell death occurs before cell division (Ionescu ME et al. 2011). Our findings showed decreased BNCS and NDI in the x-ray irradiated samples

in comparison to the controls subjects. if all viable cells complete one division during the cytokinesis-block phase the binucleated cells will be formed and they will contain more than two nuclei If some viable cells complete more than one nuclear division (Ionescu ME et al. 2011 and Fenech M 2007). Analysis of nuclear division index revealed significant differences in lymphocyte proliferation rate upon irradiation; this agrees with an earlier study reporting that DNA damage response was altered by irradiation (Shahane SA, et al. 2016).

A reduction in the dose rate may favor the arrest of cells with DNA damage in the G1 and G2 phases over cell death, which is mediated by the transducer protein kinase ataxia-telangiectasia mutated (ATM). ATM prevents cells from replicating damaged DNA and provides time for DNA repair, in contrast to the induction of apoptosis of damage cells that occurs at a high dose rate (Konopacka M & Rogoliński J 2011). Micronuclei are formed because of chromosome breaks or when entire chromosomes fail to engage with the mitotic spindle fibers and lag behind when cells divide. In 1985, Fenech established the CBMN assay in HPBL (Fenech M & Morley AA 1985) and it is now a well-established cytogenetic dosimetry method. This assay has several advantages, such as speed and ease of analysis, no requirement for metaphase cells, and reliable identification of cells that have completed only one nuclear division (IAEA 2001; Yang H, 2014). In an emergency, radiation dose estimates should be provided as soon as possible with sufficient accuracy to support clinical decision-making. Cells producing micronuclei die quickly after large doses of radiation exposure and, combined with delays in cell-cycle progression, this can result in fewer cells reaching mitosis. The CMBN assay requires 72 hours of culture time, after which cell processing can occur followed by slide preparation. Scoring of micronuclei is easier with this assay than the DCA method and requires less skilled technical staff (AFRRI 2010). For standard biodosimetry it is recommended that 1,000 binuclear cells be scored (Voisin P, et al. 2001) and, as such, counting can be performed in approximately 2 hours. Recent work by Lindholm and colleagues demonstrated that scoring of 200 binuclear cells was sufficient to identify radiation doses of >1 Gy, and took about 15 minutes (Lindholm C et al. 2010).

There are some drawbacks to the CBMN assay; however, new improvements have made the assay more specific to radiation exposure (Fenech M 2010) and enabled automated scoring of the assay for high-throughput analysis (Decordier I, et al. 2008; Willems P, et al. 2010). The CBMN assay has a dose range of approximately 0.3–5 Gy, although it has been suggested that a range of 0.1–15 Gy may be attainable with modifications to the method (WHO 2014; Fenech M 2010; Willems P, et al. 2010; Darroudi F, et al. 1998; Darroudi F 1998; AFRRI 2010; de Lemos Pinto MM, et al. 2010; Vral A, et al. 2011.Use of an automated scoring system could result in a lower dose limit of 1 Gy, however, it is unclear how accurate this measurement would be. A blood sample can be drawn immediately, with the first results available 3-4 days after culturing and processing has begun Voisin P, et al. 2001; Fenech M 2010; Willems P, et al. 2010). Experiments have shown that this method is reliable for up to 6 months after exposure (Thierens H, et al. 2005), but with a correction factor the time can be extended to approximately 1 year (Vral A, et al. 2011; Fenech M, et al. 1990; Fenech M 1993). ISO standardization is currently pending for this method, although scoring standards have been published (Fenech M, et al. 2003).

The present study was designed to examine the micronuclei frequency in HPBL. To this end, we incubated samples at 37°C with added Phytohaemagglutinin (PHA), stimulated the cells to enter the cell cycle, and then processed them for the CBMN assay. Our results suggest that there was a significant increase in the number of micronuclei in irradiated blood samples. Previous studies have reported that the yield of dicentric chromosomes and micronuclei is increased by the prolonged culture of lymphocytes with PHA at different time intervals (Hoffmann GR, et al. 2002; Krishnaja AP, Sharma NK 2006). Similar results have been reported for chromosomal aberrations, in which delayed stimulation of lymphocytes followed by radiation exposure resulted in levels of aberration that were elevated compared to lymphocytes stimulated immediately (Wilkins RC, et al. 2008). Furthermore, our results strongly support the idea that storage of blood samples for 24 hours and delayed mitogenic stimulation (24 hours post-irradiation, stored at 37°C) reduces the frequency of micronuclei. A significant reduction in micronuclei frequency in stimulated lymphocytes at twenty hours post-irradiation, compared to two or six hours post-irradiation, might be caused by checkpoint activation and cell-cycle arrest or by repair of radiation-induced DNA damage. It has been

demonstrated that A damage can induce cell-cycle arrest by activating numerous signaling molecules and pathways, and the G1 checkpoint could have played a dominant role, as circulating blood lymphocytes are arrested in the G0/G1 stage in an ATM- and P53-dependent manner (Lavin MF, Khanna KK 1999).

CONCLUSIONS

As a result of this study we can conclude, accumulation of genetic damage is detectable in peripheral lymphocytes of healthy individuals exposed to x-ray radiation. The MN frequency increases and affected by gender while the BNCs and NDI decreases with increase the dose rate. Our results suggest that Establishing a laboratory which competent enough to perform cytogenetic analysis for biodosimetry is very important in Saudi Arabia for measuring micronuclei in BNCs cells as best biomarker to assess radiation damage evaluated by CBMN assay

REFERENCES

1. [AFRRI] Armed Forces Radiobiology Research Institute (USA) AFRRI TRIGA Reactor Facility to satisfy the requirements of U.S. 2010 1-31 Dec. Nuclear Regulatory Commission License No. R-84 (Docket No. 50-170), Technical Specification 6.6.b
2. Ainsbury EA1, Bakhanova E, Barquinero JF, Brai M, Chumak V, Correcher V, Darroudi F, Fattibene P, Gruel G, Guclu I, et al. 2010. Review of retrospective dosimetry techniques for external ionising radiation exposures. Radiation protection dosimetry;147(4):573-92
3. Bolognesi C, Bruzzone M, Ceppi M, Kirsch-Volders M. 2017. The lymphocyte cytokinesis block micronucleus test in human populations occupationally exposed to vinyl chloride: A systematic review and meta-analysis. Mutation Research/Reviews in Mutation Research;774:1-1.
4. Darroudi F. 1998. Detection of total-and partial-body irradiation in a monkey model: a comparative study of chromosomal aberration, micronucleus and premature chromosome condensation assays. International journal of radiation biology;74(2):207-15.
5. Darroudi F, Fomina J, Meijers M, Natarajan AT. 1998. Kinetics of the formation of chromosome aberrations in X-irradiated human lymphocytes, using PCC and FISH. Mutation Research/Fundamental and Molecular Mechanisms of Mutagenesis; 404 (1):55-6.
6. Decordier I, Papine A, Plas G, Roesems S, Vande Loock K, Moreno-Palomo J, Cemeli E, Anderson D, Fucic A, Marcos R. 2008. Automated image analysis of cytokinesis-blocked micronuclei: an adapted protocol and a validated scoring procedure for biomonitoring. Mutagenesis;24(1):85-93.
7. De Lemos Pinto MM, Santos NF, Amaral A. 2010. Current status of biodosimetry based on standard cytogenetic methods. Radiation and environmental biophysics;49(4):567-81.
8. Deng B, Hou J, Quan Y, Dong L, Tan Z. 2015. Cytogenetic Effects of Low-Dose Tritiated Water in Human Peripheral Blood Lymphocytes—Experimental Studies on the Relative Biological Effectiveness and Chromosome Aberration Rate and CBMN in Human Blood Lymphocyte Irradiated by Tritium Low Dose Tritium â-Rays and 60Co ã-Rays. Open Journal of Clinical Diagnostics;5(04):125.
9. Fenech M. 1993. The cytokinesis-block micronucleus technique: a detailed description of the method and its application to genotoxicity studies in human populations. Mutation Research/Fundamental and Molecular Mechanisms of Mutagenesis. 31;285(1):35-44.
10. Fenech M. 2007. Cytokinesis-block micronucleus cytome assay. Nat Protoc; 2: 1084-104.
11. Fenech M. 2010. The lymphocyte cytokinesis-block micronucleus cytome assay and its application in radiation biodosimetry. Health physics;98(2):234-43
12. Fenech M, Chang WP, Kirsch-Volders M, Holland N, Bonassi S, Zeiger E. 2003. HUMN project: detailed description of the scoring criteria for the cytokinesis-block micronucleus assay using isolated human lymphocyte cultures. Mutation Research/Genetic Toxicology and Environmental Mutagenesis;534(1):65-75.
13. Fenech M, Denham J, Francis W, Morley A. 1990. Micronuclei in cytokinesis-blocked lymphocytes of cancer

patients following fractionated partial-body radiotherapy. International journal of radiation biology;57(2):373-83.

14. Fenech M, Morley AA. 1985. Measurement of micronuclei in lymphocytes. Mutation Research/Environmental Mutagenesis and Related Subjects;147(1-2):29-36.
15. Fenech, M., Neville, S. and Rinaldi, J. 1994. Sex is an important variable affecting spontaneous micronucleus frequency in cytokinesis-blocked lymphocytes. Mutat. Res., 313, 203–207.
16. Fucic A, Brunborg G, Lasan R, Jezek D, Knudsen LE, Merlo DF. 2008. Genomic damage in children accidentally exposed to ionizing radiation: A review of the literature. Mutat Res;658:111-23
17. Garty G, Chen Y, Salerno A, Turner H, Zhang J, Lyulko O, Bertucci A, Xu Y, Wang H, Simaan N, et al. 2010. The RABIT: a rapid automated biodosimetry tool for radiological triage. Health physics;98(2):209.
18. Hall EJ, Giaccia AJ. 2012. Radiobiology for the Radiobiologist. 7th ed. Philadelphia: JB Lippincott Company
19. IAEA] International Atomic Energy Agency. 2001. Cytogenetic analysis for radiation dose assessment. IAEA technical reports series no. 405. Vienna: International Atomic Energy Agency; p. 1–127.
20. Heimers A, Brede HJ, Giesen U, Hoffmann W. 2005. Influence of mitotic delay on the results of biological dosimetry for high doses of ionizing radiation. Radiation and environmental biophysics;44(3):211-8.
21. IAEA. 2011. Cytogenetic dosimetry: Applications in preparedness for and response to radiation emergencies. Vienna: IAEA-EPR.
22. Hoffmann GR, Sayer AM, Littlefield LG. 2002. Higher frequency of chromosome aberrations in late-arising first-division metaphases than in early-arising metaphases after exposure of human lymphocytes to X-rays in G 0. International journal of radiation biology;78(9):765-72.
23. Ionescu ME, Ciocirlan M, Becheanu G, Nicolaie T, Ditescu C, Teiusanu AG, et al. 2011. Nuclear division index may predict neoplastic colorectal lesions. Maedica (Buchar); 6: 173-8
24. Iyer R, Lehnert BE. 2000. Effects of ionizing radiation in targeted and nontargeted cells. Arch Biochem Biophys; 376(1): 14-25.
25. Konopacka M, Rogoliński J. 2011. Clastogenic effects in human lymphocytes exposed to low and high dose rate X-ray irradiation and vitamin C. Nukleonika;56(4):253-7.
26. Krishnaja AP, Sharma NK. 2006. Differential radiation effects in smokers–culture time dependence of the yield of gamma ray-induced chromosome damage in first division metaphases. International journal of radiation biology;82(5):363-77
27. Lavin MF, Khanna KK. 1999 Jan. ATM: the protein encoded by the gene mutated in the radiosensitive syndrome ataxia-telangiectasia. International journal of radiation biology.1; 75 (10):1201-14.
28. Lindholm C, Stricklin D, Jaworska A, Koivistoinen A, Paile W, Arvidsson E, Deperas-Standylo J, Wojcik A. 2010. Premature chromosome condensation (PCC) assay for dose assessment in mass casualty accidents. Radiation research;173(1):71-8.
29. Mill AJ, Wells J, Hall SC, Butler A. 1996. Micronucleus induction in human lymphocytes: Comparative effects of X-rays, alpha particles, beta particles and neutrons and implications for biological dosimetry. Radiat Res:145:575-85.
30. Müller WU, Rode A. 2002. The micronucleus assay in human lymphocytes after high radiation doses (5–15 Gy). Mutation Research/Fundamental and Molecular Mechanisms of Mutagenesis;502(1):47-51
31. Rothkamm K, Beinke C, Romm H, Badie C, Balagurunathan Y, Barnard S, N. Bernard N, Boulay-Greene H, Brengues M, De Amicis A, et al. 2013. Comparison of established and emerging biodosimetry assays. Radiation research.;180(2):111-9
32. Sari-Minodier I, Orsière T, Auquier P, Martin F, Botta A. 2007. Cytogenetic monitoring by use of the micronucleus assay among hospital workers exposed to low doses of ionizing radiation. Mutat Res;629:111-21.
33. Shahane SA, Nishihara K, Xia M. 2016. High-Throughput and High-Content Micronucleus Assay in CHO-K1 Cells. High-Throughput Screening Assays in Toxicology:77-85.
34. Singh VK, Ducey EJ, Brown DS, Whitnall MH. 2012. A review of radiation countermeasure work ongoing at the Armed Forces Radiobiology Research Institute. International journal of radiation biology. 88(4):296-310
35. Sram RJ, Svecova V, Rossnerova A. 2016. Systematic review of the use of the lymphocyte cytokinesis-block micronucleus assay to measure DNA damage induced by exposure to polycyclic aromatic hydrocarbons.

Mutation Research/Reviews in Mutation Research.;770:162-9.

36. Steenken S. 1989. Purine bases, nucleosides, and nucleotides: aqueous solution redox chemistry and transformation reactions of their radical cations and e– and OH adducts. Chem Rev; 89(3): 503-520.
37. Thierens H, De Ruyck K, Vral A, de Gelder V, Whitehouse CA, Tawn EJ, Boesman I. 2005. Cytogenetic biodosimetry of an accidental exposure of a radiological worker using multiple assays. Radiation protection dosimetry;113(4):408-14.
38. Thierens H, Vral A, Barbé M, Meijlaers M, Baeyens A, Ridder LD. 2002. Chromosomal radiosensitivity study of temporary nuclear workers and the support of the adaptive response induced by occupational exposure. Int J Radiat Biol;78:1117-26.
39. Thierens H, Vral A, de Ridder L, Touil N, Kirsch-Volders M, Lambert V, et al. 1999. Inter-laboratory comparison of cytogenetic endpoints for the biomonitoring of radiological workers. Int J Radiat Biol:75:23-24.
40. Tucker JD, Vadapalli M, Joiner MC, Ceppi M, Fenech M, Bonassi S. 2013. Estimating the lowest detectable dose of ionizing radiation by the cytokinesis-block micronucleus assay. Radiation research;180(3):284-91.
41. Voisin P, Benderitter M, Claraz M, Chambrette V, Sorokine-Durm I, Delbos M, Durand V , Leroy A , Paillole N. 2001. The cytogenetic dosimetry of recent accidental overexposure. Cellular and molecular biology (Noisy-le-Grand, France);47(3):557-64.
42. Varga D, Johannes T, Jainta S, Schuster S, Schwarz-Boeger U, Kiechle M, et al. An automated scoring procedure for the micronucleus test by image analysis. Mutagenesis 2004; 19:391–7[
43. Vral A, Fenech M, Thierens H. 2011. The micronucleus assay as a biological dosimeter of in vivo ionising radiation exposure. Mutagenesis;26 (1):11-7
44. Vral A, Thierens H, De Ridder L. 1992. Study of dose-rate and split-dose effects on the in vitro micronucleus yield in human lymphocytes exposed to X-rays. International journal of radiation biology;61(6):777-84
45. {WHO} World Health Organization. 2014. Cytogenetic Dosimetry: Applications in Preparedness for and Response to Radiation Emergencies (Spanish Edition). International Atomic Energy Agency
46. Wilkins RC, Romm H, Kao TC, Awa AA, Yoshida MA, Livingston GK, Jenkins MS, Oestreicher U, Pellmar TC, Prasanna PG. 2008. Interlaboratory comparison of the dicentric chromosome assay for radiatiobiodosimetry in mass casualty events. Radiation research;169(5):551-60.
47. Willems P, August L, Slabbert J, Romm H, Oestreicher U, Thierens H, Vral A. 2010. Automated micronucleus (MN) scoring for population triage in case of large scale radiation events. International journal of radiation biology;86(1):2-11.
48. Yang H, Feng R, Liu J, Wang H, Wang Y. 2014. Increased frequency of micronuclei in binucleated lymphocytes among occupationally pesticide-exposed populations: a meta-analysis. Asian Pac J Cancer Prev;15:6955-60.

Table 1: The average values of binucleated cells, micronuclei and division index scored in 1000 lymphocyte cells of male and female after X-ray exposure

Irradiated Dose (Gy)	Gender	BNCs (Mean ± SE)	MNi (Mean ± SE)	NDI (Mean ± SE)
Dose 0 Gy	M	920.40 ± 30.038	1.800 ± 14.343	0.918 ± 0.03
	F	893.1 ± 30.038	0.700 ± 14.343	0.89 ± 0.03
Dose 0.5 Gy	M	816.7 ± 30.038	82.500 ± 14.343	0.816 ± 0.03
	F	816.8 ± 30.038	88.100 ± 14.343	0.817 ± 0.03
Dose 1 Gy	M	613.40 ± 30.038	164.600 ± 14.343	0.613 ± 0.03
	F	679.5 ± 30.038	166.900 ± 14.343	0.679 ± 0.03
Dose 2 Gy	M	555.4 ± 30.038	242.500 ± 14.343	0.555 ± 0.03
	F	604.0 ± 30.038	256.900 ± 14.343	0.604 ± 0.03
Dose 3 Gy	M	374.4 ± 30.038	333.800 ± 14.343	0.374 ± 0.03

	F	410.80 ± 30.038	321.100 ± 14.343	0.411 ± 0.03
Dose 4 Gy	M	188.299 ± 30.038	291.800 ± 14.343	0.188 ± 0.03
	F	205.60 ± 30.038	399.700 ± 14.343	0.206 ± 0.03
Dose 5 Gy	M	120.40 ± 30.038	224.700 ± 14.343	0.120 ± 0.03
	F	136.60 ± 30.038	400.700 ± 14.343	0.137 ± 0.03

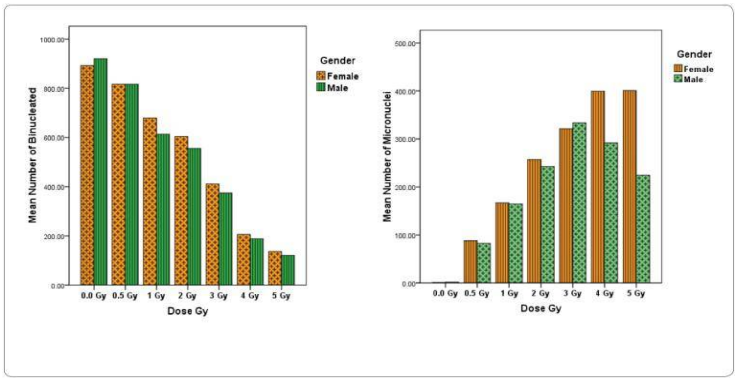

Figure 1. Mean of micronuclei (A) scored in binucleated cells (B) in 1000 non-irradiated and irradiated PBLs sample based on gender

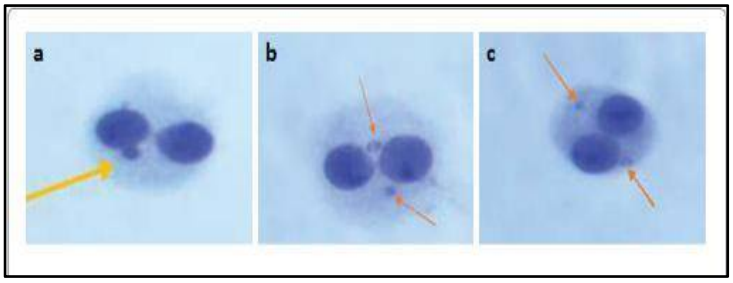

Figure 2. A typical binucleate cells with one micronucleus (a) or two micronuclei (b, c) in PBIs samples exposed to x- ray and observed at 100-fold magnification..

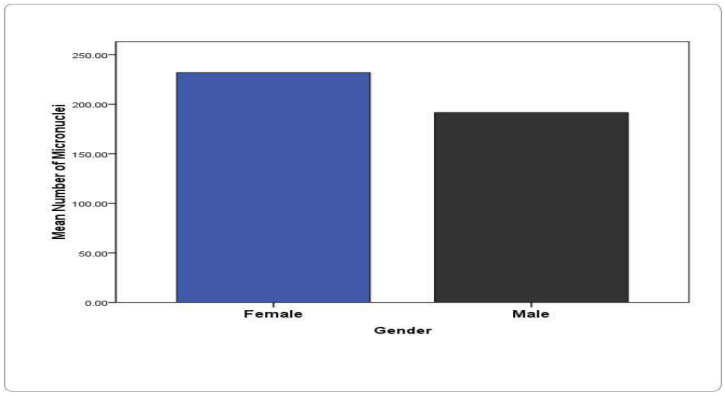

Figure 3: Frequencies of micronuclei based on gender

Indian Journal of Natural Sciences www.tnsroindia.org.in ©IJONS

Vol.9 /Issue 50 /October / 2018 *International Bimonthly* *ISSN: 0976 – 0997*

RESEARCH ARTICLE

Effect of Adding Fibrolytic Enzyme and or *Lactobacillus acidophilus* on Some Productive and Biochemical Traits in the Rams

Iman Sahib Maatoq[1]* and Tamara N. Dawood[2]

[1]Veterinary Public Health Department, Veterinary College, University of Baghdad, Baghdad, Iraq.
[2]Assistant Professor inVeterinary Public Health Department, Veterinary College University of Baghdad, Baghdad, Iraq.

Received: 02 July 2018 Revised: 03 Aug 2018 Accepted: 05 Sep 2018

***Address for Correspondence**
Iman Sahib Maatoq
Veterinary Public Health Department,
Veterinary College,
University of Baghdad,
Baghdad, Iraq
Email : shakirnezal@gmail.com

ABSTRACT

This study was aimed to examine the effect of using *Lacotbacillus acidophills* and /or fibrolytic enzyme on some productive traits on the local lamb rams. Sixteen local lamb rams aged between 3-4 months and weighted 20-24kg were divided randomly into four equal groups (4 lambs of each). The first group (G1) was feed 2.5% of the body weight concentrated diet free of any additives. The second group (G2) was feed (6g) orally EFE (xylanases, B-glucanases and cellulases) with concentrated diet. Third group (G3) was fed the same as G1 and fed orally (100 mg) *Lacotbacillus acidophills*, and fourth group (G4) was fed the concentrated diet 2.5 % of the body weight and the animals were feed EFE and *Lacotbacillus acidophills*. Cholesterol and triglyceride concentrations were taken the same trend of glucose that's its concentrations were decrease significantly (P< 0.05) with time progress and all treated groups decreased significantly (P< 0.05) compared with the control group. On other hand, the blood glucose concentration of all groups decreased with time progress along studied period, but the treated groups showed significantly (P< 0.05) lower value than control group in the 2nd and 5th periods.

Keywords: *Lacotbacillus acidophills,* animals, treated, Cholesterol, triglyceride

INTRODUCTION

Lactobacillus family is a highly heterogeneous genus, involves bacteria with a wide range of biochemical and physiological properties (Felis and Dellaglio, 2015). The members of this species are classified as the ''acidophilus complex,'' including six species of widely related *lactobacilli* that have isolated from the gastro-intestinal (GI) tract of

humans and animals (Altermann*et al*., 2005). *Lactobacillus acidophilus* has first isolated in 1900 by Moro from infant faeces and at this time was classified as *lactoacillus acidophilus* (Matthew *et al*., 2013). The term probiotic, meaning 'for life' was first established in 1960s in order to describe "substances secreted by one microorganism that stimulate the growth of another" (Paturi, 2007).*Lactobacillus acidophilus* remnant to be the most widely known andcommercially distributed probiotic culture (Altermann*et al*., 2005). Several researchers reported that *Lactobacillus acidophilus* and *L. sporogenes* were found to take up cholesterol in the presence of bile and in the absence of oxygen, both conditions present in the intestinal tract (Sanders and Klaenhammer, 2001*)* Lipid peroxidation can be prevented by*Lactobacilli* (Cerbo et al., 2015) and free oxygen radical production (Sun *et al*., 2010) because their ability to create the low oxidation-reduction potential required for their perfect growth (Cerbo et al., 2015). Probiotics also, increase plasma levels of bacterial endotoxin concentrations, at least in part, by restrain translocation of bacteria across the GI lumen into the blood streamand lessening in translocation of bacteria may occur as a result of the ability of probiotics to strain the mucosal barrier (Madsen *et al*, 1999).

MATERIALS AND METHODS

Animals

This study was carried out at the Animal Farm – College of Veterinary Medicine / Baghdad University, from 26/12/2017, up to 1/4/2018.Sixteen healthy local Awassi lambs rams were bought at the age of 3-4 months and body weight (20-24 kg). They were fed concentrate diet and freely grazed for 3-4 hours /day on the College fields as a preliminary period for 2-3weeks. The lambs were divided equally (body weight was considered) into four groups (four each)**.**Control group (G1) were daily fed on 2.5 % of the body weight concentrate diet /head, and kept as control group.Enzyme group (G2) were daily fed on 2.5 % of body weight concentrate diet /head, and giving (6g) orally exogenous fibrolytic enzymes (xylanases, B-glucanases and cellulases) daily.*Lactobacillus acidophilus* group (G3) were daily fed on 2.5 % of body weight concentrate diet/head, and giving (100 mg) orally*lactobacillus acidophilus* daily.Mixed group (G4) were daily fed on 2.5 % of body weight concentrate diet /head, and giving (100 mg) orally*lactobacillus acidophilus*and (6g) orally exogenous fibrolytic enzymes (xylanases, B-glucanases and cellulases) daily.

Estimation of blood glucose concentration

Blood glucose determined as (Trinder (1969) in which glucose is oxidized after enzymatic oxidation in the presence of glucose oxidase enzyme (GOD) with the formation of hydrogen peroxide. H2O2 reacted under catalysis of peroxidase with phenol and 4-aminoantipyrine to a red- violet quinoneimine dye proportional to the concentration of glucose in the sample.

Estimation of blood serum cholesterol concentration

Cholesterol concentration was determined after enzymatic hydrolysis and oxidation by using three enzymes: cholesterol esterase (CE), cholesterol oxidase (CO) and peroxidase (POD)(Thomas.,2012)

RESULTS

Serum Cholesterol concentration

Serum cholesterol concentration showed significant decrease ($P<0.05$) in all treated groups (78.52±3.07, 86.90±3.32 and 82.29±3.40) G2, G3 and G4 respectively, compared with the control group (85.13±2.44) in the fourth period of the study while in the fifth period the G2, G3 and G4 showed significant decrease compared with G1. In addition, table

(4-11) showed that all groups decline in their cholesterol concentration significantly ($P<0.05$) along the study experiment

Serum glucose concentration

Serum glucose level of the treated group in the second and fifth periods of the experiment were decrease significantly ($P<0.05$) compared to the control group (Table 4-10). The results also showed that all groups decline significantly ($P<0.05$) in their blood glucose concentration along studied period.

DISCUSSION

Blood glucose concentration of all groups decreased with time progress along studied periods (Table 4-10). While, G3 and G4 group showed significantly ($P< 0.05$) lower value than other groups from the 2ed period while all treated groups showed lower values than control group in the 5th period of the study On the other hand cholesterol concentration decline along the studied period significantly ($P<0.05$) also all treated groups showed significant decrease ($P <0.05$) compared with G1 (Table 1). However, triglyceride take the same trend of the glucose and cholesterol concentrations that serum triglyceride concentration showed there were significant decrease in concentration between the treated groups and the control group from the fourth period of the study to the end (Table 2).The significant decrease ($P <0.05$) in glucose concentration may due to the effect of the probiotic (*Lactobacillus* species) possess anticholesterolemic and antilipidemic factors (Tahri et al.,1995). People that consume probiotics have experienced lowered cholesterol (Fuller, 1992).

Probiotics has a protein-sparing effect (*lactobacillus*) primarily use carbohydrates as a growth medium, therefore more protein is made available for assimilation and less glucose concentration (Fuller, 1992). However, the activity of cellulolytic bacteria acting on cellulose degradation and thus produced more glucose and increased the glucogenic precursor propionate in rumen or decreased plasma insulin and insulin-glucose ratio leading to an increase in gluconeogenesis (Dawson, 1994). While Mohamed *et al*. (2013)did not found that the adding of fibrolytic enzymes influence blood glucose and urea in all levels. Also Viktor (2006) concluded that there was no significant difference in blood plasma glucose concentrations for Holstein dairy cows fed diet supplemented with fibrolytic enzyme (xylanase). The reduction in cholesterol concentrations were agreed with Wang et al. (2012) who noticed a significant reduction in liver cholesterol content and an increase in fecal cholesterol content compared with the control group. Animals fed diets containing lactic acid bacteria strains had significantly higher propionic acid and butyric acid concentrations in the feces compared with the control. Results indicated that the three screened Lactobacillus strains were able to lower cholesterol in vitro, and reduce cholesterol effectively in vivo. The mechanisms behind the hypocholesterolemic effect of three strains are likely to be diverse and will need further investigation and these results, were agreed with Smet et al. (1994) who found that a daily intake of a realistic amount of highly active *Lactobacillus* cells, e.g. in the form of yoghurt, lead to a significant reduction of cholesterol.

The lower effect of the EFE on the cholesterol concentration agreed with by Abd El-Kareim (2004) who found thatcholesterol were declined significantly by fibrozymes supplementation. While these results were not agreed with Mohamed *et al*.(2013) who found that glucose, triglycerides and urea were not differing significantly due to fibrozymes supplementation to early lactating dairy cows. Broderick *et al*. (1997) studied the effect of treated alfalfa silage with four levels of fibrolytic enzymes mixture (xylanase and cellulase) and fed dairy cows, they found that the adding of fibrolytic enzymes did not influence blood glucose and urea in all levels these diferent in the results may related to the kind of animal, species, environments, the dose of the EFE and the type of feed and the its content.

CONCLUSION

The present study concluded that the positive effect of probiotic including *Lactobacillus acidophilus* and fibrolytic enzyme to reduce the cholesterol in blood also decrease of blood glucose concentration.

Recommendations

1- Using both fibrolytic enzyme and *L*. A*cedophilus* in the diet of rams feeding to improve their performances.
2- Study the effect of probiotic and fibrolytic enzyme with different concentration of ram.
3- Study the effect of probiotic and /or fibrolytic enzyme on the productivity of rams and biochemical traits.

ACKNOWLEDGEMENTS

I would like to thank all those who have helped make this research a success especially Dr. ShakirFrayyehNazzal who works in veterinary directorate/ Ministry of Agriculture.

REFERENCES

1. Abd El-Kariem, M. A., Deyab, H. E., Ahmadi, E. A., & Abdel-Samee, A. M. (2004). Heat stress of hot summerand its amelioration techniques effects on post-partum Friesian cows under Egyptian conditions. 3rdInter.Conf.Anim. poultry, Fish prod. and Health in Semi-Aired Areas, El-Arish-North- Sinai, Egypt.; pp.172-183.
2. Altermann, E.; Russell, W. M. ; Azcarate-Peril M. A. ; Barrangou R. ; Buck, B. L.;McAuliffe, O.; Dobson, A. ;Dobson, A.; Callanan M.; Lick S.; Hamrick, A.; Cano R. H. and Klaenhammer T. D. (2005). Complete genome sequence of the probiotic lacti acid bacterium *Lactobacillus acidophilus*. PNAS; 102 (11): 3906-3912.
3. Broderick, G. A.; Derosa, R. andReynal, S. (1997).Value of Treating Alfalfa Silage with Fibrolytic Enzymes Prior to Feeding the Silage to Lactating Dairy. US Dairy Forage Res. Center, Res. Sum.; pp: 71–73.
4. Cerbo, A. D.; Palmieri, B.; Aponte, M.; Morales-Medina, J. and Iannitti, T. (2015). Mechanisms and therapeutic effectiveness of *lactobacilli*. J. Clin. Pathol.; 69:187–203.
5. Dawson, K. A. (1994). Current and future role of yeast culture in animal production. A review of research over the last six years. Proc. Alltech's 8th Ann. Symp., Alltech. Tech. Publ., Kentucky, USA. Pp: 350.
6. Felis, G. E. and Dellaglio F. (2015).Taxonomy of *Lactobacilli* and *Bifidobacteria.* Cur. Issues Intes. Micro. 8: 44–61.
7. Fuller, R. (1992). Problems and prospects. In: Probiotics- The scientific basis. Fuller, R. pp. 377 – 386.
8. Madsen, K. L.; Doyle, J. S.; Jewell L. D.; Tavernini, M. and Fedorak, R. F. (1999).Lactobacills species prevents colitis in inter leukin 10 Gene –Deficint Mice.Gas. Tro.; 116:1107–1114.
9. Matthew , B.; Plummer, S.; Marchesi, J. and Mahenthiralingam, E.(2013*).* The life history of Lactobacillus acidophilus as a probiotic: Atale of revisionary taxonomy, misidentification and commercialSuccess. FEMS Micro. Lett.; 349 :77–87.
10. Mohamed, D. A.; Borhami, B. E., El-Shazly, K. A. and. Sallam, S. M. A. (2013). Effect of Dietary Supplementation WithFibrolytic Enzymes on the Productive Performance of Early Lactating Dairy Cows. J. Agri. Sci.; 5(6): 146-155.
11. Paturi, G. (2007). Probiotic characteristics of *Lactobacillus acidophilus* and *Lactobacillus paracasei* and their effects on immune response and gene expression in mice .Unv. West. Sydney Aus.; Pp: 202.
12. Sanders M. E. and. Klaenhammer T. R. (2001). Invited Review: The Scientific Basis of *Lactobacillus acidophilus* NCFM Functionality as a Probiotic.J. Dairy Sci.; 84: 319–331.
13. Smet, I.; Hoorde, L.; Saeyer, N.; Woestyne M. and Verstraete W.(1994). In Vitro Study of Bile Salt Hydrolase (BSH) Activity of BSH Isogenic Lactobacillus plantarum 80 Strains and Estimation of Cholesterol Lowering through enhanced bsh activity. Micro. Eco. inHea. and Dis.; 7: 315-329.

14. Sun, B.; Chen, H.; Fang, H.; Zhu, L.; Gao, N. and Zhu, J. (2010). The Effects of Lactobacillus acidophilus on the intestinal smooth Muscle contraction through pkc / mlck/ mlc signaling pathway in TBI mouse model. PLOS ONE DOI:10.1371/J. pone.0128214.
15. Tahri, K.; Crociani , J; Ballongue, J. and Schneider, F.(1995). Effects of three strains of *Bifidobacterria* on cholesterol. Lett. Appl. Micro.; 21 (3): 149-151.
16. Thomes, L. (2012). Laboratory and Diagnose, 8th ed.
17. Trinder, P.(1969) . Determination of blood glucose using an oxidase with an alternative oxygen acceptor. Ann. Cli. Biochem.; 6: 24.
18. Viktor, J.D.V. (2006). Use of Fibrolytic Enzymes produced by fungus Thermomyceslanuginosus in ruminant nutrition. PhD Thesis, Szentistvan University, Hungry. Pp: 200.
19. Wang, Q.; Dong, J. and Zhu, Y. (2012). Probiotic supplement reduces risk of enterocolitis and mortality in preterm very low- birth- weight infants: an updated meta- analysis of 20 randomized, controlled trials. J. of Ped. Sur.; 47: 241-248.

Table 1. Effect of *lactobacillus acidophilus* and *fibrolytic enzyme* on serum blood Cholesterol (mg / dl) of local ram lambs.(Means ±SE).

Group / Biweeklyperiod	G_1 chol		G_2		G_3		G_4	
1	84.58±2.87	B a	87.22±2.97	B a	82.31±0.83	B a	86.28±4.79	BC a
2	90.19±1.94	AB a	90.86±2.66	B a	86.71±0.94	B a	92.30±1.66	AB a
3	94.18±2.17	A a	97.75±0.85	A a	97.66±0.96	A a	97.25±0.47	A a
4	85.13±2.44	B a	78.52±3.07	B b	86.90±3.32	B b	82.29±3.40	C ab
5	86.41±0.87	BC a	80.88±2.31	B b	80.45±2.12	B b	80.17±1.55	C b
6	77.47±1.25	C a	76.46±2.01	C a	76.32±1.13	C a	74.34±1.50	C a
LSD	6.3642							

Means with a different small letter in the same row significantly different (P<0.05)
Means with a different capital letter in the same column significantly different (P<0.05)

Table 2. Effect of *lactobacillus acidophilus* and *fibrolytic enzyme* on serum glucose (mg / dl) of local ram lambs. (Means ±SE)

Group / Biweeklyperiod	G_1 gluc		G_2		G_3		G_4	
1	86.75±2.35	AB a	87.25±2.75	A a	88.00±2.94	A a	86.50±2.02	A a
2	69.50±0.64	C a	61.75±7.55	B ab	62.25±2.13	C ab	55.25±5.32	C b
3	78.75±3.90	BC a	71.00±3.58	B a	72.75±1.49	B a	76.00±3.31	B a
4	80.25±2.86	B a	77.50±3.66	AB a	76.25±1.88	B a	72.50±4.25	B a
5	97.50±0.64	A a	86.25±3.77	A b	88.00±6.12	A ab	95.00±3.67	A ab
6	70.25±1.65	BC a	65.75±4.46	B a	62.00±2.16	C a	65.00±3.67	C a
LSD	10.099							

Means with a different small letter in the same row significantly different (P<0.05)
Means with a different capital letter in the same column significantly different (P<0.05)

Indian Journal of Natural Sciences www.tnsroindia.org.in ©IJONS

Vol.9 /Issue 50 /October / 2018 *International Bimonthly* *ISSN: 0976 – 0997*

RESEARCH ARTICLE

Characterization of Radiation Attenuation Properties of 0.662MeV Gamma Ray Energy for Epoxy Fe_3O_4 Composite Shields

HananObaidkathem*, Mohammed Jebur Resen and NajwaJasimJubier

Department of Physics, College of Science, University of Wasit, Iraq.

Received: 28 June 2018 Revised: 04 Aug 2018 Accepted: 05 Sep 2018

***Address for Correspondence**
HananObaidkathem
Department of Physics,
College of Science,
University of Wasit, Iraq.

ABSTRACT

In this present search, the gamma ray photons emitted from the Cs-137 radioactive source (0.662MeV gamma photons energies) was used to study the gamma ray attenuation in the epoxy/Fe_3O_4composite using the scintillation detector system (NaI (TI)) ,Where the linear attenuation coefficient (**μ**), the transmission coefficient (T.F), relaxation length (***λ***), half value layer (HVL) and tenth value layer values (TVL) were measured by study of photons intensity decreasing that passing through the composite material, from the linear equations of the graphical results between the natural logarithm of the intensity ratio and the thickness X(cm) of the shield.Five types of nuclear shields were prepared, one of them was made of pure epoxy resins and the other four were made of epoxy resins reinforcementby nano-powder of Fe_3O_4 (3, 6, 10, 15) % , where it turns out that the linear attenuation coefficient (**μ**) is increased and the transmission coefficient (T.F) decreased by increasing the concentration of the reinforced powder in the sample and the relationship is inverse between the thickness X of the shield and the transmission coefficient.The results showed that the relaxation length values (***λ***), half value layer (HVL) and tenth value layer (TVL) were decreased by increasing the concentration of the reinforced powder in the resin epoxy

Key words: transmission, gamma ray, material, intensity, concentration.

INTRODUCTION

Exposure or using of ionizing rays can produce damage and since everything on the surface of the earth is exposed to the influence of ionizing radiation, such as cosmic rays and radioactive materials located in the subsoil or industrial sources used for medical and other purposes, but such damage can be reduced so that become equal to the damage caused by any other technology or industrial process. There are many ways in which external exposure to radiation can be controlled so that it reaches the minimum, especially the shielding method, because it gives a good working safety level. [1] As a result of the increased use of radioactive isotopes for industrial, medical and agricultural

purposes, it has become necessary to study the coefficients of the various substances due to their biological and technological significance. It has therefore become important to develop materials that are used in shielding [2] This research is an extension of what has been studied in previous research in this field. In 2012, V.harish*et.al.* examined the shielding properties of the ethylene resin (ISO) supported by lead oxides (Pb_3O_4, PbO_2 and PbO) and various concentrations using three radioisotopes (Cs-137,Co-60 and Ba-133). The study showed that PbO gives the best results in the gamma rays, and the coefficient of attenuation increases with the concentration of oxides in the polymer [3].In 2015, ZuhairSalimkhamees prepared nuclear radiation shield using polymers. He attended high density polyethylene with 38% lead weight (additive) and epoxy with 33% lead weight and epoxy with 33% aluminium weight (Al as additive). Theattenuation coefficient and buildup factor measured these types as individual shields. It has been found that the coefficient of attenuation increases by increasing the additive and decreases in energy. Conversely, the buildup factor is found to be lower by increasing the additive and increasing by energy [4].In 2016, Abdul Rahim manufactured radiation shields from composite materials component of epoxy as matrix material and various supporting materials (C, Ni, PbO and Bi) with varying reinforcement ratios, the coefficient of linear attenuation, half value layer, and relaxation length, as well as the buildup factor, are measured, the scintillation detector system NaI (Tl) was used with various sources Eu-152, Co-60 and Cs-137. It turns out that the increase in the reinforcement ratio of shields has led to an increase of the linear attenuation coefficient. In contrast, there is a decrease in their respective values during the increase in the gamma ray energy for used source. It was also found that the relaxation length and the half value layer were lower with increased concentration [5].

Theoretical Concepts

When the gamma rays pass through the substance, the photons of those rays either pass through the material without any reaction or react by the absorption and scattering reactions, and the gamma rays passing through the material are attenuated by the removal of the reactive photons. [9]:

$I = I_\circ e^{-\mu x}$……………………………………………………..…………………(1)

Where (I): represents the intensity of the beam which passed through the shield material (X), ($I_\circ$): represents the measured radiation intensity without the presence of the shield and (μ) represents the linear attenuation coefficient of the gamma rays in the material. The linear attenuation coefficient can be calculated from equation (1) by taking the logarithm of the ratio ($I_\circ/I$) and as in the following equation:

$Ln(I_\circ / I) = \mu x$ …………...(2)

According to the linear relationship graph between the $Ln(I_\circ/I)$ and the thickness (x) values, we get a slope of the straight line representing the amount (μ). Scientists have agreed on the formula and concept of relaxation length (λ), which is defined as the distance between two consecutive reactions of the radiation falling on the substance and can be calculated by the following equation [11]:

$\lambda\ (cm) = (1/\mu)$ ……………………………………………………………..…….(3)

Other quantities are also used to compare substances used in the shielding and preference of radioactive sources in gamma rays, such as thehalf values layer (HVL), which are known as the shield thickness required to reduce the value of the incident rays to half of its original value at the specified energy and given by the following equation:

$HVL = Ln(2) / \mu$ ……………..…………………………………………………(4)

The tenth value layer (TVL) is defined as that the thickness which will reduce the radiation intensity to one-tenth of its original value, as in the follows [12]:

TVL = Ln(10) / μ ……..... (5)

Transmission factors (T.F) of any type of matter, T(E, x) for gamma-rays energy of E through thickness x (cm) of shield material was defined by dividing gamma-rays intensity I(E, x), or I, of shielding material thickness x to the gamma-rays intensity in the absence of shield material I(E, 0), or I**o**, as shown in the following equations, [10]:

T(E, x) = I(E, x)/ I(E, 0) ……..... (6)

The Absorption factor can also be calculated by the following equation:

A = Ln(1/ T.F) ……..……(7)

MATERIALS AND METHODS

The materials used in this work to prepare the nanocomposite samples as an absorbent at different concentrations are epoxy resin of the type (Euxit-50 KI) that was produced by (Swiss Chem) as a matrix material andnano iron oxide powder (Fe_3O_4) as areinforcement material , its chemical stability in the form of nano-powder (20-30nm) of Sky Spring nanomaterial production. The hand lay-up method was used to prepare five samples of shields, the nano iron oxide powder (Fe3O4) with a weight ratio of (0, 3, 6, 10, 15) % was added to the epoxy resin, the mixture is well mixed, then the hardener was added to the mixture until it becomes homogeneous after that the mixture is poured into four square-shaped molds to be the shape of each specimen of the shield with length 4cm and thickness 0.4cm.
To measure the coefficients of attenuation, thescintillation detector system (NaI (Tl)) and the radioactive source of the Cs-137 withactivity of 0.0283μCi (1.05kBq) emits gamma ray photons with energy of 0.662MeV.Figure (1) shows the system used in this search.

RESULTS AND DISCUSSION

The symbols were used to represent the used shields in this search for ease of reference in the Tables and drawn graphs and as shown in the table (1).Linear attenuation coefficients (**μ**) were calculated from the relationship between $Ln(I_\circ/I)$ and the shield thickness(x) in unit of(cm) as in Figure(2),Where the slope of the straight line of the relationship to any one of shields represents the linear attenuation coefficient of that shield against the gamma rays at the energyvalue of 0.662MeV.Values of these coefficients were ranged from ($0.0869cm^{-1}$) for the pure epoxy shield (S1) to ($0.0971cm^{-1}$) for the Epoxy/Fe3O4 composite Shield with a 15% concentration (S5), where it turns out that (S5) is the best shield that usedto attenuate of gamma rays compared to the other shields used in this search as shown in Figure(3), which represents a chart of the values of the linear attenuation coefficient (**μ**) for each of the used shield. The value of the linear attenuation coefficient (μ) of the S1 Shield, which represents pure epoxy, increases with increase the concentration of the nano iron oxide powder due to the increased intensity the shield thus increases the probability of the photon reaction with the material and this is accordant with the results of previous researches [5, 11]. The experimental calculations for the Ln(I**o**/I)values, transmission coefficient (T.F), linear attenuation coefficient (μ), half value layer (HVL), tenth value layer (TVL) and relaxation length (λ) are illustrate in Tables (2) and (3). The relationship is charted fortransmission factor values (T.F) as a function of the shield thickness for each type of samples used shown in Figure (4), as it is evident from the observation of the figure thetransmission factor decreases by increasing the shield thickness for all types of shields and this behavior is fully applicable to the theoretical concept of the equation (6). Also, the values of T.F at any shield thickness value decrease with increasing the concentration of the used reinforcementnano-powder as well as the smallest value is observed for S5 shield and this behavior is explained by the same explanation of the behavior of the linear attenuation coefficient The behavior ofthe transmission factor andthe linear attenuation coefficient (μ) are different because the relationship between them is inversely.

The plotted absorption factor (A) as a function of the shield thickness for each used shield type shown in figure (5), This figure shows that the absorption factoris increased by increasing the thickness of the shield substance and for all types of shields, this behavior is fully applicable to the theoretical concept of equation (7). The values of relaxation length (λ), HVL and TVL calculated by the (3, 4 and 5) equations are drawn as a function of the shield type as in Figure (6). These Figure shows that the values of these quantities are large in the case of the S1 shield and are gradually decreased by increasing the concentration of the nanoiron oxide powder because the beam will suffer more attenuate for each unit of path length .Increased concentration causes the increased probability of radiation interaction with the substance as a result, the length of the radiation path decreases during the material and this is consistent with the results of previous studies [13, 12, 4and 4].

Figure (7) shows the relationship of each of HVL, TVL and relaxation length (λ) of the used shields with the linear attenuation coefficient (μ) of the gamma rays emitted from cesium radioactive isotope (Cs-137). As it is shown in this figure, the values of these amounts are decreasing with increasing the linear attenuation coefficient of those rays in the shield material, which is exactly agreeable with theoretical concepts of equations (3, 4 and 5).

CONCLUSIONS

In this research it was found that the value of the linear attenuation coefficient values of the gamma rays in the shield samples is increasing with increasing the concentration of Fe_3O_4 nano-powder in composite material. Transmission factor (T.F), relaxation length (λ), half value layer (HVL) and tenth value layer (TVL) are reduced by increasing the concentration of Fe_3O_4 nano-powder and increasing shield thickness.

REFERENCES

1. Ahmed, Khaled Obeid (1993). "Introduction to Health physics". Dar al-Bookshop for Printing and publishing University of Mosul, p. 8.
2. J.F. Krocher, R.E. Browman, (1984), "Effects of Radiation on Materials and Components, Reinhold (Eds)." New York.
3. V. Harish ,Nagaiah and H. G. Harish Kumar, (2012), "Lead Oxides filled with Isophthalic resin polymer composites for Gamma radiation shielding applications", Indian Journal of Pure & Applied Physics, Vol. 50, pp 847-850.
4. ZuhairSalimKhamees , (2015),"Multilayered Shielding Preparation and Buildup Factor Calculation Using Different Type of Polymers" ,Master's Thesis, University of Wasit , College of Science .
5. Abdel Rahim Ziya Ibrahim,(2016) "manufacture of radiation shield and study of some of its properties", Master's thesis, Baghdad University, Faculty of Education for Pure science (Ibn al-Haytham), Department of Physics.,.
6. G. Knoll, (2010),"Radiation Detection and Measurement" John Wiley and Sons.NewYork ,Third Edition.
7. Sh.Sharifi, R. Bagheri, s.p. shirmardi,(2013), comparison of shielding properties for ordinary, barite,sepentine and steel-magnetite concretes using MCNP-4C code and available experimental results "Annals of Nuclear Energy, 53, 529-534.
8. N. Tsoulfanidis, (1983), "Measurement and Detection of Radiation" MC GrawHill, New York Company, 2nd ed.
9. I. Akkurt, B. Mavib, K. Gunoglua, H. Akyildirim and H. Canakcic, (2013), Photon Attenuation Coefficients of Iron Doped Clayat 662 keV , Proceedings of the 2nd International Congress APMAS2012, April 26_29, 2012, Antalya, Turkey, ACTA PHYSICA POLONICA A, Vol. 123 No. 2.
10. Gh. A. Eid[1], A. I. Kany[2] , M.M. El-Toony[3] , I.I. Bashter[4] and F. A. Gaber[1] (2013) "Application of Epoxy/ Pb3O4Composite for Gamma Ray Shielding",Arab Journal of Nuclear Science and Applications, 46(2), (226-233)
11. Isra' a M. Hassan, Laith A. Najim ,(2014)" Studying the Linear and the Mass AttenuationCoefficient of Gamma Rays for Certain Building Materials used in Iraq", Journal of Rafidain Science,Vol.25,No.3,85-75.

12. Ali N. Mohammed* [1] ,Mahmood S. Karim[1] , Hassan H. Daroysh1 , Luma Y. Abbas[2] (2017)," Monte Carlo assessment of gamma ray attenuation properties for MCP-96 alloy using transmission technique",The Fifth Scientific Conference of the College of Science University of Kerbala .
13. NajwaJassimJubier,(2017)," Estimation of Radiation Shielding Properties for Composites Material Based Unsaturated Polyester Filled with Granite and Iron Particles",Journal of Multidisciplinary Engineering Science Studies (JMESS) ISSN: 2458-925X Vol. 3 Issue 1, January.

Table 1. Composition, density and symbols of used nuclear shields

Composition	Symbol
Epoxy pure	S1
Epoxy +3% Fe_3O_4	S2
Epoxy +6% Fe_3O_4	S3
Epoxy +10% Fe_3O_4	S4
Epoxy +15% Fe_3O_4	S5

Table (2): The values of (Ln (I_o/I)), transmission factor(T.F) as a function of the shield thickness X(cm)for all used shields by using the Cs-137 radioactive isotope

Shield Type	Ln (I_o /I)					T.F				
	X(cm)					X(cm)				
	0	0.4	0.8	1.2	1.6	0	0.4	0.8	1.2	1.6
S1	0	0.0406	0.0690	0.1042	0.1419	1	0.9601	0.9332	0.9013	0.8680
S2	0	0.0430	0.0785	0.1046	0.1470	1	0.9578	0.9283	0.9005	0.8632
S3	0	0.04452	0.0758	0.1120	0.1478	1	0.9564	0.9269	0.8940	0.8625
S4	0	0.04607	0.0738	0.1147	0.1512	1	0.9549	0.9263	0.8916	0.8596
S5	0	0.04739	0.0848	0.1241	0.1557	1	0.9537	0.9186	0.8832	0.8557

Table 3. The values of linear attenuation coefficient (μ (cm^{-1})), HVL, TVL and λ (cm) as a function of the shield material type by using the Cs-137 radioactive isotope.

Shield Type	μ (cm^{-1})	HVL (cm)	λ (cm)	TVL (cm)
S1	0.0869	7.974684	11.50748	26.50173
S2	0.0889	7.795276	11.24859	25.90551
S3	0.0908	7.632159	11.01322	25.36344
S4	0.0928	7.467672	10.77586	24.81681
S5	0.0971	7.136972	10.29866	23.71782

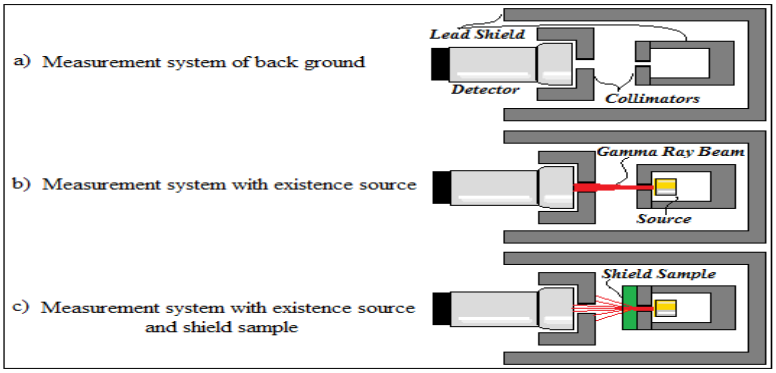

Figure 1. Geometrical arrangement of the detector system

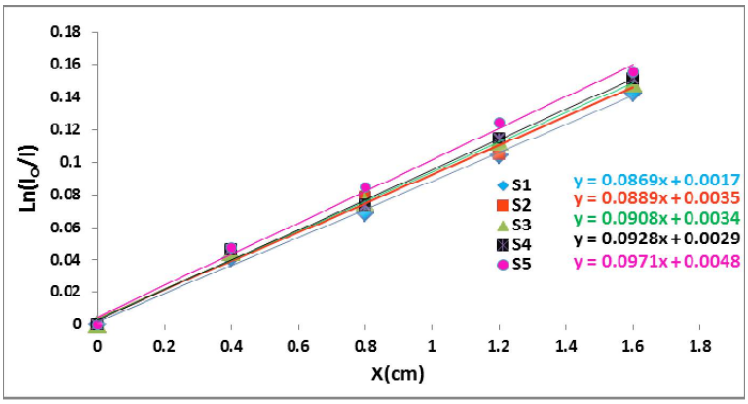

Figure 2. The relationship of the Ln(I₀/I)values as a function of the shield thickness X(cm) for all used shields types using Cs-137 radioactive isotope

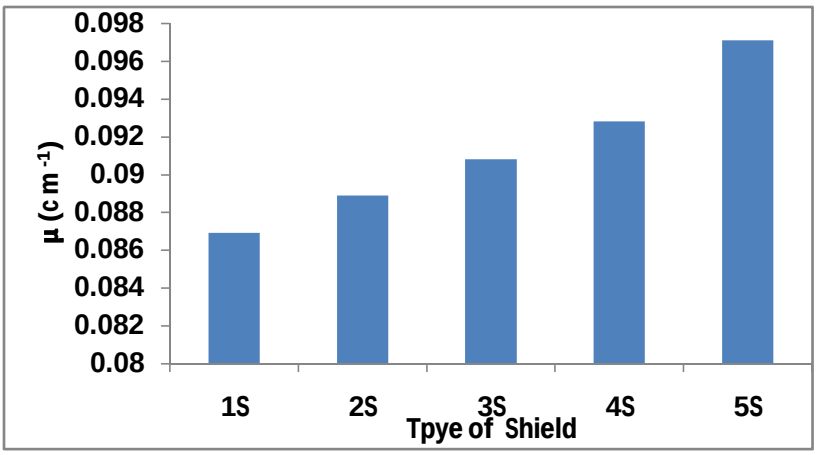

Figure 3. A chart of the values of the linear attenuation coefficient (μ) in units (cm^{-1}) of the gamma emitted from the CS-137 radioactive isotope as a function of the type of shield material

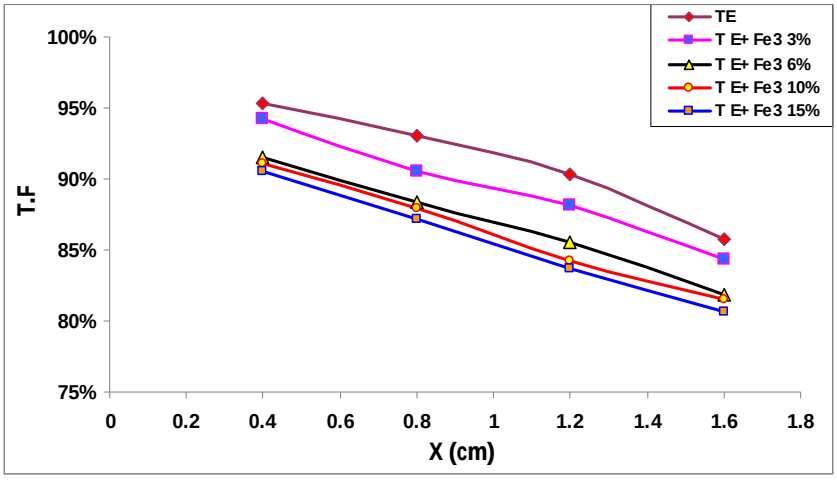

Figure 4.The relationship of the T.F values as a function of the shield thickness X(cm)) for all types of shields by using the gamma rays emitted from Cs-137

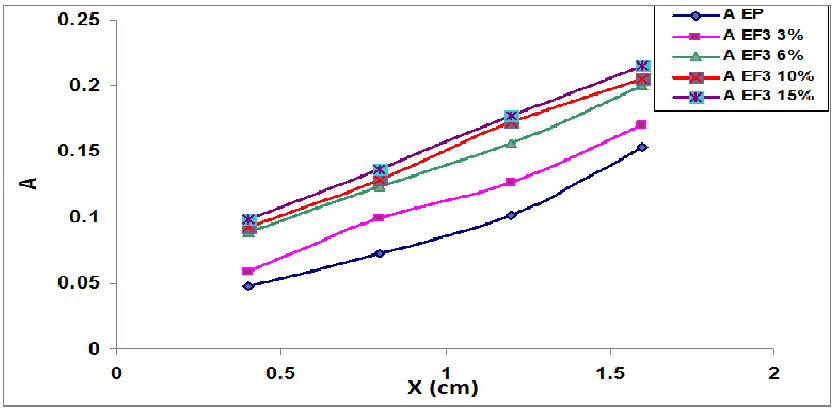

Figure 5. The relationship between the absorption factor (A) values of a gamma rays emitted from the Cs-137 radioactive isotope and the shield thickness (X(cm)) for all types of used shields

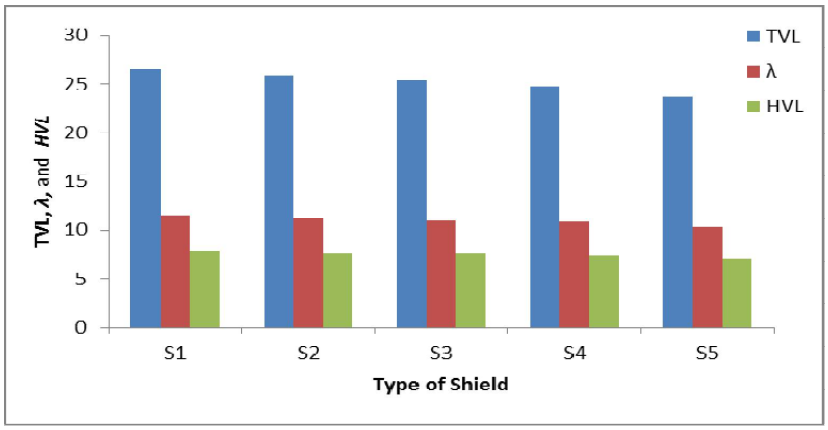

Figure 6. The HVL and TVL values, and relaxation length (λ) in units of (cm) as a function of the shield type by using the Cs-137 radioactive isotope

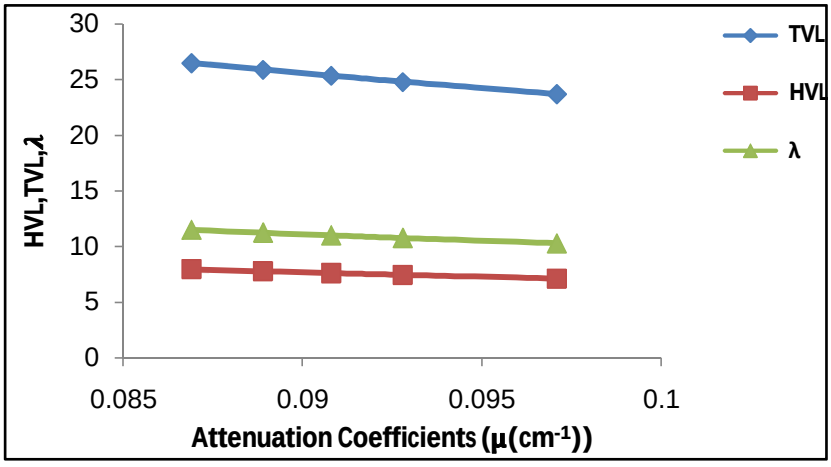

Figure 7: The relationship between the values of TVL, HVL and relaxation length λ in units of (cm) and the linear attenuation coefficient ((cm^{-1})) values for all used shields by using the Cs-137 radioactive isotope

Indian Journal of Natural Sciences www.tnsroindia.org.in ©IJONS

Vol.9 /Issue 50 /October / 2018 *International Bimonthly* *ISSN: 0976 – 0997*

RESEARCH ARTICLE

Studying the Characterization of the Zinc Oxide (ZnO) Thin Film Prepared by a Drop Casting Method

Aula A. Manaty[1*], Eidan A.Abdullah[2] and Ahmed K.Abbas[3]

[1, 2, 3]Deprtmentof Physics, College of Science, University of Wasit, Iraq.

Received: 29 June 2018 Revised: 03 Aug 2018 Accepted: 05 Sep 2018

[*]**Address for Correspondence**
Aula A. Manaty
Department of Physics,
College of Science,
University of Wasit, Iraq.
Email : alaaa224@uowasit.edu.iq

ABSTRACT

In this study, nanostructured zinc oxide (ZiO) thin film was prepared by a simple drop casting processfrom nanocrystalline powder of zinc oxide onto glass substrateat room temperature.Structural and morphological characteristics of the grown ZnO film was studied using X-ray diffraction (XRD), Scanning Electron microscopy (SEM) and atomic force microscope (AFM). Chemical analysis and opticalproperties of film was characterized via Fourier transform infrared spectroscopy (FTIR) and UV–visible spectroscopy, respectively.The (XRD) result explained the structure of thethin film has *polycrystalline* structure at 2θ= (31.5330,34.1990, 36.0170, 47.2890, 56.3180, 62.6000, 67.6900, 68.8220)^{o}with the preferred orientation at (101) plane.The (SEM) showed that the good imaging of then anostructure of thin film and the (AFM) explained that formation of ZnO has uniform grain distribution and low Co efficientroughness with average grain size of (53.40) nm. The FTIR spectroscopy result showed the distinct bonds of the ZnO film and the lastfound the energy gap equal 3.0eVof it by UV-Vis.

Key words: nanostructure, Zinc Oxide, Chemical, temperature, microscopy, film

INTRODUCTION

Transparent conducting oxides (TCOs) are materials that illustrate both conducting and transparent properties, TCOs such as In_2O_3, Al-doped ZnO Sn-doped, Sb-doped SnO2 and CdO are attracting attention due to their wide applications in electroluminescent devices as transparent electrodes, light-emitting diodes, solar cells and liquid crystal displays [1-3]. The transparent properties mean TCOs show low absorption in the visible region of the Electromagnetic spectrum, which requires an band gap larger than 3.5 eV. The conducting properties indicate that TCOs explain high electrical conductivity in the range from 1 to 10^4 S cm^{-1}[4,5].ZnO is one of the most important transparent conducting oxides and it is semiconductors of n-type with hexagonal structure.A II-VI group semiconductor material ZnO has wide energy gap (~2.9- 3.3 eV at room temperature) and large excitonic binding

energy ~ 60 meV[6,7].through the few years ago, ZnO has attracted the attention of many researchers due to its good transparency, high luminous transmittance , high electron mobility and high chemical stability [8,9]ZnO has several advantages such as non-toxicity , better electrical as well as optical performance and low cost,. These advantages make it a promising material for many applications in solar cells, gas sensing and anti refecting coating [10,11]. Especially, research on improve defficiency of solar cells in recently. Properties of ZnO can be changed favourably via doping with unknown materials as well as via altering annealing condition. So, ZnO is wholesome as electron transport material in solar cells[12].ZnO thin films are grown by variety techniques have been employed such as spray pyrolysis, sputter deposition, metal organic chemical vapour deposition (MOCVD), laser ablation, ion beam assisted deposition, chemical vapour deposition, template assisted growth and drop casting [13-15]. Drop casting a easy method to prepared, low cost, no waste the solution or material but difficult to control the thickness [16].In this work we report the preparation of ZnO thin film by drop casting method, and study the Structural, morphological and optical properties of the as deposited film.

MATERIALS AND MATHODS

Thin film of ZnO was deposited on glass substrate by drop casting deposition technique at room temperature (300 K). Atfirst, we used in this experiment zinc oxide powder and then compressed itunderpressure 10 Ton. During 5 min. and turn powder to Pellet with diameter 1cm and 2cm thick.At last, by pulsed laser Nd:YAG of energy 600MJ,wave length 1064nm ,width of pulse 10 ns and frequency 6Hz 1with 1000 pulses shots to dissolved the ZnO pellet in ethanol.The glass substrate have dimensions (75mm × length 25mm × thickness1.2 mm),it were cleaned chemically and ultrasonically by standard methods.The prepared film showed that the complete surface of the substrate is covered via a homogeneous layer of ZNO film. The structural characterization was investigated with XRD method (SHIMADZU 6000). Surface morphology was studied by FESEM (Hitachi (S-4160), AFM (Digital Intruments, CSPM-AA3000), while the atomic bonds in ZnO were analyzed with the Fourier transformed infrared spectroscope (FT-IR, Shimadzu IRAffinity-1) and optical property of the flmwas measured by UV–Vis–NIR spectrophotometer (Metertech- SP8001) in the spectral range 300–900 nm. The energy gap in this analysis is measured via the absorption coefficient of diverse wavelengths, calculated using transmittance and reflectivity data.

RESULTS AND DISCUSSION

The XRD pattern of ZnO thin film preparedviadrop casting method on glass substrates is shown in Fig. 1.ZnO was obtained in the scanning range (2θ) of 20°–80°, with using Cu-Ka (λ_{max}= 1.5406 Å) radiation. All the main peaks were matched with the standard (JCPDS S6-314) code no., distinctive of hexagonal wurtzite structure as that of ZnO. Diffraction peaks are obtained at 2θ = 31.5330°,34.1990°, 36.0170°,47.2890°,56.3180°,62.6000°,67.6900° and68.8220°, corresponding to (100),(002),(101),(102),(110),(103) and (112)diffraction peaks are observed in the XRD pattern, viewing the growth of ZnO crystallites along diverse directions[6,17,18]. The major peak is observed along (101) plane indicating that the film is oriented along c-axis [6].As well as peak is sharp, which conforms that the film is polycrystalline and hexagonal wurtzite in nature.The values of lattice parameters were calculated by the following relationship[19].

$$\frac{1}{d^2} = \frac{4}{3}\left(\frac{h^2 + hk + k^2}{a^2}\right) + \frac{l^2}{c^2} \quad \text{.....(1)}$$

where d is the inter planer spacing; h k l are theMille indices corresponding to peak; and a, b, c are lattice parameters.The crystallites sizes (D) ofthe thin film is estimated by the Scherer formula [17]:

$$D = \frac{K\lambda}{\beta \cos\theta} \qquad \text{……..(2)}$$

where kis a constant equal(0.94), $\lambda$is the wavelength of X-Ray (λ = 1.54 Å) and $\beta$is the full width at half maximum of (101) peak of XRD pattern, Bragg angle, 2θ, is around 36.0170°. The average value of grain size is 48.1 nm.The results of crystallite size and inter planer spacingof ZnO obtained from XRD measurement shown in Table1.

SEM analysis

SEM is used to study the morphology of the film. An electron beam is focused on the film to get the information about the microstructure of it. The surface morphology of the thin film plays an important role in different applications interrelated of optoelectronics.Fig.2 expose surface morphology of ZnO thin film.The image show their regular distribution of well-defined grain and shows agglomeration to large extent of grainswith their definite boundaries.The average grain size of thin film estimated by of SEM micrograph is 75nm.

AFM Analysis

The analysis of AFM image led to investigation morphological surface and granularity distribution of thin film deposited on glass at 300k by drop casting. Perfect 3D AFM image of the ZnO thin is shown in Fig.3. AFM results indicated homogenous with regular grain arrangement andlow coefficient of roughness this is due to the columnar grain growth in the structure of ZnO film. The average diameter, root mean square (RMS) roughness, average roughness andPeak to peakfor ZnO,expected from AFM, are given in Table2.

FTIR analysis

Fig. 4 show the FTIR pattern for as deposited ZnO thin film at 300 K. The set peaks were locations and match with the standard values which done in prior researches [20].In ZnO thin film, the spectrum of FTIR shows the bands at (435.24,487.96,507.54) cm^{-1} refer to Zn-O interaction. The band weak at 904.55 $cm^{-1}$is indicate to C-O-H bending vibration. The stretch vibration band C-O is located at 1066.56 cm^{-1}. The band at 1512.09 $cm^{-1}$is assigned to symmetric bending of –CH3 group and the peak at 1623.95 cm-1is due to symmetric stretching vibration of C=O group. The weak band around 2881.45 cm^{-1} is due to the symmetric C—H stretching modes at last the broad band is indicates the presence of O-H stretching vibration.

Optical Properties

Fig. 5 is show the optical transmission spectrum of the ZnO film prepared on glass substrates. The value of transmittance of thin film in the visible range is found to be 64%. In the visible region of electromagnetic spectrum, transmission spectra of ZnO thin film show sinusoidal behavior; this may be due to the layered structure of ZnO film. Fig.6 shows the plot $(\alpha h\nu)^2$vs. hν. The energy gapvalue of thin film are calculated by this plot. The presence of a single slope in the plot suggests that the ZnO have direct and allowed transition. The Eg is obtained by extrapolating the straight line portion of the plot to zero absorption coefficient. The Eg value of ZnO thin film is found to be 3.0 eV.

CONCLUSIONS

In the present paper, hexagonal nanostructured ZnO thin film was deposited by drop casting of ZnO powder. The properties of the thin filmdepend on energy of pulsed laserand the number of pulses.XRD studiesrevealed that the ZnO deposited on glass substrateare polycrystalline with preferred orientation along (101) plane. Further it is confrmed that the SEM analysis appear that the ZnO thin film are irregular distributedwith a granular

agglomeration. However, the AFM showed uniform distribution of thin film with low coefficient roughness.the thin film show high transmittance (64%), thus making the thin film suitable for optoelectronic devices. The thin film shows a direct transition in the range 3.0 eV.

REFERENCES

1. D. S. Ginley, O. D. Perkins" Handbook of Transparent Conductors" Springer Science+Business Media, LLC,PP 1-25,(2011).
2. K. Ellmer," Past achievements and future challenges in the development of optically transparent electrodes", Nature Photonics vol. 6, P.P 809–817, (2012).
3. R. Ismail, S. Ghafori and G. Kadhim," Preparation and characterization of nanostructured nickel oxide thin films by spray pyrolysis ",Appl Nanosci No. 3, p.p 514,(2013).
4. S. Kasap, P. Capper," Springer Handbook of Electronic and Photonic Materials" Springer International Publishing AG, pp 1-1,(2017).
5. A. Stadler," Transparent Conducting Oxides—An Up-To-Date Overview", Materials (Basel).; vol.5,No.4,P.P 661–683,(2012).
6. L. Mustafaa,, S. Anjum, S. Waseem, S. Bashir, K. Mahmood, M. Saleemand E. Ahmad,"Structural and optical properties of ZnO co-doped with Co and Ni thin films deposited by pulse laser deposition technique",Optik ,vol. 161,p.p. 54–63,(2018).
7. Y. Aoun, B. Benhaoua, S. Benramache, B. Gasmi, " Efect of annealing temperature on structural, optical and electrical properties of zinc oxide (ZnO) thin flms deposited by spray pyrolysis technique", Optik ,Vol.126, p.p 5407–5411 ,(2015).
8. G. Balaji, R. Sivakami, M. Sridharan and K. Jeyadheepan, " Preparation and characterization of refractory ZnO bufer layers for thin flm solar cell applications", Mater. Today Proc, vol. 3, p.p1730–1736, (2016).
9. C. Manoharan,G. Pavithra, M. Bououdina, S. Dhanapandian and P. Dhamodharan," Characterization and study of antibacterial activity of spray pyrolysed ZnO: Al thin flms", Appl. Nanosci,vol. 6, p.p 815–825, (2016).
10. K. Dhanakodi, P. Thirunavukkarasu, R. Mariappan and A.T. Rajamanickam, ," Efect of substrate temperature on the nebulizer sprayed zinc oxide thin flms", Optik, vol. 127, p.p 2516–2520, (2016).
11. G. Kenanakis, N. Katsarakis and E. Koudoumas, " Infuence of precursor type, deposition time and doping concentration on the morphological, electrical and optical properties of ZnO and ZnO: Al thin flms grown by ultrasonic spray pyrolysis", Thin Solid Films, vol. 555, p.p 62–67, (2014).
12. J. Ge, C.R. Grice, andY. Yan, " Cu-based quaternary chalcogenide Cu_2 $BaSnS_4$thin flms acting as hole transport layers in inverted perovskite CH_3NH_3 PbI_3 solar cells", J. Mater. Chem. A, vol. 5, p.p 2920–2928, (2017).
13. R. A. Ismail, N. F. Habubi and H. R. Abid," Effect of annealing temperature on the optical properties of ZnO nanoparticles" International Letters of Chemistry, Physics and Astronomy, Vol. 23, pp 37-47,(2013).
14. J. B. Lee, S. H. Kwak and H.J. Kim, "Effects of Surface Roughness of Substrates on the c-Axis Preferred Orientation of ZnO Films Deposited by r.f. Magnetron Sputtering," Thin Solid Films, Vol. 423, pp. 262-266,(2003).
15. R. Dounia, A. Migalska-Zalas, M. Addou, J.C. Bernede, A. Outzourhit and M. Benbrahim," Preparation and characterization of highly transparent and conductive indium-zinc oxide thin flms deposited by pyrolysis spray technique" Opt. Quantum Electron, vol. 48, p.p.1–10, (2016).
16. D. G. Larrude, M. E. H. Maia, and F. L. F. Jr, "Synthesis and Characterization of Silver Nanoparticle-Multiwalled Carbon Nanotube Composites", Thin Solid Films, vol. 201, (2014).
17. N. Kumari, S. R. Patel and J. V. Gohel," Optical and structural properties of ZnO thin flms prepared by spray pyrolysis for enhanced efciency perovskite solar cell application", Opt Quant Electron, vol. 50,pp.180,(2018).
18. Z. R. Khan, M. S. Khan, M. Zulfequar and Mohd Shahid Khan," Optical and Structural Properties of ZnO Thin Films Fabricated by Sol-Gel Method", Materials Sciences and Applications, vol. 2, pp.340-345, (2011)..
19. S.Benramache, A. Rahal, B. Benhaoua, " The efects of solvent nature on spray-deposited ZnO thin flm prepared from $Zn(CH_3COO)_2{\cdot}2H_2O$", Optik , vol. 125, pp.663–666, (2014).

20. C. R.Martinez, P. Joshi, J. L.Vera, J. E. Ramirez-Vick, O.Perales and S.P. Singh," Cytotoxic studies of PEG functionalized ZnO Nanoparticles on MCF-7 cancer cells",NSTI-Nanotech,vol.3, pp.420-423, (2011).

Table 1.Values of the grain size (GS) and inter planer spacing (d) of ZnO calculated from XRD

2θ (Deg.)	FWHM (Deg.)	d_{hkl} Exp.(Å)	G.S (nm)	d_{hkl} Std.(Å)	Phase	hkl	card No.
31.5330	0.1722	2.8349	47.9	2.8174	Hex. ZnO	(100)	96-900-4180
34.1990	0.1769	2.6198	47.0	2.6037	Hex. ZnO	(002)	96-900-4180
36.0170	0.1738	2.4916	48.1	2.4780	Hex. ZnO	(101)	96-900-4180
47.2890	0.2155	1.9207	40.2	1.9122	Hex. ZnO	(102)	96-900-4180
56.3180	0.2888	1.6323	31.2	1.6266	Hex. ZnO	(110)	96-900-4180
62.6000	0.1983	1.4827	46.9	1.4778	Hex. ZnO	(103)	96-900-4181
67.6900	0.2588	1.3831	37.0	1.3795	Hex. ZnO	(112)	96-900-4182
68.8220	0.4438	1.3631	21.7	1.3598	Hex. ZnO	(201)	96-900-4183

Table 2. AFM parameters (Average Diameter, RMS roughness, Surface Roughness and Peak-peak distance) for ZnO thin film at 300K

Material	Average diameter(nm)	RMS	Surface Roughness(nm)	Peak to peak (nm)
Zinc oxide	53.40	0.55	0.454	2.48

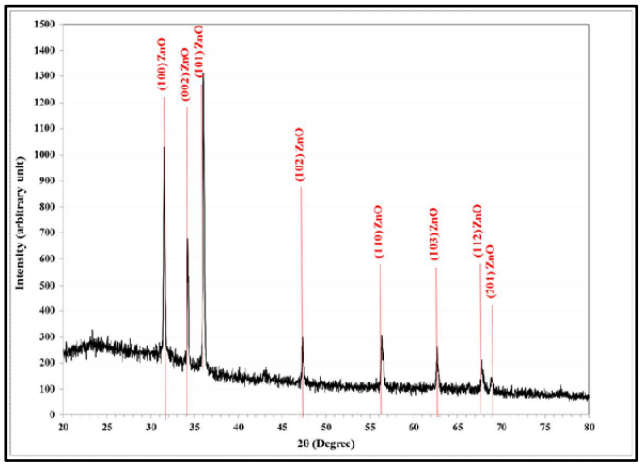

Figure 1. XRD pattern of ZnO thin film

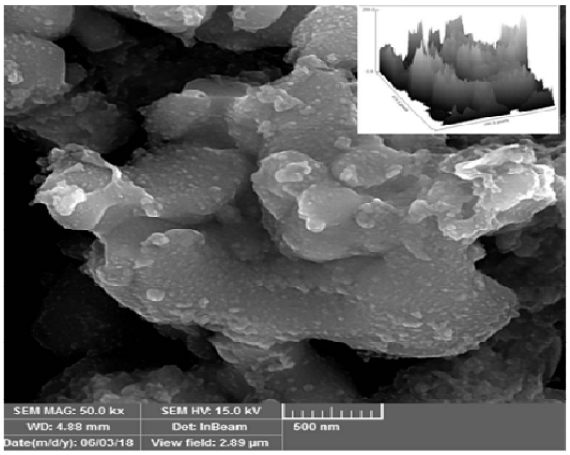

Figure 2. SEM image of ZiO film, scale bar 500 nm

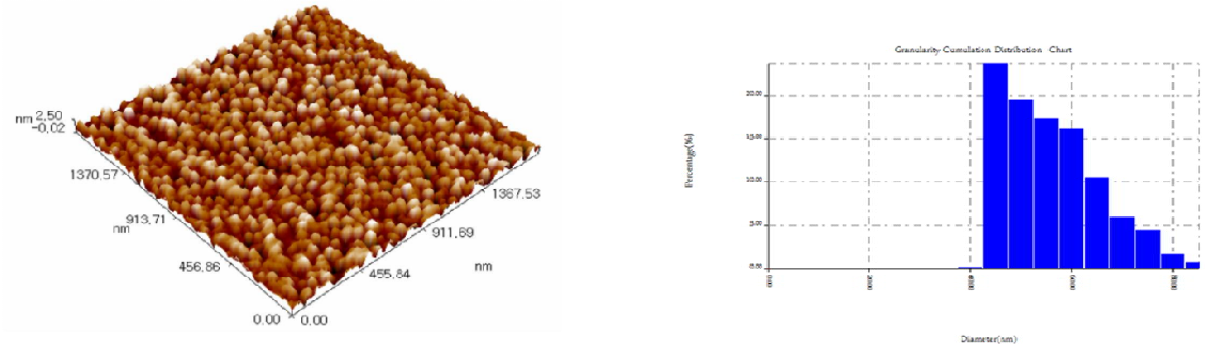

Figure 3.3D image AFM and granularity distribution of nanostructured ZnO film

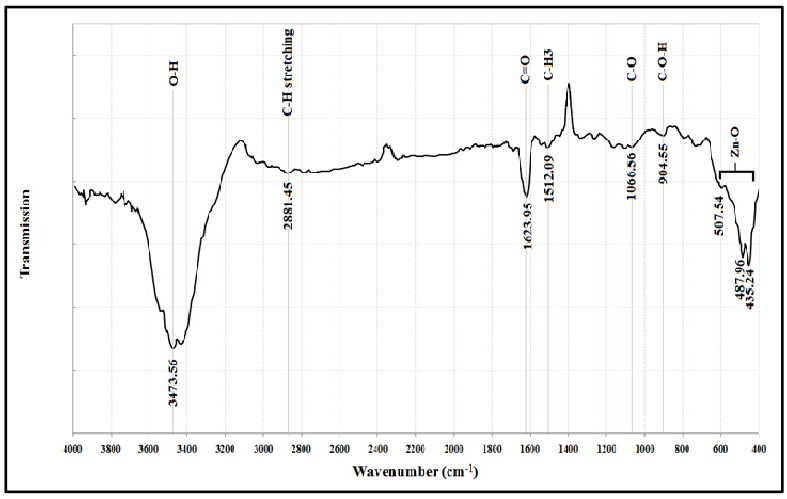

Figure 4. FT-IR spectrum of the ZnO thin film synthesized at 300K

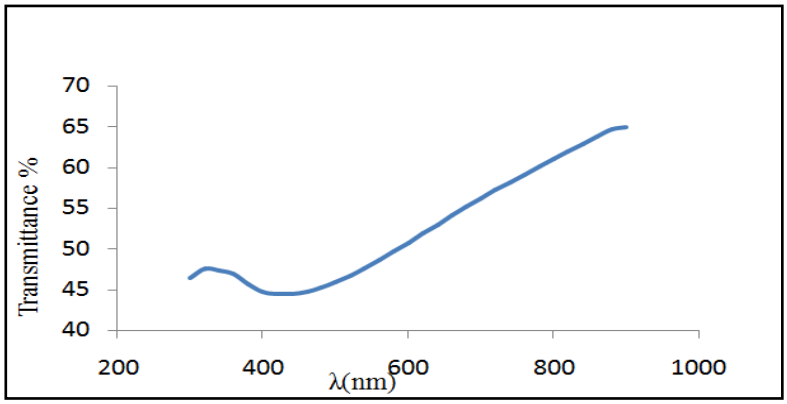

Figure 5. Transmittance spectra of the ZnO thin film prepared at 300K.

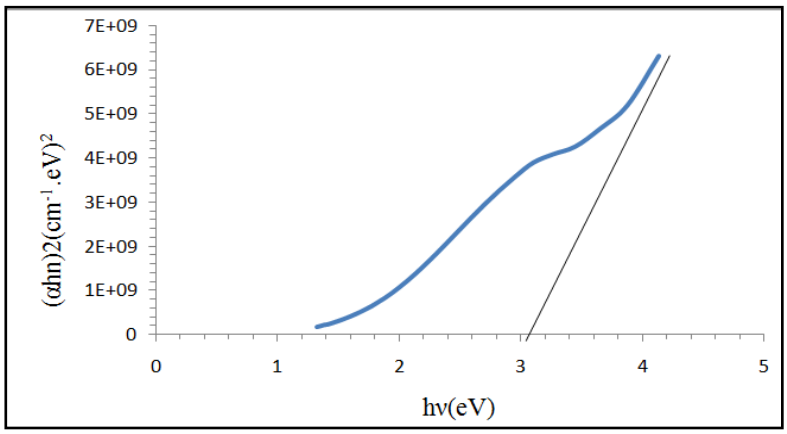

Figure 6.(αhν)² versus (hν) plot

Indian Journal of Natural Sciences www.tnsroindia.org.in ©IJONS

Vol.9 /Issue 50 /October / 2018 *International Bimonthly* *ISSN: 0976 – 0997*

RESEARCH ARTICLE

Molecular Detection of *Lucilia sericata* in Wasit Province, Iraq

Algorany, AsmaaFadhil Abdul Ridha*

Department of Biology, College of Science, Wasit University, Kut, Iraq.

Received: 02 July 2018 Revised: 04 Aug 2018 Accepted: 05 Sep 2018

*Address for Correspondence
Algorany, AsmaaFadhil Abdul Ridha
Department of Biology,
College of Science,
Wasit University, Kut, Iraq.

ABSTRACT

The greenbottle blow flies, are extremely hard to recognize based on their outside morphology. Detection of Blow flies (Diptera: Calliphoridae) to species is vital for evaluating posthumous interims, since bug species create at various rates. The sub-atomic location is vital to recognize the Luciliasericata, particularly there is three blow fly species *L.coeruleiviridis*, *L.cuprina*, and *L.sericata* are comparative morphologically, making ID troublesome. Luciliasericata (Diptera: Calliphoridae) is the regular green container fly found in many territories of the world, and the most understood of the various green jug fly species. *L. sericata* has much significance in the field of measurable entomology. A PCR for identification of *Lucilia sericata* from 50 examples in Wasit, Iraq. 43 examples were observed to be sure and 7 examples were Negative. Sub-atomic strategies are exceptionally valuable particularly on the off chance that it is important to distinguish little sections of bug material or extremely youthful hatchlings we propose to utilize it just not with standing the traditional technique.

Key words: *Lucilia sericata*,Morphological,Molecular,Iraq.

INTRODUCTION

The green container blowflies have a place with the variety *Lucilia* and despite the fact that there are more than 200 ostensible species, just two happen in South Africa. These two species – *L. sericata* and *L. cuprina* – are cosmopolitan, happening on six mainlands (1, 2, 3). L. sericata is the most ordinarily utilized fly species for worm debridement treatment (MDT) (4) and it has as of late been demonstrated that *L. cuprina* can likewise securely be utilized for MDT (5, 6). The hatchlings of both of these species feast upon breaking down creature tissue and are in this manner helpful in criminological entomological examinations to decide after death interims (PMI). *Lucilia cuprina* is regularly alluded to as the sheep-strike blowfly (7) since it is in charge of cutaneous myiasis in sheep which causes a huge number of dollars of harm in the sheep cultivating industry every year. *L. sericata* does not seem to strike sheep in the southern side of the equator however has been accounted for to cause sheep-strike in parts of Europe (8). Distinguishing proof of these flies is in this way essential for use in MDT, legal entomology and controlling sheep-strike. A few creators have recommended that these flies ought to be delegated three species or that L. cuprina ought to be named two

subspecies – *Lucilia c. cuprina* (9, 10). *Lucilia sericata* and *L. cuprina* are morphologically fundamentally the same as and the grown-ups are hard to recognize utilizing the accessible keys in light of morphological characters without utilizing the male genitalia, which typically requires damaging examining (11). Be that as it may, with some experience, the females can typically be dependably recognized utilizing the qualities depicted by (12). Atomic strategies are helpful in affirming the ordered status of these two species (5,13). The utilization of in excess of one quality for ordered and phylogenetic investigations is suggested as utilizing just a single quality may not give a genuine picture of connections or examples of quality stream (14, 15, 12). In the present examination, the sequencing of core S28 quality of *Lucilia sericata* has been done which can be utilized as its standardized tag for ordered recognizable proof. *L. sericata* is an imperative species to criminological entomology as it ascertains the posthumous record.

MATERIALS AND METHODS

Collection of Samples

60 larvae were collected during May, 2018 to June, 2018 in different area of Wasit, Iraq. The larvae were collected by hanging beef outside, and the larvae were placed in a clean, dry plastic container and transported to the laboratory for analysis.

Identification of Specimens

The identification of hatchlings was performed by analyzing the respiratory pores and back of cephalopharyngeal skeleton of the parasites which brought about the larval passing (16).

Genomic DNA Extraction

The extraction of genomic DNA from hatchling tests was finished by organization directions by utilizing DNA Extraction convention with Proteinase K and chaotropic salt (Gsync™ DNA extraction Kit, Geneald Biotech Ltd). From that point forward, the separated DNA was checked by spectrophotometer (A260/A280), and after that put away at - 20C at cooler until utilized as a part of PCR intensification.

PCR amplification

PCR test was performed for identification of *Lucilia sericata* in light of one enhancement PCR keep running by utilizing ground works for distinguish a locale of roughly 650bp in the Domain 1-2 of the 28S quality which increased utilizing the preliminaries 5` CCCCCTGAATTTAAGCATAT-3` and 5`-TTAGACTCCTTGGTC¬CGTG-3` (17). Ground works were given by (Bioneer organization. Korea) (Table-1). The PCR was set up by using (AccuPower PCR PreMix unit. Bioneer. Korea). The PCR premix tube contains cement dried pellet of (Taq DNA polymerase 1U, dNTPs 250µM, Tris-HCl (pH 9.0) 10mM, KCl 30mM, MgCl2 1.5mM, stabilizer, and following shading) and the PCR pro mix reaction was set up according to pack rules. Polymer¬ase chain response (PCR) intensification was performed utilizing 1µL of DNA in a 25µL response. Enhancement times were 94 °C for 5 min denaturation, trailed by 36 cycles of 94 °C for 30 seconds, 55 °C for 1 min, 72 °C for 30 seconds and a last augmentation period at 72 °C for 7 min (Table-2). PCR items were affirmed by gel electrophoresis recolored in ethidium bromide (17).

Statistical analysis

The statistical analysis done SAS (Statistical Analysis System - version 9.1)(18).

RESULTS

After the larvae have been identified depending on their morphological characteristic, the PCR was performed in an aggregate of 50 specimens which identified as *Lucilia sericata* larvae, the outcomes were 43 (86%) specimens were sure, where 7 (14%) were negative. PCR created, assessed in existent investigation which demonstrated extent off indicative sections of PCR items (650bp) (Table-3), (Fig-1), (Fig-2). Various investigations have been led on *L. sericata*, taking a gander at morphological ID (13, 19, 20). This investigation centers around *L. sericata*, in Wasit, Iraq which utilized one atomic quality (S28 quality) where most past examinations have either utilized just a single mitochondrial quality or a blend of mitochondrial qualities and one atomic quality (21). The point of our examination was to affirm the sub-atomic identification techniques to identify the *L. sericata* hatchlings. The portrayed technique was performed effectively on 50 *L. sericata* hatchlings which were 43 (86%) examples were certain, where 7 (14%) were negative. Our perception concurrences with (22) which discovered 77 examples were sure out of 84 examples utilizing S28 quality which base sets were 654 bp. And furthermore concur with (23) which discovered S28 quality base sets were 654 bp. Our finding is additionally concurring with (24) which demonstrated that base combine 656 bp for 28S and an aggregate of 46 examples were sequenced for 28S The ILD test for 28S demonstrated this quality to be exceptionally consistent. Our examination is contradicting (9, 13, 19, 20) which demonstrated that sometimes both atomic and mitochondrial qualities are required for solid species distinguishing proof. It is notable that the utilization of only one quality can for the most part, be deceiving yet where utilizing atomic (S28) qualities in conjunction with the mitochondrial quality, a conceivably deceptive circumstance can be stayed away from (5, 23). we propose to utilize atomic strategies just notwithstanding customary recognizable proof techniques. The last are quicker, less expensive, and besides, speak to the reason for adjust sub-atomic species recognizable proof.

CONCLUSION

This can be useful when harmed examples or protected hatchlings are to be broke down to expand the nature of distinguishing proof. It is, in this way, impractical to choose from which nation examples of intrigue started from.

ACKNOWLEDGMENTS

Authors sincerely wish to acknowledge the members of the Laboratory of the College of Science, Wasit University for supporting.

REFERENCES

1. Liu Q-L, Cai J-F, Chang Y-F, Gu Y, Guo Y-D, Wang X-H, Weng J.-F, Zhong M, Wang X, Yang L, Wu K-L, Lan L-M, Wang J-F, Chen Y-Q. 2011. Identification of forensically important blow fly species (Diptera: Calliphoridae) in China by mitochondrial cytochrome oxidase I gene differentiation. Insect Science 18: 554–564.
2. Boehme P, Amendt J, Zehner R. 2012. Differentiation for molecular identification of forensically important fly species in Germany. Parasitology Research 110: 2325–2332.
3. GilArriortuaM, Salona Bordas MI, Caine LM, Pinheiro F, de Pancorbo MM .2013. Cytochrome b as a useful tool for the identification of blowflies of forensic interest (Diptera, Calliphoridae). Forensic Science International 228: 132–136.
4. 228 :132-136.4. Vilcinskas A. 2011. From traditional maggot therapy to modern biosurgery. InVilcinskas A, ed. Insect Biotechnology. Springer, Netherlands, pp. 67-75
5. Tantawi TI, Williams KAand Villet MH. 2010. An Accidental but safe and effective use of Luciliacuprina (Diptera: Calliphoridae) in maggot debridement therapy in Alexandria, Egypt. Journal of Medical Entomology 47(3): 491-494.,

6. KinguHJ, Kuria SK, Villet MH, Mkhize JN, Dhaffala A and Iisa JM. 2012. Cutaneous myiasis: is *Luciliacuprina* safe and acceptable for maggot debridement therapy? — J. Cosmet. Dermatol. Sci. Appl. 2: 79–82.
7. Heath AC and Bishop DM. 2006. Flystrike in New Zealand: An overview based on a 16-year study, following the introduction and dispersal of theAustralian sheep blowfly, *Luciliacuprina*Wiedemann (Diptera:Calliphoridae). Veterinary Parasitology 137: 333-344.
8. Ullyett GC. 1945. Species of *Lucilia* attacking sheep in South Africa. Nature 155, 636-637.
9. WallmanJF, Leys R. andHogendoorn K. 2005. Molecular systematicsof Australian carrion-breeding blowflies (Diptera, Calliphoridae) based on mitochondrial DNA. — InvertebrateSyst. 19: 1–15.
10. Wells JD, Wall R. and Stevens JR. 2007. Phylogenetic analysis of forensicallyimportant Lucilia flies based on cytochrome oxidase I sequence: a cautionarytale for forensic species determination. International Journal of Legal Medicine121(3): 229-233.
11. Holloway BA. 1991. Morphological characters to identify adult *Lucilia sericata*(Meigen, 1826) and *L. cuprina*(Wiedemann, 1830) (Diptera: Calliphoridae). New Zealand Journal of Zoology 18: 415–420.
12. Holloway B.A. 1991a: Morphological characters to identify adult *Lucilia sericata*(Meigen, 1826) and *L. cuprina*(Wiedemann, 1830) (Diptera: Calliphoridae). — N. Z. J. Zool. 18: 415–420
13. TourleR, Downie DA. and Villet MH. 2009. A morphologicaland molecular comparison of Luciliacuprina and L. sericata. Diptera: Calliphoridae) in South Africa. Med. Vet. Entomol 14-6: 23
14. Nelson LA, Wallman JFandDowton M. 2007. Using COIbarcodes to identify forensically and medically important blowflies. Med. Vet. Entomol. 21: 44–52.
15. Whitworth TL, Dawson RD, Magalon H andBaudry E. 2007. DNA barcoding cannot reliably identify species of theblowfly genus Protocalliphora (Diptera: Calliphoridae)Proc. R. Soc. (B) 274: 1731–1739.
16. FiroozfarF , Moosa-KazemiH , BaniardalaniM , AbolhassaniM ,Khoobdel M and RafinejdJ .2011. Mass rearing of *Luciliasericata* Meigen (Diptera: Calliphoridae). Asian Pac J Trop Biomed. 1(1): 54–56.
17. Kirstin A, Williams1,2, Jennifer L, Martin H. Villet2. 2017.Phylogenetic radiation of the greenbottle flies Diptera, Calliphoridae, Luciliina. ZooKeys 568: 59-86.
18. SAS. SAS/STAT Users Guide for Personal Computer. Release 9.13.SAS Institute, Inc., Cary, N.C., USA.2010
19. Harvey ML, Gaudieri S, Villet MH. and Dadour IR. 2008. Aglobal study of forensically significant calliphorids: Implications for identification. Forensic Sci. Int. 177: 66–76
20. Debry R, Timm AE, Dahlem GA and Stamper T. 2010. mtDNA-based identification of LuciliacuprinaWiedemannand Luciliasericata (Meigen) (Diptera: Calliphoridae) in thecontinental United States. Forensic Sci. Int. 202: 102–109
21. Stevens J. and Wall R. 1996. Species, sub-species and hybridpopulations of the blowflies Luciliacuprina and Luciliasericata:Diptera: Calliphoridae Proc. Biol. Sci. 263. 1341-1335
22. Kirstin Wand Martin HV.2013. Ancient and modern hybridization between *Lucilia sericata*and *L. cuprina*(Diptera: Calliphoridae).Eur. J. Entomol.110(2): 187–196, 2013
23. Williams KA, Cronje FJ, Avenant L. and Villet MH. 2008. Identifying flies used for maggot debridement therapy. S. Afr. Med. J. 98: 196–197.
24. Kirstin Alexa Williams. June 2014.Molecular Systematics and Biologyof TwoLuciliaSericata, LuciliaCuprina Closely Related Blowflies. Ph. D. Rhodes University

Table 1. List 0f primers that used in PCR amplification

PCR	Primer	Sequence		Amplicon
Cycle	*28S* gene	F	CCCCCTGAATTTAAGCATAT	650bp
		R	TTAGACTCCTTGGTCCGTG	

Table 2. The Cycles of PCR

PCR step	Temperature	Time	Repeat cycle
Initial Denaturation	94 °C	5 Min	1
Denaturation	94 °C	30 Sec	36
Annealing	55 °C	1 min	
Extenation	72 °C	30 Sec	
Finial Extension	72 °C	7 min	

Table 3: Results of Polymerase chain reaction PCR.

Result	Samples	Percentage %
Positive	43	86 %
Negative	7	14 %
Total	50	100 %

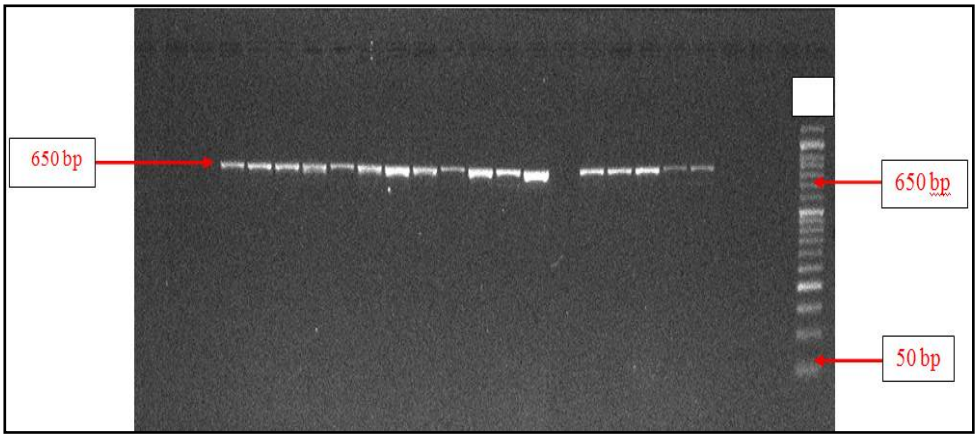

Figure 1.Gel electrophoresis image that shown the PCR product of *28S* gene that using in detection *Lucilia sericata* larvae. Where M: Marker (50-1000bp), Samples some positive at 650bp PCR product size

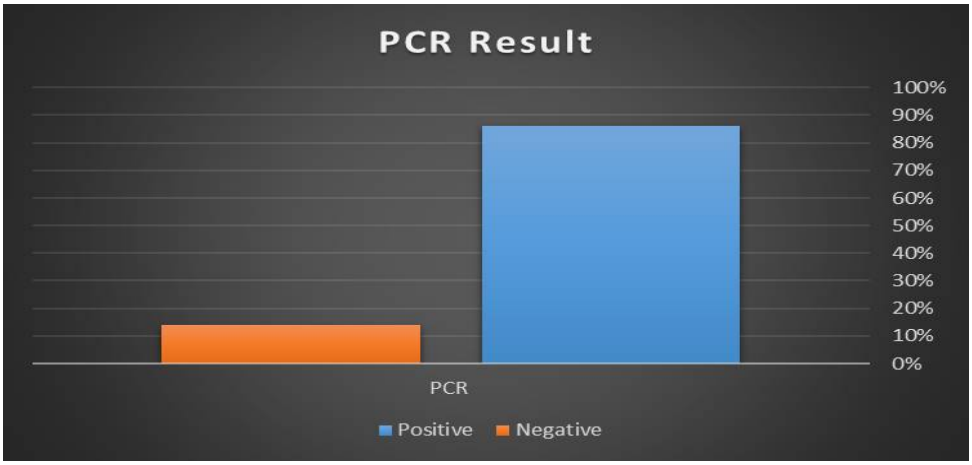

Fig 2.PCR Result show in percentage for the *S28* gene

Indian Journal of Natural Sciences *www.tnsroindia.org.in ©IJONS*

Vol.9 /Issue 50 /October / 2018 *International Bimonthly* *ISSN: 0976 – 0997*

RESEARCH ARTICLE

Used *Carum carvi* Powder in Broiler Feed to Reduce *Salmonella typhimurium* Effects on Some Health Performance

Munqith Abdulmajeed Alwan[1*] and Mohanad F. Hamood[2]

[1]Biotechnology Research Center, Nahrain University, Iraq
[2]Department. of Vetneray, Public Health, College of Veterinary Medicine, University of Baghdad, Iraq

Received: 01 July 2018 Revised: 03 Aug 2018 Accepted: 05 Sep 2018

[*]**Address for Correspondence**
Munqith Abdulmajeed Alwan
Biotechnology Research Center,
Nahrain University, Iraq.

ABSTRACT

This study was conducted to evaluate the effect of dietary supplementation with Carum carvi to reduce contamination by *salmonella Typhimurium*. And enhance immunity for broiler chicks. This study was conducted during the period from 7/11/2017 to 18/12/2018. The study includes differentness parameters (isolation of bacteria, productive performance, and biochemical test). A total 400 chicks were equally divided into eight groups each group contain (50 chicks) for 42 days. Results demonstrated that the differences in live body weight, weight gain, feed intake, feed conversion ratio were significantly increased($p<0.05$)in broiler chicks (G5, G6 andG7) provided feed supplement with *Carum Carvi* (750 mg/1000mg/ 1500mg / kg. feed) as compared to eight group(basil diet). However Carum Carvi (750mg, 1000mg, and 1500mg/kg.feed) showed significant increasing ($p<0.05$) in PCV, RBC, Hb, and WBC but showed significant decreasing in H/L ratio compared with other groups (infected by *salmonella typhimurium* group 4).

Keywords: Carum *carvi salmonella typhimurium* broilers.

INTRODUCTION

Today one of the methods for increase in productive of broilers is append medical plants to poultry diets as a nutritional and medical source such as carium carvi *carvi* L., (*Bunium persicum*) commonly known as *Caraway* (*Umbelliferae*) which is a globally distributed spice with a history as a medicinal plant since ancient times. *Carum carvi* L. is biennial herb, widely cultivated in west Asia, Europe and North America. Caraway is grown for its content of essential oils that are present in the whole plant, but their concentration is highest in achene's (Sedlakova.*et* al., 2003; Ibrahim et al., 2007). Al-Kassie, (2010) stated that approximately 30 compounds were contained in this plant while carvone and limonene account for about 95% of them. Seeds contain trace amounts of other compounds such as acetaldehyde, furfural, carveole, pinene, thujone, camphene, phellandrene, etc.The main constituents of *Carum Carvi* are the volatile oils including carvone (40-60%), limonene, carveol, dihydrocarveol and thymol in addition to

glycosides and flavonoids. Experimental studies have shown its anti-dyspeptic antispasmodic antinuclear genic, antibacterial, antitumor, antiproliferative, antioxidant ant hyperglycemic, anti-hyperlipidemia and diuretic activities (Sedlakova et al., 2003; Ibrahim et al., 2007; AlKassie, 2010). Salmonellosis is considered one of the anthropozoonotic diseases of a serious medical problem and raises great concern in the food industry. Poultry is the most potential source of Salmonella food poisoning in man (Khajeali et al., 2013). With the great expansion of the poultry industry, the wide spread occurrence of the avian salmonellosis has ranked it as one of the most important egg- borne bacterial diseases of poultry**.**Therefore, the objectives of the Studying the protective, immunological effect to reduce the bacterial infection caused by *Salmonella typhimurium* and productive, physiological qualities and histopathological changes of the internal organs resulting from the use of *carium carvi* powder.

MATERIALS AND METHODS

Fourteen hundred (400) broiler chicks strain (Ross 308) one day old were used in our experiment. The chicks were divided randomly into eight groups. Each group contains 50 chicks with two replicates. G1: Carum Carvi 750mg/kg + infected *Salmonella Typhimurium*.G2: Carum Carvi 1000mg/kg + infected *Salmonella Typhimurium*. G3: Carum Carvi 1500mg/kg + infected *Salmonella Typhimurium*. G4: infected with Salmonella Typhimurium only. G5: Carum Carvi 750mg/kg. G6: Carum Carvi 1000mg/kg + infected *Salmonella Typhimurium*. G7: Carum Carvi 1500mg/kg. G8: feed only without Carum carvi or infected with *Salmonella Typhimurium*

Plant samples collection

The seeds of *carium carvi* samples were bought from local markets of Baghdad. The powder of *carium carvi* seed add to chicken feed in three different concentration (750 mg/kg, 1000 mg/kg ,1500 mg/kg). All these concentration were supplied all the period of experiment.

Bacterial Isolation for Feces Sample

One loop full of undiluted feces sample was spread on blood agar and MacConkey agar plates. Plates then were incubated over night at 37˚C. Single colonies which were lactose fermenters, and gave negative reaction to oxidase test were transferred to blood and MacConkey agar. The process was repeated several times for purity before use for further diagnosis.

Identification of *Salmonella typhimurium*

A loop full of *Salmonella typhimurium* isolates was fixed on a microscopic slide, then stained by gram stain to examine cells shape, grouping, reaction and non-spore forming (Atlas *et al*., 1995). Identification *Salmonella typhimurium* isolates by biochemical test (Oxidase , Urease and Triple Sugar Iron test Atlas *et al*., 1995). and
Identification was carried out by sub culturing of selected colonies grown on MacConkey agar into Api 20E micro tubes gallery.

Parameters that have been studied

Growth performance

Mean body weight (gm.), Weekly mean weight gain (gm.), Feed intake (gm.), Feed conversion ratio (F.C.R).

Blood sampling

All hematological parameters (Erythrocytes and leukocytes count, PCV%, and Hb concentration) were calculated by using Hematology analyzer which it is specific for veterinary blood tests. These tests were conducted in the hematology unit/ laboratories department of Veterinary Directorate.

Statistical Analysis

Data were analyzed statistically by using one way –ANOVA. Means were compared using LSD.The differences in mortality among groups were assessed using chi-square test. $P<0.05$ is considered significant.

RESULTS AND DISCUSSION

The results demonstrated that the differences in the body weight , weight gain, feed intake, feed conversion ratio were significantly increased($p<0.05$)in broiler chicks (G5, G6 andG7) provided feed supplement with Carum Carvi (750 mg/1000mg/ 1500mg / kg. feed) as compared to eight group(basil diet). While (G8) showed significant increasing ($p < 0.05$) in the body weight, weight gain, feed intake, feed conversion ratio as compared to G1 , G2 and G3 during the all period of experiment (Table 1, 2, 3 and 4).The results of the current study were showed a significant increasing ($p<0.05$) in Live body weight and weekly weight gain of G1 , G2 and G3 during the all period of experiment as compared with control positive groups (infected group). The result showed that carium carvi has a significant role in growth and health of chick because the improvement in digestion and absorption availability of nutrients accompany with a positive effect on intestine activity and increasing digestive enzymes. These results are in agreement with Khajeali et al., (2013) who stated that *Caraway* can enhance the performance and quality of meat for broilers chicks. This improvement may be due to the biological functions of *Caraway* to improve growth or that may be due to its role as stimulant, carminative, enhanced digestibility, anti-microbial properties and the prevention of gastric toxicity.
Caraway has many unsaturated fatty acids such as myristic acid, palmitic acid, palmitoleic acid, stearic acid, oleic acid, linoleic acid (omega-6), linolenic acid (omega-3) and arachidonic acid that to be effective on saturated fat metabolism in the body(Ketels andGroote,1989; Jalc et al., 2007).

A number of phyto-nutrients have been found in caraway seeds, including different vitamins, amino acids, proteins, and minerals, also starch, sugars and other carbohydrates, tannins, phytic acid and dietary fibres (Al-Bataina *et al.*, 2003). The results of feed intake (FI) and (F.C.R) showed significantly ($p<0.05$) differences in feed intake in groups (G7, G6, and G5) when using *carum carvi* in different levels. While in feed conversion ratio the results showed significantly decreasing ($p<0.05$) in groups (G7,G6, and G5). These results are agreed with Khajeali *et.al*., (2013)who reported that caraway caused decrease in FCR with increasing BW because of some herbal plant could provides some compounds that enhance digestion and absorption of some nutrients in these diets. Other researchers proved that there is an increase in BW, FCR with decreasing hematological values of some important blood parameters in broiler diets(Ibrahim et al,.20007; AlKassie, 2010).Other a previous study, reporting that body weight and fat loss might be linked to anti-oxidant, anti-inflammatory, and anti-bacterial properties of caraway phytochemicals, especially phenolic compounds, such as carvacrol, and the unsaturated fatty acids (UFA) **(**Laribi *et al.*, 2013**).** The intake of such bioactive ingredients with high antimicrobial activity, prevents the proliferation of pathogenic microorganisms, and thus enhances the growth and multiplying of beneficial gut bacteria (Iacobellis *et al.*, 2005; Hawrelak *et al.*, 2009;).

The results of current study may support other opinions which have recommended caraway as a safe natural product with several therapeutic effects for humans (Westphal *et al.*, 1996; May *et al.*, 2000; Sadowska & Obidoska, 2003; Samojlik *et al.*, 2010). The results confirmed that the differences in the red blood cells (RBCs), packed cell volume (P.C.V.), hemoglobin (Hb) and white blood cell count (WBCs).Significantly ($p < 0.05$) higher values in (G7) than

those all other groups followed by G6 which recorded significantly ($p < 0.05$) higher values than those G5 and G8, while G5 recorded significantly ($p < 0.05$) higher values in the P.C.V , RBCs and Hb than those G8. However G3 showed significantly ($p < 0.05$) higher values than those of G2, G1 and G4. While the H/L ratio in this experiment of G4 conducted significantly ($p < 0.05$) higher values than those all other groups, followed G1 which showed significantly ($p < 0.05$) higher than those of all groups, while G7 showed significantly ($p < 0.05$) lower values than those all groups (table 5). The results demonstrated that adding *carum carvi* to the broilers diets increases the RBC, P.C.V, and HB.These results agreed with other study which suggested that caraway water extract may have protective properties against anemia through stimulating the absorption of iron in the gastrointestinal tract (El-Shobaki *et al*., 1990).The results appear in blood components (RBCs, PCV, Hb, H/L ratio) significantly higher in groups treated with *carium carvi* this components of *carium carvi* enriched with many important nutrients like vit A, B complex, C and E. And minerals such as calcium, iron, copper, zinc, potassium, magnesium each of them has it own health purposes to help improve and maintain the blood constituent.

There are a number of in vitro and in vivo studies which report different therapeutic potentials and biological activities for caraway oil/aqueous extract and its derivatives, anti-microbial, anti-inflammatory, antioxidant, anti-cancer, and anti-spasmodic effects (Alhaider *et al*., 2006; Can Baser, 2008; Johri, 2011).The aqueous extracts of the roots of caraway have afforded a variety of phenolic and aromatic compounds including different flavonoids, iso-flavonoids, flavonoid glycosides, mono-terpenoids, such as carvone and its derivatives, glucosides, lignins and alkaloids, as well as poly-acetylenic compounds (Kunzemann & Herrmann, 1977; Nakano et al., 1998; Matsumura et al., 2001; Matsumura et al., 2002a, 2002b; Najda et al., 2008). A number of phyto-nutrients have been found in caraway seeds, including different vitamins, amino acids, proteins, and minerals, also starch, sugars and other carbohydrates, tannins, phytic acid and dietary fibres (Al-Bataina et al., 2003)**.** In conclusion: the results of the add *Carum carvi* (1500 mg/kg. feed) to the broilers feed to reduce the infection of *salmonella Typhimurium* on broilers health, enhance the production parameters reduce mortality rate from the infection by *salmonella typhimurium* .

REFERENCES

1. Al-Bataina, B. A., Maslat, A. O., & Al-Kofahi, M. M. Element analysis and biological studies on ten oriental spices using XRF and Ames test. *Journal of Trace Elements in Medicine and Biology.* 2003;*17*(2), 85-90.
2. Alhaidar, I.A., I.A.Al. Mofleh, J.S. Mossa, M.O. Al-Sohaibani, S. Rafatullah and S. Qureshi. Effect of *Carum carvi* on experimentally induced gastric mucosal damage in wistar albino rats. Int. J. Pharma. 2006;2(3): 309-315.
3. Al-Kassie, G.A.M.. Effect of feed cumin (*Cumin cyminum*) on the performance and some blood traits of broiler chicks. Pakistan Journal of Nutrition .2010; 1: 72-75.
4. Atlas, R. M.; Brown, A. E.; Parks, L. C.. Laboratory Manual of Experimental Microbiology. (1st ed). Mosby. 1995;Inc. Missouri.
5. Can Baser, K.Biological and pharmacological activities of carvacrol and carvacrol bearing essential oils. *Current Pharmaceutical Design.* 2008;*14*(29), 3106-3119.
6. El-Shobaki, F., Saleh, Z., & Saleh, N. The effect of some beverage extracts on intestinal iron absorption. *Zeitschrift für Ernährungswissenschaft,.* 1990; *29*(4), 264-269.
7. Hawrelak, J. A., Cattley, T., & Myers, S. P. Essential oils in the treatment of intestinal dysbiosis: A preliminary *in vitro* study. *Alternative Medicine Review.*2009; *14*(4), 380-384.
8. Iacobellis NS, Lo Cantore P, Capasso F, Senatore F. Antibacterial activity of *Cuminum cyminum* L. and *Carum carvi* L. essential oils. J Agric Food Chem. 2005; 53(1): 57-61 . doi: 1 0.1 021 /jf0487351.
9. Ibrahim, I.A., S.M.A. EIB Adwi, A.O. Bakhiet, W.S. Abdel Gadir and S.E.I. Adam. A week feeding 9 Study of *Cuminum cyminum.* J. Pharmacol. Toxicol.2007; 2: 666-671.
10. Jalc, D., M. Certik, K. Kundrikova and P. Namestkova.Effect of unsaturated C18 fatty acids (oleic, linoleic and -linolenic acid) on ruminal fermentation and production of fatty acid isomers in an artificial rumen. J.Veterinarni Medicina. 2007;52(3): 87-94.

11. Johri, R. K. *Cuminum cyminum* and *Carum carvi*: An update. *Pharmacognosy Reviews.*2011; *5*(9), 63-72. doi: 10.4103/0973-7847.79101.
12. Ketels, E. and G. De Groote. Effect of ratio of unsaturated to saturated fatty acids of the dietary lipid fraction on utilization and metabolizable energy of added fats in young chicks. J. Poult Sci. Nov.1989;68(11): 1506-12.
13. Kunzemann, J., & Herrmann, K. Isolation and identification of flavon (ol)-O-glycosides in caraway (*Carum carvi L.*), fennel (*Foeniculum vulgare Mill.*), anise (*Pimpinella anisum* L.), and coriander (*Coriandrum sativum* L.), and of flavon-C-glycosides in anise. I. Phenolics of spices (author's transl)]. *Zeitschrift für Lebensmittel-Untersuchung und-Forschung.*1977; *164*(3), 194-200.
14. Laribi, B., Kouki, K., Bettaieb, T., Mougou, A., & Marzouk, B. Essential oils and fatty acids composition of Tunisian, German and Egyptian caraway (*Carum carvi* L.) seed ecotypes: A comparative study. *Industrial Crops and Products.*2013; *41*(0), 312-318. doi: http://dx.doi.org/10.1016/j.indcrop.2012.04.060.
15. Matsumura, T., Ishikawa, T., & Kitajima, J. New p-menthanetriols and their glucosides from the fruit of caraway. *Tetrahedron.*2001;*57*(38), 8067-8074.
16. Matsumura, T., Ishikawa, T., & Kitajima, J. Water-soluble constituents of caraway: Aromatic compound, aromatic compound glucoside and glucides. *Phytochemistry.*2002a;*61*(4), 455-459.
17. Matsumura, T., Ishikawa, T., & Kitajima, J. Water-soluble constituents of caraway: Carvone derivatives and their glucosides. *Chemical and Pharmaceutical Bulletin.*2002b;*50*(1), 66-72.
18. May, B., Kohler, S., & Schneider, B. Efficacy and tolerability of a fixed combination of peppermint oil and caraway oil in patients suffering from functional dyspepsia. *Alimentary Pharmacology & Therapeutics.*2000; *14*(12), 1671-1677. doi: 10.1046/j.1365-2036.2000.00873.
19. Najda, A., Dyduch, J., & Brzozowski, N. Flavonoid content and antioxidant activity of caraway roots (*Carum carvi* L.). *Vegetable Crops Research Bulletin.*2008; *68*(1), 127-133.
20. Nakano, Y., Matsunaga, H., Saita, T., Mori, M., Katano, M., & Okabe, H. Antiproliferative constituents in Umbelliferae plants II. Screening for polyacetylenes in some Umbelliferae plants, and isolation of panaxynol and falcarindiol from the root of Heracleum moellendorffii. *Biological & Pharmaceutical Bulletin.*1998;*21*(3), 257-261.
21. Sadowska, A., & Obidoska, G. Pharmacological uses and toxicology of caraway. In É. Németh (Ed.), *Caraway; The Genus Carum.*2003; (pp. 186-196). Amesterdam, The Netherlands: Taylor & Francis e-Library.
22. Samojlik, I., Lakic, N., Mimica-Dukic, N., Dakovic-Svajcer, K., & Bozin, B. Antioxidant and hepatoprotective potential of essential oils of coriander (*Coriandrum sativum* L.) and caraway (*Carum carvi* L.) (Apiaceae). *Journal of Agricultural and Food Chemistry.*2010;*58*(15), 88488853. doi: 10.1021/jf101645n.
23. Sedlakova, J., B. Kocourkova, L. Lojkova and V. Kuban. The essential oil content in caraway species (*Carum carvi* L.). J. Hort. Sci., (prague).2003;30(2): 73-79.
24. Steel, R.G.D. and Torrie, J.H. Principles and procedures of statistics. A biometrical approach.1980 ;2nd Edition, McGraw-Hill Book Company, New York.
25. Westphal, J., Horning, M., & Leonhardt, K. Phytotherapy in functional upper abdominal complaints - Results of a clinical study with a preparation of several plants. *Phytomedicine,* .1996;*2*(4), 285-291.
26. *Y. Khajeali, F. Kheiri, Y 1 1 2 . Rahimian, 1M. Faghani and 3A.N amjo*., Effect of Use Different Levels of Caraway (*Carum carvi* L) Powder on Performance,Some Blood Parameters and Intestinal Morphology on Broiler Chicks. World Applied Sciences Journal .2013;24 (8): 1044-1048.

Table 1. Effect of different levels of Carum carvi powder with or without *Salmonella T.* on weekly live body weight (gm.) at 42 days (Means ± SE)

Group	1st day	1st week	Week 2	Week 3	Week 4	Week 5	Week 6
G1	39.400 ± 0.476 B	124.700 ± 0.61 g	223.700 ± 0.63 g	403.10 ± 0.98 g	682.20 ± 0.89 g	1192.20 ± 085 g	1621.40 ± 1.00 g
G2	39.300 ± 0.472 B	127.400 ± 0.400 f	239.00 ± 1.02 f	413.50 ± 0.96 f	758.60 ± 1.35 f	1308.70 ± 0.59 f	1886.40 ± 0.70 f
G3	39.900 ± 0.458 b a	133.800 ± 0.64 e	242.80 ± 0. 61 e	424.50 ± 1.09 e	786.80 ± 1.28 e	1381.80 ± 1.18 e	2008.10 ±0.88 e
G4	38.900 ± 0.433 B	115.900 ± 0.84 h	203.50 ± 1.43 h	360.30 ± 3.49 h	552.80 ± 2.60 h	885.00 ± 0.97 h	1214.90± 0.73 h
G5	39.600 ± 0.54 b a	147.500 ± 0 .84 c	382.60 ± 1.52 c	573.10 ± 0.93 c	494.400 ± 0.94 c	1664.90 ± 0.56 c	2374.50 ± 1.06 c
G6	39.400 ± 0.47 B	150.200 ± 0.51 b	389.60 ± 0.85 b	593.20 ± 0.91 b	1005.00 ± 1.01 b	1804.30 ± 0.96 b	2553.20 ± 4.09 b
G7	39.400 ± 0.561 B	159.400 ± 0.70 a	408.50 ± 1.60 a	615.20 ± 1.17 a	1026.50 ± 0.68 a	1934.20 ± 0.90 a	2734.50 ± 1.04 a
G8	41.00 ± 0.632 A	139.300 ± 0.98 d	360.00 ± 0.95 d	540.00 ± 0.55 d	935.20 ± 1.28 d	1634.00 ± 1.89 d	2295.50 ± 1.36 d
LSD	1.4387	2.0253	3.2169	4.3167	3.8713	3.0047	4.8486

Different letters in columns show significant difference at levels (P<0.05)

Table 2. Effect of different levels of CARUM CARVI powder with or without *Salmonella T.* on weekly weight gain (gm.) at 42 days (means ± SE)

Group	Week 1	Week 2	Week 3	Week 4	Week 5	Week 6
G1	85.30 ± 0.89 g	99.00 ± 1.03 f	179.40 ± 1.30 Dc	279.10 ± 1.42 f	510.00 ± 1.34 g	429.20 ± 0.84 g
G2	88.10 ± 0.62 f	111.60 ± 0.90 e	174.50 ± 1.52 D	345.10 ± 1.26 e	550.10 ± 1.77 f	577.70 ± 1.03 F
G3	93.90 ± 0.70 e	109.00 ± 0.88 e	181.70 ± 1.52 C	362.30 ± 1.70 d	595.00 ± 1.82 e	626.30 ± 1.70 E
G4	77.00 ± 0.77 h	87.60 ± 0.90 g	156.80 ± 3.73 E	192.50 ± 2.27 g	332.20 ± 2.06 h	329.70 ± 0.98 H
G5	107.90 ± 1.20 c	235.10 ± 2.21 c	190.50 ± 1.93 B	421.30 ± 1.09 a	670.50 ± 0.89 d	709.60 ± 1.16 C
G6	110.80 ± 0.78 b	239.40 ± 1.10 b	203.60 ± 0.94 A	411.80 ± 0.91 b	799.30 ± 1.33 b	748.90 ± 3.82 B
G7	120.00 ± 0.78 a	249.10 ± 1.31 a	206.70 ± 2.46 A	411.30 ± 1.15 b	907.70 ± 1.28 a	800.30 ± 1.61 A
G8	98.30 ± 0.90 d	220.70 ± 0.84 d	180.00 ± 1.09 Dc	395.20 ± 1.28 c	698.80 ± 2.24 c	661.50 ± 2.74 D
LSD	2.4016	3.4641	5.6595	4.0797	4.6571	5.6213

Different letters in columns show significant difference at levels (P<0.05)

Table 3. Effect of different levels of CARUM CARVI powder with or without *Salmonella Typhy meurm* on weekly feed intake (g/bird) at 42 days (means ± SE)

Group	Week 1	Week 2	Week 3	Week 4	Week 5	Week 6
G1	106.50 ± 1.50 E	197.50 ± 2.50 e	496.50 ± 4.50 E	555.50 ± 5.00 f	826.50 ± 1.50 F	898.00 ± 2.00 E
G2	107.00 ± 1.00 E	217.50 ± 2.50 c	535.00 ± 1.00 D	642.50 ± 2.50 e	872.50 ± 2.50 e	976.00 ± 10.00 D
G3	112,50 ± 2.50 D	207.50 ± 2.50 d	541.00 ± 1.00 D	661.50 ± 1.50 cd	902.50 ± 2.50 d	996.50 ± 1.50 D
G4	98.50 ± 1.50 F	177.50 ± 2.50 f	310.50 ± 9.50 F	387.50 ± 2.50 g	542.50 ± 2.50 g	794.50 ± 5.50 F
G5	119.50 ± 1.50 Cb	260.00 ± 4.00 a	560.00 ± 1.00 C	696.50 ± 1.50 a	938.00 ± 8.00 c	1072.50 ± 10.50 B
G6	121.00 ± 1.00 B	261.50 ± 1.50 a	581.00 ± 7.00 B	672.50 ± 2.50 b	988.00 ± 8.00 b	1093.50 ± 5.50 Ba
G7	127.50 ± 2.50 A	626.50 ± 2.50 a	599.50 ± 3.50 A	652.50 ± 2.50 d	1027.00 ± 1.00 a	1104.50 ± 4.50 A
G8	115.50 ± 0.50 Cd	249.50 ± 1.50 b	546.50 ± 0.50 Dc	666.50 ± 3.50 cb	1015.00 ± 5.00 a	1045.00 ± 11.00 C
LSD	5.3463	8.2944	15.253	9.4201	15.253	23.58

Different letters in columns show significant difference at levels (P<0.05)

Table 4. Effect of different levels of CARUM CARVI powder with or without *Salmonella T.* on feed conversion ratio at 42 days (means ± SE)

Group	Week 1	Week 2	Week 3	Week 4	Week 5	Week 6
G1	1.2350 ± 0.005 C	1.99 ± 0.03 ba	2.805 ± 0.065 c	1.985 ± 0.025 a	1.615 ± 0.005 A	2.085 ± 0.005 C
G2	1.21 ± 0 Dc	1.945 ± 0.015 bc	3.065 ± 0.045 a	1.855 ± 0.005 b	1.58 ± 0 b	1.685 ± 0.015 D
G3	1.195 ± 0.015 D	1.88 ± 0.06 c	2.975 ± 0.005 ba	1.825 ± 0.005 b	1.515 ± 0.005 c	1.59 ± 0 E
G4	1.275 ± 0.025 B	2.025 ± 0.015 ba	1.98 ± 0.05 d	2.01 ± 0.05 a	1.63 ± 0.01 a	2.405 ± 0.035 B
G5	1.105 ± 0.015 E	1.10 ± 0 d	2.935 ± 0.035 bac	1.65 ± 0 dc	1.395 ± 0.015 d	1.48 ± 0.04 F
G6	1.085 ± 0.005 Fe	1.085 ± 0.015 d	2.90 ± 0 bc	1.63 ± 0 dc	1.23 ± 0.01 e	1.455 ± 0.005 F
G7	1.055 ± 0.005 F	1.05 ± 0.01 d	2.895 ± 0.065 bc	1.585 ± 0.005 d	1.13 ± 0 f	1.375 ± 0.005 G
G8	1.332 ± 0.005 A	2.0665 ± 0.145 a	3.036 ± 0.03 ba	1.686 ± 0.011 c	1.013 ± 0.001 g	3.164 ± 0.007 A
LSD	0.0395	0.0854	0.1418	0.0664	0.0252	0.065

Different letters in columns show significant difference at levels (P<0.05)

Table 5. Effect of different levels of CARUM CARVI powder with or without salmonella typh on blood The cellular Pictures in different Groups of broilers (Mean ± S.E.).

Groups	WBC	HP	RBC	PCV	H/L ratio
	X10³/ml	g/100ml	X106/ml	%	Ratio
G1	42.876 ± 0.01	7.809 ± 0.01	2.216 ± 0.007	31.6040 ± 0.01	0.575 ± 0.005
	c	g	f	g	B
G2	49.340 ± 0.13	7.95 ± 0.01	2.548 ± 0.03	33.529 ± 0.01	0.506 ± 0.006
	b	f	e	f	C
G3	67.151 ± 4.79	8.112 ± 0.01	2.924 ± 0.009	33.988 ± 0.011	0.426 ± 0.006
	a	e	d	e	D
G4	35.247 ± 1.49	7.393 ± 0.008	2.078 ± 0.01	29.82 ± 0.017	0.66 ± 0.009
	d	h	g	h	A
G5	62.372 ± 0.008	8.969 ± 0.01	3.216 ± 0.009	34.862 ± 0.008	0.382 ± 0.006
	a	c	c	c	E
G6	64.227 ± 0.009	9.881 ± 0.015	3.41 ± 0.009	35.139 ± 0.009	0.346 ± 0.006
	a	b	b	b	F
G7	67.179 ± 0.015	10.12 ± 0.011	3.73 ± 0.01	35.995 ± 0.02	0.286 ± 0.01
	a	a	a	a	G
G8	64.792 ± 3.619	8.399 ± 0.012	2.945 ± 0.09	34.256 ± 0.01	0.421 ± 0.006
	a	d	d	d	D
LSD	6.1733	0.0362	0.1036	0.0407	0.021

Different letters in columns show significant difference at levels ($P<0.05$)

Indian Journal of Natural Sciences www.tnsroindia.org.in ©IJONS

Vol.9 /Issue 50 /October / 2018 *International Bimonthly* *ISSN: 0976 – 0997*

RESEARCH ARTICLE

Bathymetry of Iraqi Territorial Water (Coast of Faw Peninsula) by Using GIS Techniques (IDW and Kriging Interpolation Methods)

Omar Mohammed Sultan Ali[1*], Nawal K.Ghazal[2], and Khalid I. Hassoon[3]

[1]M.Sc. Student, Department of Physics, College of Science, University of Baghdad, Baghdad, Iraq.
[1]Department of Remote Sensing and GIS College of Science, University of Baghdad, Baghdad, Iraq.
[3]Center of Remote Sensing, Directorate of Space Technology and Communications, Ministry of Science & Technology, Baghdad,Iraq.

Received: 02 July 2018 Revised: 04 Aug 2018 Accepted: 05 Sep 2018

[*]**Address for Correspondence**
Omar Mohammed Sultan Ali
M.Sc. Student,
Department of Physics,
College of Science,
University of Baghdad,
Baghdad, Iraq.
Email: omer90goleto@gmail.com, dr.nawal@yahoo.co.in , Dr.Khalid68@yahoo.com.

ABSTRACT

The Bathymetry process in depth of Iraqi territorial waters is obtained by three possible directions.First, the technical method using modern technologies (Synthetic aperture radar SAR), Echo Sounder,and Airborne Electromagnetic (AEM),Airborne Laser,and Multi-beam). Since Iraq doesn't have these techniques, there it can be used in other ways.Second, the practical way in the fieldwork: This trend requires large financial resources(specialized companies)and the specialized worker hands, and determine accurately the maritime borders of Iraq (the territorial sea). Third, the way of the office work application (special programs in this direction, such as GIS, ARDAS, and satellite images), which is the direction that can be taken in this work.After using GIS techniques [interpolation (IDW, kriging methods)], which found the unknown points (points in between) for the depth of water near the coast of the Faw peninsula. Through these methods are obtained five classifications of depths within the range (0, 6.3 m), these classifications are as follows: the first classification, which falls within the range (0 - 3.7), represents the limits of industrial strength at the end of the continental shelf of Iraq, while the second class, that falls within the range (0.37 - 0.979), shows the archipelagic region (sometimes land areas, sometimes covered by water, according to the tidal phenomena). The third class which falls within the range (0.979 - 1.978), represents the first shallow water area containing the mud deposits. The fourth classification, which falls within the range (1.978, 3.615), represents the second shallow water area containing industrial and oil waste. The fifth classification, which falls within the range (3.615, 6.3), represents the third shallow water area containing sunken ships and war debris. After the practical

application of the GIS techniques (methods of interpolation), which found that the best way in this field to find the unknown points of the depths (in-between points), then found from that, that the kriging method is (which gave us RMS about 0.662) better than the IDW method (which gave us RMS about 0.727).

Keywords: Bathymetry, territorial water, GIS techniques, interpolation, IDW, Kriging.

INTRODUCTION

Estimating the bathymetry of the ocean is one of the important Parameters, which play an important role in planning nearshore construction activities such as engineering work, port management pipeline laying, fishing, dredge operation, oil prospecting, and aquaculture, and it is also significantly important to determine the underwater topography and movement of sediments and to generate hydrographically charts for safe transportation. Moreover, in the port, defend on the depth of man-made channels throughout the year is important for the smooth navigation of large ships. Typically, the measurement of ocean depth is done using ordinary methods such as pre-measured rope or cable passage, placed on the side of the vessel and allowed to reach the seabed. This method can explore the depth of a single point in time. Hydrographic ships carrying echo sounder instruments such as single-beam and multi-beam echo sounders rapidly replaced this method. The echoes sounding the method are able to determining the depth precisely over the clear water, coastal environment, whereas in turbid water, the method lacks performance due to filtering of sound waves to the bottom of the ocean. In general, the speed of ship limitation the surveyors to map the ocean the region at a slightly different scale than the desired scale. It is to be noted that the method would take 200 years of survey time to complete swath survey of the deep ocean, and it would take even more time for shallow coastal areas [1]. In order that overcome this inadequacy, various airborne laser Bathymetric (ALB) and light detection and ranging (LiDAR) systems such as scanning hydrographic operational airborne LIDAR survey (SHOLAS), compact hydrographic airborne rapid total survey (CHARTS), laser airborne depth sounder (LADS), an experimental advanced airborne research LIDAR (EAARL) was established to conclude the Bathymetry of oceans. This method can effectively determine the depth of both shallow and Clearwater coastal environments, but this technique is limited by its high purchasing and conservation costs. Almost all of the above methods take a long interval of time to revisit the same location and thus it is difficult to observe the frequent changes in seabed morphology [2].

It is very hard to infer the Bathymetry of shallow water region, as those areas are tough to access by Hydrographic ships carrying echo-sounding tools. Accurate estimation of Bathymetry of shallow water the region is important for the navigation, security of small boats like fishing and for benthic studies. Remote sensing technology can be observed as one of the most promising substitutional tools to map the bathymetry of shallow water regions by coupling remote sensing data with ground-based measurements. Remote sensing technology has different advantages such as wide coverage of Area, receptivity of the area over the sure period, and easy access to data. Therefore, this technology supply a fast solution to map Bathymetry of the region, where a rapid change of coastal environment is spotted. Bathymetry mapping using remote sensing technology is obtained from the principle in which the total amount of Electromagnetic energy observed and reflected from the Water body determines the water depth [3]. The remote sensing a technique is ready to determine the depth of the ocean, for the reason that the water, relax signal from the bottommost part of the ocean with a strong wavelength dependency. However, breakthrough of electromagnetic wave energy is limited. Therefore, remote sensing technique is mostly adopted to infer the depth of clear and shallow water region. The two important approaches such as analytical method and experimental method are adopted to retrieve the bathymetry of the ocean using satellite image. A number of analytical algorithms are available in the literature, which are proposed by Lyzenga (1978, 1981), In order to use the analytical method for mapping the bathymetry of the ocean, a number of input parameters such as water pole, properties of the

atmosphere and bottom reflectance, and spectral signatures of suspended and dissolved materials are required. Although the analytical method is moderately complex and difficult, have adopted it. Otherwise, the empirical method establishes the relationship between the remotely sensed radiance of a water body and the depth at observed locations is established empirically without regard to how light is transmitted in water. In comparison, empirical the method requires only a few parameters as input, which are simple and do not require water pole parameters [4].

MATERIALS AND METHODS

Study area and Data used

The Iraqi coast of the Arabian Gulf. The coast is located in the extreme south of Iraq between latitude 29° 49´000 ´´ and 30° 05´ 012 ´´ N and longitude 48° 01 ´ 006 ´´ and 48 ° 44 ´ 000 ´´ E. This coast consists of a Coastal Sabkha which extends about (27 km) towards the north , covering on area of (736 km^2), see fig (1).The other part of the area is tidal flats with a gentle slope toward the Gulf. The length of the tidal flat is 64 km and its width varies with the sedimentation nature, it is 15000 m near the Shatt Al-Arab estuary to 100 m a narrow strip near the southern entrance of Khour Al-Zubair [5].

Topographic changes of water (Khour Abdallah)

There Have Been Erosion And Retreat Of The Zero Line Towards The Iraqi Coast At The Entrance Of Khour Abdullah By 284 M During The 46 Years Or 6.17 M / Year Depending On The Nature Of The Coastal Soil And The High Speed Of The Tide In Particular, While Erosion In The Iraqi Side At Khour Shitaneh 370 M At A Rate Of 8.04 M / Year, Because The Acceleration Of Tidal Currents Is Also Greater In This Region. The Sedimentation Occurs In The Opposite Direction, And There Have Been Erosion And Sedimentation In Some Areas Of The Kuwaiti Coast, That The Erosion Amounted To 375 M Or 8.15 M /Year, Sedimentation Which Reached 540 M During 46 Years, An Average Of 11.73 M / Year, Which Adds Large Areas To Kuwaiti Side. And The Possibility Of The Emergence Of New Islands, Later Effect On The International Boundary Between The Two Countries And The Navigational Channel, Due To The Adoption Of The Principle Of The Midline Of The Channel Presentation From The Beginning Of The Baseline For Both Countries In Accordance With The United Nations Resolution (833) In 1993 [6].

Data used

- Satellite image (landsat8)
- GIS software

Methodology of work

The entirety of this study was conducted using ArcGIS software specifically, remapping and topology the toolsets used for this project analysis, chose Point in the area, selection by location, union and Path Distance. These techniques are chosen to provide the most optimal outcome for this site suitability analysis. Especially, both interpolation methods (IDW, Kriging).

Interpolation

Interpolation tools available in the geographical information systems are useful and allow the operator to easily perform a different kind of elaborations and to display them graphically in order to show the results in a way intelligible also to non-skilled subjects. Interpolators are divided into two typologies: 1. Deterministic., 2. Stochastic.

These interpolators use a linear combination of known functions with different weighting and neighboring search schemes: data that are closer to interpolation point have more influence (weight), during the computations, in comparison with faraway ones, according to the First Law of Geography (Tobler, 1970). Interpolation is the process of estimating unknown values that fall between known values. The Interpolators could be defined as weighted average methods with similar processing concept. The operator in fact, needs to compute an unknown value, at an ensample location, given a set of neighboring sampled values, collected at locations neighboring the unknown one; the quantity of neighboring points included in the search radius directly affects the final surface smoothing and the computing time. The interpolation procedure consists in the definition of the search area or neighborhood around the unknown point, the detection of the observed data points within the previously defined neighborhood and, finally, the assignment of appropriate weights to each of the observed data points [7].

Inverse Distance Weighted (IDW)

IDW works best for dense, evenly spaced sample point sets. It does not consider any trends in the data, so, for example, if actual surface values change more in the north-south direction than they do in the east-west direction (because of slope, wind, or some other factor), the interpolated surface will average out this bias rather than preserve it. IDW interpolation considers the values of the sample points and the distance separating them from the estimated cell. Sample points closer to the cell have a greater influence on the cells estimated value than sample points that are further away. Inverse Distance Weighting cannot make estimates above the maximum or below the minimum sample values. For an elevation surface, this has the effect of flattening peaks and valleys (unless their high and low points are part of the sample). Because the estimated values are averages, the resulting surface will not pass through the sample points [8].

As the following formula:

$$Z^*(\mathbf{u}) = \sum_{i=1}^{n} \lambda_i Z(\mathbf{u}_i),$$ ……..(1)

Where u is the estimation location u_i, i=1….. n, are the locations of the sample points within the search neighborhood, Z *(u) is the inverse distance estimate at the estimation location, n is the number of sample points, λ_i, Are the weights assigned to each sample point, and Z (u_i), i=one…, n, are the conditioning data at sample points [9]. The weights are determined as:

$$Z^*(\mathbf{u}) = \sum_{i=1}^{n} \lambda_i Z(\mathbf{u}_i),$$ ……..(2)

Where di are the Euclidian distances between estimation location and sample points, and exponent p is the power or distance exponent value. Note that the sum of the inverse distance weights, λ_i, i=1…, n, is equal to 1, that is:

$$\lambda_i = \frac{\left(\frac{1}{d_i^p}\right)}{\sum_{i=1}^{n}\left(\frac{1}{d_i^p}\right)}, \quad (i = 1, \ldots, n),$$ ……..(3)

Where di are the Euclidian distances between estimation location and sample points, and exponent p is the power or distance exponent value. Note that the sum of the inverse distance weights, λ_i, i= 1…, n, is equal to 1, that is:

$$\sum_{i=1}^{n} \lambda_i = 1. \quad \text{.....(4)}$$

Kriging method

In general, Kriging is a relatively fast interpolated that can be exact or smoothed depending on the method. The method is flexible with input and output data: many outputs can be generated besides the prediction maps like predictions of errors and probabilities. The drawback of the flexibility is that it may require a lot of decision-making. A measure of success is through the prediction errors or through cross-validation. Another method of interpolation can be applied that is more complex than the method (IDW-POW). In this way, unknown values can be calculated from the actual values that take upper and lower real recorded values. For example, if the range of real values is between (0, 6.3) it can be obtained the unknown values (points in between). This method has two types (ordinary, universal); the first type ordinary does not need to a direction of a slope or direction of the wind, while the second type universal needs direction. This is why taking the first type ordinary only because do not need the direction in the process of finding depths [10].

Ordinary Kriging

Ordinary Kriging is the basic form of Kriging. The prediction by ordinary Kriging is a linear combination of the measured values. The spatial correlation between the data, as described by the variorum, determines the weights. As the mean is unknown, fewer assumptions are made.The method assumes intrinsic stationarity; unfortunately, meteorological variables are often not stationary. In some case, this problem can be eliminated by using different sizes and shapes of the search neighborhood. Ordinary Kriging is frequently applied in meteorology [11].

$$\begin{bmatrix} \gamma(Z_1-Z_1) & \gamma(Z_1-Z_2) \dots & \gamma(Z_1-Z_n) & 1 \\ \gamma(Z_2-Z_1) & \gamma(Z_2-Z_2) \dots & \gamma(Z_1-Z_n) & 1 \\ & & & 1 \\ \gamma(Z_n-Z_1) & \gamma(Z_n-Z_2) \dots & \gamma(Z_n-Z_n) & 1 \\ 1 & 1 \quad \dots & & 0 \end{bmatrix} \times \begin{bmatrix} \lambda_1 \\ \lambda_2 \\ \\ \lambda_n \\ \mu \end{bmatrix} = \begin{bmatrix} \gamma(X_1-X) \\ \gamma(X_2-X) \\ \\ \gamma(X_n-X) \\ 1 \end{bmatrix}$$

Where:
γ: Variogram values,
$z_1 \dots z_n$: real value at location 1 to n,
X: Location where new value is estimated,
μ: Lagrange factor.

RESULTS AND DISCUSSION

Inverse Distance Weighted (IDW)

The values of depth in the area where measurements are not taken by giving weights to nearby values. This method is the simplest method of interpolation, where it takes the concept of spatial autocorrelation. The (IDW) will give relative weight to the nearest points greater than the distant points in the calculation of the unknown values. It does

not exceed the maximum value and not less than the minimum value. Any unknown values will fall between the highest and lowest values only, see fig (2).When the power value increasing, the relative weights for the proximal points will be greater than the distance points. However, while reducing the value of the fall, all points will take relative weight ratios, and this is contrary to the first law of the geography ((Tobler law)). This law states that nearby points take relative weights greater than distant points.

After analyzing the values that found in the figure above and match them with reality, these values came from applying (IDW-POW) method, and make classes close to five classes, that value was set within the range (0 - 6.3).The first class ratings within the range (0 - 0.37) represent the boundary of the industrial dam at the end of the continental shelf. The second class that falls within the range (0.37- 0.979) shows the archipelago area (which is sometimes the land areas. In addition, sometimes water, land according to the phenomenon of tides).The third class within the range (0.979- 1.978) represents the first shallow that contains a Clay deposits area. The fourth class with rang (1.978- 3.615) represented the second shallow water area that contains industrial and oil waste. The fifth class with rang (3.615- 6.3) represented the third shallow water area that contains Ships drowned and war debris. The (third, fourth, fifth) class area that needs to Clean up and the Cree's operations to reach the appropriate depths that suit with submersible of large commercial vessels, from figs (3 and 4) can be seen the graphic between real and expected values and the percentage of error through applying Regression function for each value. In the end, that found the value of the RMS from applying the IDW-POW method, see table (1).

Ordinary Kriging

After analyzing the values that found in the figure above and match them with reality, these values came from applying (kriging-ordinary) method, and make classes close to five classes, those values were set within the range (0, 6.3), see fig (5). The first class ratings within the range (0 - 0.37) represent the boundary of the industrial dam at the end of the continental shelf. The second class that falls within the range (0.37 - 0.979) shows the archipelago area that is sometimes the land area. In addition, sometimes water, land according to the phenomenon of tides. The third class within the range (0.979 - 1.978) represents the first shallow water that contains a Clay deposits area. The fourth class with rang (1.978 - 3.615) represents the second shallow water area that contains industrial and oil waste. The fifth class with rang (3.615- 6.3) represents the third shallow water area that contains Ships drowned and war debris.

The (third, fourth, fifth) class area that need to Clean up the Cree's operations to reach the appropriate depths that suit with submersible of large commercial vessels. From figures (6, 7, 8 and 9) can be seen the graphics representing the predicted, error, standardized error and normal QQ plot through application regression function for each value. In the end, that found the value of the RMS from applying the Kriging-ordinary method, see table (2). After applying the two methods (IDW-POW and Kriging-Ord) and observing the values of the Root-Main-Square that is inspired by, the two methods find that (Kriging-Ord) method is the best way to find any unknown values of the depths, as shown in table (3). This work is focused to find the best way to calculate the unknown values of the depths of our territorial waters (Coast of the Faw Peninsula).

CONCLUSIONS

1. Nature of most the Iraqi coast in this region is a shallow water and contains shipwrecks, Industrial waste. In addition, Iraq must carry out cleaning and Cree of mud deposition the coast to allow ships to approach the Iraqi coast.
2. By Using GIS techniques (methods of interpolation, IDW, kriging methods), we found the unknown points(in between point) of the water's depth near the coast of the Faw Peninsula, [as shown in first stage of part two from practicel work (chap 4)] that get five classes of depths at range (0-6.3 m). These classes are as follows:

- The first class ratings within the range (0- 0.37) represent the boundary of the industrial dam at the end of the continental shelf.
- The second class that falls within the range (0.37- 0.979) represents the archipelago area (which is sometimes the land areas. In addition, sometimes water, land according to the phenomenon of tides).
- The third class within the range (0.979 - 1.978) represents the first shallow that contains a glacial area.
- The fourth class with rang (1.978 - 3.615) represented the second shallow water area that contains industrial and oil waste.
- The fifth class with rang (3.615 - 6.3) represented the third shallow water area that contains Ships drowned and war debris.

3. After the practical application of the GIS techniques (methods of interpolation), which found that the best way in this field to find the unknown points of the depths (in-between points), and then found that the kriging method (which gave us RMS about 0.662) better than the IDW method (which gave us RMS about 0.727).

REFERENCES

1. J.Pushparaj, A. Hegde, *Estimation of bathymetry along the coast of Mangalore using Landsat-8 imagery*, The International Journal of Ocean and Climate Systems, Vol. 8(2) 71-83, 2017.
2. R. Abileah, , *Mapping Shallow Water Depth From Satellite*, ASPRS Annual Conference Reno, Nevada, 2006.
3. F. Bandini, D. Olesen, J. Jakobsen, C. Kittel1, S. Wang, M. Garcia, P. Gottwein, *Bathymetry observations of inland water bodies using a tethered single-beam sonar controlled by an Unmanned Aerial Vehicle*, Hydrol. Earth Syst. Sci, 4.0 License, 2017.
4. N. D. Volp, B. C. van Prooijen, G. S. Stelling, *A finite volume approach for shallow water flow accounting for high-resolution bathymetry and roughness data*, Water Resources Research, VOL. 49, 4126–4135, 2013.
5. H. K. H. Al-Mahmood, , *the Properties of Iraqi Coast, Geographical Study*, PhD thesis, 2006.
6. J. T. Al Ali, H. K. Hassan, O. I. Hamoud, *Study Of Topographic And Navigational Changes Of Khawr Abd Allah Channel*, Basra Research Journal, Issue: 34, Part 4, p 2012.
7. E. A. Mortada, K. Mohamed, E. M. Abdallah, M. Abderrahmane, , *A Descriptive Model For Developing A Hydraulic Geodatabase By Using The GIS Software*, International Journal of Computer Science & Information Technology (IJCSIT), Vol 3, No 2, 2011.
8. M. W. Sielicka, I. B. Olkowska, A. Stateczny, *Application of geodatabase dedicated for bathymetric data during the production of electronic navigational charts for inland shipping*, Scientific Journals Zeszyty Naukowe Maritime University of Szczecin Akademia Morska w Szczecinie, Vol 35, Iss 107, pp. 168–173, 2013.
9. T. Tunçaya, I. Bayraminb, F. Atalayc, I. Ünverb, , *Assessment of Inverse Distance Weighting (IDW) Interpolation on Spatial Variability of Selected Soil Properties in the Cukurova Plain*, Tarim Bilimleri Dergisi, Journal Of Agricultural Sciences, Vol: 22, PP: 377-384, 2016.
10. S. Bhattacharjee, P. Mitra, O. K. Ghosh, *Spatial Interpolation to Predict Missing Attributes in GIS Using Semantic Kriging*, Transactions On Geoscience And Remote Sensing, Vol. 52, No. 8, 2014.
11. A. Tyagi, P. Singh, *Applying Kriging Approach on Pollution Data Using GIS Software*, International Journal of Environmental Engineering and Management, ISSN 2231-1319, Vol: 4, No: 3 , pp. 185-190, 2013.

Table 1. Showing the result after applying the predicted values (IDW-POW)

Value of Error	Type of Error
Sample	136 of 136
Mean	0.03565258107606679
Root-Mean-Square	0.7271175227425816

Table 2. Represents the result after applying the predicted values (kriging-ordinary method)

Type of Error	Values of Error
Sample	136 of 136
Mean	-0.005276242444205131
Root-Mean-Square	0.662480711860391
Mean Standardized	-0.004398992449118254
Root-Mean-Square Standardized	0.6940081936618238
Average standard Error	0.9974120556391727

Table 3. Compare the RMS values for both methods

Method type	Amount of RMS
IDW_POW	0.7271175227425816
KRIGING-ORDINARY	0.662480711860391

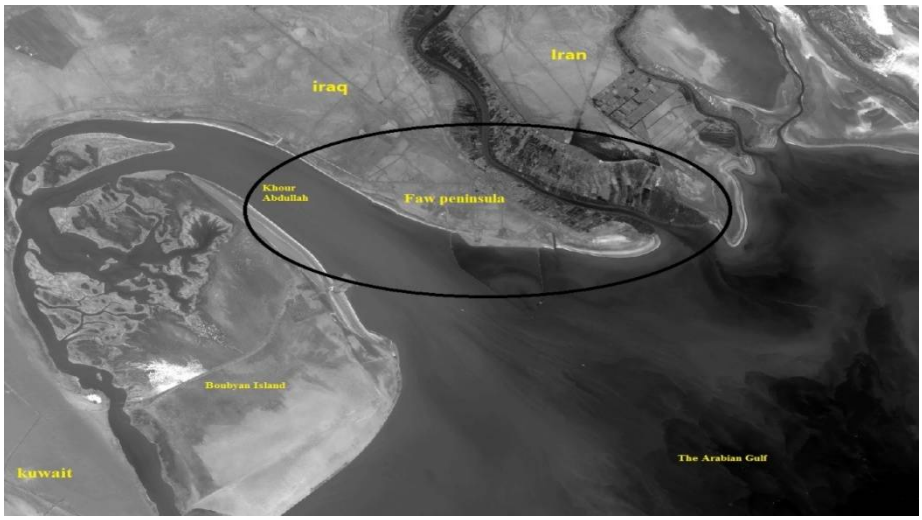

Fig 1. The highlights on the coast of the Faw peninsula [Landsat 8]

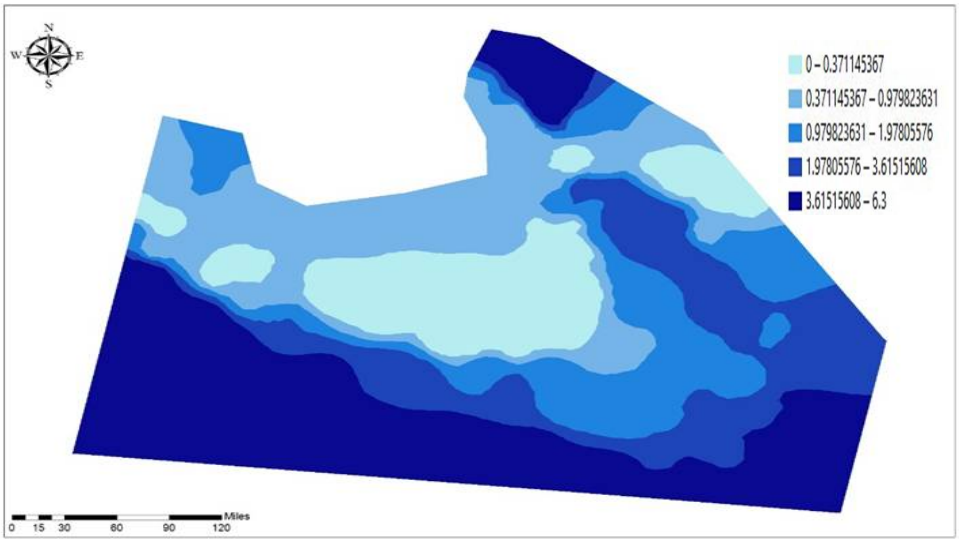

Fig 2. The final shape after applying IDW-POW method

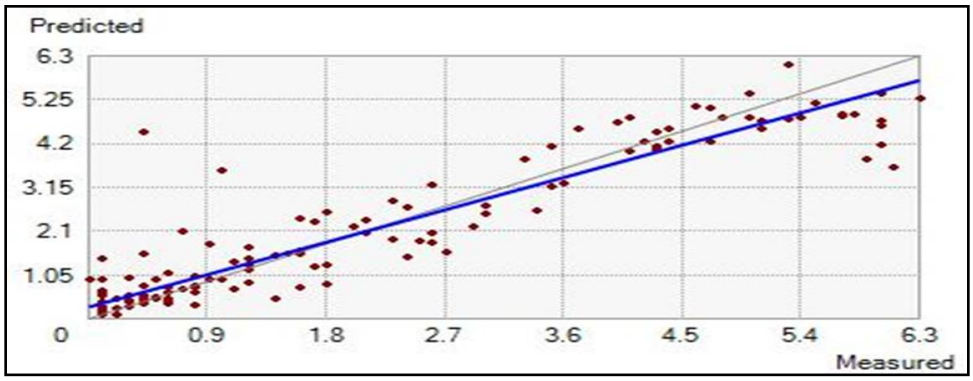

Fig 3. Representing the predicted values

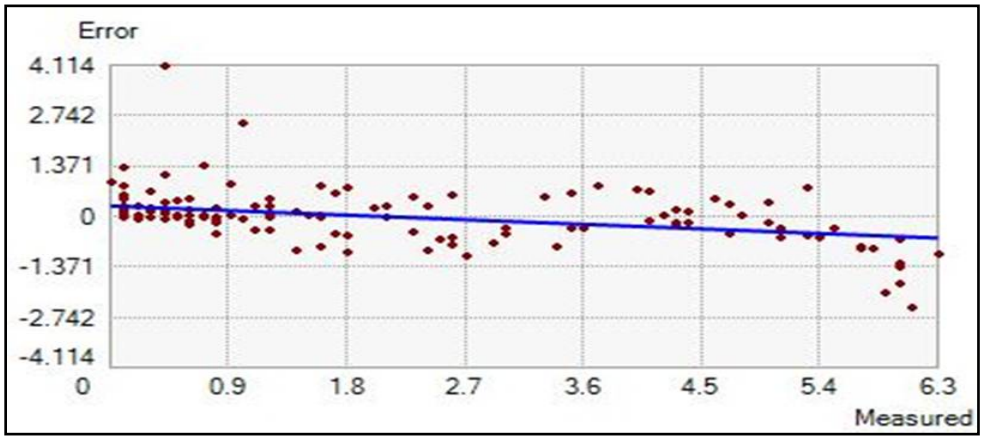

Fig 4. Representing the error value

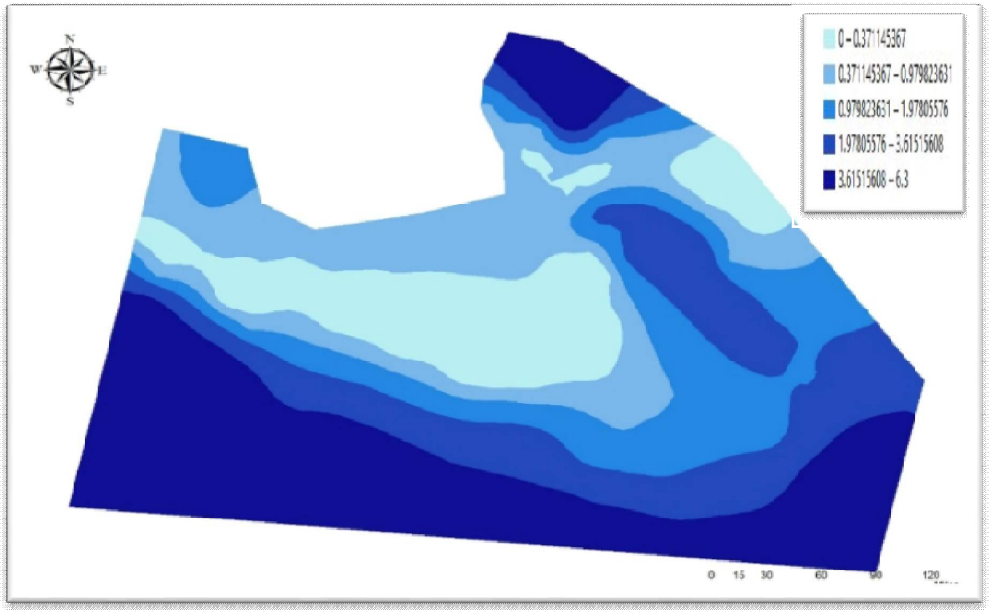

Fig 5. The final shape of the in-between points representing the depth values after applying Kriging Ordinary method.

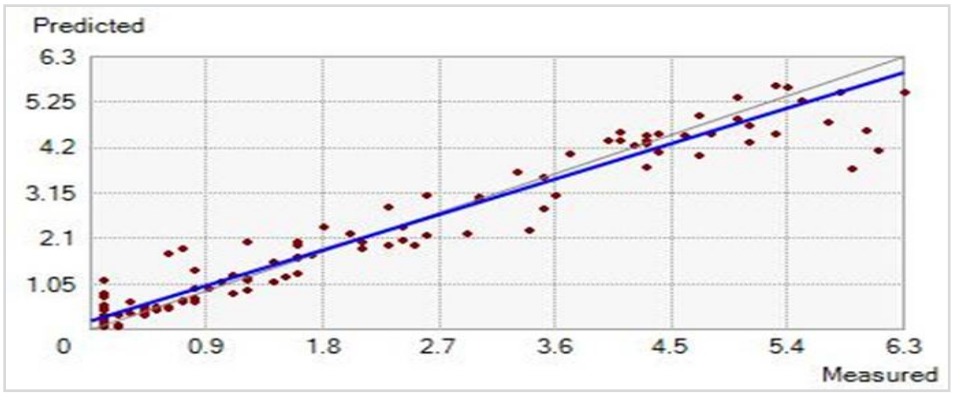

Fig 6. Representing the predicted values (kriging-ordinary method)

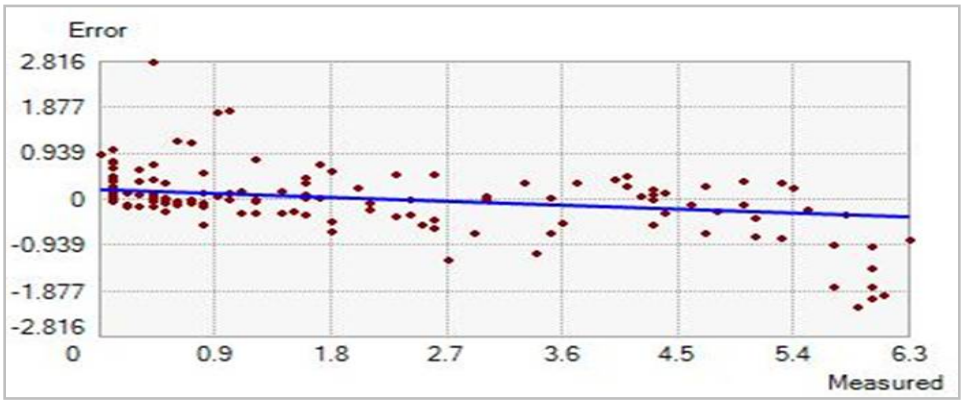

Fig 7. Showing the error values (kriging-ordinary method)

Fig 8. Illustrated the Standardized Error value (kriging-ordinary method)

Fig 9. Represented the QQ plot (kriging-ordinary method)

Indian Journal of Natural Sciences www.tnsroindia.org.in ©IJONS

Vol.9 /Issue 50 /October / 2018 *International Bimonthly* *ISSN: 0976 – 0997*

RESEARCH ARTICLE

Study the Immunogenisity of Enterobacterial Common Antigen Against Challenge with *Brucella melitensis* in Guinea Pigs

Ibrahim A.H. Al-Zubaidy[1*] Ban S.Al-Nasiry[1] and ZeenaQ.Al-Khafajee[2]

[1]College of Veterinary Medicine, Unit of Zoonotic Diseases, University of Baghdad, Iraq
[2]Ministry of Agricultures, Iraq.

Received: 04 July 2018 Revised: 03 Aug 2018 Accepted: 06 Sep 2018

[*]**Address for Correspondence**
Ibrahim A.H. Al-Zubaidy
College of Veterinary Medicine,
Unit of Zoonotic Diseases,
University of Baghdad, Iraq.

ABSTRACT

Enterobacterial common antigen (ECA) appears to be required for the resistance of *E. coli* to bile salts and short-chain fatty acids. Enterobacterial common antigen occurs as two distinct forms immunogenic form and the haptenic form, the imunogenic form is found only in certain rough mutants that possess a complete lipopolysaccharid core structure but which lack O-specific side chains, the teropolysaccharide chains are covalently linked to the lipopolysaccharid core region. The total protein concentration of ECA that extracted was 8.2 mg/ml. The result of culturing of the extract was negative for any bacterial contamination. The results of the study first experiment showed on the six groups of guinea pigs showed clinical signs of illness after 7 days that included fever, dullness, decrease appetite, in the 5th and 6thgroups.Two animals in the 6th group were died after 5 days.

Keywords:. Enterobacterial, immunogenic, extract, guinea pigs, lipopolysaccharid.

INTRODUCTION

Enterobacterial common antigen(ECA) appears to be required for the resistance of *E. coli* to bile salts and short-chain fatty acids. However, the role of ECA in the resistance of these organisms to these compounds remains to be established. Furthermore, it is not known if ECA has a similar function in other gram-negative enteric bacteria. In contrast, there are no reports concerning the function of ECA. In this regard, the periplasmic location and cyclic structure of ECA are similar to those of the osmoregulatedperiplasmicglucans synthesized by many gram-negative *Proteobacteria* (**1**). The idea of using ECA to induce an immune responses against other gram - negative bacteria obtained from the fact that some antigens included by enterobacteriaceae family have some similarity to some outer membrane proteins consisted by the cellular membrane of other gram - negative bacteria like *Brucella*(2). Enterobacterial common antigen occurs as two distinct forms immunogenic form and the haptenic form, the imunogenic form is found only in certain rough mutants that possess a complete lipopolysaccharid core structure but

which lack O-specific side chains, the teropolysaccharide chains are covalently linked to the lipopolysaccharid core region (3,4). In contrast, the haptenic form is found in all members of the Enterobacteriaceae, including those organisms that possess the immunogenic form, the heteropolysaccharide chains of the haptenic form are O-glycosidically linked to the phosphate residue of a phosphatidic acid moiety (5) This study was designed in order to:

1. Extraction of Enterobacterial common antigen from *E. coli.*
2. Study the immunogenicity of Enterobacterial common antigen against challenge with virulent *Brucella melitenses* as compared with the Rev-1 vaccine in guinea pigs.

Objective of the study

1. Skin test and ELISA test for detection immune responses (before challenge).
2. Clinical observation and pathological changes in control immunized animal groups (post challenge).

MATERIALS AND METHODS

E.coli l vaccine strain

The standard *E.coli*was obtained from Zoonotic Unit in the College of Veterinary Medicine ,University of Baghdad. Which was confirmed by bacterial isolates by gram stain, biochemical tests, to be sure it was *E.coli* according to (6) .

Brucella melitense challenge strain

The Virulent*Brucella melitenses* was prepared in Zoonotic Unit in the College of Veterinary Medicine, University of Baghdad. After diagnosis of bacterial isolates by gram stain and Modified Ziehl – Nelessenstain (MZN), biochemical tests according to (7) .

Rev-1 vaccine

It was provided from National Project of control on brucellosis and tuberculosis, State Company of veterinary, Ministry of agriculture produce from Syva animal health, Spain .

Experimental design

Experiment I-Dose Selection

In order to obtain the most proper dose of immunization, a study for extraction enterobacterial common antigen (ECA) dose was done. Thirty healthy adult local guinea pigs were fed on commercial assorted pellets, kept in clean and disinfected cages 10 days before the primary dose of immunization and divided randomly into six groups, each group contained 5 guinea pigs, they all injected subcutaneously with 1 ml contained 0.5 mg,1 mg,1.5 mg, 2 mg, 2.5 mg and 3mg of ECA.In this way the safe dose which represented the maximum dose of each common antigen that gave no obvious clinical signs of illness was selected.

Experiment II- immunization study

Twenty of both sexes guinea pigs were divided into four group as following: The first group immunized S/C with 1 ml of ECA contain 2 mg/ml for two doses with 14 days intervals. The second group immunized S/C with 0.5 ml of 1×10^9cfu/ml for two doses with 14 days intervals.The third group (control positive) and fourth group (control

negative) was S/C injected with 1 ml of PBS. After 16 days post immunization, skin test was done first, second and third group for measuring DTHT(skin test) and blood collected and control group to measure antibody titer by ELISA test.After 21days animals of first, second and third group were inoculated I/P with 1 ml of 1×10^6 cfu/ml of virulent *Brucella melitenses* (8), viable bacterial counting was done according to using Miles and Misra,(9)After 25 days animals were scarified then post mortem gross lesion where recorded and specimen pieces from internal organs(liver,heart,lung and kidney), where taken for bacterial isolation after 25 days of post immunization and challenge dose injection, guinea pigs from the control group and the other two immunized groups were killed for postmortem examination and isolation of *Brucellamelitenses* from the internal organs Liver, Heart ,Lung and Kidneyon(10).

Immunological tests

Delayed Type HypersensitivityTest Skin test (DTHT)

ELISA Test

ELISA test was done using a kit produce by SYNBIOTIC France

RESULTS AND DISCUSSION

Enterobacterial common antigen extraction

The total protein concentration of ECA that extracted was 8.2 mg/ml. The result of culturing of the extract was negative for any bacterial contamination.

Dose selection Results

The results of the study first experiment showed on the six groups of guinea pigs showed clinical signs of illness after 7 days that included fever, dullness, decrease appetite, in the 5th and 6thgroups.Two animals in the 6th group were died after 5 days.The others in this group were inapptance for (3 days).No obvious clinical signs of illness was recorded on the fourth group which received a dose 2mg/ml animal (Table 1).

Results of Immunological test

Delayed Type Hypersensitivity Test (Skin test)

All animals in the control group which are not immunized with any antigen did not expose any degree of erythema or induration where as animals in groups that vaccinated with ECA and Rev-1 gave positive reaction after 24 and 48 hours in compared with the control group.The positive reactions represented by redness around the injected area with increasing in skin induration. These alterations differ between each other according to the ability of each antigen to make a reaction. The mean diameter erythema of the first group that vaccinated with ECAwas11.6± 2.608 mm (Table 2) .Whereas it is 9.4±1.673 mm in the second group that vaccinated with Rev-1 vaccine (Table 3) .This is due to the specifity of ECA when examined using the same antigen in skin test.The results of skin erythema after 48 hours appeared in the same picture with an obvious decrease in the values that represented by 6.2 ± 1.789 mm in the first group (Table 2) and 3.6± 2.302mm in the second group (Table 1).The overall result of skin test appeared to agree with the most studies that used different antigens (AL-Zubaidy, 2007).With regard to skin induration all vaccinated groups showed positive results with some differences in their values. The first group showed a mean of 4±1.871mm after 24 hours and 6 ± 2 mm after 48 hours (Table 2). The second group mean was 4.8±0.837 mm after 24 hours and 6

±1.414 mm after 48 hours(Table 3). The differences in erythema in general refereed to the cellular immunity stimulated by the presence of the antigen that led to the accumulation of macrophages and other non-specific inflammatory cells. The differences between the values of the two antigens illustrated the differences related to the ability of each antigen to give immunity (11,12). The higher immune response in the first group that vaccinated by ECA and tested by ECA referred to specifity of this antigen which is the important factor that gives a high skin reaction (13). The high cellular immune responses that appeared in this study may be due to the smooth character of the strains that used which have a higher immunogenicity than rough strains due to their consisting of O-side chain as mentioned (14).

The results of delayed type hypersensitivity of the two vaccinated groups showed the presence of significant differences at $p<0.01$in the first group 24 hours and $p<0.05$ in the 48 hours after the experiment .This difference may be related to the ability of the antigens (Rev-1and ECA) to induce a cellular immunity and the molecular complex of these antigens that led to induce this large immune response (15). The induration of the skin at the site of inoculation of antigen may be due to the accumulation of immune cells like macrophages and other inflammatory cells. This evidence is supported by (12)who explained that in the first exposure of the antigen the phagocytic cells engulf the antigen and present it on MHC–II molecules then proliferation and differnation in memory immune cell and T. cell occur.The skin induration of group two that vaccinated with Rev-1 gave a higher mean than ECA group, this result related to that the Rev-1 antigen contained all types of Brucella antigens but ECA antigen contain antigens that resemble to some outer membrane proteins of brucella(16).

Results of indirect ELISA

The results of indirect ELISA showed differences in the mean of optical density among the three group. These are illustrated in the (Table 4) all animals of the 1st and 2nd groups showed positive result and there is a negative result in the 3th group which is the control group.The mean of the 1stgroup which vaccinated with ECA was higher and recorded 1.805nμ which indicated a higher antibody titer whereas the mean of the 2nd group which vaccinated Rev-1 record a mean of 1.346 nμ. These results indicated a high humoral immune response in the 1st group than that in the 2nd group.These results agree with previous many studies which indicated many differences when using different types of antigens even of the same bacteria (17). The results in the optical density revealed to the antibody titer in each group, according to the kit manufacturer leaflet the higher records in the 1st and 2nd group indicated the existence of protein components that have a high molecular weight with a complex protein molecule that can give a high ratio of a humoral immunity in the serum of the vaccinated animals. These results of skin test in the second group are in agreement with those of (18) who studied the relation between skin test and serological test.

Challenge Experiments

First group (ECA group)

Animals of the first group which vaccinated with ECA showed apparently normal carcass this indicate an immune response against challenge dose that prevent any pathological lesion through of the body

Second group (Rev-1 group)

The results of gross pathological concerning to the second group which vaccinated with Rev-1 showed generalized congestion specially the liver which showed enlargement due to immune response occur by the vaccination with Rev-1 group(8).The bacterial isolation showed low bacterial growth of *Brucella melitenses* in liver and spleen .

Third group (Control group)

With regard to gross pathological lesion the result showed generalized congestion throughout the carcass with whitish spots on the surface of the liver.The liver was very congested and enlarged these changes may related to what mentioned by (19) about the fact that the first organ that affect from these infections the deliver than the infection with spread to make another spots of abscesses in other organs. The bacterial isolation showed positive*Brucella melitenses* isolates from liver, spleen, lung, kidneys and heart with higher number of colonies in liver.

Histopathological Changes

First group (ECA group)

Liver

The mean microscopic feature was characterized by mononuclear cell infiltration in liver parenchyma mainly in portal area and blood vessels consisting of macrophage and lymphocyte(Figure 4).The liver in another section showed vacuolar degeneration of hepatocyte with the appearance of some apoptotic cells associated with proliferation of kupffer cell.

Kidney

The histopathological examination showed inflammatory cell particular macrophage ,neutrophil and lymphocyte aggregation in the wall of papillary ducts (Figure 5).

Second group (Rev-1 group)

Liver

The liver showed proliferation of kupffer cell together with slight mononuclear cells infiltration in dilated sinusoids in addition to hyper atrophy of some hepatic cord (Figure 6).

Kidney

No clear lesions were reported in the kidney(Figure 7).

Third group (Control group)

Liver

showed a large diffuse necrotic areas associated with small granulomatous lesion which included granulomatous lesions consisted from aggregation of macrophage as well as vacuolar degeneration of hepatocyte and proliferation of kupffer cell (Figure 8).More over there was sever dilation and congestion of the sinusoids which led to atrophy of hepatic cord with congestion of the sinusoids and necrotic of hepatocyte and RBC with inflammatory cell particular neutrophil replacement the necrotic area(figure 9).

Kidneys

There was sever hemorrhage in the adrenal gland with vacuolar degeneration of their cell (Figure 10).The pathological lesions in internal organs of the vaccinated groups were correlated with an immune responses indicated by DTH test and this indicated the stimulation of cellular and humeral immunity as a response to the injection of the two antigens.The group that vaccinated with ECA gave an immune response against challenge with *Brucella melitenses* that differ in the degree with that of Rev-1group and showed a result that gave rise to very good immunity. This may be related to the close similarity of some outer membrane proteins of Brucella to outer membrane protein F of *E. coli* (20).Both groups that vaccinated with Rev-1 and ECA showed histopathological changes through all internal organs like congestion and aggregation of phagocytic and other inflammatory cells. The liver was the most affected organ with these changes then lung, kidney and heart.

This may be due to the importance of the liver in maintaining nutritional metabolic balance in the body and this include all nutrient materials.The liver has a big role in elimination of toxins and body waste products, metabolic substances ,moreover the liver gross by portal circulation. These all mean that all poisons metabolites and protein materials cross through liver tissue then go to other parts of the body (21). The reason that leads to accumulation of neutrophils, macrophages and mononuclear cells may be related to the antigens that were injected (Rev-1 and ECA) which have the ability to induce cellular immune response which produce these cells to migrate and localized in liver and other tissues to phagocyte and eliminate these foreign proteins by their enzymes. The presence of foreign body giant cells in the liver of the group that vaccinated with ECA indicated the higher immune response in this group (22).The presence of infiltration neutrophils in liver and lung in vaccinated animals may be due to active production of TNF-α which is a proximal mediator for neutrophic chemotactic factor (23) and neutrophils are essential for host defense (24). Neutrophils also can produce pro-inflammatory mediators such as IL-12 (25)

REFERENCES

1. Bohin, J. P. (2000*).Osmoregulatedperiplasmicglucans in Proteobacteria.* FEMS Microbiol.Lett.186:11-*19.*
2. Verstreate; Creasy;Caveneya;Baldwin;Blab and Winter (1982) .Outer membrane proteins of Brucellaabortus isolation and characterization .Infect .Immun. march vol.35 no.3 979-989.
3. Mayer, H. and Schmidt,G. (1979).Chemistry and biology of the enterobacterial common antigen(ECA). Curr.Top.Microbiol.Immunol., 85:99-153.
4. Ramia, S.; Neter, E. and Brenner, D. (1982).Production of enterobacteria common antigen as an aid to classification of newly identified species of the families Enterobacteriaceae and Vibrionaceae. Int.J.System.Bacteriol 32:395 - 398.
5. Kuhn,HM.; Meier-Dieter, U. and Mayer, H. (1988). ECA, the enterobacterial common antigen. FEMS Microbiol Rev 54:195-222.
6. Quinn, P. J.; Carter, M. E.; Markey, B. and Carter, C. R. (2004).Clinical Veterinary Microbiology. Mosby, Spain.
7. Alton, G. G.; Jones, L. M.; Angus, R. D. and Verger, J. M. (1988).“ Techniques for the Brucellosis laboratory” Institute national de La rechercheagronomique 147, rue de l’ university. 75007.
8. AL-Zubaidy, I. A. (2007). “Study of cellular and humoral immune response to Brucellins extracted from some vaccine strains" PhD. Vet. Med. College /Baghdad University.
9. Miles, A.A.; Misra, S.S. and Irwin, J.O. (1938). The estimation of the bactericidal power of blood .J. Hyg .Camp., 38:739-749.
10. Al-Oubaidy,S.S.A.(2008).Immunopathological study of the cross immunization between *Brucellaabortus* and *Brucellamelitensis* in guinea pigs .Msc .Thesis .Vet .Med .Coll .Bagh .Univ.
11. Bercovich, Z.; Laak, E.A. ter, and Lipzigj, H.H. Van. (1995). Detection of brucellosis in dairy herds after an outbreak of the disease using a delayed-type hypersensitivity test. Prev. Vet. Med., 13:277-285.

12. Kindt, T.J.; Goldsby, R.A. and osborne, B.A. (2007). "Kuby Immunology". 6th Ed. Library of Congress, Publisher, S. Tenney, W.H. Freeman and Company, Printing and Binding , R.R. Donnelley New York, U.S.A.
13. Davis, D.B.; Dulbecco, R.; Eisen, N.H. and Ginsborg, S.H. (1990). Microbiology . Lippincott Company. 4th Ed. pp.539-549.
14. Cheville, N.F.; Stevens, M.G.; Jensen, A.E.; Tatum, F.M. and Halling, S.M. (1994). Immune responses and protection against infection and abortion in cattle experimentally vaccinated with mutant strains of *Brucellaabortus* Am. J. Vet. Res., 54:1591-1597.
15. AL-Tardy, O. J. M; Badeh, M.M;AL-Ratrot, M.A and K.U(2000). Principles of immunology and Blood serum . first edition .Dar AL-Thakfa edition house Jordan
16. AL-Haddad, Z.A.Z.A.(2009)."Immuno pathological Study of *Cryptococcus neoformans* isolated from human and cows' milk in mice" ph D thesis .Vet. Med. college / Baghdad Universit
17. Joklik, W. and Amos, Z. (1984). Microbiology, 8thed Appleton – Century Crofts, Norwalk – Connecticut..
18. Fensterbank, R.; Pardon, P. and Marly, J. (1985).Vaccination of ewes by a single conjunctival administration of *Brucella melitensis* Rev1. Vaccine. Ann. Rech. Vet. 16: 351-356.
19. Cerwenka H.S.(2010). Pyogenic liver abscess :Differences in etiology and treatment in Southeast A sia and Central Europe.WorldJ.Gastroenterol .16(20):2458-2462.
20. Verstreate; Creasy;Caveneya;Baldwin;Blab and Winter (1982) .Outer membrane proteins of *Brucella abortus* isolation and characterization .Infect .Immun. march vol.35 no.3 979-989.
21. Kumar,V.; Mitchell, R.M.; Abbas, A.K. andFausto, N. (2009). Basic Pathology. 8th edition .pathology.bsd.uchicago. edu/faculty/VKumar. html .
22. Tizard, I.R.(2009).Veterinary Immunology : an Introduction 8th ed. Black well scientific . publ :London.UK.
23. Netea, M.G.; VanTits, I.J.; Curfs, J.H.; Amiot, F.; Mers, J.F.;Vandermeer, J.W. and Kullberg, B.J. (1999). Increased susceptibility of tumor necrosis factor-α lymphotoxin-alpha double knockout mice to systemic candidiasis through impaired recruitment of neutrophils and phagocytosis of *Candida albicans*. J. Immunol., 163: 1498-1505.
24. Herring, A.C. and Huffnagle, G.B. (2001).Innate immunity and fungal Infection. In Kaufmann S.H.E. ,spher A., and Ahmed R. (eds).Immunology of Infectious Diseases. American Society for Microbiology, Washington, DC,PP.127-137.
25. Cassatella, M.A. (1995).The production of cytokines by polymorph nuclear neutrophils.Immunol. Today, 16: 21-25

Table 1.Show result of dose selection of ECA(+)observed (-)non observed

Group of animal	Dose	Clinical behavior	Live animal	Dead animal
1	0.5	+	5	-
2	1	-	5	-
3	1.5	-	5	-
4	2	-	-	-
5	2.5	+	-	-
6	3	+	3	2

Table 2. Delayed type hypersensitivity skin test in immunized guinea pigs with ECA group after 24 and 48 hours post Intradermally injection.

Number of Animals	Skin erythema (mm)		Skin induration (mm)	
	24 hrs	48 hrs	24 hrs	48 hrs
1	15	9	4	5
2	11	5	4	7
3	8	5	3	5

4	13	7	2	4
5	11	5	7	9
Mean± SD	11.6± 2.608	6.2 ± 1.789	4 ± 1.871	6 ± 2

Mean of skin induration ± Standard Deviation

Table 3.Delayed type hypersensitivity skin test in immunized guinea pigs with Rev-1 group after 24 and 48 hours post Intradermally injection.

Number of Animals	Skin erythema (mm)		Skin induration (mm)	
	24 hrs	**48 hrs**	**24 hrs**	**48 hrs**
1	8	0	4	6
2	8	5	6	6
3	9	6	5	8
4	10	4	5	6
5	12	3	4	4
Mean ± SD	9.4 ± 1.673	3.6 ± 2.302	4.8 ± 0.837	6 ±1.414

Mean of skin induration± Standard Deviation

Table 4. Results of the optical density (O.D) innμ of ELISA test in the three groups of the experiment

No of animal	(O.D) innμ ECA group	(O.D) innμ Rev-1 group	(O.D) innμ Control group
1	1.909	1.408	0.019
2	1.593	1.331	0.188
3	1.921	1.306	0.092
4	1.800	1.341	0.290
Mean ± SD	1.805±0.151	1.346±0.043	0.147±0.117

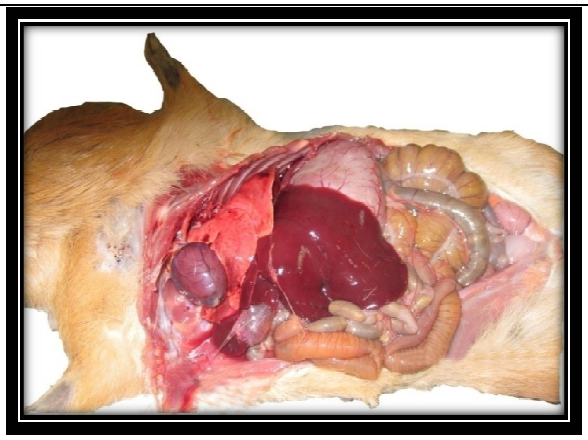

Figure 1.ECA group immunized animal with *E.coli* and infected animal with *Brucella melitenses* showed normal internal organs.

Figure 2.Rev-1 group immunized animal and infected animal with *Brucella melitenses* showed generalized congestion specially the liver which showed enlargement.

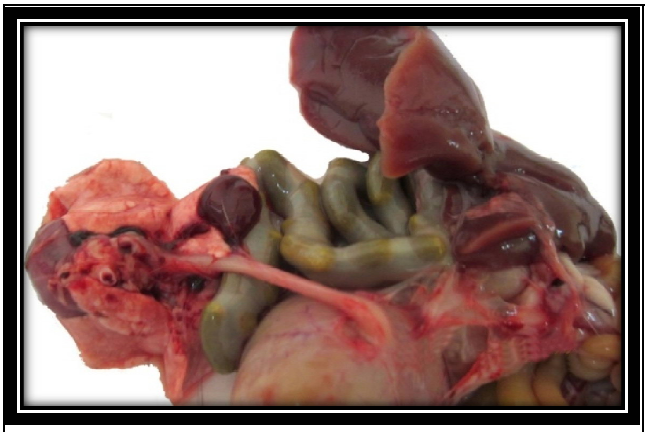

Figure 3. Control group infected animal with *Brucella melitenses* showed generalized congestion throughout all internal organs

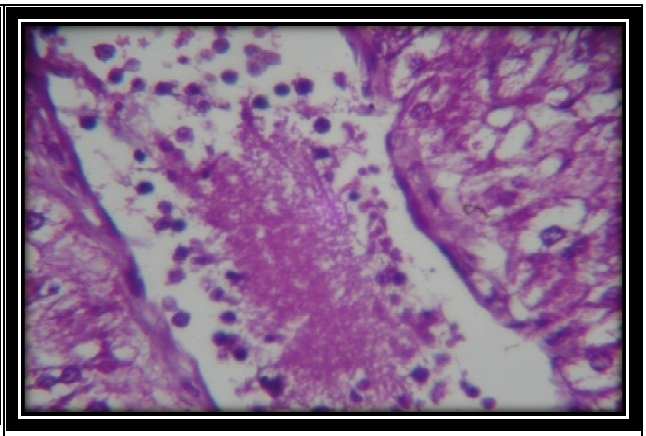

Figure 4. Histopathological section in the liver of immunized animal with ECA at 25 days post-challenge shows mononuclear cell infiltration in liver parenchyma mainly in portal area and blood vessels consisting of macrophage and lymphocyte (H&E stain 40X).

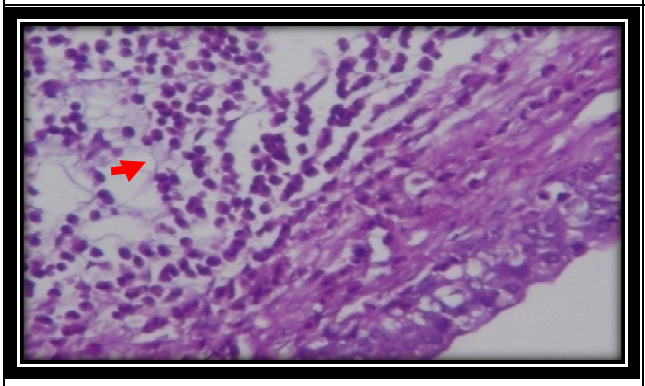

Figure 5. Histopathological section in the kidney immunized animal with ECA at 25 days post-infection showed mononuclear cells infiltration in the wall of papillary ducts (H &E stain40X).

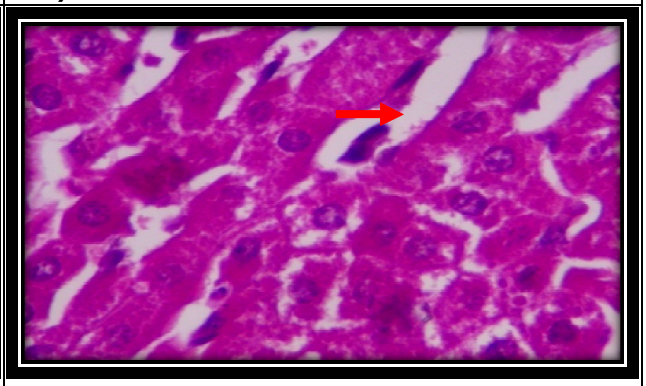

Figure 6. Histopathological section in the liver of immunized animal with Rev-1 at 25 days post - challenge showed proliferation of kupffer cells (H&E stain 40X).

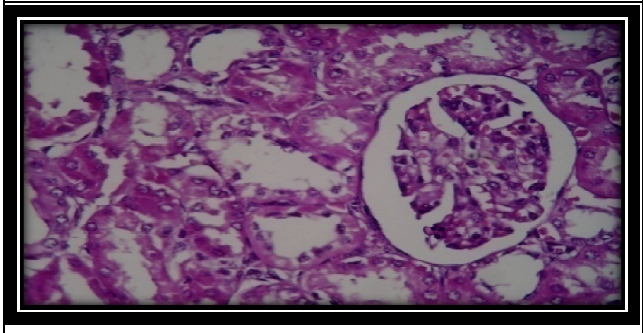

Figure 7. Histopathological section in the kidney of animal immunized with Rev-1 at 25 days post-challenge showed no clear lesions (H&E stain 40X).

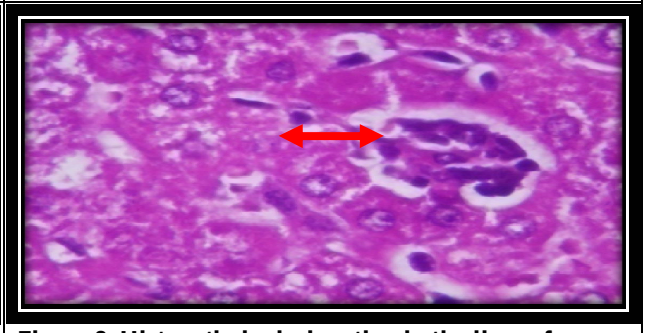

Figure 8. Histopathological section in the liver of non-immunized infected animal showed granulomatous lesion in the liver parenchyma with kupffer cells proliferation (H&E stain 40X).

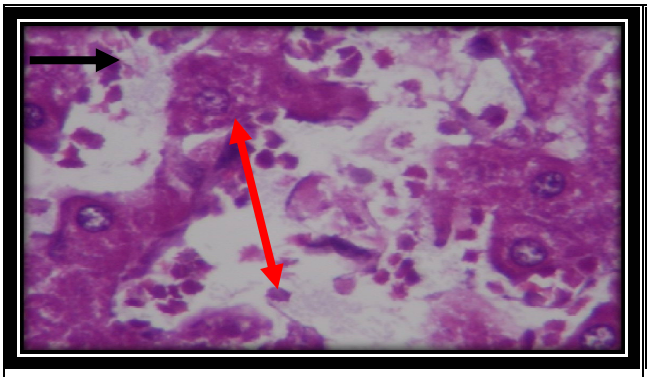

Figure 9. Histopathological section in the liver of non-immunized animal showed sever dilation of sinusoids with necrosis of hepatocytes which replaced by inflammatory cells and RBCs (H&E stain 40X).

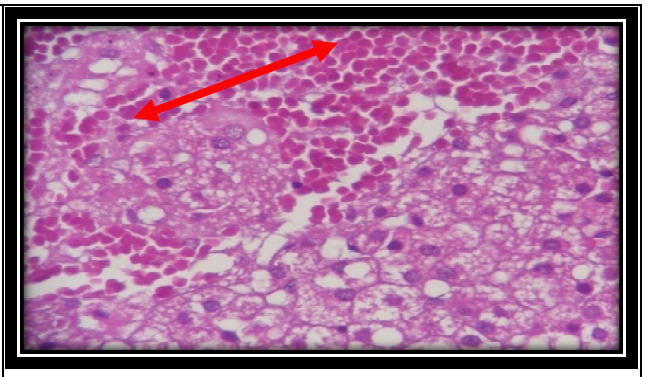

Figure 10. Histopathological section in the adrenal gland of non-immunized animal shows severe hemorrhage (H&E stain 40X).

Indian Journal of Natural Sciences www.tnsroindia.org.in ©IJONS

Vol.9 /Issue 50 /October / 2018 *International Bimonthly* *ISSN: 0976 – 0997*

RESEARCH ARTICLE

The Ability of *Staphyllococcus aureus* antigen to Protect Mice against Challenge with Some Pathogenic Bacteria

Ban Sahib Al-Nasiry*

College of Veterinary Medicine, Unit of Zoonotic Diseases, University of Baghdad, Iraq.

Received: 02 July 2018 Revised: 04 Aug 2018 Accepted: 06 Sep 2018

***Address for Correspondence**
Ban Sahib Al-Nasiry
College of Veterinary Medicine,
Unit of Zoonotic Diseases,
University of Baghdad, Iraq..

ABSTRACT

This study designed to investigate the ability of sonicated *Staphylococcus aureus* Ag in protection against challenge with some gram positive bacteria in mice .the result indicate a high degree of protection represented by positive delayed type hyper sensitivity which reflect cellular immunity . Also the result of positive optical density reflects the humeral immunity moreover this study show no obvious pathological lesion in immunized groups. Isolation of bacteria showed negative results in immunized groups while there are a high number of colonies in non immunized groups.

Keywords:. *Staphylococcus aureus* gram positive bacteria mice

INTRODUCTION

Staphylococcus is a group of bacteria that cause multiple infections. Either direct infection or due to production of toxins .Boils,impetigo,food poisoning, cellulites and toxin shock syndrome are all infections caused by Staphylococcus.(1) Methicillin –resistant *Staphylococcus aureus* which known as MRSA is a type of this bacteria that is resist antibiotic methicillin and other drugs.(2)Cross reactivity between *Staphylococcus aureus* and some other Gram-positive bacteria was obtained using cross immune electrophoresis and rabbit antisera.(3) The aim of this study is to use an antigen prepared from *Staphylococcus aureus*to immunize agianist mice infected experimentally with other important pathogenic bacteria.

MATERIALS AND METHODS

Thirty nine healthy mice of both sexes were used and devided into four groups, 3 groups contain 10 mice .and (1,2,3) immunized with 0.2ml contain 1.3mg whole sonicated staphylococcus antitigen which prepared according to(4).into two doses with 14 days intervals. One group contain 9 mice divided into 3groups 4,5,6 did not immunized (control).

Cellular & humeral immunity were estimated using skin delayed hypersensetivity& ELIZA test respectivly to each group against staph. Peptidoglycain prepared according to(5), at day 27 of the first immunization dose. Challengewasobtained by injection of all 39 mice as fallowed:

1. 1 x 10^{9} CFU \ ml *Listeria monocytogens* for (group.1), &3 mice of group 4
2. 6 x 10^{6} CFU \ ml *Streptococcus pneumona*e for (group.2),&3 mice of group 5
3. 1 x 10^{9}CFU \ ml *Corynbacterium.pyogense* for (group.3),&3 mice of group 6

After 48h.of challenge all animals were euthanized, macroscopicaland microscopicalexamination were done.

RESULTS

All animals of the groups (1,2,3), shows positive skin reaction after 24 &48 h. by presence of increase skin thickness(table 1), while no skin thickness in animal of group 4,5 & 6. The results of indirect Elisa testindicate to positiveoptical densityrecordes in the groups 1,2,3 illustrated in table (2) while negative record was noticed in group 4,5,6. The results of colonies isolation from some internal organs show large numbers of colonies in groups 4,5,6 especially in liver and spleen while very low numbers in groups 1,2 and no any isolats in group 6.Gross examination shows sever congestion of internal organs of animal in groups (4,5&6) especially liver,spleen&kidneys & some whitish spots disseminated on kidney surface. Figure (1)No obvious pathological lesion in animal of groups 1,2,3. All animal groups gave positive reaction after 24 and 48 hours of skin test except group 4,5,6.

The positive reaction represented by presence of increased skin thickness. Our gained skin thickness gave an impression that whole staph. Ag had highest means of thickness diameter this may be related to the high immunological ability caused by this Ag.And have an across immunological activity agaist infection with*Listeria monocytogens, Streptococcus pneumonae & Coryn bacterium pyogense*. In the skin test, residual macrophages in the epidermis pick up the peptidoglycan that enter through the skin and transport into regional lymph nodes, where T-cells are activated by Ags and rapidly differentiate to Th-1 cells, which produce various cytokines and chemokines like IL8, so that macrophages and other cells are activated and attracted to the site of skin test (6).

Groups 1,2,3 gave an immune response with little differences between animal groups these differences related to the ability of wholeStaphylococcus to give cross immunity.In general the results of skin test were relatively high. All smooth strains evolve higher cellular immune response than that of rough strains due to their consisting of O-side chain (7) (8). Group 4,5,6 show sever signs of inflammation accompanied with presence of high number of bacterial colonies due to virulent infections caused by*Listeria monocytogens,Streptococcus pneumona*e &*Coryn bacterium pyogense*, with no anyimmunization that lead to ability of these virulent bacteria to colonies and infect the internal organs.The overall results indicate the ability of Staphyllococcal Ag to produce immunity against*Listeria monocytogens,Streptococcus pneumona*e & *Coryn bacterium pyogense* as a result of the ability of Staphyllococal antigen to induce a cellular immunity and the molecular complex of this antigen that led to induce this large immune response(9).

REFERENCES

1. Klevens RM,Morrison MA,Nadle J, Petits, Gershman K, Ray S, HarisonLH,Lyntield R, DumyatiG,Townes JM, Craig AS, Zell ER, FosheimGE,McDougal LK, Carey RB,FridkinSK (2007). Invasive Methicillin – resistant *Staphylococcus aureus*infections in united State JAMA 298 : 1763- 1771.
2. Park, B.Nizet, V.;Liu,G.Y. (2008). Role of *Staphylococcusaureus*catalase in niche Completitionagainst *Streptococcus Pneumonia* . J.Bact. 190: 2275- 2278.

3. Esmaily, F. and Sharifi- Yazdi(2002). Amodefied method for preparation of *Staphylococcus aureus* peptidoglycan towards making or sub- unit vaccin.Iranian J. Publ. Health. 31, (1-2):37-44.
4. Mitove,I.; Denchen, V. and Linde,K. (1992). Humeral and cell mediated immunity in Mice after immunization with live and vaccins of salmonella typhimurium:Auxotrophic mutants with two attenuating markers. Vacc., 10: 61- 66.
5. AL- Zubaidy, I.H. (2007). Extraction and characterization of different Antigens from Vaccination strains of Brucella. PHD Thesis.College of Vet.Med.Dept.of Med. University of Baghdad.
6. Kindt,T.J.; Goldsby, R.A. and Osbone, B.A.(2007). KubyImmunology 6th Ed. Library Of Congress, publisher, S. Tenney, W.H. Freeman and Campany, printing and Binding, R.R. Donndley New york, USA.
7. Cheville, N.F. ; Steven, M. G.; Jensen, A.E.; Tatum, F.M. and Halling, S.M. (1994). Immune responses and protection against infection and abortion in cattle Experimentally vaccinated with mutant strain of Brucellaabortus. Am. J.Vet. Res.,54: 1591- 1597.
8. Herring, A.C. and Huffnagle, G.B.(2001).Innate immunity and fungal infection. In Kanfmann S.H.E., Spher A., and Ahmed R.(eds). Immunology of infections diseases American society of Microbiology, Washington, DC.PP.127- 137.
9. AL-Tardy, O. J. M; Badeh, M.M;AL-Ratrot, M.A and K.U(2000). Principles of immunology and Blood serum .first edition .Dar AL-Thakfa edition house Jordan.

Table 1. Mean of skin thickness due to delayed type hypersensitivity test after 24 & 48 hours in millimeter of all groups.

Group	Skin induration	
	24 hrs	48 hrs
1	2.5	1.8
2	2.8	1.8
3	2.5	1.9
4	0.4	0.1
5	0.2	0.1
6	0.2	0.1
Mean+-SE		

Table 2. mean of optical density value of all groupsin nanometer at 450 nanometer

Group	Optical density
1	0.941
2	0.952
3	0.878
4	0.013
5	0.026
6	0.041

Table 3. Mean of colony numbers isolated from internal organs

Organ / Group	Spleen	Liver	Heart	Kidney
Mean of immunized group(1)	3	5	0	0
Mean of immunized group(2)	4	1	0	0
Mean of immunized group(3)	0	0	0	0
Mean No.of group 4	40	66	24	28
Mean No.of group 5	36	74	31	23
Mean No.of group 6	42	56	28	22

Figure 1.No obvious pathological lesion in one animal of group 1.

Figure 2. Congestion of internal organs of animal in group's 6especially liver, spleen& kidneys.

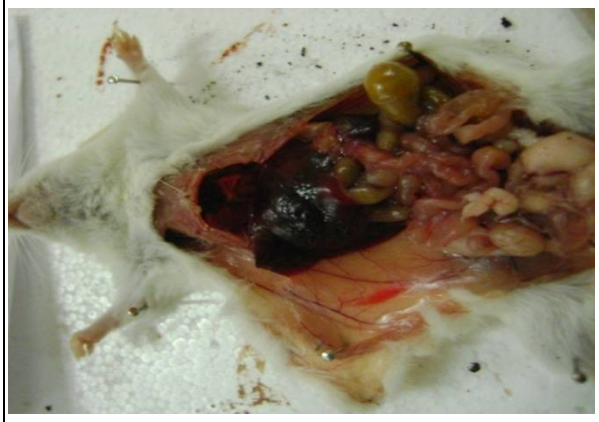

Figure 3. Show sever congestion of liver, spleen and small intestine of one animal of group 5.

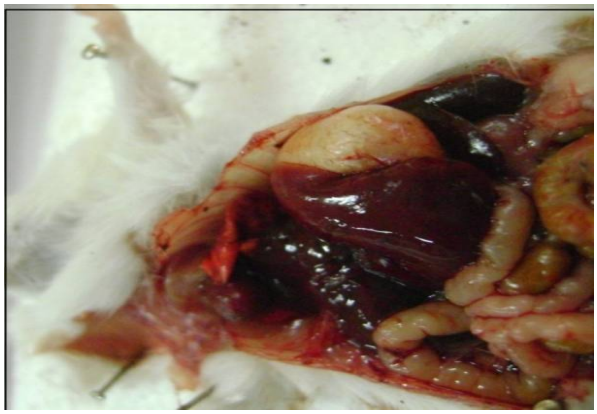

Figure (4) Show sever congestion of all carcass with present of white spots in liver of animal of group 4.

RESEARCH ARTICLE

Study the Effect of the Different Weights of Nano Graphene on Super Capacitor

Hanaa H. Salman[1]* and HarithI.Jaafer[2]

[1]College of Education, University of A1-Qadisiyah, Iraq.
[2]College of Science, University of Baghdad, Iraq.

Received: 05 July 2018 Revised: 08 Aug 2018 Accepted: 10 Sep 2018

***Address for Correspondence**
Hanaa H. Salman
College of Education,
University of A1-Qadisiyah, Iraq.
Email : hanahs7379@gmail .com, harithibrahem@yahoo.

ABSTRACT

In this study ,the electrical properties of super capacitor were investigated using nanomaterial (graphene) as active material , The electrodes were prepared from aluminum plates with dimensions (5×5)cm^2 and covered by Nano graphene material with different weights (0.04,0.06,0.08,0.1,0.2and 0.3)gm.,and phosphoric acid(H_3PO_4) was used with 1M concentration as an electrolyte solution .The capacitor is charged with 3volt ,the method fortesting these super capacitors were including charge – discharge curve. the results showed an increase in the charge current by increasing the weight of graphene ,while the discharge current became stable .There was an improvement in the voltage drop and an increase in storage energy.

Keywords: super capacitor, graphene, EDLC, capacitance, stored energy

INTRODUCTION

Supercapacitors (SCs) a type of important electrochemical energy device, also known as ultra-capacitor or electric double layer capacitors(EDLCs)[1]supercapacitor with very high capacity and a low internal resistance with higher capacitance value than conventional capacitors, marvelous ability to charge and discharge[2], EDLCs operate on principles similar to these of conventional electrostatic capacitors which is contain two conducting electrodes separated by an insulating dielectric materials.EDLC store charge non –faradaic ally or electrostatically, and there is no transfer of charge between electrolyte and electrode in SCs using the electrode/electrolyte interface of a highly porous electrode, because of the properties for supercapacitorsmade it different than other power source such as fuel cells and batteries[3]. Supercapacitorsconsists of three essential components the electrolyte, electrodes and the separator[4]. Electrode must have good conductivity, high temperature stability high surface area per unit mass and volume, high corrosion resistance, other materials used in electrodes such us graphene, carbon nanotubes, conduction polymersetc. In most of supercapacitors, activated carbon coated the electrodes, which is a very porous

substance and high specific surface area, The electrochemical interface between an electrolyte and electrode has long been known to behave like capacitor and thus name "double-layer"[5]. Graphene materials have a larger electrochemical available surface andhigher conductivity, graphene materials an formidable potential to improve the energy density of supercapacitors [16,17] .

Electrolytes are inserted between the two electrodes ,it is electrically conductive.electrolytes used in SCs consist of dissolved chemicals that dissociate into actions and anions and solvent . It is must be, not chemically react with other materials in the SCs, low viscosity, chemically inertthere are two kinds of electrolyte aqueous and organic electrolyte, aqueous electrolyte ha a much smaller resistance and larger power density and organic electrolyte whose ions are bigger, higher resistance and smaller power density [6]. Separators, materials used in separator include, nonwoven porous polymeric films, woven glass fibers and porous woven ceramic fibers, the separator lets the transfer of the charged ions however forbids the electronic contact betweenthe electrodes, generally separator is very thin, very porous to the conducting ions, chemically inert, stability and conductivity[2,7]

.study graphenebased ultra-capacitors,uses aqueous and organic electrolytes .A capacitance as determined from galvanostatic charge/discharge was measured using $C = I\,(dv/dt)$with dv/dt calculated from the slope of the discharge curves.Specific capacitance of 135 and 99F/g in aqueous and organic electrolytes" [8]." study supercapacitorsusing graphene coated paper electrode , two types of contacting materials silver and graphite foil were tested. Also investigatedthe influence of the paper used as separator. aspecific capacitance of up to 100f/g and energy density of 1.27 wh/kg. the energy density can further be increased by using other electrolyte" [9]."Investigated fabrication of supercapacitor using an electrode layer covered with polyaniline layer .The electrochemical measurements were assessed using electrical impedance spectroscopy(EIS) , cyclic voltammetry (cv), , and charge-discharge measurements.The result indicated that graphene/PANIdouble layers exhibited high porosity and large surface area. Specific capacitance as high as 915.78 f/g at scan rate of 5 mv/s in the scanning potential window from -0.8 to 0.8 with 4 mg active material ."[10] .Study the effect and significance of separator thickness of electrochemical double layer capacitors. Various thicknesses of separator are studied is compared with different types of separator, polyethylene separators of high thickness has high capacitance value and low internal resistance value compared to high thicknesses of the same separator at three layer after this ESR increased due to increase in thickness of separator. Also to four layer ,after this the ESR is decreased during increase in thickness of separator [11].

"Study supercapacitor Nano fiber electrodes graphene, in 1M H_2SO_4.Electrodes fabricated from a lower carbon mixture containing PAN and graphene showed the highest capacitances whereas electrodes fabricated from higher carbon mixtures of PAN ,graphene and carbon black had significantly lower capacitance values"[12],and study and supercapacitor, different polymers which are used to form composite materials for supercapacitor applications are reviewed. properties of graphene and polymer composites, graphene and polymers for flexible supercapacitors are also discussed [13]. Flexible paper electrodes for supercapacitors, Graphite was coated on paper with pencil drawing and then electrochemically exfoliated using the cyclic voltammetry (CV) technique to obtain the exfoliated graphite (EG)-coated paper .polypyrrole (PPY)doped with β-naphthalene sulfonate anions was deposited on EG-paper through in situ polymerization , the as-prepared PPY –EG –paper showed a high electrical conductivity of 10.0S.cm-1 and could be directly used a supercapacitors electrodes .The PPY-EG-paper electrodes gave a larger specific capacitance of 2148F.g-1, compared to PPY-graphite-paper (848 F.g-1),the capacitance value of PPY-EG-paper could be preserved by 80.4% after 1000 charge /discharge cycles. The PPY-EG paper electrodes a good rate capability and high energy density of 110.3 Wh.Kg-1at a power density of 121.9 W.Kg-1"[14] .

MATERIALS AND METHODS

1. Graphene Nano powder, manufactured by company sky springnanomaterial's, Inc.., the particle size was:6-8nm and surface area:120-150m^2/g.

2. Commercial Aluminum plates were used of electrodes with thickness (0.99mm) and dimensions (5×5) cm^2.
3. Fibrous texture as separator between electrodes fig.(2).
4. Phosphoric acid with 1M concentration.

Sample Preparation

Two aluminum plates were used based electrode , the end of the plates were punctures with adiameter(3mm), for the purpose of the placing the wires at the ends of the plates as positive and negative electrode and connecting them to the circuit, and The two plates of aluminum are coated with polyurethane epoxy as adhesive and conductive material. A layer of Nano graphene is placed according to the weights (0.04,.0.06,0.08,0.1, 0.2and0.3) gm on the aluminum plates fig(3).anda thin sheet (fibrous texture) as used separator insertedbetween aluminum plates(electrodes) of super capacitor before adhesion together, and infused with electrolyte solution H_3PO_4.and electrodes are then bounded to gather by nylon warp.In this way, the supercapacitors were manufactured to be connected to the circuit for the purpose of conducting tests.The charging and discharging curve was used to calculate the capacitance of manufactured capacitors and thus calculate stored energy.

After connected the capacitor with electric circuit described in the figure (4) switch is closed and charging is capacitor with 3volt for (30min) where the charge is draw by the graph between the V(volt) in the Y-axis and the time (second) in the X-axis, the charging curve appears. After 30 min of charge, and then discharge is capacitor for a period of time 30 min .The charging and discharging process is plotted in one curve as shown in fig.5 This method was used for all sample groups (capacitors) manufactured.

To calculated capacitance by using formula 3-1 where
V1: is 80% of 3V
V2:is 40% of 3 V
T1:Time with voltage V1
T2:Time with voltage V2
I:Discharge current

$$\boldsymbol{C = I\frac{dt}{dv}} \qquad \boldsymbol{Eq(3-1)}$$

Were $\boldsymbol{C}$: capacitance(f).
$\boldsymbol{I}$: discharge current(A).
The stored energy in supercapacitors calculated by multiplying the capacitance $\boldsymbol{C}$ by the voltage v to the power of 2, Eq.3-2

$$\mathbf{E = \frac{1}{2}.c.v^2} \qquad \mathbf{Eq\ (3-2)}$$

RESULTS AND DISCUSSION

Many parameter will effect on electrical properties for supercapacitors (SCs), one of these was the mass of active materials which influence on results. The applied volt which used to be charge the(SCs) was3 volt, the supercapacitors have electrodes(aluminum) and the electrolyte solution is phosphoric acid(H_3PO_4) and separator as shows in the fig .2 The electrolyte solution is placed on the separator between electrodes and when connecting the supercapacitor with electrical circuit, we charged the capacitor with 3volt, the current will be moves between two electrodes and will lead to decay of the electrolyte solution(H_3PO_4) to (H^+) and (PO^-) ions .The positive ions(H^+) will transfer to negative electrode and the negative ions (PO^-)) will transferto positive electrode, and these ions will stay at that surface of active material(graphene).The increasing in active materials will effect on properties for (SCs),it was

observed that, when the ratio for (graphene) increased(table 1), the charging current(I_{ch}) will increase dueto the increased surface area of the electrode with presence of graphene.i. e the nanoparticles will spread on the surface of the electrode will increase the effective area which associated(adjacent) with electrolyte solution. This leads to direct contact points with the ions which dissolved in the solution. For the discharge current (I_{dch}), it was found(table 1) that the current is constant except at the value of mass ratio(0.08,0.3). the constant current maybe due to the large amount of ions stay on the electrode.The variable in current at the mass ratio (0.08,0.3)gm. for graphene were(0.15,0.13)mA. its maybe to the internal impudence.For the drop voltage(V_{drop}), the presence of voltage after the charging process and before the closure of the circuit depends on the number of ions accumulated on the electrode . The voltage drop, it was found the increase in ratio for graphene will decrease the voltage drop.

To explain this phenomenon, the increased of active materials will increased the surface area of electrodes so that a lot of positive and negative ions will lay on the electrodes. The accumulated of ions will lead the voltage for each electrode constant. At discharge process , the ions will moves and re-bonding ,so that the voltage drop will decrease. From (table 1) the capacitance for SCs will increase with increase of weight ratio for graphene due to the large surface area of graphene. This lead to increase the stored energy.

REFERENCES

1. P.Mandake,P.karandikar,"signifance of separator thickness for supercapacitor", (IJRASET), 2016, issue II,Vol.4
2. S.Chauhan, "graphene oxide/pdyanilinecompsite as electrode material for supercapacitors", journal of chemical and pharamaceutical research, 2017,p p.285-291.
3. J .Triqueiro, R.Borges, R.lavall, h. Calado, and G. Silva, "polymeric Nano materials as electrolyte and electrodes in supercapacitors" ,2009,p p.733-739
4. T. Chen & l. Dai,"carbon Nano materials for high-performance supercapacitors", centerof advanced science and engineering for carbon, 2013, vol.16 no.718.
5. F .lufrano, p.Staiti, "Mesoporous carbon materials as electrodes for electrochemical supercapacitors", int.j.electrochem sci., 2010,pp.903-916.
6. Y.Zhang, l.wei,X.Shen, H.liang, "study of supercapacitor in the application of power electronics", 2009,issue 6, vol.8.
7. A .Shneuwly and R.Gallay, "properties and applications of supercapacitors from the state-of-the-art to future trends", proceeding pcim 2000.
8. M.Stoller,S.park, Y .Zhu, J.An, and R.Ruoff, graphene-based ultracapacitors", Nano letters , 2008, vol.8, no.10, pp.3498-3502.
9. B. Andres ,S. Forsberg ,A.Vilches,R.Zhang,H.Andersson, M .Hummelgard,J.Back , and H. Olin, "supercapacitors with graphene coated paper electrodes".Nordic Pulp paper Research 2012,Vol.27,no.2
10. M .Tayel, M.Soliman, and M.Harb, "fabrication of supercapacitor based and graphene and polyaniline for energy storge applications", international journal of advanced research in electrical , electronics and instrumentation enginerring", 2015, vol.4, issue 10.
11. P.Mandake, P.Karandikar,"Significance of Separator Thickness for Super capacitor",(IJRASET),2016,Vol. 4,issue II.
12. M .Mustafa and A.Zdunek,"supercapacitornanofiber electrodes graphene-based', int.j.electrrochem. sci, 2017, pp.2917-2932.
13. Y.Gao,"graphene and polymer composites for supercapacitor Applications :AReview",Gao Nanoscale research letters,2017.
14. L.Huang ,W.Ra,L.Fan,J,Xu,Z.Bai,W.Xu,and H.Bao,"Paper Electrodes Coated With Partially-Performance Flexible Supercapacitors",Journal/Polymers,2018
15. S Ban, J.Zhang, L. Zhang, K.Tsay, D. Song and X.Zou, "charging and discharging electrochemical supercapacitors in the presence of both parallel leakage process and electrochemical decomposition of sovlentt", acta 90 ,2013, pp. 542-549.

16. Hayes, R.; Warr, G.G.; Atkin, R. Structure and nanostructure in ionic liquids. Chem. Rev. 2015, 115,6357–6426.
17. P .Lu ,Q. Dai, L. Wu and X. Liu ,"Structure and Capacitance of Electrical Double Layers at the Graphene–Ionic Liquid Interface", applied sciences, 2017, 7, 939

Table 1. shows electrical properties of SCs with different weights of active materials (nano-graphene)

Material(graphene)gm.	I_{ch} mA	I_{dch} mA	V_{drop}	C(farad)	E(stored energy)Wh
0.04	1.03	0.16	1.5	0.007	28.8
0.06	2.2	0.16	1.25	0.013	68.4
0.08	2.8	0.15	1.09	0.0176	126
0.1	6	0.16	1.25	0.0177	108
0.2	6	0.16	1	0.02	144
0.3	8.7	0.13	0.6	0.0270	2520

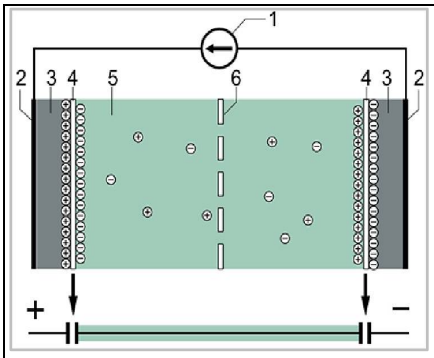

Figure 1. Atypical supercapacitor: 1) Power source 2) collector 3) polarized electrode 4) Helmholtz double layer.5) electrolyte having positive and negative ions 6) separator

Figure 2. Fibrous texture as separator in supercapactiors.

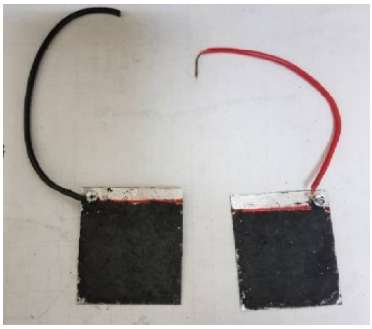

Figure 3. electrode in supercapactor

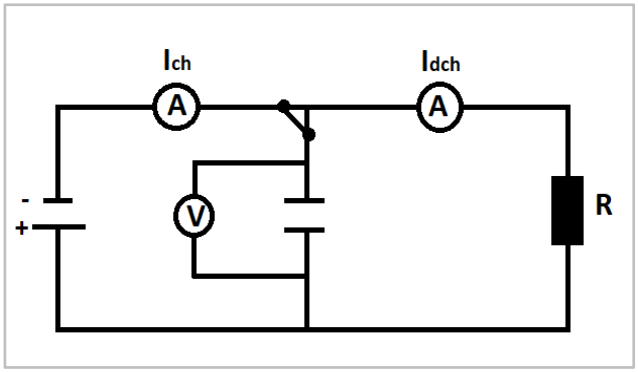

Figure 4: Charge and discharge circuit diagram[15]

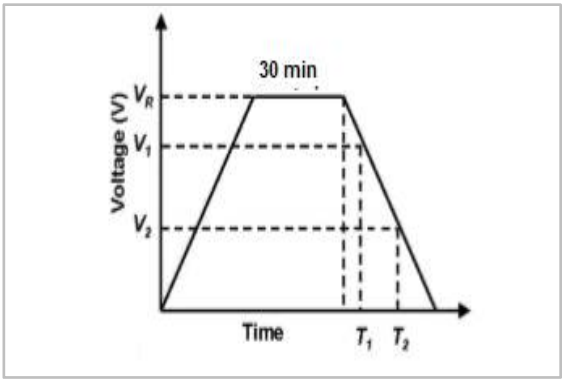

Figure 5 :charge and discharge curve

Indian Journal of Natural Sciences www.tnsroindia.org.in ©IJONS

Vol.9 /Issue 50 /October / 2018 *International Bimonthly* *ISSN: 0976 – 0997*

RESEARCH ARTICLE

Structural and Electrical Properties of Pure Lithium Nickel Oxide Composite as Cathode Materials for Rechargeable Batteries

Hind Mohammed Hasan* and Zainab Raheem Muslim

Department of Physics, College of Science, University of Baghdad, Iraq.

Received: 04 July 2018 Revised: 07 Aug 2018 Accepted: 10 Sep 2018

***Address for Correspondence**
Hind Mohammed Hasan
Department of Physics,
College of Science,
University of Baghdad, Iraq.
Email : hindmoh_1990@ yahoo.com

ABSTRACT

Lithium nickel oxide with layered structure have been successfully prepared by sol-gel method with a new precursor agents. The structure, morphology electrical and dielectric properties which includes σac and σdc were characterized by X-ray diffraction (XRD), atomic force microscopy (AFM) and LCR electrometer IA(impedance analyzer) The XRD structural properties show that $LiNiO_2$ have layered oxide .The AFM results shows that $LiNiO_2$ grains are up to around 73.66 nm in diameter. The σac is found to increase with the increasing frequency. It is observed that the C value decrease with the increasing frequency. The values of the ε' and ε'' are found to decrease with the increasing frequency. σdc is found to decrease with increasing temperature.

Keywords: Lithium nickel oxide; Lithium ion battery; Cathode material; Powder fabrication, Composites.

INTRODUCTION

In recent years, lithium ion batteries have been considering as one of the important power sources for energy storage, electric vehicles and hybrid electric vehicles [1]. For several years lithium nickel oxide is very much known for its electro chromicity, where protons serve as the guest, intercalating into the nickel oxide host structure at a lower voltage. Possibly, this compound might have been the origin of $LiNiO_2$, wherein the Li^+ ion exchange occurs at a voltage as high as 4V [2,3].Nickel compounds find application as electrode materials in battery systems, for instance, in the form of NiO(OH) in Ni–Cd and Ni–MH batteries[4]. $LiMO_2$ (M = Co, Ni) materials exhibit excellent electrochemical features as cathodes in lithium batteries. Particularly, $LiNiO_2$ offers some significant advantages such as it is cheaper and exhibit a higher specific capacity [5]. Despite the fact that materials based on sulfides and oxides are known to be viable cathodes, oxides are only considered to be the preferred materials that can be synthesized and employed as cathode materials in an extensive range of lithium battery applications [6].Since cathode materials for

lithium ion batteries have lower capacity compared with anode materials and it has a high free energy of reaction with the lithium the overall electrochemical performance of lithium –ion batteries is significantly determined by the properties of the cathode materials [7,8]. In this work, lithium nickel oxide as cathode material for lithium ion batteries was prepared by sol-gel method by new precursor agents. The structural and electrical properties for lithium nickel oxide are reported

MATERIALS AND METHODS

Preparation of lithium nickel oxide ($LiNiO_2$)

$LiNiO_2$ composite were prepared using sol gel method. Stoichiometric weighs (1:1:1) of $LiNO_3$, Ni $(CH_3COO)_2 . 4H_2O$, and citric acid were dissolved in (60ml) deionized water which were used as precursor agents. The mixture were heated under stirring at (70-80) °C for several hours, which made the mixture denser and formed the gel. The gels were heated at (100) °C in air for 8hours so that all the distilled water gets evaporated .The dried gel were calcined in air at (750) °C for2hours . After calcination, the powder was ground and remade to a pellet. The crystalline phase of the sample was performed using SHIMADZU (XRD-6000) diffractometer Japanese –made with cu $k\alpha$ radiation ($k\alpha$=1.5405A°).The morphology of the sample was characterized under an atomic force microscope AA3000 scanning probe microscopy by Angstrom Advanced Inc (USA). The measurement of Ac-electrical conductivity σAc , and its variation with frequency was carried out using a LCR electrometer IA(impedance analyzer) (2494A Aglient) over a frequency range (50 Hz -5MHz). The samples of (1.4cm) in diameter and (0.2cm) in thickness for a shape of a pellet were employed for this study. The electrical conductivity has been measured as a function of temperature for a pellet over the range (T =293-423) K by using the electrical circuit. The measurements have been done using sensitive digital electrometer type keithley (616) and electrical oven.The production powder are shown in Fig (1). A block diagram for preparation of powders using sol-gel method, was shown in Fig (2)

Structural properties

X-ray diffraction analysis

The x-ray diffraction spectra for lithium nickel oxide $LiNiO_2$ synthesis by sol-gel method are reported in Fig (3). The x-ray spectra indicate the formation of hexagonal layered structure $LiNiO_2$ with space group (R3m) (JCPDS NO. 9-63). The main peaks at 36.69°, 38.26°, 44.37°,49.36°.59.2°64.12°and 76.94° corresponding to (101), (012), (104), (015), (107), (018) and (021) indicates the formation of pure $LiNiO_2$, which mean there is no impurity phases .

Atomic force microscopy analysis

Atomic force microscopy (AFM) micrograph of $LiNiO_2$ is shown in Fig (4), It can be seen in Fig (4) that samples are consist of regular spherical shape and the grain

Electrical properties

AC conductivity (σa.c)

The variation of AC electrical conductivity as a function of frequency over frequency range 50Hz to 5MHz at room temperature for $LiNiO_2$ is shown in Fig (5). It obviously that $\sigma_{a.c}(\omega)$ increase with increasing frequency. Thus, a.c. conductivity, derived from the classical point of view, implies that the conductivity of a material increases when a large number of free electrons exist and the relaxation time τ, i.e. the average time between collisions, is long. The

conductivity in these crystalline compounds is due to the mobile ions hopping among energetically favorable sites in the surrounding potential. The motion of the surrounding ions simply provides the activation energy for mobile ions to move through channels in the crystalline framework. The exponent 's' is the frequency exponent which represents the degree of interaction between mobiles ions and the environments surrounding them ($0<s<1$) . The value of s is found to be 0.741 which corresponding to hopping correlated model (C.H.B) [9].Distribution over the surface which seem to be uniform.The average grain size was found to be 73.66nm which indicate a nanostructure dimension for the samples. The average roughnesses were found to be 0.765nm.

Capacitance dependent frequency

The variation of capacitance with angular frequency at room temperature for $LiNiO_2$ is shown in Fig (6). At low frequency there is a sharp decrease of capacitance with increasing frequency, this can be appropriately explained on the basis of decreasing in space charge region at the electrodes. At high frequency region, there is a slight decrease of capacitance, this can be attributed to the partially blocked charge carriers near the electrodes.

Dielectric properties

The variation of real (ε') and imaginary parts(ε'') of dielectric constant as a function of frequency (50 Hz to 5 MHz) at room temperature for$LiNiO_2$ are shown in Fig(7) and Fig(8). The decrease in ε' and ε'' with the increasing frequency is explained by the fact that as the frequency is raised, the interfacial dipoles have less time to orient themselves in the direction of the alternating field. As the frequency increases, charges can no longer follow the field and their contribution to the dielectric constant ceases [10].The dielectric constant was calculated from the measured value of C (farad) in the range of frequency (50Hz-5MHz). It is seen in Fig (8) that the dielectric loss decreases with increase of frequency and attains constant value at higher frequencies. The mechanism in low frequency is polarization process, while in high frequency the ion cannot oscillate as quickly.

DC conductivity

Variation of dc conductivity (σdc) with inverse of absolute temperature for $LiNiO_2$ is shown in Fig (9).The curve show two linear regions with different activation energy in low and high temperature region. This indicates it has multiple activation processes in different temperature regions. The change of slope of conductivity graph indicates a change from trapped to mobile carriers with increase in temperature. The values of activation energies (Ea_1), (Ea_2) was calculated from the straight line fitting of plots. The values of activation energies (Ea_1), (Ea_2) and D.C conductivity at room temperature for $LiNiO_2$is listed in Table (1).

CONCLUSIONS

Lithium nickel oxide with layered structure have been successfully prepared by sol-gel method with new precursor agents. XRD pattern confirmed the formation of pure $LiNiO_2$ with no impurity phases. AFM result indicate that $LiNiO_2$ is in the nanostructure dimension. $\sigma_{a.c}(\omega)$ was found to increase with increasing frequency, which is mean that a large number of free electrons exist and the relaxation time τ, i.e. the average time between collisions, is long. The decrease in ε' and ε'' with the increasing frequency is explained by the fact that as the frequency is raised, the interfacial dipoles have less time to orient themselves in the direction of the alternating field. As the frequency increases, charges can no longer follow the field and their contribution to the dielectric constant ceases. The result of

σdc show that there is two different activation energy in low and high temperature region. And this result indicate that the sample is polycrystalline.

REFERENCES

1. A.K. Padhi, K.S. Nanjundaswamy, J.B. Goodenough. "Phospho-olivines as positive electrode materials for rechargeable lithium batteries" Journal of The Electrochemical Society. 144(1997) ,1188–1194.
2. P. Kalyani, N. Kalaiselvi"Various aspects of $LiNiO_2$ chemistry: A review" Science and Technology of Advanced Materials 6 (2005) ,689–703.
3. H. .R. Shaaria and Sethuprakhashb . "Review of Electrochemical Performance of $LiNiO_2$ and Their Derivatives as Cathode Material for Lithium-ion Batteries" Jurnal Teknologi (Sciences & Engineering) 70:1 (2014), 7–13.
4. A.J. Salkind" Capacity of layered cathode materials for lithium-ion batteries—a theoretical study, in: A.J. Salkind (Ed.), Proceedings of the Symphosium on History of Battery Technology"Pennington, NY, 1987, 87–114.
5. Y. Zhang and Ch.Wang "Cycle-Life Characterization of Automotive Lithium-Ion Batteries with $LiNiO_2$ Cathode "Journal of the electrochemical society .156;7, (2009)A527-535,.
6. Tsuyoshi Sasaki, Takamasa Nonaka, Hideaki Oka, Chikaaki Okuda, Yuichi Itou, Yasuhito Kondo, Yoji Takeuchi, Yoshio Ukyo, and Shunsuke Muto"Capacity- fading mechanisms of $LiNiO_2$-based lithium-ion batteries I. analysis by electrochemical and spectroscopic examination" J. Electrochemical Society. 156; 4, (2009)A289- A293.
7. Zaiping Gua"Investigation on cathode materials for lithium ion batteries", PhD. University of Wollongong, 2003. Available from: University of Wollongong Research online.
8. H .Tavassol, J. W .Buthker, G. A .Ferguson, L. A .Curtiss, A.A.Gewirth. Journal of .Electrochemical Society. 159,(2012), A730.
9. Hannachi. N, I. Chaabane, K. Guidara, A. Bulou and F. Hlel, . AC electrical Properties and dielectric relaxation singlecrystal. Materials of $[N(C_3H_7)_4]_2Cd_2Cl_6$ Science and Engineering: B. 172 ;(2010) ,24-32.
10. Mahato. D. K, Alo Dutta and T. P. Sinha, "Dielectric relaxation and ac conductivity of double perovskite oxide Ho_2ZnZrO_6", Physica B. 406, (2011), 2703- 2708.

Table 1. DC activation energies, their ranges and conductivity at room temperature for $LiNPO_2$

Sample	Ea1 (eV)	Range (K)	Ea2 (eV)	Range (K)	σRT ($\Omega^{-1}.cm^{-1}$)
$LiNiO_2$	0.067	289-323	0.109	323-423	6.25E+01

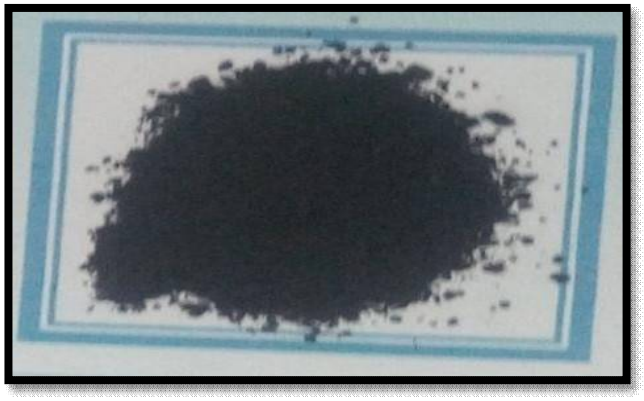

Figure 1. .Final powders of $LiNiO_2$

Figure 2. A block diagram for preparation of powder by sol-gel method.

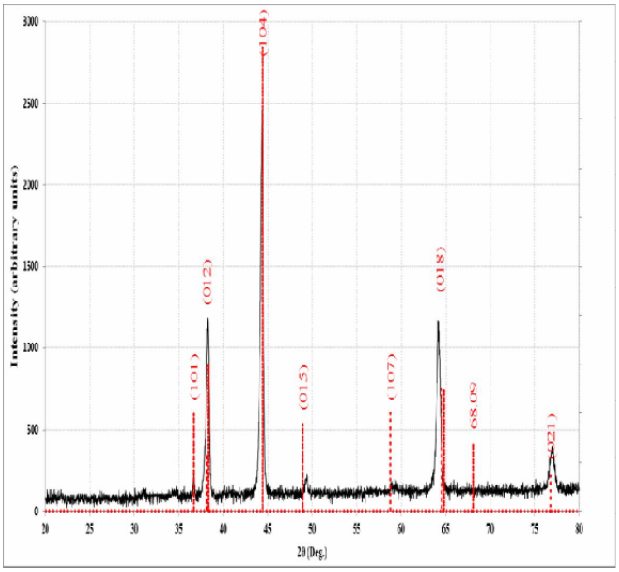

Figure 3. X-ray diffraction spectra of $LiNiO_2$

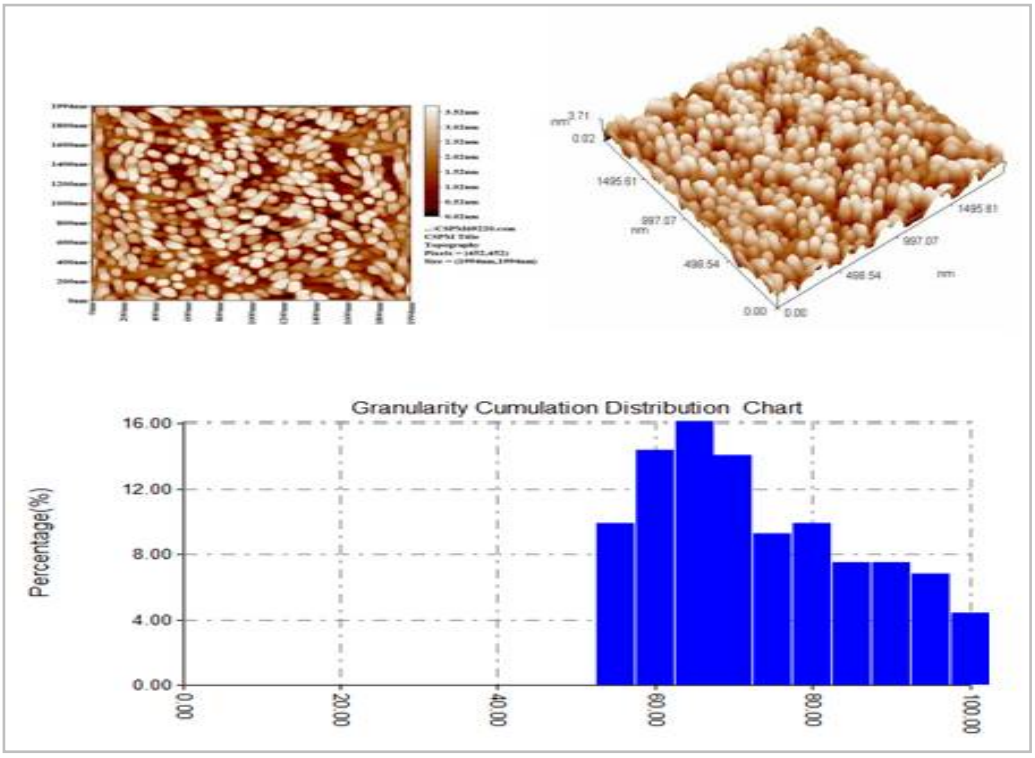

Figure 4. AFM micrograph for $LiNiO_2$

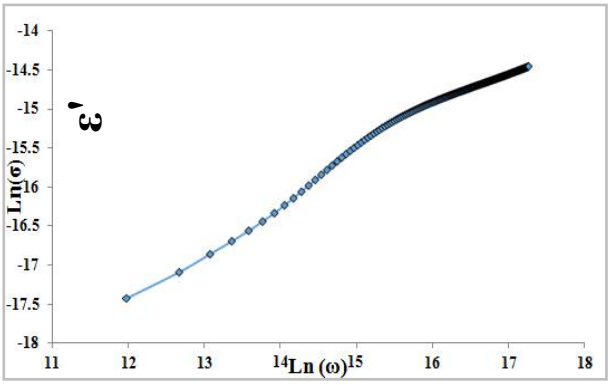

Figure 5. Variation of AC conductivity with frequency for $LiNiO_2$.

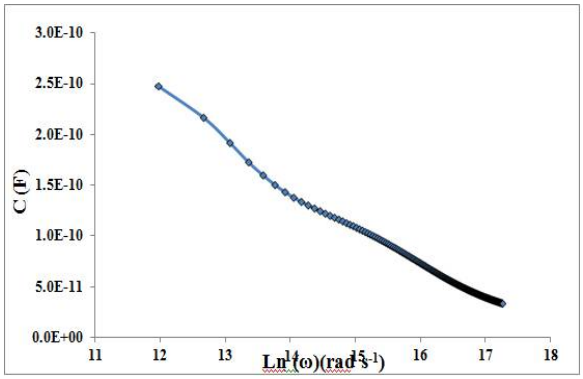

Figure 6. Variation of capacitance (C) frequency for $LiNiO_2$.

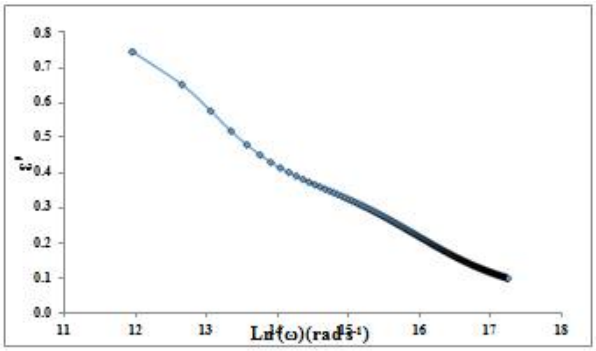

Figure 7. Variation of real part (ε') of dielectric constant with frequency for $LiNiO_2$

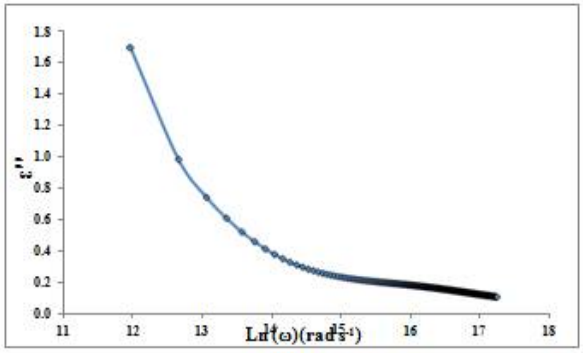

Figure 8. Variation of imaginary part (ε'') of Dielectric loss with frequency or $LiNiO_2$

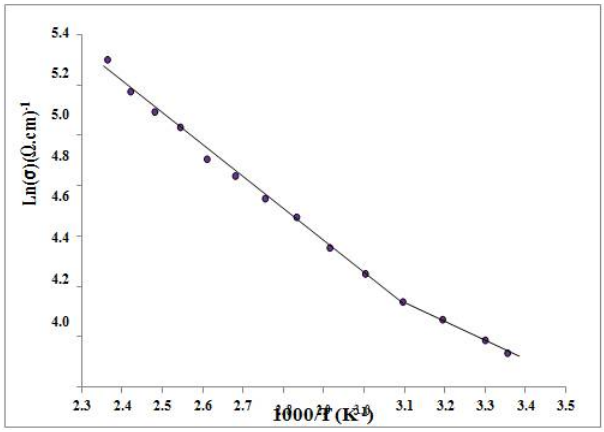

Figure 9. Variation of Ln (σ) with reciprocal temperature for $LiNiO_2$

Indian Journal of Natural Sciences www.tnsroindia.org.in ©IJONS

Vol.9 /Issue 50 /October / 2018 *International Bimonthly* *ISSN: 0976 – 0997*

RESEARCH ARTICLE

Structure, Optical and Sensing Properties of Nanocrystalline (β-Ga_2O_3) Thin Films Prepared by Pulse Laser Deposition (PLD) Technique

Mohaimen M. Khalaf[1]*, Asmiet Ramizy[2], and Kadhim A. Aadim[3]

[1]Ministry of Education, Direction of Education in Al-Anbar, Iraq.
[2]Department of Physics, College of Science, University of Anbar, Anbar, Iraq
[3]Department of Physics, college of Science, University of Baghdad, Baghdad, Iraq

Received: 02 July 2018 Revised: 05 Aug 2018 Accepted: 10 Sep 2018

*Address for Correspondence
Mohaimen M. Khalaf
Ministry of Education,
Direction of Education in Al-Anbar, Iraq.

ABSTRACT

Beta gallium oxide thin films were prepared using pulse laser deposition technique using Nd-YAG laser source (λ=1064 nm, pulse width=10 ns, f=6 Hz, P=600 mj) at different number of pulses. Structural, morphological and optical properties were investigated in terms of X-ray diffraction, atomic force microscopy and optical transmittance. An (XRD) result showed that all films have a polycrystalline structure. As the number of pulses increases, an (AFM) result indicates that the grain size and roughness was increased accordingly. It has been found that the band gap of (β-Ga_2O_3) thin films decreased from 4.92 to 4.40 ev when the number of pulses increased from 400 to 700 pulse. We analyzed the effects of the preparation conditions on the (NO2) sensor performances (as sensitivity, recovery/response time) of (β-Ga_2O_3) sensors at different temperature. The results showed that the films had a good sensitivity even at room temperature, and that the highest sensitivity was (150.4202 %) at (200 ^oC).

Keywords; Beta gallium oxide ; Nanocrystalline; Pulse Laser Deposition.

INTRODUCTION

Gallium oxide (Ga_2O_3) were belongs to a family of Transparent Semiconducting Oxides (TSO). Historically, gallium oxide dates back to (1875) when newly discovered element gallium and described its com+pounds. Although gallium oxide has been known for many decades, it has remained on the margins of mainstream research, where scientific research of gallium oxide has intensified significantly over the past decade. Where research and applications based on gallium oxide have been developed [1]. The (Ga_2O_3) material has five phases, α- , β- , γ- , δ- and ε-. Among these, the (β-Ga_2O_3) phase with the monoclinic system has more chemical and structural stability than the other phases. It is considered one of the most promising materials, with a wide bandgap of (4.9 ev) and melting point at (1780 ^oC) [2,3]. Furthermore, (β-Ga_2O_3) contains many super-characteristics, which can be applied in electroluminescent devices, gas sensors at room temperature and hotter, solar-blind ultraviolet (UV) detectors, field-effect transistors, and insulating

tunnel barriers. Several methods for the growth of (β-Ga_2O_3) thin films have been reported, such as: pulse laser deposition (PLD), molecular beam epitaxy, sputtering, thermal evaporation, and metal organic chemical vapor deposition [3,4]. (PLD) has many advantage such as: short experiment period, high deposition rate, and low substrate temperature, [5].In this work, (β-Ga_2O_3) films grown by pulse laser deposition (PLD) on glass substrate at various number of pulses were investigated by X-Ray diffraction (XRD), atomic force microscope (AFM) and spectrophotometer measurements. And study the sensing properties for gas sensor at various operating temperature

MATERIALS AND METHODS

(β-Ga_2O_3) films were prepared on glass substrate by PLD technique, showed in fig. 1, using a Nd-YAG laser source (λ=1064 nm, pulse width=10 ns, f=6 Hz, P=600 mj). Before to deposition, the Glass slides were cleaned using distilled water in the ultrasonic device for (30 min), and using ethanol alcohol for (30 min), and then blown dry with air before they were introduced in deposition chamber. Facing the substrate, (β-Ga_2O_3) with purity of (99.999 %) were set as the target. And the distance between substrate and target was about (3 cm), the laser energy for deposition was (600 mj). So that the pressure value inside the discharge chamber is (2.5×10^{-2} mbar) for the purpose of contributing to ionizing the target material. Then it annealing the films to (500 ^oC) for (2 h). After deposition, the structural properties of films were measured by conventional X-Ray diffraction (XRD) using a radiation source (Cu-kα). The surface topography and roughness were examined by atomic force microscopy (AFM). The optical properties were studied by spectrophotometer. The (NO_2) properties of (β-Ga_2O_3)/PS films were measured in the device shown in Fig. 2.

RESULTS AND DISCUSSION

Fig. 3 shows the (XRD) patterns of (β-Ga_2O_3) thin films deposited on glass substrates with a different number of laser pulses. We note that all films have a polycrystalline structure. These patterns show peaks centered at 2θ = (30.1° , 30.42° , 31.74° , 35.23° , 38.46° , 64.77°) which corresponds to (400 , 40-1 , 002 , 111 , 31-1 , 512) planes, these value exhibit a good agreement with (JCPDS No. 96-200-4988) card. However, when the number of pulses increased, the intensity of the peaks and their grain size increases accordingly, as shown in the table 1. The average grain size was estimated by Scherrer's equation [6]:

$$D = 0.9 \lambda / (\beta \cos \theta) \quad \ldots\ldots(1)$$

Where: D, λ , β and θ are the average crystalline size, wavelength of X-ray radiation , full width at half maximum (FWHM) of peak diffraction, Bragg diffraction angle.Fig. 4 indicates to the three dimension (3D) AFM images of gallium oxide films at different number of laser pulses. The AFM results showed an increase in grain size with the laser pulse increased, which corresponded with (XRD) results, and indicated to increase roughness as the laser pulse increased, this is due to the grain size enlarged [6].Fig. 5 shows the transmittance spectra as a function of wavelength. It clears that when number of laser pulse increase, the transmittance decrease accordingly, as shown in the table 1. This occurs due to the increase in the thickness of the film with the increase number of pulses, which leads to higher absorption [7]. Using Tauc's relation to direct transitions, (β-Ga_2O_3) optical band gap was estimated graphically [8]:

$$(\alpha h\upsilon) = B(h\upsilon - E_g)^{1/2} \quad \ldots\ldots(2)$$

Where: (α) is the absorption coefficient, ($h\upsilon$) the energy of incident photon, (B) constant, (Eg) the bandgap. From fig. 5 noted that the energy gap decreases by increasing the number of pulses, which was explained by the increase in particle size [9] and because of the increase in film thickness [10].Fig. 7 indicates to the variation in resistance with time for (β-Ga_2O_3)/PS thin films at different operating temperature (35,100,200) ^oC towards (NO_2) gas. When gas (NO_2) was introduced into the chamber, resistance of the films increases because of oxidizing behavior of (NO_2) gas. On the (Ga_2O_3) surface, (NO_2) gas reacts with (Ga) sites and captures electrons, this leads to a decrease in

conductivity and thus increased films resistance[11]. Table 1 shows the calculated values of sensitivity, response time and recovery time for (β-Ga_2O_3) films, which are deposited on substrates of porous silicon and under the influence of (NO_2). We note that the value of sensitivity increases with increasing temperatures, this increasing may refers to the saturation of the conduction band with electrons elevation from shallow donor levels caused by oxygen vacancies, where the adsorption process at high temperatures are occur on the surface of (Ga_2O_3)[12]. The highest value for sensitivity was (150.4242%) at the operating temperature (200 ° C), which is called the optimum temperature.Fig. 8 shows the relationship of response time and recover time with temperature. The greatest sensitivity was obtained in response time (14.1 s), recover time (23.4 seconds) through operating temperature (200 ° C).

CONCLUSIONS

In this paper, (β-Ga_2O_3) thin films are prepared by PLD technique. Structural, morphological, optical and sensing properties were studied. An (XRD) result indicates that all films have a polycrystalline structure, and the intensity of the peaks and their particle size increases with the number of laser pulses increased. (AFM) results indicate that grain size and roughness increases as the number of pulses. The optical properties show an increase in the energy gap by increasing the number of pulses. The (NO_2) sensing characteristics were studied for (β-Ga_2O_3)/PS at different operating temperatures. We found that the value of sensitivity increases with increasing temperatures.

REFERENCES

1. Stepanov, S. I., V. I. Nikolaev, V. E. Bougrov, and A. E. Romanov. "Gallium oxide: properties and applica a review." Rev. Adv. Mater. Sci 44 (2016): 63-86.
2. Cheng, Yi, Jixiang Chen, Kun Yang, Yizhuo Wang, Yan Yin, Hongwei Liang, and Guotong Du. "Structural, morphological, FTIR and photoluminescence properties of gallium oxide thin films." Journal of Vacuum Science & Technology B, Nanotechnology and Microelectronics: Materials, Processing, Measurement, and Phenomena 32, no. 3 (2014): 03D119(1-4).
3. Ghose, Susmita, Md Shafiqur Rahman, Juan Salvador Rojas-Ramirez, Manuel Caro, Ravi Droopad, Abraham Arias, and Nicola Nedev. "Structural and optical properties of β-Ga2O3 thin films grown by plasma-assisted molecular beam epitaxy." Journal of Vacuum Science & Technology B, Nanotechnology and Microelectronics: Materials, Processing, Measurement, and Phenomena 34, no. 2 (2016): 02L109.
4. Pandeeswari, R., and B. G. Jeyaprakash. "High sensing response of β-Ga2O3 thin film towards ammonia vapours: Influencing factors at room temperature." Sensors and Actuators B: Chemical 195 (2014): 206-214.
5. Feng, Qian, Fuguo Li, Bo Dai, Zhitai Jia, Wenlin Xie, Tong Xu, Xiaoli Lu, Xutang Tao, Jincheng Zhang, and Yue Hao. "The properties of gallium oxide thin film grown by pulsed laser deposition." Applied Surface Science 359 (2015): 847-852.
6. Ou, Sin-Liang, Dong-Sing Wuu, Yu-Chuan Fu, Shu-Ping Liu, Ray-Hua Horng, Lei Liu, and Zhe-Chuan Feng. "Growth and etching characteristics of gallium oxide thin films by pulsed laser deposition." Materials Chemistry and Physics 133, no. 2-3 (2012): 700-705.
7. Ayad, Z. M., Kadhim, A. A. and May A. A. "Laser Energy Impact on CdO NPs Prepared By PLD Technique" Indian Journal of Natural Sciences 8(49) (2018): 14106-14111.
8. Zhang, F. B., Saito, K., Tanaka, T., Nishio, M., and Guo, Q.X. "Structural and optical properties of Ga2O3 films on sapphire substrates by pulsed laser deposition" Journal of Crystal Growth 387(2014) ,96-100.
9. Raju, N. Ravi Chandra, K. Jagadeesh Kumar, and A. Subrahmanyam. "Physical properties of silver oxide thin films by pulsed laser deposition: effect of oxygen pressure during growth." Journal of Physics D: Applied Physics 42(13) (2009): 135411(1-6).
10. Ghaith, H. J. "Spectroscopic study of a Lead-Copper plasma produced by pulses Nd-YAG laser" M.Sc. thesis, College of Science, University of Baghdad, (2018).

11. Sonker, Rakesh Kumar, Anjali Sharma, Md Shahabuddin, Monika Tomar, and Vinay Gupta. "Low temperature sensing of NO2 gas using SnO2-ZnO nanocomposite sensor." Adv. Mat. Lett 4(3) (2013): 196-201.
12. Mohammed, A.S., "Synthesis and Characterization of Rare Earth Doped NiO Nanostructure on Si and PSi H_2S Sensor and Photodetector" Ph.D. Thesis , College of Science , University of Anbar , (2018).

Table 1 : shows the structural and optical parameters of the (β-Ga_2O_3) films, for the different pulses number

No. pulses	Average grain size (nm)	Roughness (nm)	Transmittance %	Energy gap (ev)
400	15.7	1.76	76.82	4.92
500	18.2	1.95	67.69	4.74
600	19.0	2.05	65.60	4.62
700	26.4	2.21	51.68	4.40

Table 2 : Sensitivity, recover time and response time of the (β-Ga_2O_3)/PS, for different operation temperature

Temperature (°C)	Sensitivity (%)	Recover Time (Sec)	Response Time (Sec)
35	116.0338	23.27	21
100	147.695	15.2	13.01
200	150.4202	23.4	14.1

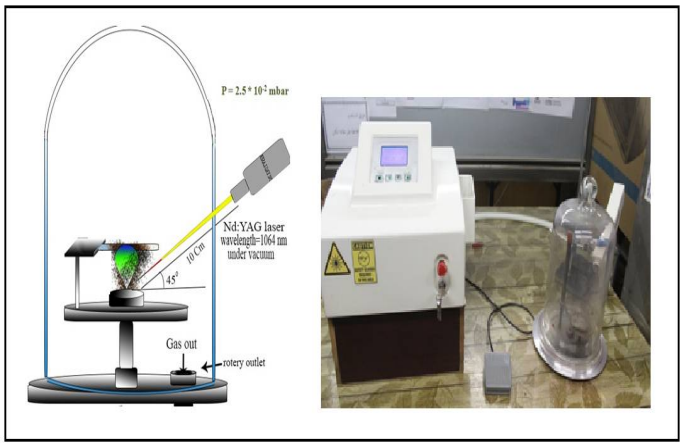

Figure 1. PLD system

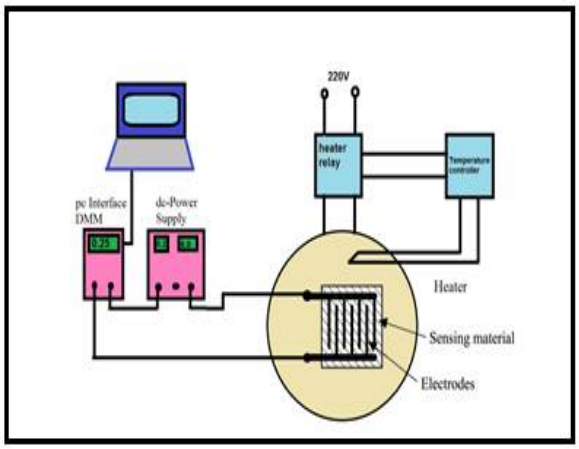

Figure 2. Measuring system of (NO2) sensing properties

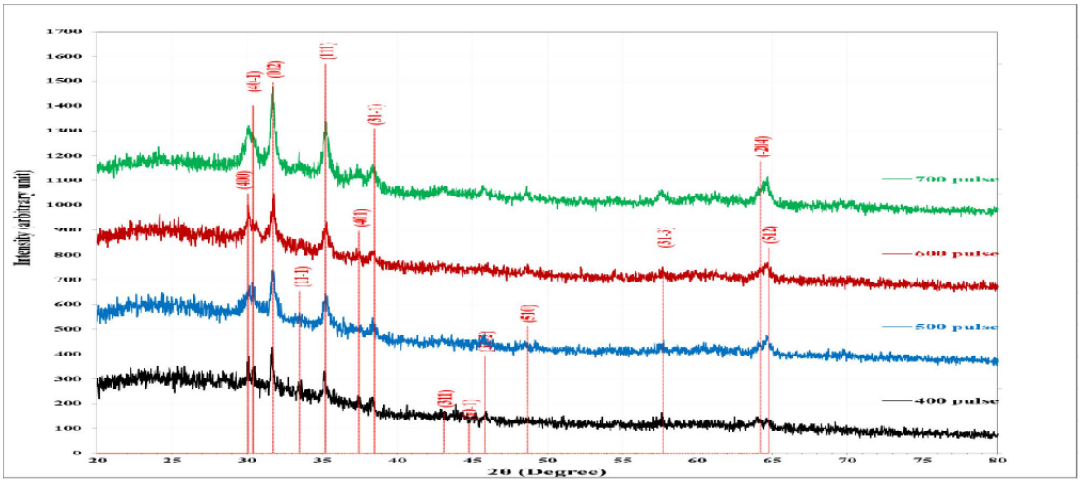

Figure 3. X-ray diffraction patterns of (β-Ga_2O_3) films, for different number of laser pulses

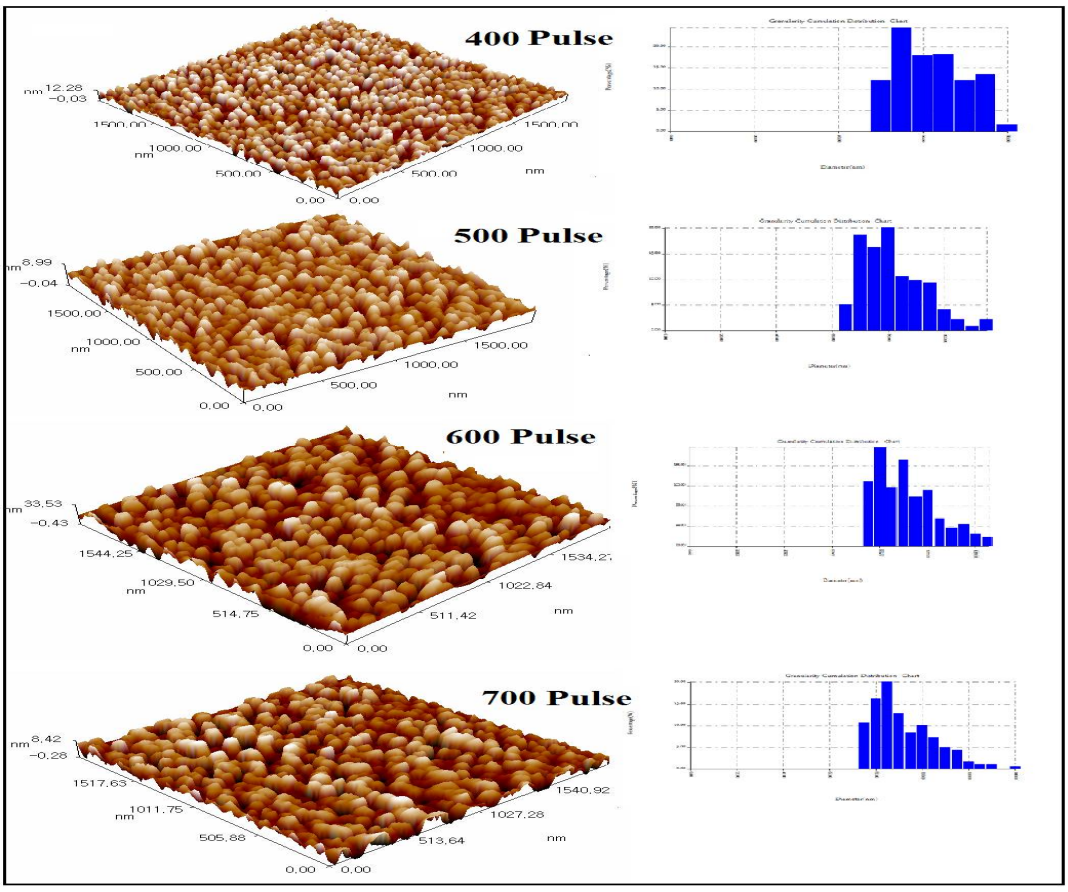

Figure 4: 3D AFM images of (β-Ga_2O_3) films at different Laser pulses

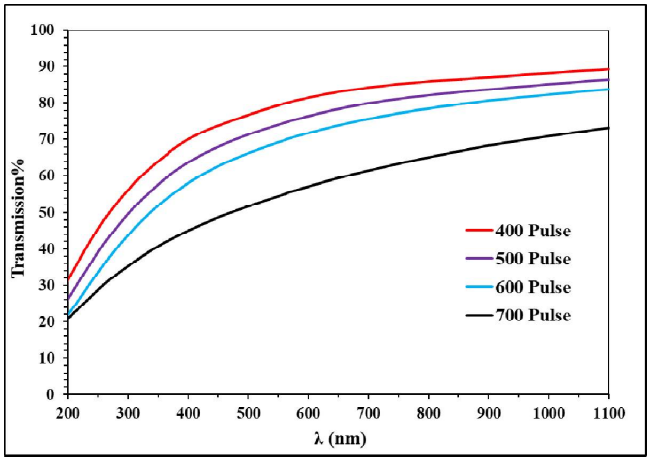

Figure 5. Transmittance spectra for (β-Ga_2O_3) films as a function of wavelength.

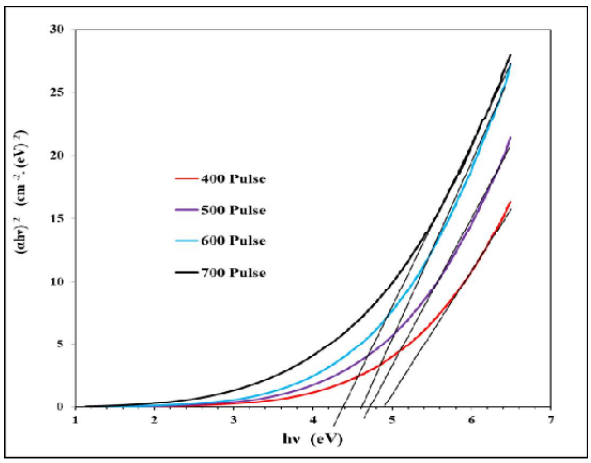

Figure 6. The energy gap for (β-Ga2O3) films at different number of pulses

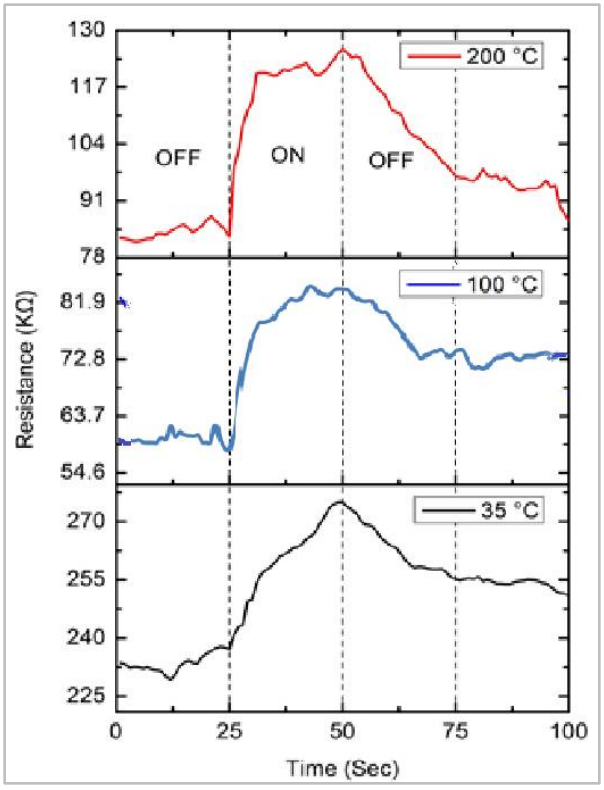

Figure 7: The resistance for (β-Ga2O3) films at different temperature

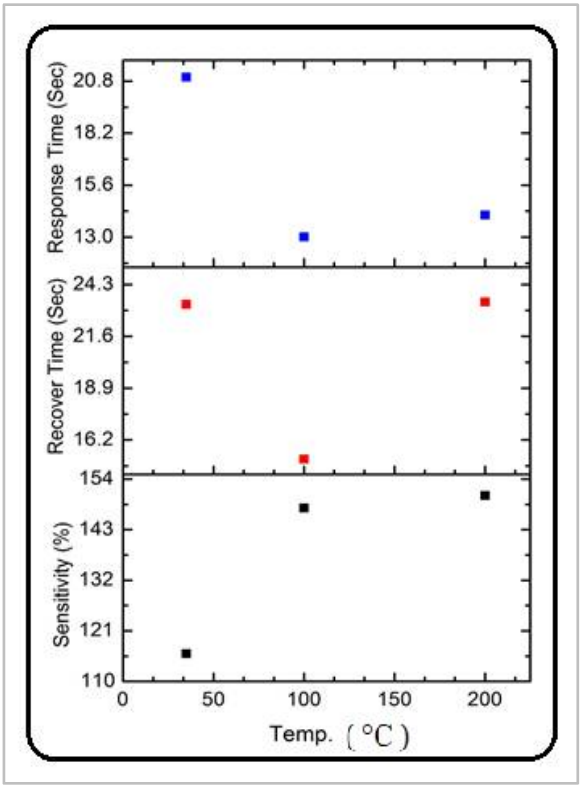

Figure 8 Relationship of the sensitivity, response time and recover time with temperature of the (β-Ga_2O_3)/PS

Indian Journal of Natural Sciences www.tnsroindia.org.in ©IJONS

Vol.9 /Issue 50 /October / 2018 *International Bimonthly* *ISSN: 0976 – 0997*

RESEARCH ARTICLE

Assessment of Irrigation Water Quality for Dabdaba formation by Using GIS Techniques in Karbala Province, Iraq

Muthanna M. Abd[1], Fouad K. Mashee Al Ramahi[2] and Fadhil M. Al- Mohammed[3*]

[1]Department of Physics, College of Science, University of Baghdad, Baghdad, Iraq,
[2]Remote Sensing Unit, College of Science, University of Baghdad, Baghdad, Iraq,
[3]Kerbala Technical Institute, AL-Furat Al-Awsat Technical University, 56001 Kerbala, Iraq.

Received: 05 July 2018 Revised: 09 Aug 2018 Accepted: 10 Sep 2018

[*]**Address for Correspondence**
Fadhil M. Al- Mohammed
Kerbala Technical Institute,
AL-Furat Al-Awsat Technical University,
56001 Kerbala, Iraq.
Email: fmhmjme@yahoo.com

ABSTRACT

The present study was conducted in Karbala province /Iraq for evaluating a groundwater for dabdaba formation and to determining its water quality index and studying the possibility of its use for irrigation purpose. One hundred and forty seven wells were selected within the dabdaba formation area to take water samples during 2017. Chemical analysis for samples of water included evaluation of the total dissolved solids TDS, the major positive elements (calcium, Ca^{++}, magnesium Mg^{++}, sodium Na^{+}, potassium K^{+}) and major negative elements (sulfates So^{-2}, bicarbonate, $HCO3^{-}1$,chloride Cl^{-}) in addition to hydrochemical transactions (electrical conductivity EC, sodium adsorption ratio,SAR, pH,). The results showed that there are no values from IWQI within range 85≤ 100 in all wells in the Dabdaba area, which are considered to be best range, this range of water index ensures that no damage to the plant and soil when water is used for irrigation. The maximum value of IWQI was in well number 70, and the minimum value of IWQI was 27.5 in well number 110. After making (IWQI) map by using IDW method, the results obtained showed 66% of wells study area falls within the high restriction. The map of IWQI shows that 66% of the Dabdaba wells water is classified as being used for irrigation should be within the high restriction for the preservation of soil and plant.

Keywords: Dabdaba formation, Irrigation, Water quality index, Karbala province, Groundwater.

INTRODUCTION

Groundwater is the water below the earth's surface. It is stored in the pores of rocks and soil particles. The quality and quantity of groundwater is vary from area to another, that depends upon the depth of geological formations and amount of rainfall [1].The aquifer may be divided into two types, unconfined and confined aquifers. Groundwater is one of the most important water sources in the study area. Because it is located within the dry areas. Therefore, attention to the study quality of groundwater is very important in determining the methods of using this water in irrigation of plants, or irrigation of animals in addition to their validity for human drinking. The crop yield, irrigation water quality and the associated to soil characteristic is often a complex phenomenon that includes the effect of many parameters [2].Although the water quality index WQI is created to rehabilitate urban water supply. This index was used for researchers and environmental planning scientists to determine the water quality of different purposes. The quality of irrigation water should be assessed to avoid, or at least minimize, the effects on crops [3].
The purposes of this study are to:

1. provide an overview of groundwater quality,
2. determination of the spatial distribution of the quality of the groundwater such as (EC, Na, Cl, Mg, HCO_3 , and SAR), and
3. Draw an interpolation map of irrigation water quality index, which shows the best quality within the study area by using IDW method (IDW: one interpolation method called invers distance weighting [9]).

The Study Area

The study area covers all administrative boundaries of the holy Karbala province, located between latitudes 32° $50^{'}$ $24^{''}$ and 32° $01^{'}$ $11^{''}$ north and longitudes 44° $18^{'}$ $03^{''}$ and 43° $01^{'}$ $04^{''}$ east [4]. The area of Karbala is about (5034) km^2 and represents 1.2% of the total area of Iraq [5]. Karbala geographical location is very important because it is located in the center of Iraq almost, it is has administrative borders with the provinces of Anbar, Baghdad, Hilla and Najaf.As in figure (1).

Groundwater Aquifer In Study Area

The geological formations for the study area, which contain groundwater, consist of the following basins: Dammam, Zahra, Dabdaba, Umm Er-Radhuma, Tayarat, Euphrates, Injana, and Alnafayl formations [6]. Figure (2) show the extension of the Dabdaba formation and the strati graphical position with other formations within study area

MATERIALS AND METHODS

The quality of groundwater was determined in karbala province by taking samples from 147 wells within the study area and within the Dabdaba aquifer. The locations of these wells were identified by using GPS technique, which is called Global Positioning System [8], it was processed using ArcGIS 10.2,thus was made map showing the locations of these wells, as in figure(3). The concentration of the chemical and physical (EC, Na, Cl, Mg, HCO_3) elements was measured laboratory and results were as in Appendix A

Permeability and Infiltration Hazard

The amount of water infiltration into agricultural soil depends on of several factors. These factors including irrigation water quality, and soil factors, such as permeability, and organic content. The high concentration of sodium ions in irrigation water can reduce soil permeability and thus reduce infiltration rate. The presence of sodium in the soil in

exchangeable form Lead to dispersion of soil granules. This dispersion leads to the breakdown of structure of the soil. After that, the soil becomes compact and solid in drought periods. This state reduces the infiltration rate of water and air to the soil, thus reducing productivity. The infiltration problem is related with other factors such as soil type and soil salinity. The value of Sodium adsorption ratio (SAR) for irrigation water quantifies the relative proportions of sodium concentration to the concentrations of magnesium and calcium 11].this ratio is defined as below:

$$SAR = \frac{Na}{\sqrt{\frac{(Ca+Mg)}{2}}} \quad \text{.....(1)}$$

Where the concentrations of calcium, sodium, and magnesium are expressed in units, milli equivalents per liter

Interpolation by Using (IDW Method)

Interpolation maps were made by using (IDW) method for chemical and physical elements (EC, Na, Cl, Mg, HCO_3), in addition SAR, showing the variation is clear in the distribution of the spatial concentrations elements in the study area, as in figures from 4 to 9.

The Model of Irrigation Water Quality Index (IWQI)

IWQI is an acronym for irrigation water quality index. This index represents the effect of several variables in determining the quality of irrigation water and its suitability for irrigation. It can be calculated from equation (2) and (3) and using Tables (2) and (3).

$$q_i = q_{imax} \_ \{[(x_{ij} - x_{inf}) \times q_{iamp}]/x_{amp}\} \text{.....(2)}$$

where q_{imax} is the maximum value of qi for the class; x_{ij} is the observed value for the parameter; x_{inf} is the corresponding value to the lower limit of the class to which the parameter belongs; q_{iamp} is class amplitude; x_{amp} is class amplitude to which the parameter belongs. Where q_{imax} is the maximum value of qi for the class; x_{ij} is the observed value for the parameter; x_{inf} is the corresponding value to the lower limit of the class to which the parameter belongs; q_{iamp} is class amplitude; x_{amp} is class amplitude to which the parameter belongs

The irrigation water quality index (IWQI) is calculated as:

$$IWQI = \sum_{i=1}^{n} qiwi \quad \text{.....(3)}$$

The analytical results were taken in to GIS environment to generate the numerical spatial distribution of the parameter and IDW (invers distance weight) technique adopted to create the spatial distribution maps water quality parameters, as in figures(5) and (6). IWQI is dimensionless parameter ranging from 0 to 100; qi is the quality of the i^{th} parameter, a number from 0 to 100, function of its concentration or measurement; w_i is the normalized weight of the i^{th} parameter, function of its relative importance to groundwater quality.

RESULTS AND DISCUSSIONS

The highest electrical conductivity was 19701 (µs/cm) at 57 well. The highest value of sodium concentration was 1413(mg/l) in well number 108, and lowest value was 128(mg/l) in well number 1. The highest value of Magnesium concentration was 1330(mg/l) in well number 30, and lowest value was 21.8(mg/l) in well number 144. The highest value of Calcium concentration was 2162(mg/l) in well number62, and lowest value was 129(mg/l) in well number 20. The highest value of Bicarbonates concentration was 482.6(mg/l) in well number 57, and lowest value was 118.4(mg/l) in well number 146. The highest value of Chloride concentration was 17.5(mg/l) 1/2 in well number110, and lowest value was 0.72 (mg/l) 1/2 in well numbers 1. The highest value of IWQI concentration was 62.4 in well number 70, and lowest value of IWQI concentration was 27.5 in well number 110.

CONCLUSIONS

From the results and compared with table 3,it was conclude the following: There are no values from IWQI within range 85≤ 100 in wells study area, which are considered to be best ratios, and no restriction use in soil and plant. There are no values from IWQI within range 70≤ 85 in wells study area, which are low restriction for water use in soil and plant. 9.5% of wells in dibdiba formation, contains IWQI values within range 55≤ 70 (number of wells 14),which are moderate restriction for water use, therefore may be used in soils with moderate to high permeability values, being suggested moderate leaching of salts, and plants with moderate tolerance to salts may be grown. 66.7% of wells in dibdiba formation, are contains IWQI values within range 40≤55 (number of wells 98), which are high restriction for water use, therefore may be used in soils with high permeability without compact layers. High frequency irrigation schedule should be adopted for water with EC above 2000µs/cm and SAR above 7,0 .And should be used for irrigation of plants with moderate to high tolerance to salts with special salinity control practices, except water with low Na,Cl, and HCO3 values. 23.8% of wells in dibdiba formation, are contains IWQI values within range 0≤ 40 (number of wells 35), which are severe restriction for water use, therefore should be avoided its use for irrigation under normal conditions. In special cases, may be used occasionally. Water with low salt levels and high SAR require gypsum application, IN high saline content water soils must have high permeability, and excess water should be applied to avoid salt accumulation. Only plants with high salt tolerance, except for waters with extremely low values of Na, Cl, and HCO3

REFERENCES

1. Salah,Hamed,geostistical analysis of groundwater levels in the water resource department, south AL Jabal ALAKHDAR area using GIS, Benghazi,Libya,GIS Ostrave,2009,32718, General water Authority
2. APHA (American Public Health Association) Standard method for examination of water and waste water, NW, DC 20036, (1994)
3. Mohammed, M.N. (2011): "Quality assessment of Tigris river by using water quality index for irrigation purpose", European Journal of Scientific Research, Vol. (57), No.1, pp.15-28.
4. Hatem Khudair Salih Al-Juburi , 2002, "Hydrological and Hydrochemical Study of the Karbala Panel Area", State Company for Geological Survey.
5. State Directorate of Urban Planning, 2011, Karbala Province, Basis Design Update for the City of Karbala and Al-Hur.
6. Al-Jawad, S.B., Al-Dabagh R.H. , Mussa ,M.S. , and Al-Hady H.A. (2002): "Hydrogeology of the Aquifers In the Western Desert -west and south of the Euphrates River, sections I and II", the national program, unpublished.
7. Consortium-Yugoslavia, (1977): "Water development projects, western desert-Blook7, hydrogeological explorations and hydro technical work, hydrogeology", Vol. (5), Republic of Iraq, Directorate of western desert development projects.

8. Kennedy M., 2010, "The Global Positioning System and ArcGIS", pp1-227.
9. Victoria,2010,"A Modified Spline Interpolation Method for function Reconstruction from its zero-Grossing", University of Lativa,19 Raina,LV-1459,Riga,Lativa,Scientific paper, University of Lativia,vol,756,computers Science and Information Technologies.
10. Msek, C., and Gunduz, O. (2007): "IWQ index: A GIS integrated technique to assess irrigation water quality", Environmental Monitoring and Assessment, Vol. (128), pp. 277–300.
11. Ayers, R.S. and Westcot, D.W. (1999): "The water quality in agriculture", 2nd. Campina Grande: UFPB. (Studies FAO Irrigation and drainage, 29).
12. Al-Mussawy, Waqed, 2013, "Optimum Management Models for Groundwater Use in Karbala Desert Area", Thesis of the degree of doctor, College of Engineering, University of AL-Mustansiryah, pp57.

Table 1.Results of water quality analysis for the aquifer in the study area

No. of Wells	Na(mg/l)	Ca(mg/l)	Mg(mg/l)	EC (µs/cm)	HCO_3 (mg/l)	SAR (meq/l)½
1	128	2080	160	8300	211.6	0.726584999
2	251	1360	1336	4380	315.4	1.152471974
3	482	2160	40	3570	195.7	2.808805029
4	720	1840	320	7000	327.3	4.064014854
5	251	1280	1320	11150	186.3	1.170001071
6	482	800	480	3480	239.6	3.313517027
7	720	1920	440	4510	237.1	3.843604999
8	133	1480	520	3480	198.3	0.754967225
9	480	880	120	4510	417.5	4.016349699
10	590	1400	480	10340	237.9	3.458938425
11	800	145	38	5300	328.1	15.24097551
12	330	193	55	2850	189.6	5.378334281
13	331	521	219	5140	367.8	3.057829685
14	266	134	95	2490	389.5	4.278037892
15	322	143	34	2910	234.4	6.26621436
16	1127	431	145	12300	296.4	11.94885035
17	138	569	54	2550	258.1	1.478218179
18	155	592	585	1679	269.6	1.07671152
19	325	462	487	4370	258.2	2.50413437
20	162	129	85	3630	341.3	2.707695274
125	325	1365	92	345.6	301.1	2.293516967
126	346	2165	98	345.6	205.3	1.971767394
127	133	1845	97	345.6	327.4	0.816424788
128	256	1285	90	259.2	361.5	1.858301487
129	487	805	96	345.6	283.3	4.310895191
130	725	1925	95	259.2	291.8	4.367780297
131	256	2085	94	345.6	228.9	1.486813884
132	595	1405	33	259.2	248.2	4.281960902
133	805	150	35	259.2	252.8	15.33623161
134	335	198	37	259.2	391.6	5.716613956
135	336	526	39	259.2	327.7	3.800560905
136	271	139	43	259.2	418.2	5.134208942
137	327	148	38	345.6	426.5	6.185373235
138	1132	436	144	259.2	413.2	11.97223515

139	160	574	145	259.2	186.3	1.540514481
140	330	597	154	259.2	114.9	3.10578893
141	167	467	143	345.6	266.8	1.729105238
142	257	1846	285	259.2	247.3	1.466890557
143	486	1286	287	345.6	259.1	3.181618544
144	806	1406	21.8	432	319.4	5.835853502
145	336	151	22	432	349.7	6.744470617
146	966	506	141	259.2	118.9	9.758210495
147	300	165	176	345.6	311.8	3.853298848

Table 2. Weights for the IWQI parameters.

Parameter Weight (wi)	Parameter Weight (wi)
Electrical conductivity (EC)	0.211
Sodium (Na+)	0.204
Chloride (Cl-)	0.194
Bicarbonate(HCO_3)	0.202
Sodium Absorption ration(SAR)	0.189
Total	1.00

Table 3. Irrigation Water Quality Index Characteristics[12]

IWQI	Water restriction use	Recommendation of soil	Recommendation of plants
85≤ 100	No restriction	May be used for the majority of soils with low probability of causing salinity.	No toxicity risk for most plants.
70≤ 85	Low restriction	Recommended for use in irrigated soils with light texture or moderate permeability, being recommended salt.	Avoid salt sensitive plants.
55≤70	Moderate restriction	May be used in soils with moderate to high permeability values	Plants with moderate Tolerance to salts may be grown.
40≤55	High restriction	May be used in soils with high permeability without compact.	Should be used for irrigation of plants with moderate to high tolerance to salts .
0≤ 40	Severe restriction	Should be avoided its use for irrigation under normal condition	Only plants with high salt tolerance except for waters with extremely low values of Na ,Cl and HCO_3.

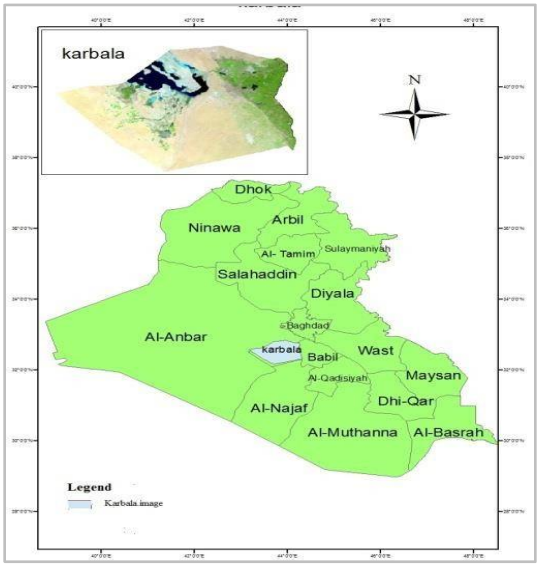

Figure 1. Location of Karbala province of the republic of Iraq (source: from work researcher).

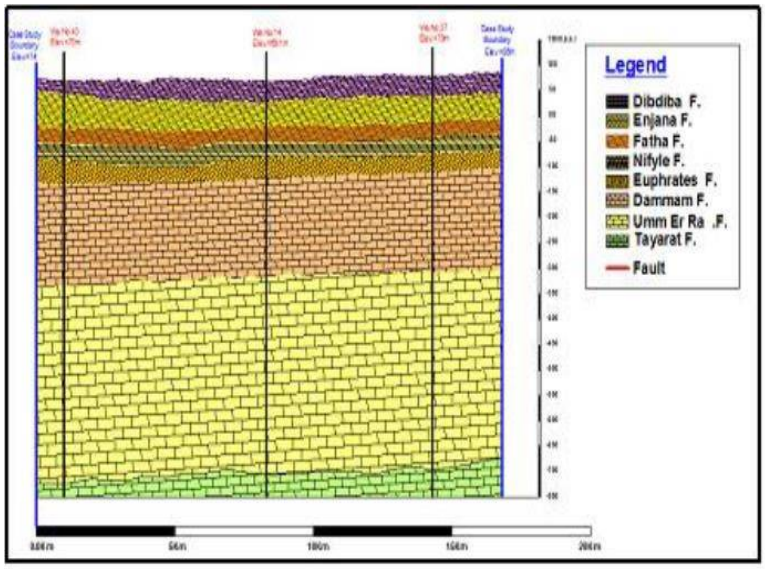

Figure 2. The Stratigraphic Correlation between the Wells in the Study Area [7]

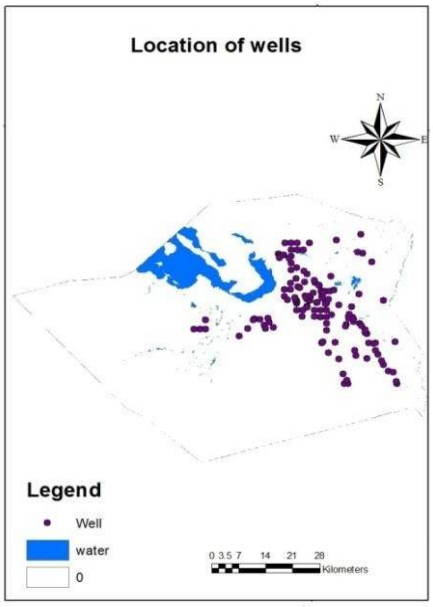

Figure 3: Locations of the Water Samples of the Well in the Study Area

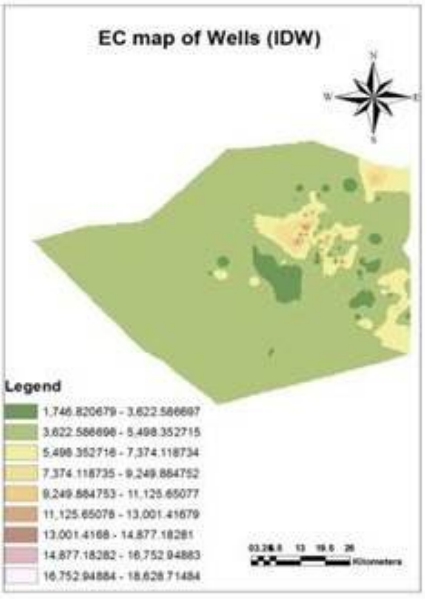

Figure 4. Spatial distribution of EC concentration by using IDW method

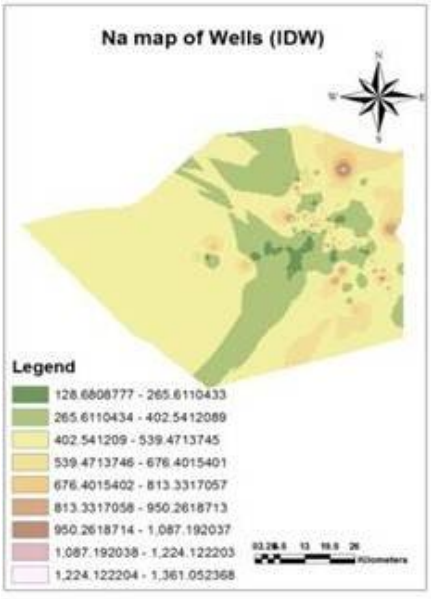

Figure 5. Spatial distribution of Na concentration by using IDW method.

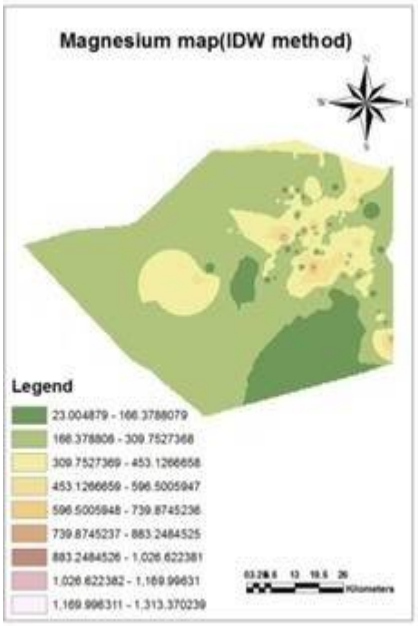

Figure 6. Spatial distribution of Mg concentration by using IDW method

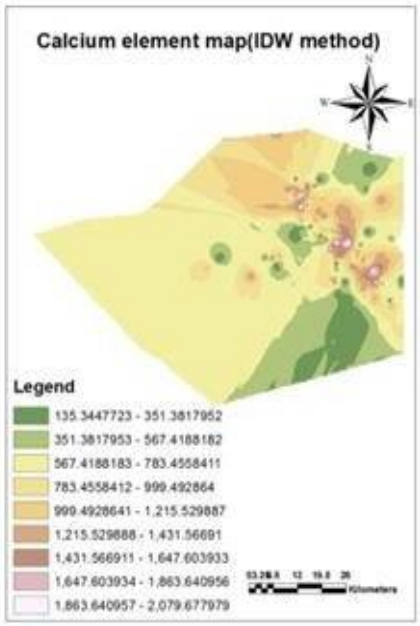

Figure 7. Spatial distribution of Ca concentration by using IDW method

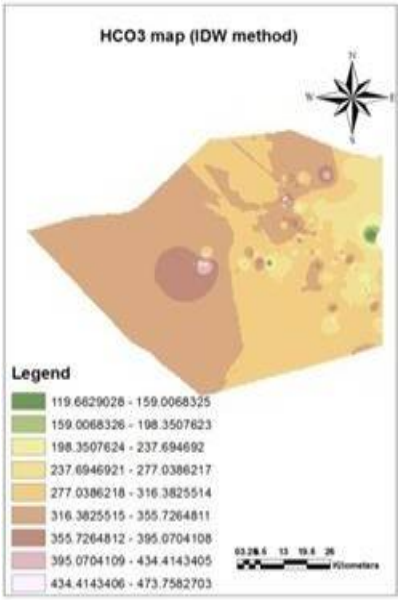

Figure 8. Spatial distribution of HCO_3 concentration by using IDW method.

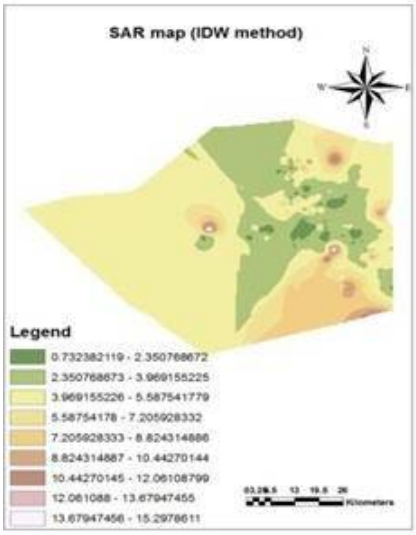

Figure 9. Spatial distribution of SAR concentration by using IDW method.

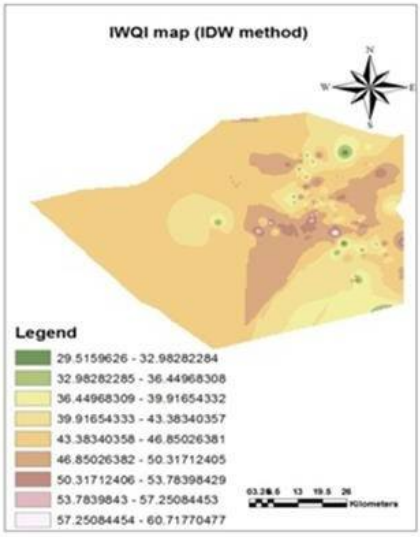

Figure 10. Interpolation of the IWQI distribution for dabdaba formation using IDW method.

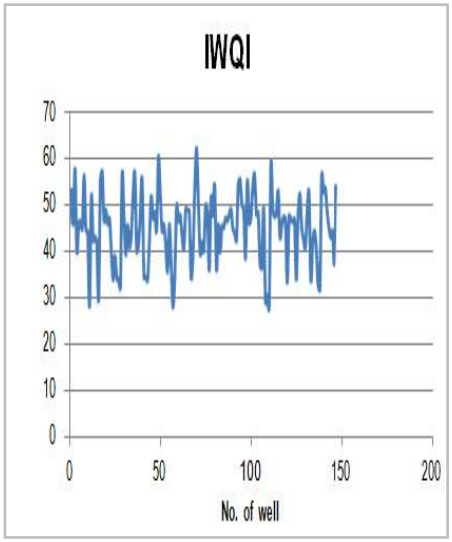

Figure 11. Spatial distribution of irrigation water quality index (IWQI) concentration in dabdaba formation.

Indian Journal of Natural Sciences www.tnsroindia.org.in ©IJONS

Vol.9 /Issue 50 /October / 2018 *International Bimonthly* *ISSN: 0976 – 0997*

RESEARCH ARTICLE

Investigation of Polymorphism Mitochondrial Gene (CD9) in Bull Semen Before and After Glycyrrhizaglabra Treatment

Saad S. AL-Dujaily[1]*, Najwa Sh. Ahmed[1] and Hayder Abdul-Kareem Hasan AL-Mutar[2]

[1]Biotechnology Research Center, Al-Nahrain University, Baghdad,Iraq
[2]Department of Surgery and Obstetrics, College of Veterinary Medicine, University of Baghdad, Iraq.

Received: 06 July 2018 Revised: 08 Aug 2018 Accepted: 10 Sep 2018

***Address for Correspondence**
Saad S. AL-Dujaily
Biotechnology Research Center,
Al-Nahrain University,
Baghdad, Iraq
Email: almutar.haydar@gmail.com

ABSTRACT

Sperm motility is a critical factor to consider in couples seeking after assisted reproductive advancements. A few examinations have exhibited the impact of sperm motility on the results of various reproductive technologies; including intrauterine insemination (IUI).CD9 has a basic part in treatment When getting semen for the artificial insemination (AI) from cattle. The outcomes demonstrate A noteworthy ($P<0.05$) diminish in sperm concentration was spotted following in vitro initiation with Glycyrrhizaglabra medium contrasted and before activation, and huge increment in dynamic sperm motility ($P<0.05$) and morphologically normal sperm ($p<0.05$).

Keywords: Bull semen, CD9 gene, Polymorphism, Glycyrrhizaglabra.

INTRODUCTION

Sperm motility is a critical factor to consider in couples seeking after assisted reproductive advancements. A few examinations have exhibited the impact of sperm motility on the results of various reproductive technologies, including intrauterine insemination (Yalti*et al*., 2004)conventional in vitro fertilization (IVF) (Repping et al., 2002), and IVF with intracytoplasmic sperm infusion (ICSI) (Stalf et al., 2005). Sperm motility gives a measure of the trustworthiness of the sperm axoneme and tail structures and additionally the metabolic apparatus of the mitochondria, and sperm morphology is a surrogate measure of the honesty of DNA bundling and the nature of spermatogenesis (Pacey, 2006). On the other hand herbal plant are used word widefor instance the Glycyrrhizaglabra (Gg).Various parts have been isolated from licorice, including water dissolvable, biologically active complex that record 40-50 percent of the aggregate dry material weight (Obolensteva, *et al* ;1999). The CD9 is closely related to other tetraspanin proteins (Kaji and Kudo 2004, Le Naour*et al*. 2000).CD9 has critical role in fertilization (Kaji*et al*. 2000), while getting semen for the artificial insemination (AI) from cattle is essential as that insemination doses

contain sufficient sperms to achieve adequate fertility. To determine appropriate sperm concentrations,semen quality is analyzed with an assortment of strategies including the percent motile sperm, suitable sperm viable sperm, sperm with intact acrosomes and sperm with normal morphology(De Jonge, 1999).In view of these measures, the quantity of sperm expected to achieve a level of fertility is computed. However there are a large number of specified tests, but they can't identifythe bull semen of lessened fertility (Brahmkshtri et al., 1999). In this manner, choosing where to set quality control limits is troublesome.Semen quality investigation constitutes an intense apparatus to assess the fertility capability of a male in many varieties (Rodriguez-Martinez and Barth 2007). Research center assessed parameters of sperm quality incorporate appraisal of the integrity of different structures, for example, genomic DNA (gDNA), acrosome, cell membrane, and mitochondria, in addition unique parameters, for example, the hyperactivated motility (Madrid-Bury *et al*. 2005,Rodriguez-Martinez 2006).Thus, the goal of present study is to found out the effect of Gg medium on *in vitro* activation of cryopreserved semen of bull for AI and to investigate of mitochondrial gene mutation and polymorphism in bull before and after Gg addition.

MATERIALS AND METHODS

The present study was conducted in the Biotechnology Research Center-Al-Nahrain University through the period from March till July 2016. Bull semen straws of proven fertility were obtained from the Department of Artificial Insemination, Ministry of Agriculture. A total of 50 strawswere used and the thawedsemen were examined the certain sperm service parameters to be specific; sperm concentricity individual sperm motility andmorphologically normal sperm percentage.Then all straw samples were treated with Gg medium after second freezing. After one month of cryopreservation the results of thawed semen were measured and certain sperm function parameters were recorded too. The thawing of semen strawswas doneby shortly inserted in a water bath kept at 39°C. After about 2 seconds, the straws were taken out of water. The motile spermatozoa were then obtained. The thawing after second cryopreservation through swim-up procedure was applied (Parrish *et al*. 1988).Ggwas added to the mediumsemen samplesaftersecond freezing.

Preparation of Gg

The major method for preparation of Ggextract was done by aqueous method.The extract was obtained by crushing the root of plant and extracted as described by Chakravarty, (1976). TheGgextract was obtained from the Al-AhliyaFlavours& Fragrances Co. Ltd. IRAQ). The Gg hasbeen stored in well-closed container protected from light and moisture (Maisonneave, 1971).The preparation of Gg stock solution of 0.1% concentration was done as described by Al-Dujaily *et al*., (2006).DNA was produced by using the standard protocol by intron kit (Korea) procedure.Two conserved primers were used (forward) 5-GAGGCAAAACTCCAAAACCA-3 and (reverse): 5-CT CCACTGTCGTTT GTCGTG-3, Accession NCBI Taxonid (NM_1739009913).The thermal cycling conditions were done as follows: Denaturation at 95 °C for 3 min, followed by 35 cycles of 94 °C for 30s, 55°C for 30s and 72 °C for 35s with final incubation at 72 °C for 7 min using a thermal Cycler (Gene Amp, PCR system 9700; Applied Biosystem). The polymerase chain reaction (PCR) products were extracted by 2% agarose gel electrophoresis and visualized by contact with ultra violet light (302nm).Sequence of nucleotides of CD9 gene by using BioEdit program, which was performed by MagrogenCompany, Biotechnology Lab, machine is DNA sequencer 3730XL, Applied Biosystem.The compatibility was conducted using Basic Local Alignment Search Device(BLAST) program which was available at the National Center Biotechnology Information (NCBI) online at (http://www.ncbi.nlm.nih.gov), then submission of CD9 gene in NCBI

Statistical Analysis

Data were analyzedusingSAS (2012) program. The differences between means were assessed using paired t test. $P<0.05$ is considered significant.

RESULTS AND DISCUSSION

Table 1. Showed the effect of Gg addition to the culture medium on the certain sperm function parameters of second cryopreservation semen samples obtained from bull semen straw. A significant (P<0.416) decrease in sperm concentration was observed following *in vitro* activation with Gg medium compared with before activation.This result was clarified the beneficial effect of preparation techniques by the removal of dead, immotile spermatozoa and semen debris in such way only high quality motile spermatozoa were harvested and poor quality spermatozoa were absent in the post activation medium (Al-Dujaily *et al*.,2013).There was a significant increase in active sperm motility (P>0.0293) and morphologically normal sperm(p<0.492) of the thawed straw samples treated with a medium containing Gg compared with before activation.Culturing of thawed sperms with licorice extract – Hams-F12 medium result in a significant increase in the percentages of sperm motility and grade activity of forward movement (grade A and grade B) of all the groups of as the no zoospermic samples.The *Glycyrrhizaglabra* has estrogenic activity (Rafi,*et al* 2002).Estrogens are known to enhance sperm qualities including sperm motility and grade activity not with standing induction of hyperactive motility (Ganong,2005).

Furthermore, it has been noticed that the *Glycyrrhizaglabra* contains Ca^{+2}, potassium, glucose, fructose, vitamin E, vitamin C and many other substances e.g.: Zn^{+2}, sucrose, amino acid (Tylor , 2004).All these substances can empower sperm motility and the review activity of forward development. The sugars are thought to be a wellspring of vitality for sperm motility.Fructose is one of the principle energy substrate for spermatozoa and an activator factor of mammal spermatozoa(Rigau*et al* 2000), the protein and amino acids, which sustain and maintain sperm osmolality and in turn integrity of sperm cell membrane (Agarwal and Prabakkaran 2005).DNA was extracted from the bull sperm by *AccuPrep*® kit / intron the procedure was very efficient and showed sharp band by gel electrophoresis showed in Figure(1). Genomic DNA of sperm was also used for amplification of CD9 gene using PCR specific primers. The amplified fragment which is yielded of single band of the desired product with a molecular weight of 658 base pair appeared sharp in agarose gel through Gel electrophoreses techno.Results showed that after activation the sperm concentration after activation (1.15 x 107) decreased significantly (P<0.05)while sperm motility increased significantly (P<0.05) (80%) and morphologically normal sperm(p<0.05) The bull fertility qualities are firmly influenced by natural impacts. Hence, impacts of single loci are relied upon to be low and require a higher number of creatures to be analyzed (Long and Langley 1999).The conservation of the sperm preparing capacity.Plasma membrane integrity is crucial to sperm survival into the female reproductive tract, and in preserve fertilizing capability (Celeghini et al. 2007). The acrosome is filled with hydrolytic enzymes which are necessary for penetration spermto zonapellucida. The acrosome must stay unblemished previously and amid the transit of the sperm to the isthmus until zona binding has been completed.

Early acrosome responses render sperm infertile (Silva and Gadella 2006), and along these lines, acrosomal integrity is a very important functional characteristic which licenses assessment of sperm treating potential (Nikolaeva et al. 1998, Silva and Gadella 2006) During preparation, the motility and surface hyaluronidase is fundamental for the entrance of sperm to the cumulus cells (Primakoff and Myles 2002). CD9 plays an imperative and basic part in gamete membrane interactions (Kaji et al. 2000), An investigation directed on CD9 null mice, demonstrated their total sterility because of scarcity in egg-sperm fusion (Xiang and MacLaren 2002). CD9 was altogether expanded amid the final oocyte development, demonstrating that to be fertilized (Li et al. 2004). Other studies demonstrate that CD9 quality which communicated in blastocysts and endometrium epithelial cells in man and in bovines (Le Naour et al. 2000, Xiang and MacLaren 2002), play a role in inhibiting embryo implantation (Liu et al. 2006). This is agreed with the outcomes that, demonstrating the up-organizing of CD9 in biopsies got from blastocysts bringing about no pregnancy (El-Sayed et al. 2006) might be involved in embryo invasive behaviors (Liu et al. 2006). In this study, SNP was found in exon 9. The sequencing of amplified product of *CD9* gene from bull , out of them appeared 100% and 99% compatibility with standard *Bostaurus*breed CD9 gene from (682 to 1111 and 682 to 1110) number of nucleotide from gene of gene Bank results as shown in Figure (2 A+B), Sequence ID: NM_173900.2, and have number score (430

and 417) bits. This result is similar to result obtained by Zhou*et al*., (2013).After addingGlycyrrhizaglabrait was founda variation of CD9 gene, and afteralignment of product amplification of CD9 gene it was found TransitionCGC>TGG, and three Transversion CCT>CCA,GTG>GAG`and CGC>TGG from the Gene Bank, The part ofCD9gene Thaving99% compatibility with standard in Gene BankCD9 gene, as shown in table(2).Thus it could be explained at the present study that of CD 9 in bullwith A and G allele and genotype A/G might be associated with litter size in Iraqi goats. However, further analysis should be performed in order to validate both the association and the physiological significance of the mutation in the CD 9gene. Thus CD9 may participate in many different cellular functions, such as increase the Ca^{++} receptor and /or activate the catsper channels that responsible of increase the Ca^{++} influx to sperm mitochondria (Tylor , 2004)·leading to increase the active sperm motility in addition to its function in adhesion, migration, differentiation, proliferation and signal transduction (Li *et al*. 2004).At the same time the constituents of Gg may enhance the sperm motility and MNS So it could be explained at the present study that Iraqi goats of CD 9with A and G allele and genotype A/G might be associated with litter size in bull. However, further analysis should be performed in order to validate both the association and the physiological significance of the mutation in the CD 9gene.

Submission of CD9 gene in NCBI

The gene CD9 were registered after the correspondence of The National Center for Biotechnology Information and obtained accession number ID: KY853664.1 and became a reference to Iraq and the Middle East and the world.

REFERENCES

1. De Jonge, C. (1999) Attributes of fertile spermatozoa: Andrology lab corner an update. Journal of Andrology 20, 463–473.
2. Brahmkshtri, B.P.; Edwin, M.J.; John, M.C.; Nainar, A.M.; Krishnan, A.R. (1999) Relative efficacy of conventional sperm parameters and sperm penetration bioassay to assess bull fertility in vitro. Animal Reproduction Science 54, 159–168.
3. Rodriguez-Martinez H & Barth AD 2007 *In vitro* evaluation of sperm quality related to *in vivo* function and fertility. Society of Reproduction and Fertility 64 39–54.
4. Zhou, G.B., Zeng, Y., Meng, Q.G., Liu, Y., Dai, Y.P., Zhu, S.E., Bunch, T.D. and Hou, Y.P. (2013). Decreased expression of CD9 in bovine oocytes after cryopreservation and the relationship to fertilization capacity. 80(6):451-9.
5. Glover T and Mitchell K.An Introduction to Biostatistics, 2nd ed. Waveland Press, Inc, 2008; 4.
6. Al-Dujaily, S.S. , Al-Janabi, A. and Nori ,M .The effect of *Glycyrrhizaglabra* on *in vitro* activation of asthenospermic patients(J. Babylon University,2006).
7. Al-Dujaily,S.S., Al-Sultani,Y.K., Shams Alddin ,N. (2013) *In vitro* sperm activation with Pentoxifylline and L-carnitine for infertile men semen using layering . Iraqi J. Embryos and Infertility Researches.3(6):26-31.
8. Rafi, M., Vastano, B., Zhu, N., *et al*.(2002). Novel Polyphenol Molecule Isolated from Licorice Root (*Glycyrrhizaglabra*) Induces Apoptosis, G2/M cell cycle arrest, and Bcl-2 phosphorylation in tumor cell lines. J. Agric. Food. Chem. 50: 677-684.
9. Ganong, W. F.(2005). Review of medical physiology .McGraw-Hill Boston, Pp:424-340.
10. Taylor, L. (2004).Database File for Licorice.Raintree Nutrition Inc. Available from:http://www.rain-tree.com/licorice .html.
11. Rigau, T., Camprubi, M. , Badia, J., *et al*.(2000). Different effects of glucose and fructose on energy metabolism in dog sperm from fresh ejaculates.14th International Congress on Animal Reproduction. 2:24.
12. Agarwal, A. and Prabakkaran, S.A.(2005) Oxidative stress and antioxidative in male infertility: a difficult balance. Iranian J Reprod Med. 3:1-8.

13. SAS. 2012. Statistical Analysis System, User's Guide. Statistical.Version 9.1th ed. SAS.Inst. Inc. Cary.N.C. USA.

Table 1. Certain sperm function parameters before and after *in vitro* activation of bull sperm cryopreserved for second time by using Glycyrrhizaglabra medium.

Certain sperm function parameters	*In vitro* activation of bull sperm cryopreserved for second time using by Gg medium		P-value
	Before	After	
Sperm concentration x 10^7	1.330 ± 0.037	1.151 ± 0.022	0.0416
Active sperm motility (%)	65.00 ± 3.62	80.00 ± 4.52	0.0293
Morphologically normal sperm (%)	68.75 ± 3.81	78.50 ± 4.19	0.0492

Table 2: Type of polymorphism of CD9 gene in bull sperm after Glycyrrhizaglabra medium used for *in vitro* activation.

location of Gene Bank	Cod Change	Type of Polymorphism
T765A	CCT>CCA	Transversion
T785A	GTG>GAG	Transversion
C805T	CGC>TGG	Transition
C807G	CGC>TGG	Transversion

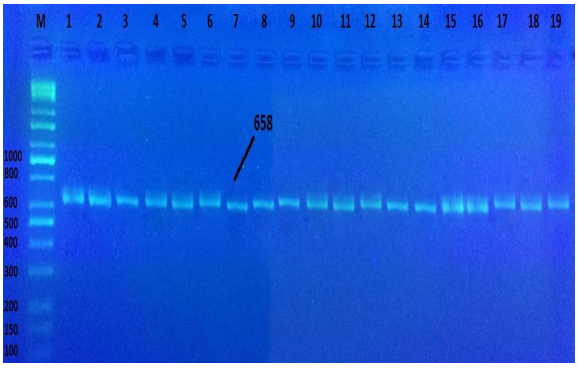

Figure 1.The product was electrophoresis on 2% agarose gel at 5 volt/cm², 1x TBE buffer for 2 hours. M: DNA ladder (100-10000bp), lane (1-19) PCR product of band size 658bp. visualized under U.V light after staining with red stain safe

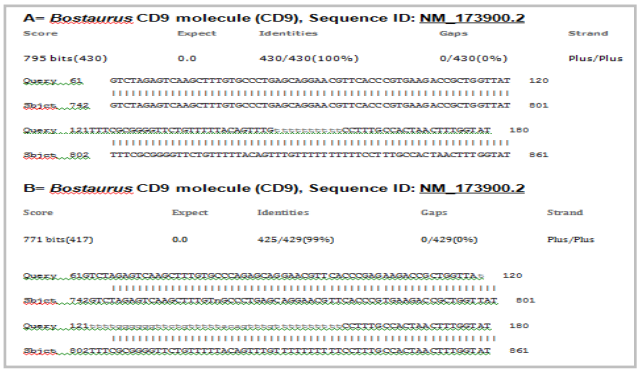

Figure (2 A+B): Sequencing of sense flanking the *CD9* For bullsperm after adding Glycyrrhizaglabra, gene, obtained from Gene Bank. Query represents of sample; Subject represent of database of National Center Biotechnology Information (NCBI).

Indian Journal of Natural Sciences www.tnsroindia.org.in ©IJONS

Vol.9 /Issue 50 /October / 2018 *International Bimonthly* *ISSN: 0976 – 0997*

RESEARCH ARTICLE

Thermal and Optical Properties of PMMA, Cu Nanocomposite

Noorhan S. Jumaah* and Salma M. Hassan

Department of Physics, College of Science, University of Baghdad, Baghdad, Iraq.

Received: 01 July 2018 Revised: 05 Aug 2018 Accepted: 10 Sep 2018

*Address for Correspondence
Noorhan S. Jumaah
Department of Physics,
College of Science,
University of Baghdad,
Baghdad, Iraq.

ABSTRACT

In this work PMMA,Cu Nano composite of Cuweights (0.1%, 0.3%, 0.4%, 0.5%, 1% of PMMA) was preparedby solubilizing Poly (methyl methacrylate) (PMMA)with Tetrahydrofuran (Thf) solvent and adding copper Nano particles. FT-IR spectrum, thermal conductivity and the optical properties was studies for the Nano composites. The results of PMMA,Cu Nano composite show that when concentration of Cu Nano particle increase, the optical energy gapdecreased and the thermal conductivity increased.

Keywords: PMMA ,Cu, Nano, thermal, energy .

INTRODUCTION

Nano composites are composed by Nano sized particles with high surface area, the particles interface assumes as key point, which defines its final properties. Depending on the dispersion and particles surface, several interfaces can be observed, which can result in special properties. [1].Nano composite materials have become increasingly important due to their extraordinary properties, which arise from the synergism between the properties of the parent components and their unique interfacial characteristics. These properties appear to be quite different from those of the conventional micrometer-sized composites. This mainly results from the nanometer-sized component which dramatically increases the available interacting surface area [2].Polymer Nanocomposites (PNCs) make the largest and most diverse use of Nanocomposites due to ease of fabrication, low cost and good properties[3].Poly(methyl methacrylate) (PMMA) is an important amorphous thermoplastic with desirable properties, including clarity (the transparency is close to the ultraviolet region and also the infrared), chemical resistance, good moldability, high strength, dimensional stability and has limitations in its thermal stability and mechanical-dynamical properties at high temperatures[4].In this work we add copper Nano particle to PMMA due tospecial physico-chemical characteristic of copper nanoparticles which include catalytic activity, electronic properties and antimicrobial activity. Cu nanoparticles have received considerable interest due to their good thermal, optical and electrical properties [5].

MATERIALS AND METHODS

Preparation of Nano composites

(25ml) of Tetrahydrofuransolvent (THF) was added to (5 g) of Poly(methyl methacrylate) then stirrering the mixture with temperature about 40°C for (2 hours) until The whole PMMA dissolve completely and having a clear sol-gel .Copper nanoparticles was weighed in a clove box filled with nitrogen gasof different weights(0.1%, 0.3%, 0.4% , 0.5% and 1% of PMMA),to prevent oxidation of copper Nano particle, then were added gradually to the PMMA sol gel during the stirring for (1 hour) until a homogenous mixture is reached. The whole process was done under nitrogen gas .Cast the mixture in a circular aluminum mold of diameter 30 mm after clean it with alcohol,then dried at room temperature for 72hour.The samples were cut into 25 mm to remove the high edge caused by surface tension. Figure 1 shows the PMMA/Cu Nano composite samples.

RESULTS AND DISCUSSION

Fourier Transform infrared spectrophotometer (FTIR)

FT-IR spectroscopy is a very informative measurement for studying the functional groups of the structure. FT-IR spectra of PMMA/Cu Nano composites were recorded and some partial changes in the absorption peaks of different concentration of Cu were observed Figure 2. From Fig.2 it can be seen that there is a distinct absorption band from 1147.65 cm^{-1} to 1195.87 cm^{-1}, which can be attributed to the C–O–C stretching vibration. The two bands at 1274.95 cm^{-1} and 752.24 cm^{-1} can be attributed to the α-methyl group vibrations. The band at 989.48 cm^{-1} is the characteristic absorption vibration ofPMMA, together with the bands at 1064.71 cm^{-1} and 846.75 cm^{-1}. The band at 1739.79 cm^{-1},is characteristic for the stretching of the C=O, shows the presence of the acrylate carboxyl group. The band at 1483.26 cm^{-1} can be attributed to the bending vibration of the C–H bonds of the –CH3 group. The band at 2995.45 cm^{-1} can be assigned to the C–H bond stretching vibrations of the –CH3 and –CH2- groups. The peak 3506.59 cm^{-1} is associated to Cu Nano particle.Our results are agree with [6]. Peaks in Figure2 show no shifts but decreasing in the transmittance when the concentration of Cu increase this is due to the fact that copper is a shiny material which increased the reflectivity of the PMMA/Cu Nano composites.Table 1shows lists of the observed peaks for the PMMA/Cu with different concentration of Cu.

Thermal conductivity of the PMMA/Cu Nano composite

Thermal conductivity (often denoted k, λ, or κ) is the property of a material to conduct heat. It is evaluated primarily in terms of the Fourier's Law for heat conduction[7]:

$$q = -k\frac{dT}{dx} \quad \ldots\ldots\ldots (1)$$

where q denotes the heat flux, or heat flow, per unit time per unit area (area being taken as that perpendicular to the flow direction), k is the thermal conductivity, and dT/dx is the temperature gradient through the conducting medium. The thermal conductivity of insulators such as polymers has traditionally been measured by Lee's disk method. In Lee's disk method of bad conductor materials, the thermal conductivity (K) can be determined as below [8]:

$$K\left((T_B-T_A)/d_S\right)=e[T_A+(2/r)(d_A+(1/4)d_S)T_A+(1/2)r\ d_S\ T_B]\ldots\ldots\ldots (2)$$

where (T_A,T_B,T_C) are the temperature degree at each disk A,B,C respectively, (d_s) is thickness of specimens, (r) is radius of each disks also the specimens (all are of same radius) and e represents the amount of the imposed heat calculated by the following equation:

$$IV = \pi r^2 e\,(T_A+T_B) + 2\pi re\,[d_A T_A + d_S \tfrac{1}{2}(T_A+T_B) + d_B T_B + d_C T_C] \ldots\ldots (3)$$

where: I is current through the heater, V is applied voltage and (d_A),(d_B) ,(d_c) are the thickness of copper disks A,B,C respectively. Figure 2 shows the thermal conductivity of PMMA/Cu Nano composite of different weight of Cu. As shown in Figure 3 the thermal conductivity of the samples is increase as the concentration of Cu is increase, for the two first concentration (0.1%, 0.3%) there is a slight increase in the thermal conductivity, this mean phonons in PMMA is still dominated in conductivity not electrons of Cu. for the (0.4%, 0.5%) electrons start to become more effective in thermal conductivity in addition to phonons. the last concentration 1% there are a noticeable increase which mean that electrons in Cu nanoparticle is become dominated in the thermal conductivity of the Nano composite.

The Optical properties

The optical properties of materials can be defined as any property that involves the interaction between electromagnetic radiation or light with the matter, including absorption, polarization, reflection, and scattering effects[9].A UV-Vis spectrometer was used to study the transmission and absorption spectra of the PMMA/Cu samples at wave length rang 200-1100 nm. The absorption was used to determine the optical energy gap and optical constants such as refractive indexand Real Dielectric constant.

Optical energy gap

the optical energy gapof the samples was evaluated from Eq.

$$\alpha h\upsilon = D(h\upsilon - E_g)^r \quad \ldots\ldots\ldots\ldots (4)$$

\Where D is a constant, hν is the energy of incident photon, which can be calculated using the equation hυ (eV) = 1240 / λ (nm).And r is the order of the optical transition depending on the nature of electronic transition. The transition is called direct if the extremities of V.B. and C.B. lie at the same point in k-space, while the transition is called indirect if the transition is possible only with phonon assisted ($\Delta k \neq 0$). Thus the value of r may be (1/2, 2, 3/2, and 3), corresponding to the allowed direct, allowed indirect, forbidden direct and forbidden indirect transition respectively.α is the absorption coefficient. The absorption coefficient was calculated using the following expression[10]:

$$\alpha = 2.303\frac{A}{d} \quad \ldots\ldots\ldots\ldots\ldots\ldots\ldots\ldots\ldots\ldots (5)$$

Where (A) is the absorption and (d) is the sample thickness. Figure 4 (a, b, c, d, e. f) shows the plot of $(\alpha h\nu)^2$ versus hν with different Cu concentration.Table 1 shows the optical energy gap of the PMMA/Cu Nano composite of weights (0.1%, 0,3%, 0.4%, 0,5% and 1%). It can be seen from figure4 (a, b, c, d, e and f) that the optical energy gap of the samples decrease as Cu concentration increase, the energy gap has changed from (5 ev) for pure PMMA to (3.8 ev) for the highest concentration (1% wt Cu).The Cu Nano particle made an intermediate energy levels for PMMA that led to minimize the energy gap.

Refractive index

The refractive index (n) of PMMA/Cu Nano composite can be calculated from the following equation [11]**:**

$$n = \left[\frac{4R}{(R-1)^2} - k^2\right]^{1/2} - \frac{(R+1)}{(R-1)} \quad \text{.....(6)}$$

WhereR is the reflectance and given by the equation:

$$R = \frac{(n-1)^2 + k^2}{(n+1)^2 k^2} \quad \text{.....(7)}$$

The extinction coefficient (imaginary part of the refractive index), which is related to the exponential decay of the wave as it passes through the medium and can be determined by using equation:

$$k = \frac{\alpha\lambda}{4\pi} \quad \text{.....(8)}$$

Whereλ is the wavelength of the incident radiation and α is α is the absorption coefficient given in eq (5). The variation of the refraction index (n) as a function of the wavelength for PMMA/Cu Nano composites has been determined. Figure 3.3 shows the variation of index refraction as function of wavelength. It was found that (n) change with (λ) in the range (360-1000) nm. It is shown that the refraction index is almost the same in the two firstCu concentration (0.1%, 0.3%), and there is a noticeable increased in (0.4%) ,but by increasing the Cu Nano particle to 0.5% and 1% cause decreasing in the refracting index that because copper start to scatter the incident UV-Visible light.

Real Dielectric constant

The real dielectric constant (εr) can be calculated by using equation [12]:

$\varepsilon r = n2 - k2$.....(9)

where n is the refractive index, k is The extinction coefficient given in equations 6, 8 respectively. The real dielectric constant (εr) which depend on the frequency of the electromagnetic wave. The variation of εr versus wavelength in the range (200-1000) nm for PMMA/Cu Nano composites has been determined. Figure 6 show the variation of εr with the increase of the wavelength of the incident radiation is due to the change of reflectance and absorbance. The behavior of εr is similar to that of the refractive index because of the smaller value of k^2compared with n^2.

CONCLUSIONS

In the present study, thermal and optical properties of PMMA/Cu Nano composite were investigated and the following conclusion can be obtained:

1. The thermal conductivity increase with increasing the concentration of Cu Nano particle, which indicate that the composites conduct heat better than the PMMA.
2. The enhancement in the thermal conductivity is mainly attributed to the heat transferred by lattice vibrations as (major contributors) and electronic contribution when addition Cu Nano composite during thermal activation.
3. The best fitting to the absorption spectra gave r=1/2, meaning it allowed direct transition for the samples.
4. Adding Cu Nano filler in PMMA matrix may cause the location states of PMMA to overlap and extend in the mobility gap. This overlap may give us an evidence for decreasing energy gap when adding Cu in the PMMA matrix.

REFERENCES

1. Azeredo, HMCd.,Nanocomposites for food packaging applications. Food Res.Intern.42,(2009).
2. M. Yuan "Tunable Conductivity Level in NanosizedPhthalcon/Polymer Composites" Geborente Tianjin, China, 2008.
3. F. Hussain, M. Hojjati, M. Okamoto, R.E. Gorga, Review article: Polymer-matrix nanocomposites, processing, manufacturing, and application: An overview, Journal of Composite Materials 40(17), (2006).
4. Silva A., Soares B. G., Zaioncz S., Dahmouche K.: Poly(methyl methacrylate)-clay nanocomposites prepared by in situ intercalative polymerization: The effect of the acrylic acid. LNLS 2007 Activity Report (2007).
5. JyotiChaudhary,Giriraj Tailor: Synthesis and thermal properties of copper nano particles, Asian Journal of Chemistry,2017.
6. Choi SUS: Enhancing thermal conductivity of fluids with nanoparticles. In Developments and Applications of Non-Newtonian Flows.FED-vol. 231/MD-vol.66.Edited by: Siginer DA, Wang HP. New York: The American Society of Mechanical Engineers; 1995:99.
7. L.A.Utraki," Introduction to polymer Blend in polymerblendsHand book ", Vol. 1, Kluwer Academic Pub. Dordrecht,2002.
8. M. S. Vijaya and G. Rangarajan ", Materials Science",Tata McGraw-Hill publishing company limited ,2003.
9. Vaibhav Jain, AkshayKokil,Optical Properties of Functional Polymers and Nano Engineering Applications,CRC Press,2017.
10. M. Alenso and J. Veen ,"Physics" second edition , John Wiley, New York (1971).
11. W. Klopffer, "Introduction to Polymer Spectroscopy", Springer Verlage, (1984).
12. K. M. Habib , "Study of the Photoconductivity of Pplyblend and Doped Polymers", Ph.D thesis submitted to the College of Science , University of Baghdad, (2005).

Table 1. The values of the energy gap of the PMMA/Cu Nano composites

sample	Pure PMMA	Cu 0.1 wt%	Cu 0.3 wt%	Cu 0.4 wt%	Cu 0.5 wt%	Cu 1 wt%
Energy gap (eV)	5	4.8	4.71	4.6	4.31	3.8

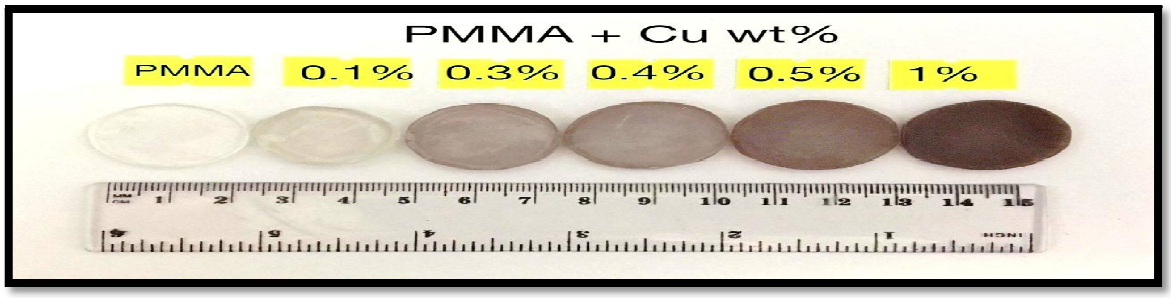

Figure 1. PMMA Cu Nano composite samples

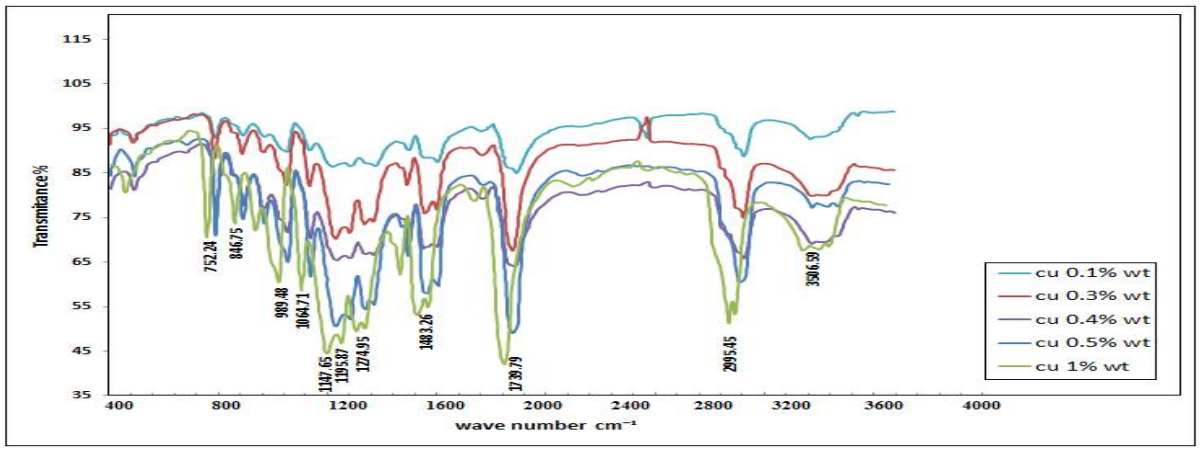

Figure 2. FT-IR spectra of PMMA/Cu Nano composite

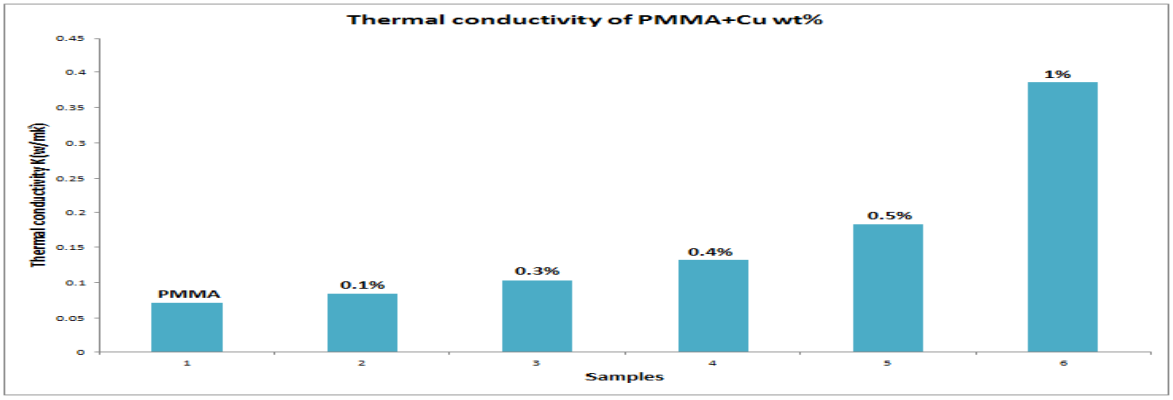

Figure 3: Thermal conductivity of PMMA/Cu Nano composite

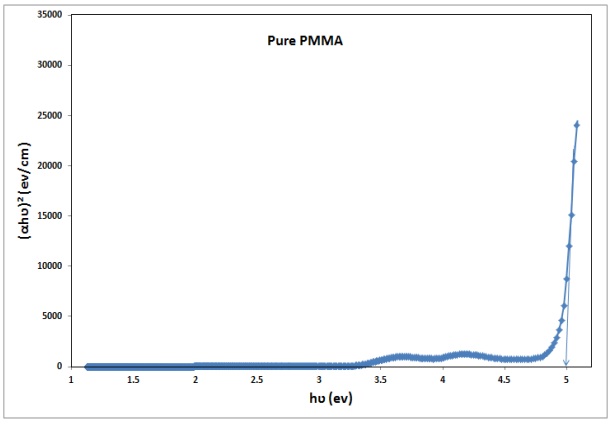

Figure 4-a energy gap of the samples decrease as Cu concentration increase

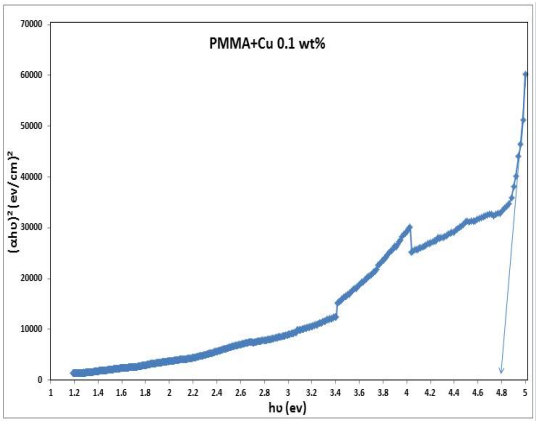

Figure 4-b energy gap of the samples decrease as Cu concentration increase

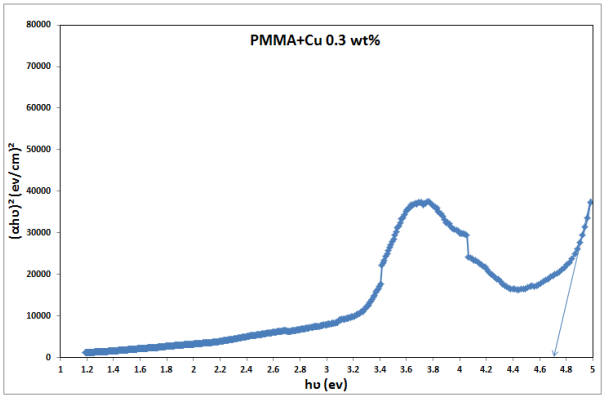

Figure 4-c energy gap of the samples decrease as Cu concentration increase

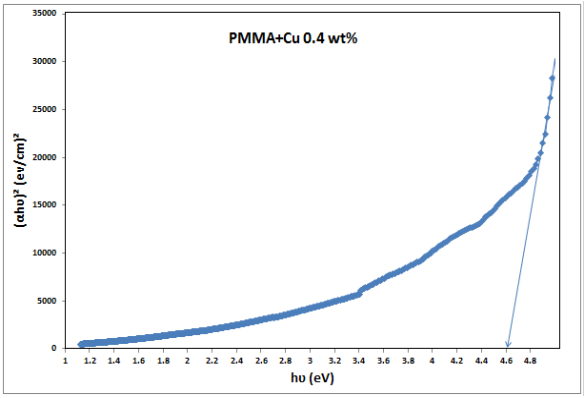

Figure 4-d energy gap of the samples decrease as Cu concentration increase

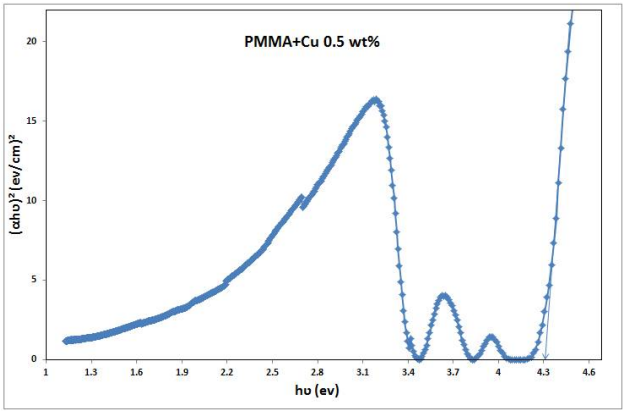

Figure 4-e energy gap of the samples decrease as Cu concentration increase

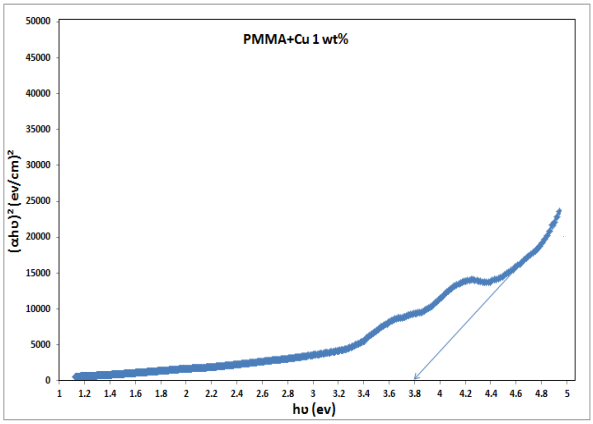

Figure 4-f energy gap of the samples decrease as Cu concentration increase

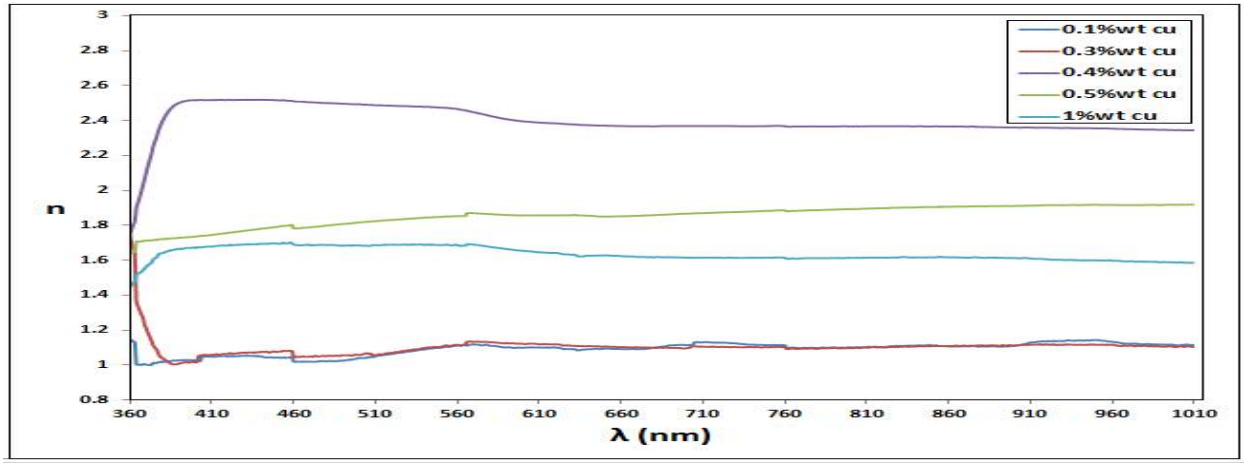

Figure 5. Variation of the index of refraction with the wavelength for PMMA/Cu Nano composites

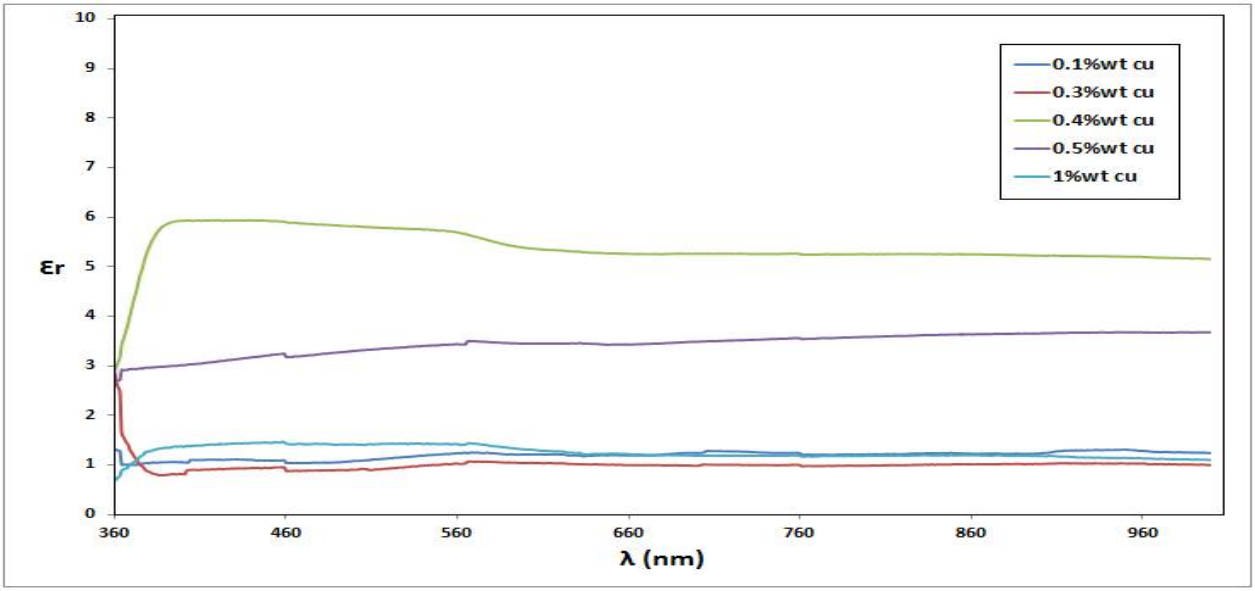

Figure 6. The real dielectric constant with the wavelength for PMMA/Cu Nano composites

Indian Journal of Natural Sciences www.tnsroindia.org.in ©IJONS

Vol.9 /Issue 50 /October / 2018 *International Bimonthly* *ISSN: 0976 – 0997*

RESEARCH ARTICLE

Synthesis, Structural and Morphological Characterization of Pure and Doped $LiNiPO_4$ Composite as Cathode Materials for Lithium Ion Batteries

Hind Mohammed Hassan* and Zainab Raheem Muslim

Department of Physics, College of Science, University of Baghdad, Iraq.

Received: 04 July 2018 Revised: 08 Aug 2018 Accepted: 10 Sep 2018

***Address for Correspondence**
Hind Mohammed Hassan
Department of Physics,
College of Science,
University of Baghdad, Iraq.
Email: hindmoh_1990@ yahoo.com

ABSTRACT

Lithium nickel phosphate $LiNiPO_4$, carbon doped $LiNiPO_4$,aluminum doped $LiNiPO_4$/C silver doped $LiNiPO_4$/C powder have been prepared by sol-gel method. Characterization of the structure and morphology of powders was performed using XRD, SEM, AFM and EDX. The XRD was carried out to confirm the formation of these powders. The calcination was achieved at (750)C° for(2h).X-ray diffraction data show the formation of olivine structure of $LiNiPO_4$ with space group (pnma) .SEM images showed a uniform distribution of the particle for $LiNiPO_4$and this distribution became less because the additives , this results were ensured by AFM results. .EDX result reveals the existence of C, O, Ni, Al Ag, and P atoms and are consistent to those of the literature, while the peak of Li is not visible because of its low activation energy.

Keywords: Lithium nickel phosphate; Lithium ion battery; Cathode material; Powder fabrication, Composites.

INTRODUCTION

In recent years, the demand for rechargeable batteries with high voltage and high energy density has grown tremendously because of the development and popularity of portable electronic devices (1).One of the most promising energy storage solutions for future automotive technologyarerechargeable battery sources. Rechargeable batteries are more portable than the resources such as flywheels, capacitors, biofuels, solar cells, and fuel cells and provide quick energy storage and release of energy (2).ZHANG Ying et al.2015(3) and LucangeloDimesso et al. 2012(4) prepared $LiNiPO_4$ and $LiNiPO_4$/C composites as cathode materials for lithium ion batteries. Among the various electrical energy storage mediums, lithium ion rechargeable batteries are the most promising power system due to their high energy density range from 100-150 Wh/kg, high operating voltage (~4V), lightweight, long cycle life, environmental friendliness and safety.Technology of Li-ion battery is applied to both thin, light, and flexible portable

electronic devices, electric vehicles and they also find applications in space (5,6,7). Cathode materials are typically oxides and phosphates of transition metals, which can undergo oxidation to higher valences when lithium is removed (8).Since cathode materials for lithium ion batteries have lower capacity compared with anode materials and it has a high free energy of reaction with the lithium the overall electrochemical performance of lithium –ion batteries is significantly determined by the properties of the cathode materials (9).The structure and morphology properties of the synthesized composite powders are discussed in this work.

MATERIALS AND METHODS

$LiNiPO_4$, $LiNiPO_4$/C, $LiAlNiPO_4$/C and $LiAgNiPO_4$/C were prepared using conventional sol-gel method. $LiNO_3$ (Fluka,India.98%) $Ni(NO_3)_2.6H_2O$(HAMEDIA,India,97%),$NH_4H_2PO_4$(Central Drug House,India,99%), $AlNO_3$,$AgNO_3$ (Fluka, India,99.9%) and citric acid (Alpha,India,99.5%) were used as started materials. The A-type $LiNiPO_4$ sample was synthesis by dissolved stoichiometric weighs (1:1:1) of $LiNO_3$, $Ni(NO_3)_2.6H_2O$ and $NH_4H_2PO_4$ in (60ml) deionized water. The mixture were heated under stirring at(70-80)°C for several hours, which made the mixture denser and formed the gel. The gels were heated at (100) °C in air for 8hours.The dried gel were calcined in air at (750) °C for 2hours.$LiNiPO_4$/C composite (B-type) was synthesized in the same way with addition 3times weight of citric acid as a chelating agent and carbon source. $LiNiPO_4$/C/G Where (G=$AlNO_3$, $AgNO_3$) composite were synthesized in the same way with addition of ($AlNO_3$ or $AgNO_3$ solution respectively), to the mixture.The structural analysis of the samples was performed byusing SHIMADZU (XRD-6000) diffractometer Japanese -made with cu kα radiation (kα=1.5405A°). The scanning angle 2Θ was varied in the range of (10-80) degree with speed of 5 degree/min. Crystallite size were calculated by using Scherer equation: $D= K\lambda/ \beta \cos\Theta$ Where K is crystallite shape factor, a good approximation is 0.9, λ is the X-ray wavelength, β is the full width at half maximum and Θ is the Braggs angle. A scanning electron microscope model inspect 50, FEI Company made in Holland was used to investigate the morphology of the samples.AFM AA3000 scanning probe Microscopy by Angstrom Advanced Inc (USA)was performed to measure the average diameter and the grain size for the composite for the samples in the shape of a pellet. The chemical composition was determined with an inductively coupled plasma spectrometer Burcker , made in England and with an energy dispersive X-ray spectrometer (EDX) coupled to a inspect 50 scanning electron microscope. The production powder yielded bright-yellow for all types of composite, as shown in Fig .1. This agrees with the results obtained by Herle et al (10).

RESULTS AND DISCUSSION

The x-ray diffraction spectra for lithium nickel phosphate $LiNiPO_4$, $LiNiPO_4$/C, $LiAlNiPO_4$/C and $LiAgNiPO_4$/C synthesis by sol-gel process are reported in Fig.2. All the x-ray spectra indicate the formation of orthorhombic olivine structure $LiNiPO_4$ with space group (pnma) (JCPDS NO.96-200-1690). The main peaks at 17.6°, 20.8°, 25.8°,30.4°.36.3° and 53.2° corresponding to (200),(101),(111),(020) , (311) and(222) indicates the formation of orthorhombic olivine structure $LiNiPO_4$ this agree with the result obtained by [3]. It can be seen from the patterns that all diffraction peaks are very sharp, which indicates that the samples have good crystal structure.The x-ray spectra showed the presence of crystalline reflections attributed to $Li_4P_2O_7$ and $Li_6P_6O_{18}$ as secondary phases, this agree with the result obtained by [4]. The formation of crystalline aluminum is not appears in the x-ray spectrathis is due to change in crystal structure or due to grain orientation of aluminum which differ from grain orientation of $LiNiPO_4$. SEM images of $LiNiPO_4$, $LiNiPO_4$/C, $LiAlNiPO_4$/C and $LiAgNiPO_4$/C were shown in Fig3 (a, b, c and d), respectively. In Fig (3a) it can be seen regions of agglomerated small particles of spherical morphology and the particles size had a wide range distribution Fig (3b) show that the addition of carbon source reduce the agglomeration of particles and lead togrowth in particle morphology for $LiNiPO_4$/C. It is clearly that the samples have developed grains of regular shape. SEM image for $LiAlNiPO_4$/C is shown in Fig (3c). It can be seen that the addition of aluminum effect on the morphology causes drastic morphology modification, leading to large particle sizethis is due to higher radius for aluminum (2.39A°) which is larger than silver (2.25A°) and carbon(1.9A°) (11).SEM image for $LiAgNiPO_4$/C is shown in Fig (3d), it is

clearly that there is a grain of different size which occur by the addition of silver to the composite. AFM micrograph of $LiNiPO_4$, $LiNiPO_4$/C, $LiAlNiPO_4$/C and $LiAgNiPO_4$/C were shown in Fig.4 (a, b, c and d), respectively .It can be seen in fig (4a) that samples areconsist of regular spherical shape and the grain distribution over the surface is more uniform. Fig.4 (b, c and d) shows that with addition of citric acid as carbon source and chelating agent causes a growth in the particle size . The average grain size were found to be 54.02nm for pure sample and 83.54,96.58 and 108.23nm for $LiNiPO_4$/C,$LiAlNiPO_4$/C and $LiAgNiPO_4$, respectively. This agree with SEM results. This result effect on the average roughness of these powders. The average roughness were found to be 0.297nm for pure samples, while the average roughness were found to be 0.48, 0.552 and 0.459nm for $LiNiPO_4$/C, $LiAlNiPO_4$/C and $LiAgNiPO_4$, respectively. Furthermore, in order to characterize the elemental composition on the surface of $LiNiPO_4$, $LiNiPO_4$/C, $LiAlNiPO_4$/C and $LiAgNiPO_4$/C particles, the corresponding energy dispersive X-ray (EDX) spectrum of were analyzed in Fig.5. The result reveals the existence of C, O, Ni, Al Ag, and P atoms and are consistent to those of the literature, while the peak of Li is not visible because of its low activation energy (12).

CONCLUSIONS

Olivine cathode materials $LiNiPO_4$, $LiNiPO_4$/C, $LiAlNiPO_4$/C and $LiAgNiPO_4$/C were successfully prepared with citric acid as carbon sources by sol-gel method. All samples showed very sharp diffraction peaks, which indicates that the samples have good crystal structure. The XRD spectra of the composite annealed in air at 750C° for 2 hour detected the reflections of the $LiNiPO_4$ crystalline phase, and $Li_4P_2O_7$ and $Li_6P_6O_{18}$ as secondary phases.SEM images showed a uniform distribution of the particle for $LiNiPO_4$and this distribution became less because the additives, this results were ensured by AFM result. EDX result reveals the existence of C, O, Ni, Al Ag, and P atoms and are consistent to those of the literature, while the peak of Li is not visible because of its low activation energy.

REFERENCES

1. Chung-Hsin Lu, Hsuan-Hao Chang and Chi Yen. Reverse Microemulsionsynthesis and electrochemical properties of $LiNiO_2$ Powders. *Tamkang Journal of Science and Engineering. 2004; 7(4):199_204*.
2. Jürgen Garche Chris K. DyerPatrick T. Moseley ZempachiOgumiDavid A. J. Rand Bruno Scrosati .Encyclopedia of Electrochemical Power Sources. Elsevier: Kurzweil, P . 2009.4538.
3. ZHANG .Y, PAN Yue, LIU Jia, WANG .G and CAO. D,"Synthesis and electrochemical studies of carbon-modified $LiNiPO_4$ as the cathode material of Li-ion batteries", Chem. Res. Chin. Univ., 2015 January12.; 31 (1): 117—122
4. Lucangelo. D & Dirk. B &Christina. S & Wolfram .J"Investigation of graphitic carbon foams/LiNiPO4 composites", Solid State Electrochem.2012 July 20; 16(12):3791–3798.
5. Yangyang Feng, Huijuan Zhang, Ling Fang, Ya Ouyang and Yu Wang. Designed synthesis of a unique single-crystal Fedoped $LiNiPO_4$nanomesh as an enhanced cathodefor lithium ion batteries. Mater. Chem. A. 2015;3(31): 15969-15976.
6. Peter G. Bruce, Bruno Scrosati, and Jean-Marie Tarascon. Nanomaterials for rechargeable lithium batteries. Chem., Int.Ed., 2008;47: 2930–2946.
7. KARTHICKPRABHU S "Study of high energy olivine phosphate cathode materials doped with transition metals and rare earths for lithium ion batteries.PhD. KALASALINGAM UNIVERSITY, 2016.
8. T.V.S.L. Satyavani ,A. Srinivas Kumar and P.S.V. Subba Rao. Methods of synthesis and performance improvement of lithium iron phosphate for high rate Li-ion batteries. , Engineering science and technology.2016;19(1):178-188.
9. Rui Qinga,1, Ming-CheYangb, Ying Shirley Mengb, Wolfgang Sigmund .Synthesis of $LiNi_xFe_{1-x}PO_4$solid solution as cathode materials for lithium ion batteries. ElectrochimicaActa 2013;108:827-832.
10. P. SubramanyaHerle, B. Ellis, N. Coombs and L. F. Nazar.Nano-network electronic conduction in iron and nickel olivine phosphates. Nature materials. 2004February 22; 3:147-152.

11. Martin Rahm, Roald Hoffmann, and N. W. Ashcroft. Atomic and ionic radii of elements 1–96. Chem. Eur. J. 2016;22: 14625 – 14632.
12. R. El khalfaouy a, H. El knidri, R. Belaabed, A. Addaou, A. Laajeb, A. Lahsini. Synthesis and characterization of $LiMnPO_4$ material as cathode for Li-ion batteries by a precipitation method and solid-state blending. *J. Mater. Environ. Sci. 2016;7 (1) :40-49*.

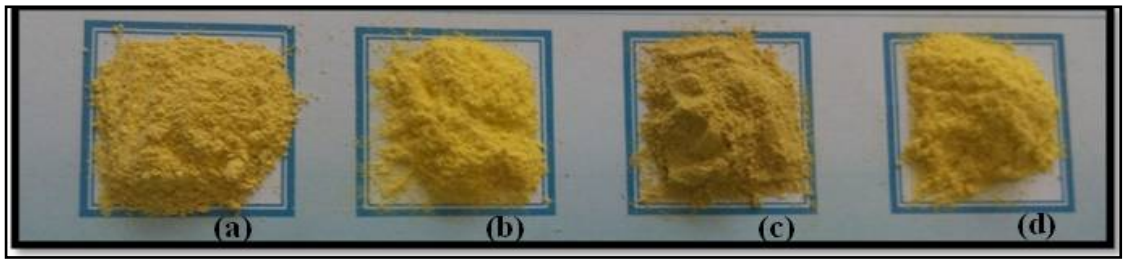

Figure1 . Final powders of a) $LiNiPO_4$, b)$LiNiPO_4$/C, c) LiAgNiPO4/C and d) $LiAlNiPO_4$/C composite.

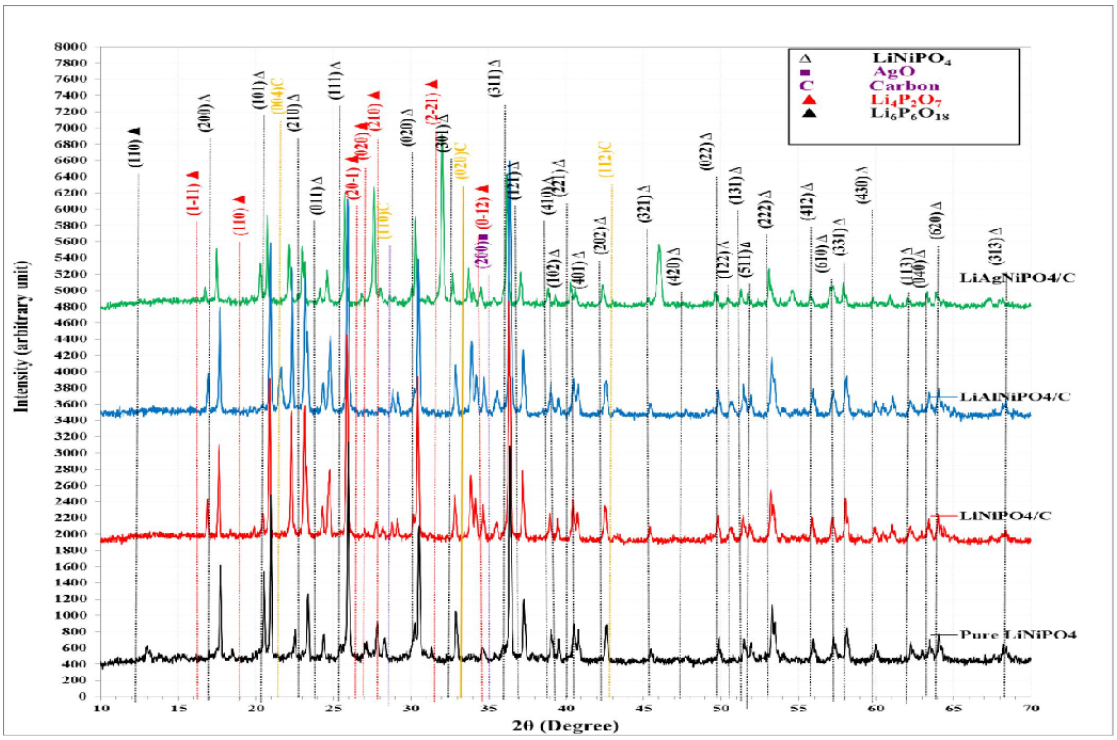

Figure.2 X-ray diffraction spectra of pure $LiNiPO_4$, $LiNiPO_4$/C, $LiAlNiPO_4$/C and $LiAgNiPO_4$/C.

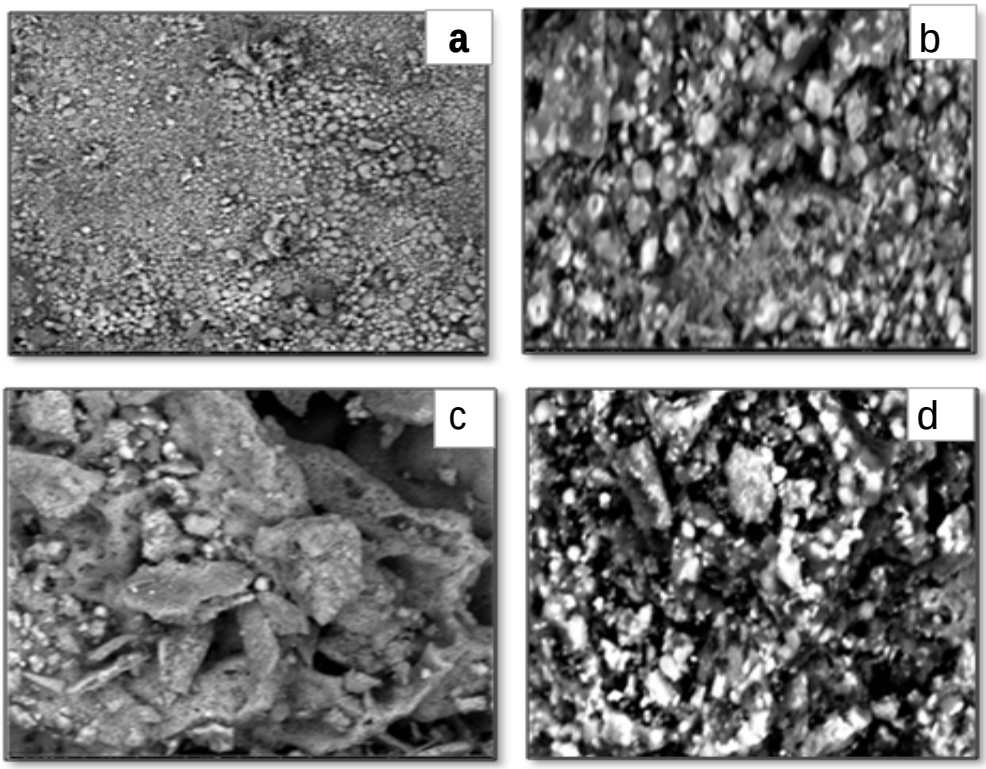

Figure.3 SEM images (scale bar50µm) of a) $LiNiPO_4$; b) $LiNiPO_4$/C; c) $LiAlNiPO_4$/C/ and (d)$LiAgNiPO_4$/C.

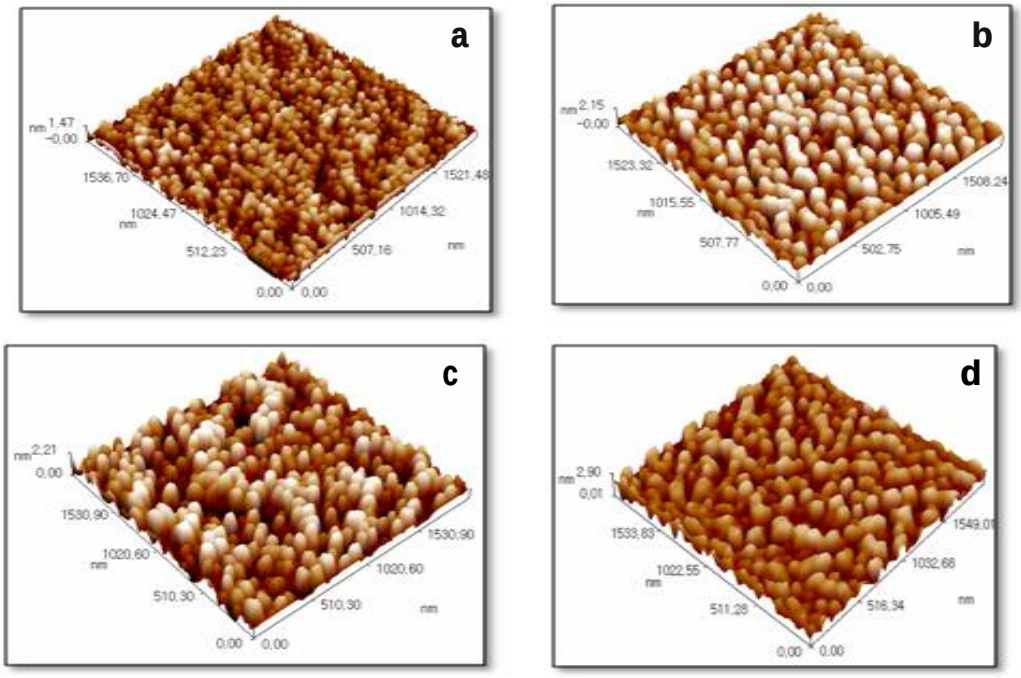

Figure.4 AFM micrograph of a)pure $LiNiPO_4$, b)$LiNiPO_4$/C, c)$LiAlNiPO_4$/C and d)$LiAgNiPO_4$/C

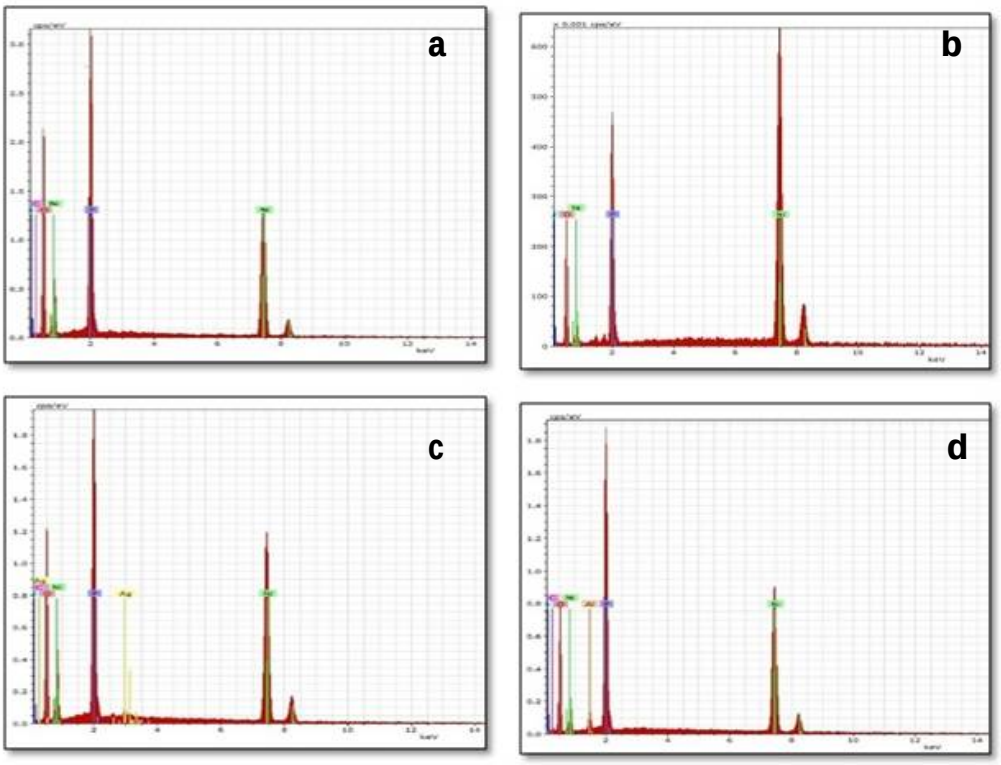

Figure5: EDX for a) $LiNiPO_4$, b)$LiNiPO_4$/C, c)$LiAlNiPO_4$/C and d)$LiAgNiPO_4$/C

Indian Journal of Natural Sciences www.tnsroindia.org.in ©IJONS

Vol.9 /Issue 50 /October / 2018 *International Bimonthly* *ISSN: 0976 – 0997*

RESEARCH ARTICLE

Histological and Histometrical Features of the Fallopian Tube in Humangenital System

Manar Khlaf Litef*, Saad Ahmed Mohammed and Samira Abdul Hussein

Department of Anatomy and Histology, College of Medicine, Tikrit University, Iraq.

Received: 08 July 2018 Revised: 15 Aug 2018 Accepted: 19 Sep 2018

*Address for Correspondence
Manar Khlaf Litef
Department of Anatomy and Histology,
College of Medicine,
Tikrit University, Iraq.
Email:sabahali503@yahoo.com

ABSTRACT

Present work wasinvestigatedthe histological and histometrical features of the fallopian tube in woman during different periods of ages.A total twenty-two samples of fallopian tube were used. The tissue sections were stained with H&E and Masson's trichrom stains. In all ages the infundibulum has cranial funnel and posterior neck parts.The mucosa of funnel has fimbria and the neck mucosa had thin branched mucosal folds. In Ampulla the mucosa has many tall branched folds whileisthmus mucosa has few simple branched folds. The mucosal folds were lined with simple-pseudo stratified columnar cells contained secretory, non-secretory and basal cells. The lamina propria- submucosa has no muscularis mucosa. Tunica muscularis of neck part composed of smooth muscle fibers that oriented in different direction while in ampulla and isthmus have thick inner circular and thin outer longitudinal smooth muscle fibers. The height of fimbria was significant in the left fallopian tube during 30years (911.4±4.2µm) into 49 years (1019.89±2.8 µm). The height of mucosal folds was significant in the ampulla of the left fallopian tube during 30 years (708.6±2.9µm) into 49 years (722.4±9.9 µm). The thickness of fimbria was significant in the left fallopian tube during 30 years (127.9±5.0µm) into 49 years (129.2±2.5 µm).The thickness of mucosal folds in ampulla was significant in the left fallopian tube during 40-49 years (124.9±5.0µm) and in isthmus was during 30-39 years (79.9±1.0 µm). The height of epithelium of fimbria was significant in the left fallopian tube during 40-49 years (19.9±1.5µm). The height of epithelium of ampulla was significant in the left fallopian tube during 30-39 years (36.5±3.0µm) into 40-49 years (38.3±2.6 µm).

Key Words: fallopian tube, histological, histometrical, woman.

INTRODUCTION

Fallopian tube is one of the most functionally significant organs of female reproductive system which serving as bridge between the ovary and the uterus, structurally and functionally equipped to carry out the sequent cascade of events from egg pickup,it is peristaltic transport to the site of fertilization (ampulla) and providing the optimal environment for fertilization and transport of embryo to the uterus for implantation [1] [2].Following fertilization, the fertilized ovum develops into an embryo and continues to pass through the oviduct into the uterus,the fallopian tube is both the conduit and the transporter of the ovum and the early concept us. Its function also aids to transport of sperm to the site of fertilization[3].The fallopian tube is divided into the fimbriae, infundibulum, ampulla and isthmus. An epithelium of fallopian tube have two types; secretory and ciliary cells. The middle tunica of fallopian tube composed of muscle layers. The tubes are fixed by doublelayer of peritoneum which forming the broad ligament of reproductive system by which the vascularization and innervation are conduit consequently supplying the fallopian tube, uterus and the ovaries[4].Fallopian tube consists of three layers: endosalpinx, myosalpinx and outer serosa which continuous of the mesosalpnix.

The endosalpinx is thrown into mucosal folds which increased in their number toward the fimbria and lined by columnar epithelium. The myosalpinx actually consists of inner circular and outer longitudinal layer of smooth muscle fibers which has a third layer is added in the interstitial portion of the tube [4] [5]. The ciliated epithelial cells consisted of 25% of total epithelial cells which disperse among secretory cells in all segments of the oviduct. The ciliated cells increase in number from the fimbriae and be absent in the distal segment of the oviduct, consequently the isthmus showed fewof ciliated cells [6].Secretory cells are involving of 55-65% of the total epithelial cells, it present in all segments of the oviduct [6]. The fallopian tube revealed cyclical changes under the influence of estrogen and progesterone. Cells of fallopian tube are low in height during the menstrual phase of the cycle and increase during the proliferative phase finally they reach their maximal height in per ovulatory period. During per ovulatory period both secretory and ciliated cells have the same size, the secretory cells forming domes between the tufts of cilia [7].[8].The current study was aimed to investigate the histological and histometrical changes that occur in different periods of ages.

MATERIALS AND METHODS

Twenty-two samples of fallopian tubes have collected from women with a mean age of 44 years. The design of study was divided into four groups; first group involved (20-29 years), second group involved (30-39 years), third group involved (40-49 years), fourth group involved (50 years). The samples of fallopian tubes were obtained from Al Qadisiyah hospital in Tikrit governorate. The study was conducted in department of Anatomy and Histology at College of Medicine-Tikrit University. Samples of fallopian tubes have obtained by bilateral salpingo-oophorectomies (removal of fallopian tubes and ovaries) and tubal ligations using a protocol. Patients with healthy fallopian tube were operated for reasons unrelated to tubal dysfunction, for benign causes or sterilization. Patients have excluded if they had received exogenous steroid treatment or chemotherapy within the last 6 months before surgery.

All patients signed informed consent letters, and the study protocol was approved by the local ethics. Then specimens of the fallopian tubes have washed up with normal saline then fixed in 10 % neutral buffered formalin solution.Samples of fallopian tubes have cut up into three segments; fimbriated funnel, ampulla and isthmus of the tubes (each segment approximately to 1cm). After well fixation the specimens havedehydrated withup graded series of ethanol (70-100%) (2 hours each), cleared with two changes of xylen solution (one hours each), embedded two changes of paraffin bath (two hours each) and sectioned at 5-7 µm. Sections have stained with hematoxylin & eosin, Masson's trichrom stain [9] [10] .The slides were captured by using future Winjoe microscopy camera, china.Statistical

analysis;the data ofepithelial height, folds height and thickness, luminal diameterwere represented by (Mean±SE). A post-hoc (Tukey &Dunkun) analysis was applied toachievesignificant differences (P<0.05) [10] .

RESULTS

Each part of fallopian tube was consisted of four tunicae (Tunica mucosa,submucosa, muscularis & serosa). In all ages the infundibulum distended cranial part showed funnel shaped part which ended by finger like projections (fimbria) and it'sposterior has constructed neck part (fig.1). The fimbria were lined by simple to pseudo stratified columnar epithelium which consisted of ciliated and non-ciliated cells, the lamina propria was composed of well vacular loose connective tissue contained many of blood capillaries and distended arterioles (fig.2).At the neck of infundibulum the mucosa showed many of thin branched mucosal folds (fig.3). The mucosal folds were lined by simple to pseudo stratified columnar epithelium consisted of ciliated, non-ciliated and basal cells. The lamina propria of these folds was very thin layer composed loose connective tissue (fig.4). The lamina propria of neck was continued with submucosa due to absence of muscularis mucosa and composed of loose connective tissue and contained collagen bundles and many of blood vessels (fig.5), the tunica muscularis of neck was composed of sparse smooth muscle fibers which appeared oriented in different direction, many of arterioles were intermingled tunica muscularis (fig.6).Ampulla; in all ages the ampulla had very thick wall and wide lumen,the tunica mucosa was thrown into several mucosal folds which branched into primary and short secondary folds. At the base of the tall fold there were few of short mucosal folds(fig.6).

All mucosal these folds were lined with simple-pseudo stratified columnar epithelium, the epithelium showed three types of cells; secretory cells and non- secretory cells and basal cells (fig.7). The secretory epithelial cells were few and showed clear and pale stained cytoplasm contained oval basally situated nuclei. The non- secretory epithelial cells (peg cells) were the predominant type showed eosinophilic cytoplasm and contained oval-elongated nuclei. The lamina propria withinsimple and primary folds was loose connective tissue contained fibrocytes (fig. 8). The tunica submucosa was continued with lamina propria due to absence of muscularis mucosa and composed of very thin layer of loose connective tissue contained fibroblasts and arterioles (fig.9).Tunica muscularis was very thick layer composed of thick inner circular oriented and thin outer longitudinal smooth muscle fibers. The two layers of tunica muscularis were separated by a layer of well vascular collagenous connective tissue showed many of blood vessels and nerve fibers (fig.10).Isthmus was characterized by thick wall and narrow lumen (fig.11), the tunica mucosa of was thrown into 7-8 simple and branched mucosal folds which were lined with pseudo stratified columnar epithelium which at the caudal part of isthmus close the uterus fold the epithelium was low simple type which line with simple columnar epithelium composed of ciliated and non-ciliated types (fig.12), the lamina propria-submucosa was thick layer composed of cellular dense connective tissue contained collagen fibers, fibrocytes and lymphocytes (fig.13). Tunica muscularis was very thick layer and it composed of very thick inner circular oriented smooth fibers and thin outer longitudinal smooth muscle fibers (fig.14). In isthmus the tunica muscularis was thicker than that of ampulla. The histometrical measurements of height of fimbria and mucosal folds were showed in (Tab.1). Thickness of fimbria and mucosal folds were showed in (Tab.2) andthe epithelial height of fimbria and mucosal folds were showed in (Tab.3).

DISCUSSION

The current results revealed presence of ideal tunicae in the wall of fallopian tube such observation have mentioned by [4], [5], [11],[12],[13].In all ages the infundibulum showed funnel shaped cranial part and posterior neck part, such observation suggests that the neck has control the abdominal ostium of oviduct and the funnel is optimized with the first function of oviduct that to capture the ovum after ovulation and serves as a conduit for its travel toward the next region of oviduct [3]. The present study showed that the at funnel part the fimbria is highly vascular structures lined with epithelium of three types of cells, this result is supported by results of [5],[14]. On the other hand the mucosa of the neck of infundibulum had many of thin simple mucosal folds this part represents the area at which the abdominal

ostium is controlled. In all ages the neck of infundibulum and ampulla were highly folded structures and their mucosa had numerous primary and secondary mucosal folds, this result suggest that these folds are play an important role in adaptation of neck and ampulla to do their function such results is supported by result of [5], [8], [14][15] and results of [16] who say that the influences of PGF2 revealed an increase in the cell height of the lining epithelium of the ampulla with increased branching of primary and secondary mucosal fold.The current results revealed that the lining epithelium of the fallopian tube is pseudo stratified type, this result is agree with result of [17], on the other hand this result is disagree with results of [5], [6], [11], [16], this variation suggest that the differences in type of epithelial lining could be attributed for variation of cyclic phase this is agree with result of [18].

The results have observed that the epithelium had three types of cells this result compatible with [6], [19], [20] [21], The current result showed that the non- secretory epithelial cells (ciliated cells) were the predominant type this result supported by results of[22] & [23] who says that "The fallopian tube serves as a passage that transports gametes and the embryo as well as provides important structural, environmental and nutritional support for early embryonic development", also result of [21] who stated that "During the follicular phase the ciliated cells are abundant).On the other hand this result disagree with result of [11]& [6] who mentioned that "The ciliated cells are consist of small group of total epithelial cells which intermingled between the secretory cells in all segments of the oviduct "and disagree with (References) who referred for that the secretory cells are consisting of 55-65% of the total epithelial cells which are more abundant in the cranial portion of the ampulla and in the fimbriae, than in the isthmus, the present result agree with result of [24]&[20] who revealed that variation in ratio of ciliated to non-ciliated epithelial cells due to influences of various hormones during various cycles, at the secretory cells reach peak activity and discharge their contents into the lumen of the tube, consequently reducing in height relative to the ciliated cells leading in greater prominence of the cilia and may enable them to move particulate material or viscous secretions more effectively.In funnel and ampulla the lamina propria was merging with tunica submucosa due to absent of muscularis mucosa and both were well vascular loose connective tissue, this compatible with result of (11) and (16). The current result revealed that the tunica muscularis composed of thick inner circular and thin outer longitudinal such results agree with results of [25], [26], [11]and disagree with result of [12] that in woman referred for three distinct layers of smooth muscle fiber. On the other hand in isthmus the tunica muscularis was thicker than that of ampulla such result was similar that mentioned by [17].The histometrical measurements revealed significant fimbrial height, thickness, height of mucosal folds and height of epithelium in the left fallopian tube in ages of 30-49 years and the same differences were recorded between group (30-49 years) and other groups.

The thickness of mucosal folds was significant in the left ampulla in ages from (30-39 years) and was significant between groups of ages in (30-49 years) and other ages in both left and right isthmus. The epithelial height of fimbria was significant the left fallopiantube in groups (40-49 years), also there were significant differences between ages (40-49 years) and other ages of the left fallopian tube, these significant differences suggests that the fallopian tube under the influence of gonadal hormones (estrogen and progesterone) and epithelial cells may be low or height during the menstrual phase of the cycle and increase during the proliferative phase finally they reach their maximal height in per ovulatory period. During per ovulatory period both secretory and ciliated cells have similar size, the secretory cells be domes between the tufts of cilia, the estrogen effected the epithelium hypertrophy, secretory activities as well as ciliogenesis, on the other hand an opposite effects (Atrophy and deciliation) are related with high levels of progesterone consequently related with provide good capacitation [22], [23] ,[7], [27], [28] , so the samples of the fallopian tubes at periods of present study could in the follicular phase and under influences of the LH hormones [16],[28] or during luteal phase where that the increase in height of epithelium of fallopian tube may be due to increase in the protein synthesis under progesterone stimulation [18].The mucosal folds of the ampulla were much higher and more highly branched than that of isthmus such results agree with results of [14], [17], also [21] mentioned that the infundibulum and ampulla have high number and height of primary folds as well as increase of the thickness of the epithelium at the follicular phase. In conclusion the histological structure of fallopian tube did not showed any significant changes, only that the histometrical parameters of the fimbria and ampulla of the left fallopian tube which revealed that the left tube was more active than the right one during periods extending from 30-49 years.

REFERENCES

1. Ropert JK, Ming shih I. The origin and pathogenesis of epithelial ovarian cancer; A proposed unifying theory. Am.J. surg. Pathol., 2010: 34.3. 433.43.
2. Gray's. Anatomy.40th Ed.Churchill living stone. 2009:1327-8.
3. DiPaola BB, Lucidi SR. FACOG, 2016.
4. Eddy CA., Pauertsein CJ. Anatomy and physiology of the Fallopian tube. Clin. Obstet. Gynecol.,1980:23: 1177-1193.
5. Eweka AO, Ferdinard AE .Histological studies of the effects of monosodium glutamate of the fallopian tubes of adult female Wistar rats; Europe PMC plus. 2010.
6. Codon SM, Casanave EB. Morphology and histological annual changes of the oviduct of Chaetophractusvillosus (Mammalia, Xenarthra, Dasypodidae). Int. J. Morphol. 2009: 27.2:355-360.
7. Lyons RA, Saridogan E, Djahanbakhch O. The reproductive significance of human Fallopian tube cilia. Hum Reprod Update. 2006.
8. Donnez J, Casanas-Roux F, Ferin J, Thomas K. Changes in ciliation and cell height in human tubal epithelium in the fertile and post-fertile years. Maturitas.1983: 5. 39-45.
9. Bancroft JD, Marilyn G. Theory and practice of histological techniques. 6th Ed. London: Elsevier Limited; 2008; 168-173.
10. Muna RA, Abood DA, Rajab JM. Histological Changes of Cervix in Ovariectomized Indigenous Rabbits. AJPS,2016;16.2:45-52.
11. Leeson CR, Leeson TS, Paparov AA. In "Textbook of Histology" 5thEd., W.B. Saunders Co., Philadelphia. 1985: 470-472.
12. Muglial U, Motta PM A. New Morpho-functional Classification of the Fallopian Tube Based On its Three-Dimensional Myoarchitecture. Histol. Histopathol. 2001; 16: 227-237.
13. Singh GK, Prakash P. Histological and histochemical studies on the ampulla of the oviduct of goat. Indian Vet. J. 1990: 67: 152 -154.
14. Abe H,Oikawa T. Immunocytochemical localization of an oviductal zona pellucida glycoprotein in the oviductal epithelium of the golden hamster. Anat. Rec.1991; 229.3: 305-14.
15. Fredericks CM. Morphological and Functional Aspects of the Oviductal Epithelium in: The Fallopian Tube: Basic Studies and Clinical Contributions Futura Publishing Company Inc., New York. 1986:67-80.
16. Singh RA,Madan ML.Histological observations on reproductive organs in response to hormone administration in cyclic ewes (P.G. Progesterone, LHRH). Indian J. Anim. Sci. 1989: 59. 250-57.
17. Rajput R, Sharma DN. Regional cyclic and genitalical studies on histology and histochemistry of oviduct of Gaddi sheep. Indian Vet. J. 1997; 74: 580-583.
18. Ramachandraiah SV, NarsimhaRao P, Rama Rao P,RamamohanRao A. . Histological, Histometrical and Histochemical changes in the uterine and oviductal epithelium of ewe during estrus cycle. Indian. J. Anim. Sci. 1980; 50.1:41 -45.
19. Paik DY, Janzen DM, Schafenacker AM, Velasco VS, Shung MS, Cheng D, Huang J, Witte ON, Memarzadeh S . Stem-like epithelial cells are concentrated in the distal end of the fallopian tube: a site for injury and serous cancer initiation Stem Cells. 2012: 30. 11: 2487–2497.
20. Crow J, Amso N, Lewin J, Shaw RW. Morphology and ultrastructure of Fallopian tube epithelium at different stages of the menstrual cycle and menopause. Hum. Reprod. 1994; 9: 2224-2233.
21. MokhtarMD.Microscopic and histochemical characterization of the bovine uterine tube during the follicular and luteal phases of estrous cycleJournal of Microscopy and Ultrastructure. 2015: 44–52.
22. Miki K, Clapham DE. Rheotaxis guides mammalian sperm. CurrentBiology, 2013;23:443–452.
23. Hunter RH.Temperature gradients in female reproductive tissues. Reproductive Bio. Medicine Online. 2012; 24:377–380.

24. Lyons RA, Djahanabakhch O, Mahmood T, Saridogan E, Sattar S, Sheaff MT,Naftalin AA, Chenoy R. Fallopian tube ciliary beat frequency in relation to the stage of menstrual cycle and anatomical site. Hum. Reprod. 2002; 17:584-8.
25. Singh GK, Prakash P. Histological and histochemical studies on the ampulla of the oviduct of goat. Indian Vet. J. 1990; 67: 152 -154.
26. Leese, The formation and function of oviduct fluid. J. Reprod. Fert. 1988; 82: 843-856.
27. Teves ME, Barbano F, Guidobaldi HA, Sanchez R, Miska W, Giojalas LC. Progesterone at the picomolar range is a chemoattractant for mammalian spermatozoa. FertilityandSterility. 2006;86: 745–749.
28. Aguilar J, Reyley M. The uterine tubal fluid: secretion, composition and biological effects. Anim. Reprod. 2005:2.2:91-105.

Table 1: Show height of fimbria and mucosal folds of the fallopian tube in of groups (1, 2, 3 &4).

Ages / Years		Height of fimbria & mucosal folds / µm (Mean ±standard error)					
		Fimbria		Ampulla		Isthmus	
		Left	Right	Left	Right	Left	Right
G1	20-29	701.9±9.**3** (aa)	699.11±6.1 (aa)	632.9±**8.3** (aa)	605.5±4.9 (aa)	100.5±**9.1** (aa)	92.8±**3.9** (aa)
G2	30-39	911.4±**4.2** * (ab)	876.8±**5.9** (ab)	708.6±2.9 * (ab)	613±9.9 (aa)	131.3±2.3 (aa)	116.4±5.4 (aa)
G3	40-49	1019.9±2.8 * (ab)	1009±3.6 (ab)	722.4±.9.9 * (ab)	717.4±**5.3** (ab)	200.8±3.5 (ab)	198.4±8.7 (ab)
G4	50	622.9±5.9 (aa)	621±9.3 (aa)	622±3.5 (aa)	588.8±7.6 (aa)	137.4±2.8 (aa)	98.9±**.83** (aa)

(*) Represent significant differences between left and right part of fallopian tube at level of (0.05). Similar litters (aa) represent non-significant differences between groups of ages at level of (0.05) & the different litters (ab) represent significant differences between groups of ages at level of (0.05).

Table 2: Show the thickness of fimbria and mucosal folds of the fallopian tube in groups (1, 2, 3 &4).

Ages / Years		Thickness of fimbria & mucosal folds / µm - (Mean±standard error)					
		Fimbria		Ampulla		Isthmus	
		Left	Right	Left	Right	Left	Right
G1	20-29	99.8±**3.6** (aa)	93.1±4.7 (aa)	100.4±2.9 (aa)	92.7±.**1.5** (aa)	64.1±1.5 (aa)	55.7±2.2 (aa)
G2	30-39	127.9±5.0* (ab)	109±9.2 (ab)	109.1±2.1 (aa)	96.1±2.8 (aa)	79.9±1.0 * (ab)	73.5±2.1 (ab)
G3	40-49	129.2±2.5 * (ab)	118.4±8.2 (ab)	124.9±7.1 * (ab)	99.0±.**6.1** (aa)	75.3±2.0 (ab)	73.9±3.1 (ab)
G4	50	102.4±6.2 (aa)	100.9±7.2 (aa)	85.2±2.5 (aa)	82.9±**1.7** (aa)	69.0±2.0 (aa)	61.5±3.4 (aa)

(*) represent significant differences between left and right parts of fallopian tube at level of (0.05). Similar litters (aa) represent non-significant differences between the groups of ages at level of (0.05) & different litters (ab) represent significant differences between groups of ages at level of (0.05).

Table 3: Show epithelial height of fimbria and mucosal folds of fallopian tube in (1, 2, 3 &4)

Ages / Years		Epithelial height of fimbria & mucosal folds / µm - (Mean ±standard error)					
		Fimbria		Ampulla		Isthmus	
		Left	Right	Left	Right	Left	Right
G1	20-29	11.9±**1.0** (aa)	11.7±0.9 (aa)	24.9±.**1.8** (aa)	22.8±.**1.0** (aa)	16.8±1.0 (aa)	14.4±1.2 (aa)
G2	30-39	14.3±1.1 (aa)	14.2±0.9 (aa)	36.5±3.0 * (ab)	26.9±1.8 (aa)	17.4±0.8 (aa)	16.9±1.1 (aa)
G3	40-49	19.9±1.5 * (ab)	15.4±0.1 (aa)	38.3±2.6 * (ab)	26.2±0.3 (aa)	17..3±1.0 (aa)	15.6±1.6 (aa)
G4	50	11.1±1.4 (aa)	11.9±0.9 (aa)	26.1±1.2 (aa)	25.0±**2.9** (aa)	16.0±3.1 (aa)	15.9±1.5 (aa)

(*) represent significant differences between left and right parts of fallopian tube at level of (0.05). Similar litters (aa) represent non-significant differences between the groups of ages at level of (0.05) & different litters (ab) represent significant differences between the groups of ages at level of (0.05).

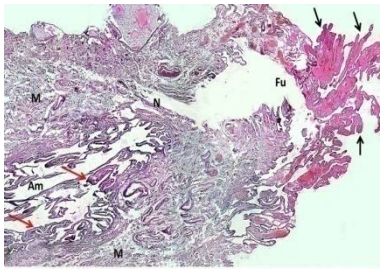

Figure1.Histological section of infundibulum (42 year old) shows: Fimbria (arrows), funnel part (Fu), fimbria (black arrows), neck part (N), ampulla entrance (Am), simple mucosal fold (Red arrow) & tunica muscularis (M). H&E stain. 40X

Figure 2. Magnified section at the tip offimbria shows: epithelium (E), lamina propria of loose connective tissue(Lc) contained blood capillaries (blue arrows), ciliated cells (Black arrows) & non-ciliated cells (red arrows) . H&E stain. 400x

Figure 3: Histological section at the neck of infundibulum shows: lumen (L), mucosal folds (arrows), tunica muscularis (M), mesosalpenix (Me), blood vessels (Bv). H&E stain. 40x

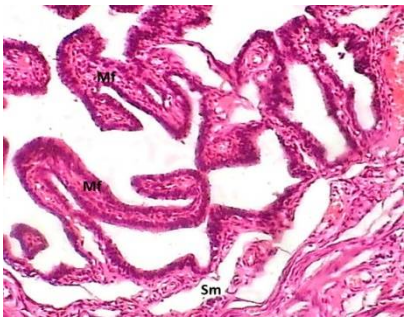

Figure 4: Magnified section at neck part shows: mucosal folds (Mf), lamina propria- submucosa (Sm) H&E stain, 100x

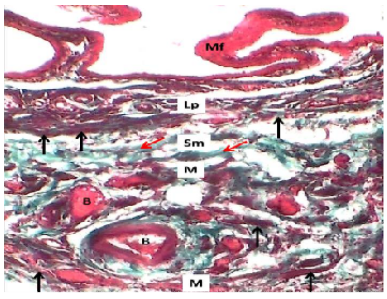

Figure 5: Section at the wall of neck part shows: mucosal folds (Mf), lamina propria- submucosa (Lp), smooth muscles fibers (Black arrows) blood vessels (Bv) H&E stain, 100x

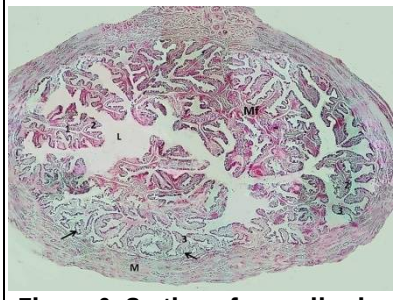

Figure 6: Section of ampulla shows: mucosal folds (Mf), simple fold (1), primary folds (2), short simple folds (3), epithelial crypts (arrows), lumen of ampulla (L) & tunica muscularis (m) H&E stain. 40x

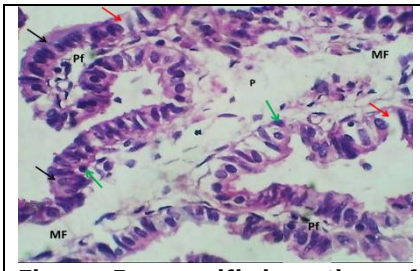

Figure 7: magnified section of mucosal fold–ampulla shows: simple mucosal fold (MF), primary folds (Pf), non-secretory epithelial cells (Black arrows), secretory epithelial cells (Red arrows), basal cells (Green arrows) & lamina propria (P).H&E stain. X400.

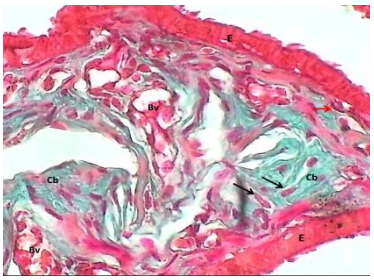

Figure 8: Magnified section of simple not branched mucosal fold of ampulla shows: epithelium (E), fibroblast (Black arrows), fibrocytes (Red arrows), collagen bundles (Cb) & blood vessel (Bv). Masson trichrom stain. X400.

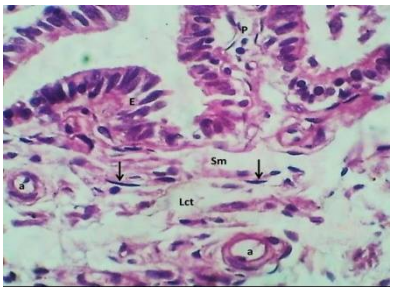

Figure 9: Magnified section of ampulla of shows: non secretory epithelial (E), lamina propria (p) & submucosa (Sm) shows: arterioles (a), loose connective tissue (Lct) with collagen fibers & fibrocytes (Black arrows). H&E stain. X400.

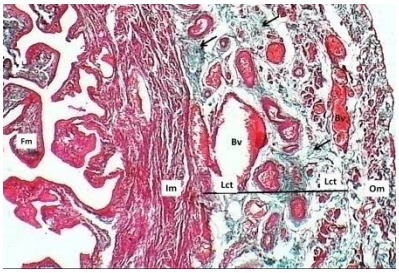

Figure 10: Magnified section of wall of ampulla shows: fimbria (Fm), circular smooth muscle fibers (Im), thin longitudinal smooth muscle fibers (Om), loose connective tissue (Lct) collagen bundles (Black arrows) &blood vessels (Bv). Masson trichrom stain. X100.

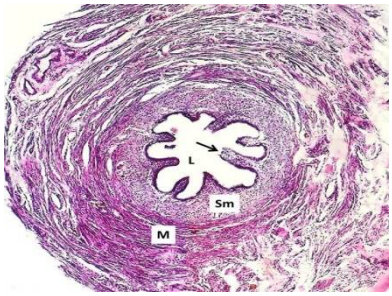

Figure 11: Transverse section of isthmus closed uterus shows: simple mucosal folds (arrows), tunica submucosa (Sm), tunica muscularis (M).H&E stain40x.

Figure 12: Magnified section of mucosal fold of the isthmus closed uterus shows: epithelium (E), lamina propria (p) &cilia (Black arrows). H&E stain. X400.

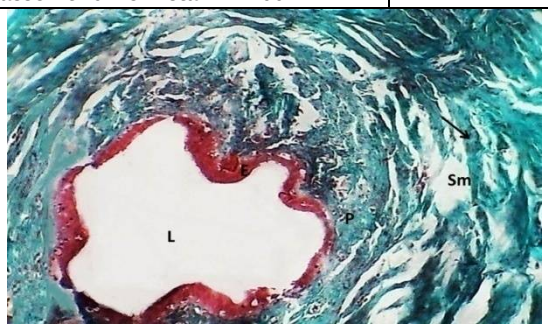

Figure 13: Magnified section of the isthmus close uterus shows: epithelium (E), lamina propria (p), tunica submucosa (Sm)&collagen bundles (Black arrow). Masson's trichrom.stain. X400.

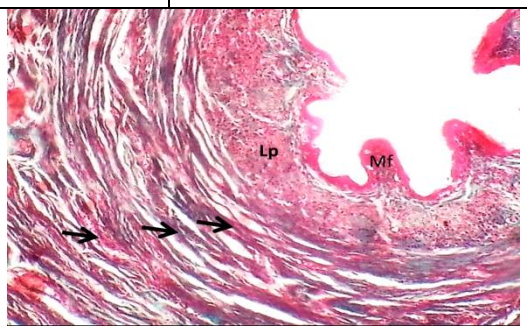

Figure 14: Magnified section of the wall of isthmus shows: mucosal fold (Mf), lamina propria (Lp)&circular smooth muscle fibers (arrows). Masson's trichrom stain. X400.